FINAL REPORT

IMPROVEMENT OF EVALUATION METHOD FOR EXISTING HIGHWAY BRIDGES

Research Report No. FL/DOT/RMC/6672-818
Contract No. BC-818

Ton-Lo Wang
Zhouhong Zong

Department of Civil & Environmental Engineering
Florida International University
Miami, FL 33199

Prepared for:
Structural Research Center
Florida Department of Transportation
Tallahassee, FL 32399

March 2002

Technical Report Documentation Page

1. Report No.	2. Government Accession No.	3. Recipient's Catalog No.
FL/DOT/RMC/6672-818		

4. Title and Subtitle	5. Report Date
Improvement of Evaluation Method for Existing Highway Bridges	March 2002
	6. Performing Organization Code
7. Author(s)	8. Performing Organization Report No.
Ton-Lo Wang and Zhouhong Zong	
9. Performing Organization Name and Address	10. Work Unit No.
Florida International University Department of Civil and Environmental Engineering University Park Miami, Florida 33199	11. Contract or Grant No. BC-818
	13. Type of Report and Period Covered Final Report October 2000 – March 2002
12. Sponsoring Agency Name and Address	14. Sponsoring Agency Code
Florida Department of Transportation Research Center, MS30 605 Suwannee Street Tallahassee, Florida 32399-0450	99700-3596-119

15. Supplementary Notes

Prepared in cooperation with the Federal Highway Administration

16. Abstract

In Florida, many short to middle span highway bridges have been in service for a rather long period. In these bridge structures, local damages can unavoidably occur due to long-term action of passing vehicle load and natural corrosion. The potential damages of these bridge structures in service are a great concern of FDOT. This study conducted the damage detection and diagnose of highway bridges by using modal parameters, such as frequencies, damping ratios, and Energy Transfer Ratios (ETR) index, as well as static data, such as deflections and strains. The project consists of the state-of-the-art report of structural health monitoring, measurement and signal treatment, ETR, model identification methods, model bridge testing and FE calculation, damage identification from static data, dynamic data, and ETR, etc. It is found that different damage index has different sensitiveness to different types of damage and extents. Modal parameters, such as frequency and damping ratio, are not sensitive to the bearing damage or girder cracking. ETR index is heavily affected by the signal-to-noise ratio and relies on the large amount of measured data. ETR hasn't been verified on real bridges.

17. Key Words	18. Distribution Statement
Highway Bridge, Damage Detection, Damage Index, Damage Identification, Bridge Evaluation, Vibration Testing, Static Testing, Energy Transfer Ratio (ETR), Structural Health Monitoring	This document is available to the public through the National Technical Information Service, Springfield, Virginia, 22161

19. Security Classify. (of this report)	20. Security Classify. (of this page)	21. No. of Pages	22. Price
Unclassified	Unclassified	183	

Form DOT F 1700.7 (8-72)

Reproduction of Completed Page Authorized

METRIC CONVERSIONS

N × 1,000 = kN

ft × 0.3048 = m

inch × 2.54 = cm

kip (force) × 4.448 = kN

kip (mass) × 454 = kg (mass)

mph × 1.609 = km/h

psi × 6.895 = kPa

ksi × 6.895 = Mpa

DISCLAIMER

The opinions, findings and conclusions expressed in this publication are those of the authors and not necessarily those of the Department of Transportation or the U.S. Department of Transportation.

Prepared in cooperation with the State of Florida Department of Transportation and the U.S. Department of Transportation.

ACKNOWLEDGEMENTS

The authors wish to express their sincere appreciation to the Florida Department of Transportation (FDOT) for funding this research. Special thanks are also extended to Mr. Marcus Ansley, Director, and Dr. Dongzhou Huang, Senior Research Scientist, Structural Research Center, FDOT for their valuable advice, suggestions, and comments during the course of this study. Finally, the authors would like to thank the following individuals and organizations for providing information and suggestions:

Professor Z. Liang, Department of Civil Engineering, State University of New York at Buffalo,
Professor D.W. Peng, College of Civil Engineering and Architecture, Fuzhou University, China,
Dr. Chunhua Liu, Parsons Brinckerhoff, Inc., and
Testing Center of Engineering Structures, Fuzhou University, China.

TABLE OF CONTENTS

LIST OF TABLES

Chapter 3

Chapter 4

Chapter 5

Appendix A

Appendix B

Appendix D

LIST OF FIGURES

Chapter 2

Chapter 3

Chapter 4

Chapter 5

Chapter 1

Introduction

Literature search demonstrates that about 40 percent of the nation's highway bridges are structurally deficient. These deficient structures potentially endanger the safety and economical use of the highway system. The National Bridge Inspection Standards (NBIS) regulates that every bridge on a public road must be inspected at least every 2 years. Highway agencies across the nation have inspection staffs and programs to collect and update critical bridge inventory and inspection data. Nowadays, there is still an evident need to perform a more precise evaluation of structural function and to find effective solutions.

In Florida, short to middle span bridges constitute the majority of highway bridges. These structures have been in service for a long period of time. In these bridge structures, local damages can unavoidably occur due to long-term action of passing vehicle load and natural corrosion. The potential damage of these bridge structures in service is a great concern of the Florida Department of Transportation (FDOT).

Recent researchers in this field have addressed some robust ways, such as using vibration monitoring of highway bridges, as a means for detecting structural deterioration. This kind of diagnosis system appears to be more applicable in the case of extra long span bridges, where the conventional human inspection method turns out to be very difficult. The latest results have demonstrated that the global modes of a subject structure is effective both in identifying the development of significant damage and in isolating its location. In this damage detection process, pre-damage and post-damage modal parameters of modes measured from the test structure are utilized to localize the damage. However, it is important to apply these new developments and to establish an improved technique in a deterioration rating system for highway bridges.

The aforementioned method of detecting deterioration is especially efficient for short and medium span bridges, which have been widely used in the state of Florida. Potential dangers may not be found merely by means of human visual inspection. It is definitely necessary to develop an advanced diagnosis method for the maintenance and management of highway bridges in the future.

1.1 Vibration-based damage detection and evaluation

The basic idea of vibration-based damage detection is that the modal parameters (notably frequencies, mode shapes, modal damping) are functions of the physical properties of the structure (mass, damping, and stiffness). Since deterioration of integrity of structures and mechanisms can be characterized by changes in vibration signature which have been indicators for condition monitoring system. Vibration-based structural damage detection and evaluation can be categorized into the following four levels: (I) detecting the existence of damage, (II) finding the location of damage, (III) estimating the extent of damage, and (IV) predicting the remaining

load-carrying capacity and fatigue life.

Detecting the existence of damage (level I) is basically equivalent to detecting a change in the dynamic characteristics. There are two approaches to extend vibration-based methods beyond level I. In the first approach, a large number of sensors are used to detect the location of the damage based upon a local mode shape change. The localization accuracy is typically limited to the spatial resolution of the measurement mesh. The second approach requires fewer sensors, but needs an analytical model of the structure. Parameters of the model that are related to damage are updated so that the dynamic characteristics of the model correspond to the measurements. *Finite Element Model Updating* methods fall in this category. To perform tasks of Level (IV) requires material constitutive information on a local level, materials aging studies, damage mechanics, and high-performance computing.

In vibration-based damage detection, lots of measurement data are generated. The process of finding a model from data is called *System Identification* (SI). The application of SI, based on the measurement and analysis of vibration signals to identify a suitable mathematical model and vibration signatures corresponding to the changing state of physical structure, is among the promising nondestructive evaluation methods. This belongs to the scope of *experimental modal analysis*. This kind of damage diagnosis method appears to be more feasible in the case of extra long span bridges, where the conventional human inspection method turns out to be very difficult. In this damage detection process, an initial measurement of an undamaged structure was treated as the baseline for the future comparison of the measured response. Health monitoring and damage assessment of civil engineering structures have become more practical in systematic inspection and evaluation of these structures during the past two decades.

1.2 Focus of the research

Nowadays, vibration-based damage detection and evaluation may contain several typical steps. The first step is establishing the *Finite Element Model (FEM)* of the structure under the intact condition, which can be treated as the baseline model. This model should be confirmed by the experimental data from indoor model or field-testing. The second step is field vibration testing and dynamic parameter identifying. An *Experimental Modal Analysis* of a vibration structure from output-only data is the key issue. The third step is *Finite Element Model Updating* in structural dynamics. The basic assumption is that the testing results, which contain the measurement noise is correct, and the calculation from FEM may be updated according to the testing results once the errors between them are acceptable. Then the updated FEM may be considered as the representative of the post-damaged structures. The fourth step is using the updated FEM, damage detection, assessment of loading-carrying capacity, seismic evaluation, etc. The above process may be facilitated by nondestructive inspection and by combining the static measurement and dynamic data. But the most important issue is to discern the damage locations and damage extents. It is also the most difficult task for structural evaluation. Enormous amount of work on vibration-based structural damage detection and evaluation has already been carried out. Nevertheless many of the proposed damage identification methods are still in the

stage of numerical simulations or the traditional laboratory “saw-out”.

The objective of this study is to address a new damage detection and diagnose method of highway bridges, based on modal parameters, such as frequencies, damping ratios, and Energy Transfer Ratios (ETR) index, as well as static data, such as deflections and strains. Contributions of present work mainly include summary of structural health monitoring system, theoretical base of measurement and signal treatment, theoretical studies on energy transfer ratio (ETR), establishment of wide-range measurement system, ambient and impact analysis, parameter identification and estimation, finite element calculation, and experimental verification. A more detailed chapter-by-chapter overview is given in the following.

Chapter 2 reviews the literature relevant to the methods used to detect and locate damage as well as to monitor structural health conditions.

Chapter 3 introduces the methods and procedures for bridge damage detection used in the research. Firstly, the theoretical foundation of measurement and signal processing are briefly summarized. Secondly, modified SDOF modal identification method in the frequency domain as well as the correlation method and traditional poly-reference identification method in the time domain are presented. Lastly, the basic theory of the modal Energy Transfer Ratio (ETR) and the foundation for the extraction of ETR are also illustrated in this chapter.

Chapter 4 discusses the design, construction, and testing conditions of a modal bridge. A 1:6 scaled model was designed and manufactured in the laboratory. Special consideration for the vibration testing is given to the following factors, namely, the effects of the added mass distribution, vehicular speed, window function for the analysis, and the excitation locations. FE modeling under different damage conditions is also presented and the calculation comparisons are illustrated.

Chapter 5 demonstrates the experimental results of model bridge damage detections. The static testing, the ambient testing, and forced vibration testing of the model bridge are discussed in this chapter. Two kinds of artificial damage, a bearing failure and girder deteriorations, are studied. Damage detections are conducted by using the changes of modal parameters and static parameters before and after damage are introduced. Damage detection by using ETR index is discussed and a summary, including advantages and disadvantages is presented.

Chapter 6 summarizes the conclusions of this research. Additionally, some unsolved problems and suggestions for future related damage detection and evaluation are mentioned.

Chapter 2

State-of-the-art Report of Bridge Health Monitoring

2.1 INTRODUCTION

Due to a wide variety of unforeseen conditions and circumstance, it will never be possible or practical to design and build a structure that has a zero percent probability of failure. Structural aging, environmental conditions, and reuse are examples of circumstances that could affect the reliability and the life of a structure. There are needs of periodic inspections to detect deterioration resulting from normal operation and environmental attack or inspections following extreme events, such as strong-motion earthquakes or hurricanes. To quantify these system performance measures requires some means to monitor and evaluate the integrity of civil structures while in service. Since the Aloha Boeing 737 accident that occurred on April 28, 1988, such interest has fostered research in the areas of structural health monitoring and non-destructive damage detection in recent years.

According to Housner et al. (1997), structural health monitoring is defined as "the use of *in-situ*, non-destructive sensing and analysis of structural characteristics, including the structural response, for detecting changes that may indicate damage or degradation". This definition also identifies the weakness. While researchers have attempted the integration of NDE with health monitoring, the focus has been on data collection, not evaluation. What is needed is an efficient method to collect data from a structure in –service and process the data to evaluate key performance measures, such as serviceability, reliability, and durability. So, the definition by Housner et al. (1997) should be modified and the structural health monitoring may be defined as "the use of *in-situ*, nondestructive sensing and analysis of structural characteristics, including the structural response, for the purpose of identifying if damage has occurred, determining the location of damage, estimating the severity of damage and evaluating the consequences of damage on the structures" (Fig. 1). In general, a structural health monitoring system has the potential to provide both damage detection and condition assessment of a structure.

Assessing the structural condition without removing the individual structural components is known as nondestructive evaluation (NDE) or nondestructive inspection. NDE techniques include those involving acoustics, dye penetrating, eddy current, emission spectroscopy, fiber-optic sensors, fiber-scope, hardness testing, isotope, leak testing, optics, magnetic particles, magnetic perturbation, X-ray, noise measurements, pattern recognition, pulse-echo, radiography, and visual inspection, etc. Most of these techniques have been used successfully to detect location of certain elements, cracks or weld defects, corrosion/erosion, and so on. The Federal Highway Administration (FHWA) sponsored a large program of research and development in new technologies for the nondestructive evaluation of highway bridges. One of the two main objectives of the program is to develop new tools and techniques to solve specific problems. The other is to develop technologies for the quantitative assessment of the condition of bridges in

support of bridge management and to investigate how best to incorporate quantitative condition information into bridge management systems. They hoped to develop technologies to quickly, efficiently, and quantitatively measure global bridge parameters, such as flexibility and load-carrying capacity. Obviously, a combination of several NDE techniques may be used to help assess the condition of the system. They are very important to obtain the database for the bridge evaluation. But it is beyond the scope of this review report to get into details of local NDE.

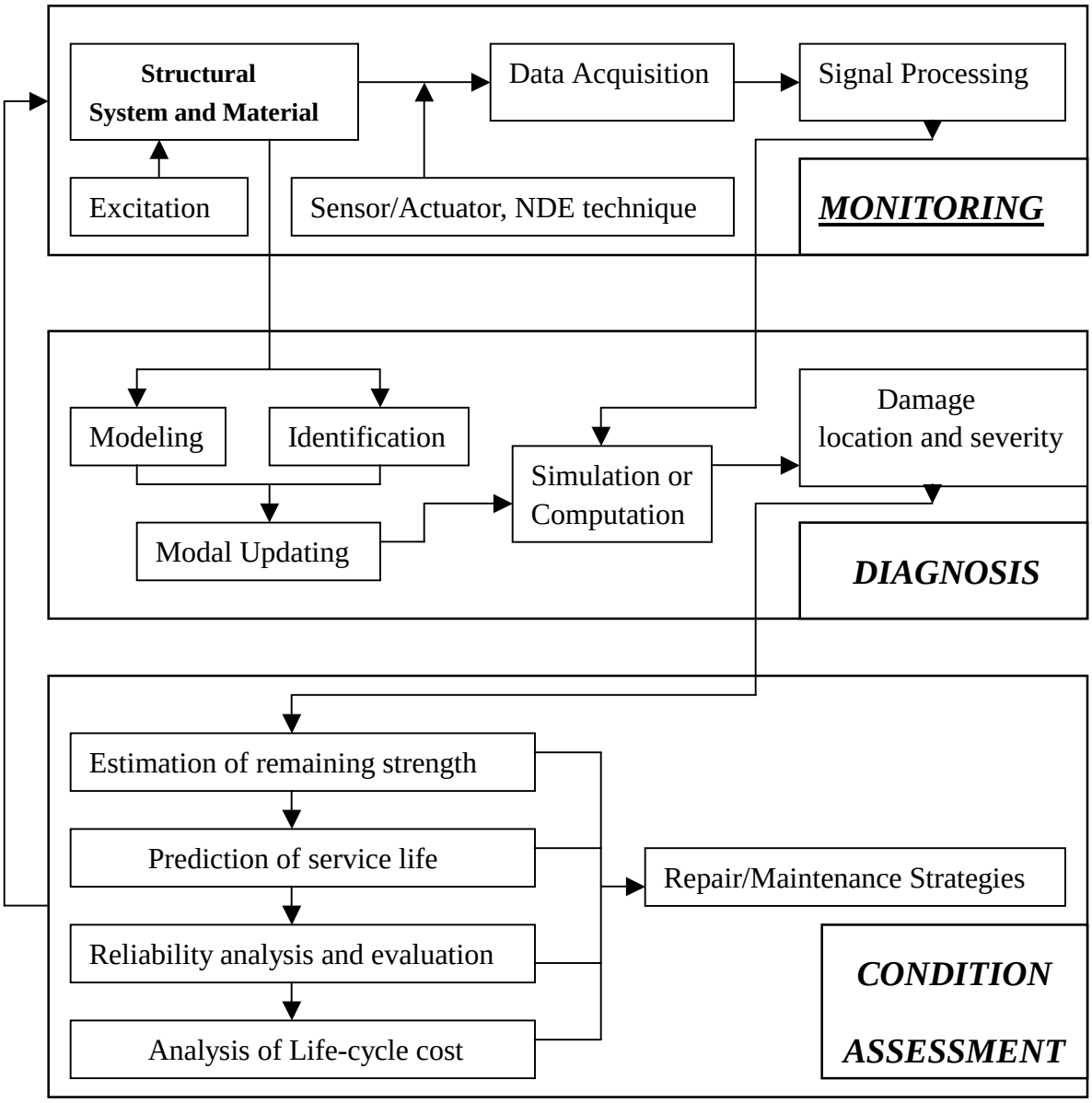

Fig 2.1 Basic Components of Structural Health Monitoring System.

Health monitoring techniques may be classified as global and local. Global attempts to simultaneously assess the condition of the whole structure whereas local methods focus NDE

tools on specific structural components. Clearly, two approaches are complementary to each other. All such available information may be combined and analyzed by experts to assess the damage or safety state of the structure.

Structural health monitoring research can be categorized into the following four levels: (I) detecting the existence of damage, (II) finding the location of damage, (III) estimating the extent of damage, and (IV) predicting the remaining fatigue life. The performance of tasks of Level (III) requires refined structural models and analyses, local physical examination, and/or traditional NDE techniques. To perform tasks of Level (IV) requires material constitutive information on a local level, materials aging studies, damage mechanics, and high-performance computing. With improved instrumentation and understanding of dynamics of complex structures, health monitoring and damage assessment of civil engineering structures has become more practical in systematic inspection and evaluation of these structures during the past two decades.

Most structural health monitoring methods under current investigation focus on using dynamic responses to detect and locate damage because they are global methods that can provide rapid inspection of large structural systems. These dynamics-based methods can be divided into four groups: (1) spatial-domain methods, (2) modal-domain methods, (3) time-domain methods, and (4) frequency- domain methods. Spatial-domain methods use changes of mass, damping, and stiffness matrices to detect and locate damage. Modal-domain methods use changes of natural frequencies, modal damping ratios, and mode shapes to detect damage. In the frequency domain method, modal quantities such as natural frequencies, damping ratio, and model shapes are identified. The reverse dynamic system of spectral analysis and the generalized frequency response function estimated from the nonlinear auto-regressive moving average (NARMA) model were applied in nonlinear system identification. In time domain method, system parameters were determined from the observational data sampled in time. It is necessary to identify the time variation of system dynamic characteristics from time domain approach if the properties of structural system change with time under the external loading condition. Moreover, one can use model-independent methods or model-referenced methods to perform damage detection using dynamic responses presented in any of the four domains. Literature shows that model independent methods can detect the existence of damage without much computational efforts, but they are not accurate in locating damage. On the other hand, model-referenced methods are generally more accurate in locating damage and require fewer sensors than model-independent techniques, but they require appropriate structural models and significant computational efforts. Although time-domain methods use original time-domain data measured using conventional vibration measurement equipment, they require certain structural information and massive computation and are case sensitive. Furthermore, frequency- and modal-domain methods use transformed data, which contain errors and noise due to transformation. Moreover, the modeling and updating of mass and stiffness matrices in spatial-domain methods are problematic and difficult to be accurate. There are strong development trends that two or three methods are combined together to detect and assess structural damages. For example, several researchers combined data of static and modal tests to assess damages. The combination could remove the weakness of each method and check each

other. It suits the complexity of damage detection.

Structural health monitoring is also an active area of research in aerospace engineering, but there are significant differences among the aerospace engineering, mechanical engineering, and civil engineering in practice. For example, because bridges, as well as most civil engineering structures, are large in size, and have quite low natural frequencies and vibration levels, at low amplitudes, the dynamic responses of bridge structure are substantially affected by the nonstructural components, and changes in these components can easily to be confused with structural damage. Moreover, the level of modeling uncertainties in reinforced concrete bridges can be much greater than in the single beam or a space truss. All these give the damage assessment of complex structures such as bridges a still challenging task for bridge engineers. Recent research and implementation of structural health monitoring and damage assessment are summarized in the following sections.

2.2 LABORATORY AND FIELD TESTING RESEARCH

In general, there are two kinds of bridge testing methods, static testing and dynamic testing. The dynamic testing includes ambient vibration testing and forced vibration testing. In ambient vibration testing, the input excitation is not under the control. The loading could be either micro-tremors, wind, waves, vehicle or pedestrian traffic or any other service loading. The increasing popularity of this method is probably due to the convenience of measuring the vibration response while the bridge is under in-service and also due to the increasing availability of robust data acquisition and storage systems. Since the input is unknown, certain assumptions have to be made. Forced vibration testing involves application of input excitation of known force level at known frequencies. The excitation manners include electro-hydraulic vibrators, force hammers, vehicle impact, etc. The static testing in the laboratory may be conducted by actuators, and by standard vehicles in the field-testing. A brief description of the laboratory and field-testing research on the damage assessment is given below.

Bakht and Jaeger (1990) summarized the valuable lessons learned form static and dynamic testing of more than 225 bridges in Ontario, Canada. They found that: (1) slab-on-girder bridges are stiffer than the corresponding calculated values; and (2) the floor systems of steel truss bridges may contribute substantially of the combined stiffness of the structure. In most cases, the actual load-carrying capacities are higher than those from calculations.

Kennedy and Grace (1990) investigated the dynamic and fatigue response of continuous composite bridges with prestressed concrete slabs. Four ¼-scale models of continuous composite bridges were tested. It was shown that prestressing the concrete deck slab in the vicinity of the pier supports eliminated transverse cracking of the slab, enhanced the natural frequencies, and increased the fatigue life as well as the ultimate load-carrying capacity.

Mazurek and DeWolf (1990) conducted ambient vibration tests of a two-span aluminum plate-girder bridge in the laboratory. They used low-mass vehicular excitation and found that the ambient vibration method provided approximately the same resonant frequencies and mode shapes as those used modal analysis.

Hearn and Testa (1991) applied a perturbation method to structural inspection through vibration monitoring. They found that changes in modal frequency and damping can be good damage indicators; and demonstrated the effectiveness of this method by testing a welded four-member steel frame with progressive cracks. They found that modal parameters (except mode shapes) could be used effectively to detect damage in these test structures

Hogue, Aktan, and Hoyos (1991) carried out a impact excitation test on local region of an 262m long, prestressed, pretensioned concrete girders bridge. Modal parameters except for damping ratios were identified, then the mass matrix was estimated, and then the flexibility matrix was derived. A static test was conducted to validate the dynamic test-based identification.

Aktan, et al. (1997, 1998, 1999, and 2000) proposed a coordinated, multi-disciplinary approach that integrated field, theoretical and laboratory research for solving large system identification problems. A 3-span steel bridge testing in field and its physical model testing in the laboratory were conducted for the damage detection. The studies indicated that modal flexibility provided a relevant/reliable measure of structural state. Also many experiences, observations, as well as challenges were summarized.

Pandey and Biswas (1994) used a simple supported W12×16 beam for experimental verification. The beam had a splice at the mid-span. Damage was simulated by opening bolts from the splice plates. Thirty-three measurement points were marked up on the top of the beam. They demonstrated the effectiveness of using changes in the flexibility matrix in detecting and locating damages.

Salawu and Williams (1995) conducted full-scale forced-vibration tests before and after structural repairs on a multi-span reinforced concrete highway bridge. A hydraulic actuator was used to excite the bridge, and four servo-accelerometers were used to measure the bridge response. They found that: (1) the natural frequencies did not change significantly due to structural repairs; and (2) the modal assurance criterion and the coordinate modal assurance criterion values were found to be good indicators of the presence and location for condition assessment of the bridge. The modal analysis gave an indication of the location of the repairs. They recommended more experimental work for condition assessment of the bridge.

Farrar et al. (1994 and 1996) has done extensive testing of damage detection methods on the Alamoso Canyon Bridge in New Mexico. Both forced and ambient vibrations were measured using a very dense array of accelerometers. Modal parameters were extracted using linear signal processing techniques and compared with those calculated using a detailed finite-element model. One of the important outcomes of this experiment was a study of the variability of various modal parameters and an attempt to quantify the statistical significance of parameter changes.

Duron, Ozisik, and Rubin (1995) conducted ambient tests of a span of the Benica-Martinez Bridge in California. The steel truss bridge was built in 1960. The test span has a 350-ft center segment. 36 accelerometers were installed in the upper and lower chords of this truss span. The measurements were used to condition assessment.

Sanayei, Imbaro, et al. (1997) used the static data of experiments on a small scale steel frame model to support the proposed approach of parameter estimation. The model used for testing is a two-story, one-bay scale steel frame. Height of each story is 350mm for a total height

of 700mm, the length of the bay is 600mm. Vertical and lateral loads are applied by hanging weights directly on the frame or with pulleys mounted to the test frame. The displacement and strain were measured at critical sections. A larger steel frame model was tested by **Shi, Law and Zhang (2000)**. They investigated changes of modal strain energy before and after damage. The damage was simulated by removing top- and seat-angles at the joints. B&K 4370 accelerometers and B&K 9202 force hammer are used to collect the vibration information. Results indicated that the presented method was effective in localizing damages, but it is noise sensitive in the damage quantification, especially in the multiple damage quantification.

Doebling, Hemez, et al. (1997) employed vibration tests of a scale suspended truss to prove that a mode selection strategy based on maximum modal strain energy produces more accurate update results than a strategy based on minimum frequency. The truss consisted of eight bays, with a span of 4m. Eight lumped masses connected to it. They made the truss as an appropriate representation of large spacecraft structures such as International Space Station Alpha. Similar tests were also conducted by **Kosmatka and Ricles (1999)**. Their experimental results showed that the proposed method in conjunction with residual forces and a weighted sensitivity analysis could accurately predict the location and severity of stiffness as well as any changes in mass for different damage scenarios.

Sennah and Kennedy (1997 and 1998) presented the dynamic characteristics results from an extensive parameter study on the free vibration and forced vibration of simply supported, two or three-span continuous, straight and curved, composite multi-cell box girder bridges. These results are helpful to the damage detection study on the composite bridges by vibration modal testing.

Chen, Yang, et al. (1999) tested a full-scaled beam both statically and dynamically. They focused on the correlation between frequency of a structure and degree of damage. Test results have confirmed that the frequency of the beam itself depends on the load history while that of the beam plus sufficient preloads can be identified independently. This was because preloads can keep cracks open so that the cracked beam vibrates in a linear fashion.

Zhang, Q.W. (1999) investigated the behaviors of a T-shape rigid bridge under vehicle loading and ambient vibration. The results from dynamic evaluation based on the system identification assorted with the analysis results from the static data. He found that different modal updating methods had different application scope, especially where lot of elements occurred damage. And the effective of nonstructural components should be considered in the FE model.

Lee and Liang (1999) have developed a portable system integrated with necessary computer software and measurement hardware, such as sensor and data-acquisition systems for bridge condition assessment. They have established the viability of using this system through a 1:6 down scaled model bridge. The bridge model is a typical 40in wide concrete slab supported by three single span parallel steel girders with a span of 8ft. On the slab, a total 16 measurement points were chosen. Ambient excitations were used for the modal testing, which is generated by pulling a model car along the bridges. The results showed that the energy transfer ratio (ETR) is a good indicator of structural damage. Ambient and impact tests on three full scaled bridges were

also carried out. Since no real damage existed in these bridges and therefore no notable changes presented in the measured parameters.

Huang, Yang, et al. (1999) presented a simple and effective procedure for conducting the free vibration test on the highway bridges. The feasibility of the procedure was demonstrated in identification of the dynamic properties of a three-span box-girder concrete bridge Using ITD technique. **Huang and Lin (2001)** also used the ARV model to identify the dynamic characteristics of a structural system.

Cui, F. (2000) conducted a static testing on a scale truss, which was made of organic glass. Damage was simulated by reduction of member areas. He used strains of members to demonstrate the algorithms of damage identification.

Chaudhary, Abe, et al. (2000) utilized the strong seismic records in the 1995 Kobe earthquake to examine the performance of various components of two base-isolated bridge, based on the method of parameter identification. It is shown that the identified system parameters could reveal useful information about the performance of the isolation system as well as about different substructure components.

Hwang, Jernigan and Lin (2000) presented a procedure for the evaluation of the expected seismic damage to bridges and highway systems in Memphis and Shelby County, Tenn. The bridge damage states considered were no/minor damage, repairable damage, and significant damage. Given an earthquake with a moment magnitude of 7.0, the expected damage to bridges and highway systems was determined. The results could be used to prioritize bridges for retrofitting, to prepare a pre-earthquake preparedness plan, to develop a post-earthquake emergency response plan, and to assess the regional economic impact from the damage to highway transportation systems.

Haritos, N. (2000) introduced the several years of experience in the dynamic testing on bridge superstructures for the structural system identification at the university of Melbourne, Australia. They developed a modal testing package by using simplified experimental modal analysis and time –domain identification method. A number of bridges were tested and analyzed using this package.

Shah, Popovics, et al. (2000) reported basic findings from several laboratory-based nondestructive evaluation techniques for the concrete infrastructure. The described techniques were based on measurements of mechanical waves that propagate in the concrete. Vibration frequencies were shown to be sensitive to the presence of fatigue-induced cracking in concrete small specimens; changes in the vibration frequency of a concrete specimen fatigue tests were related to the remaining fatigue life of the tested beam. Future effort will be directed toward practical application of the techniques to monitor the conditions of existing concrete structures.

Zhuo, W.D. (2000) studied the seismic behavior of simple supported bridge with FRP confining RC columns by shaking table tests. Different levels of input peak ground acceleration were assigned 10%, 15%, 20%, ……, of EL Centro (NS) earthquake ground motion until the failure of column occurred. The test data will be used to illuminate the proposed approach in this study.

Piombo, Fasana, et al. (2000) described the dynamic tests performed on a simply

supported bridge with a span of 20m in Northern Italy under traffic excitation. The acceleration data had been used for the identification of the natural frequencies, viscous damping ratios and mode shapes of the bridge. Modal parameters had been extracted using the wavelet estimation technique. This work represented the first attempt in using the wavelet estimation technique directly on transient data and nor on the impulse response estimates obtained via the random decrement technique.

Kim and Bartkowicz (2001) designed and built a ten-bay hexagonal truss to simulate the current space station truss sections. Modal tests were performed on this laboratory structure partially instrumented with 96 accelerometers in several damage conditions. A time-domain modal identification technique was used to extract frequencies and mode shapes from the test data. A two-step damage detection approach was developed and showed promise for large structures with limited instrumentation. Because the proposed approach is a global NDE method which uses vibration measurements and, therefore, it is limited to identifying structural damages. Several damage cases were determined to be unidentifiable.

Halling, Muhammad, and Womack (2001) carried out seven forced vibration tests on an isolated single span of a freeway overpass structures. The work focused on horizontal vibration utilizing an eccentric mass shaking machine and the data was collected with an array of accelerometers. Finite-element models were created to simulate the structure. It was shown that the structural parameters optimized from the algorithm could be used to identify the estimated location and intensity of the damage or retrofit of the structure at each state.

Mirmiran and Wei (2001) employed Ultrasonic Pulse Velocity (UPV) to assess the extent and progression of damage in FRP-encased concrete. They found that the UPV damage index had a much better resolution for stress ratios and the volumetric strains after confinement was activated. A comparison of the UPV damage index with the normalized acoustic emission counts revealed that the two methods had different sensitivities at different stages of loading and could potentially complement each other as a hybrid damage assessment tool.

Peeters and Roeck (2001) conducted one-year monitoring of the Z24-Bridge in Switzerland under ambient vibrations. They presented a method to distinguish normal eigen-frequency changes form the environmental effects, such as wind and temperature, on damage events. Further research will focus on a description of the non-linear behavior so that safety statements about bridge in cold period will be made.

Sikorsky, Stubbs, Bolton, and Seible (2001) described the integration of a non-destructive damage detection method with an on-site data acquisition system to remotely monitor a conventional concrete slab bridge and a composite bridge utilizing CFRP and GFRP and evaluate their performance. Preliminary results were also provided.

The IASC-ASCE (the International Association for Structural Control and the Dynamic committee of ASCE Engineering Mechanics Division) SHM task group (founded in 1999) is developing a series of benchmark SHM problems, beginning with a relatively simple problem and proceeding on to more realistic but more difficult problems, to evaluate the potential for this technology for civil engineering structures. Phase I **(Johnson, Lam, et al. 2000)** focused on health monitoring strategies that were applied to data generated with an analytical model of the

benchmark structure, which is 2-bay by 2-bay, 4 story steel frame structure. A total of six cases were considered to evaluate various structural health monitoring approaches for pure translational motion, coupled torsional and translational motions, and incomplete sensor information. The structure was damaged by removing the stiffness contributions of various structural members. Phase II **(Dyke, Bernal, Beck, Ventura, 2001)** considers the application of these techniques to data that is obtained experimentally. The steel frame structure used in Phase I was also used as the test specimen. The damage was simulated by removing bracing within the structure. An electromagnetic shaker and mass on the top of the structure was used to excite the structure. Accelerometers are placed throughout the structure to provide measurements of the structural responses. The task is still on the way.

The degradation of the reinforced concrete (RC) structures is a major problem in many countries. **Imbabi, Famiyesin, Tan (2001)** developed a promising method to monitor and evaluate the integrity and the strength of RC slab. The $1/3^{rd}$ –scaled slab panels were subjected to increasing point load increments at the mid span to induce damage, and unloaded at intervals to facilitate measurements of dynamic response. The resulting deflections, strains, and accelerations were recorded for each load increment, corresponding to a unique damage state. The static and dynamic response data were used to assess the strength and integrity.

From above, we can distinguish that (1) the models in the laboratory are mainly beams, columns, truss and/or frame structures; (2) the location and severity of damage in the models are determined in advance; (3) the testing has demonstrated lots of performances of damage structures; (4) the field-testing and damage assessment of real bridges are more complicated than the models in the laboratory; and (5) the correlation between the damage indicator and damage type, location, and extent still needs further improvement.

2.3 ANALYTICAL DEVELOPMENT

The bridge damage diagnosis and health monitoring are both concerned with two fundamental criteria of the bridges, namely, the physical condition and the structural function. In terms of mechanics or dynamics, these fundamental criteria can be treated as mathematical models, such as response models, modal models and physical models. Instead of taking measurements directly to assess bridge condition, the bridge damage diagnosis and monitoring system evaluate these conditions indirectly by using mathematical models. The damage diagnosis and health monitoring are active areas of research in recent years. For example, numerous papers on these topics appear in the proceedings of International Modal Analysis Conferences (IMAC) each year, in the proceedings of International Workshop on Structural Health Monitoring (once of two year, at Standford University), in the proceedings of European Conference on Smart materials and Structures and European Conference on Structural Damage Assessment Using Advanced Signal Processing Procedures, in the proceedings of World Conferences of Earthquake Engineering, and in the proceedings of International Workshop on Structural Control, etc.. There are several review papers to be referenced, for examples, **Housner et al. (1997)** provided an extensive summary of the state of the art in control and health

monitoring of civil engineering structures. **Salawu (1997)** discussed and reviewed the use of natural frequency as a diagnostic parameter in structural assessment procedures using vibration monitoring. **Doebling, Farrar, et al. (1998)** presented a through review of the damage detection methods by examining changes in dynamic properties. **Zou, Tong, and Steven (2000)** summarized the methods of vibration-based damage and health monitoring for composite structures, especially in delamination modeling techniques and delamination detection.

2.3.1 Signature Analysis and pattern Recognition Approaches

A modal model is characterized by a set of modal parameters, which can be extracted from response model by modal testing techniques. Traditionally, the major modal parameters are natural frequencies, damping ratios, and mode shapes. The modal model can be also used as a vibrational signature. For example, in mechanical engineering condition monitoring of rotating equipment is typically based on the looking for signature changes in a power spectrum of the measured vibrations. The same nonparametric approach could be used for civil structures, but it is more typical to use identified modal parameters to provide the signature characterizing the structure. In order not only to detect damage but to also locate its position, observed changes in the signature must be compared with a database of possible changes and the most likely change must be selected. This is a type of pattern recognition where the database of " pattern " is generated by analyzing various damage scenarios or " failure modes ". The representative researches on damage detection through a modal model are listed briefly in the following.

One approach to detect damage has been to use changes in the modal frequencies. With fibre-reinforced plastics, **Adams, et al. (1978)** demonstrated that damage can be detected from a decrease in natural frequencies and in an increase damping. **Biswas, Pandey, and Samman (1990)** performed experiments on a highway bridge and demonstrated that the decrease in natural frequencies can be used to detect the presence of damage. **Hassiots and Jeong (1995)** introduced a method to identify the localized reductions in the stiffness of a structure, using changes of natural frequencies only. **Capecch and Vestroni (1999)** addressed the problem of understanding when it is sufficient to measure and use only natural frequencies, thus avoiding the need to measure modal shapes in vibration beams, or beam systems. The identification procedure was based on the minimization of an objective function that accounts for the difference between the analytical and experimental quantities. Further study demonstrated that the observed changes in natural frequencies, especially the changes in fundamental natural frequencies, were unable to determine the location of crack damage (**Casas, et al. 1995)**. This occurs because a certain amount of damage at two different locations may produce the same amount of frequency change.

Sensitivity analysis has been proposed to improve the sensitivity of natural frequency change to the structural damage **(Hearn and Testa, 1991)**. The basic idea behind this was to compare the frequency changes obtained from experimental data collected on the structural with the sensitivity of the modal parameters obtained from an analytical FE model of the structure. Accuracy of sensitivity-based methods is dependent on the quality of the FE model used to computer the sensitivities. It should be kept in mind that obtaining an accurate analytical model in itself remains a difficult task. The uncertainties of analytical model may influence the results

of damage detection.

Results from some experimental and numerical studies have suggested that the lower vibration modes would probably be suited for damage detection. Using the information from the mode shapes, **Stubbs et al. (1995)** reported a method to localize damage by using the pattern recognition method. They studied a beam model with known mode shapes, and then generated mode shapes at any location using interpolation. The location of damage compared fairly well with FE analysis. Finally, they applied this method to the real bridges including a 163-ft-plate girder bridges and a two-span simply supported truss bridges (the length of each span is approximately 201-ft), and in general concluded that the method can accurately locate damage though the damage pattern was not quite distinctive.

The combination of different modal parameters, especially the combination of natural frequency and mode shapes has been used by several researchers. **Mazurek and DeWolf (1990)** found that crack propagation in a beam can cause substantial shifts in certain frequencies and mode shapes can be use to locate the damage. With the help of analytical beam models, **Pandey et al. (1991)** demonstrated the use of changes in the curvature mode shapes to detect and locate damage. **Wahab and Roeck (1999)** introduced a damage indicator called " curvature damage factor", in which the difference in curvature mode shape for all modes can be summarized in one number for each measured point. They applied the techniques to a real prestressed concrete bridge, named Z24, which crosses the highway A1 between the Bern and Zurich in Switzerland.

Another combination in terms of natural frequencies, mode shapes, and modal assurance criteria (MAC) was employed by **Alampalli, Fu, and Aziz (1992)** on a scale bridge model test. The authors concluded that natural frequencies should be used to detect damage, and mode shapes and MAC values can be further used to identify damage locations.

Lee (1995) compared the transfer function parameter change of the tested system to detect damage and locate the position by using a few of sensors. **Zhang, Schulz, and Ferguson (1999)** employed the transmittance functions (TFs) and the sensor-actuator system to detect, locate and assess damages on a composite beam. Further work was underway to use sequential TFs to detect damage on large panel and blade structures using a dense pattern of measurements formal scanning laser Doppler vibrometer.

This kind of vibraional signature analysis has been proven to be successful in localizing damage. However, it is not sensitive to most types of damage that occur to bridge structures. Model testing and field-testing have shown that the changes of natural frequencies due to local damage are very small, mode shapes (especially higher mode shapes) are sensitive to the changes of local stiffness but it is very difficult to measure them accurately. There are similar problems in other vibration signatures, such as mode shape curvature, modal flexibility, MAC, etc. None of these can provide sufficient information for the detection of both small and large defects. The successful applications of these modal model methods may rely on the development of test techniques and new findings of model-based approaches.

2.3.2 Model Updating and System Identification Approaches

2.3.2.1 System Identification Approaches

System identification (SI) is the process of constructing or updating an accurate mathematical model of a system based on input and output (I/O) observations. Among other applications, SI can be applied to structural health monitoring and damage assessment, e.g., by determining the structural stiffness values and comparing them with previously determined values or originally intended values. Research interest in this subject area has increased steadily over the years. In the context of civil engineering structures, **Caravani, Waston, and Thomson (1977)** were among the first to carry out SI study by means of a recursive least-square algorithm. **Carmichael (1979)** presented two case study of state estimate to illustrate the use of the Kalman filter and the extended Kalman filter(EKF). **Yun and Shinozuka (1980)** applied two SI algorithms, namely, the EKF and iterated linear filter-smoother, to identify the hydrodynamic coefficient matrices for an offshore structure problem. **Hoshiya and Satio (1984)** proposed a weighted global iteration algorithm to improve the convergence characteristics of the EKF process. This method was subsequently applied in the study of a running load on a beam by **Hoshiya and Maruyama (1987). Yun et al. (1988)** identified the structural parameters of a damage bridge structure by the EKF. More recently, **Sato and Qi (1998)** developed another bridge structure by the EKF. They also developed another filter-based SI approach by incorporating a memory fading function. Other recent research works include **Wang and Haldar (1994), Ghanem and Shinozuka(1995), Cobb and Liebst(1997), Herrmann and Pradlwarter (1998), and Quek, et al. (1999).**

Most of the SI studies in structural engineering have dealt with few degree of freedom (DOFs) and few unknown structural parameters. In practice, however, modeling of engineering structures often requires the contrary. The difficulty and the computational effort required for convergence increase drastically when the numbers of DOFs and unknowns increase. To this end, various means have been proposed in recent years to tackle the numerical problems generally associated with SI of large systems. **Koh et al. (1991)** formulated a sub-structural identification method to improve the convergence performance by decomposing the structural system into several smaller subsystems. Other research works adapting the sub-structuring approach include those by **Oreta and Tanabe (1994) and Yun and Lee (1997).** In another attempt towards overcoming computation difficulty for structures with relatively large number of DOFs, **Koh et al. (1995 a. b)** developed an improved condensation method suitable particularly for multistory frame buildings. With similar objective, **Hermann and Pradlwarter (1998)** proposed a two-step identification approach in time domain for finite-element models with a substantial number of DOFs. **Kim and Bartowics (1997 and 2001)** also developed a two-step damage detection and health monitoring approach for large and complex structures with a limited number of measurements. The first step is initial damage detection, based on the optimal-updating techniques and changes of stiffness. The second is detailed damage detection by the design sensitivity method and linear perturbation theory.

In all the above-mentioned works, classical SI techniques were used, such as EKF, recursive least squares, instrumental variable and maximum likelihood methods, These methods, in one way or another, search the optimal solution by exploiting the previous solution. Treating the

problem as an inverse problem, many classical methods require the use of secant, tangent, or higher-order derivatives of the objective function. As the system of unknowns grows in size, the numerical difficulty increases and often to the extent that the convergence becomes extremely difficult, if not impossible. Such "exploitation" methods perform point-to-point search and have the danger of converging to local optima. On the other extreme, a random search (e.g. trial-and-error) may be used to explore the entire search space. To overcome one trial solution with another, an error norm has to be defined as a measure of deviation of the estimated response (computed based on the estimated parameters) from the actual (measured) response. The search continues until the error norm is deemed to be small. Such a blind "exploration" strategy is obviously too time consuming for large systems due to huge number of possible combinations. For instance, if there are ten unknowns to be identified and each unknown is divided into 100 discrete values within its search range, there will be a total of 10^{20} possible combinations—an astronomical figure to work with even for today's powerful computers.

In this regard, a worthwhile attempt is to employ evolutionary algorithms, which have proved in the last decade to be a powerful search and optimization tool. The main features of these algorithms are that they attempt to imitate living things and are stochastic in nature. There are presently four main approaches, namely, genetic algorithms (GA)、evolutionary programming, evolutionary strategies, and simulated annealing. By far the most widely known approach in engineering is perhaps GA. This approach was developed to solve discrete or integer optimization problems as opposed to continuous parameter optimization problems. In the case of parameter identification, this can be tuned into an advantage of controlling the resolution of identified parameters through the (integer) length of the chromosome (number of bits). **Koh, Hong, and Liaw (2000)** conducted a GA search in modal domain of a much smaller dimension than the physical domain. The objective function was defined based on the estimated modal response in time domain and the corresponding modal response transformed from the measured response. This method had been shown to work well in terms of mean error (10-15%) for a fairly large system with 50 DOF's and 52 unknown parameters. **Hao and Xia (2002)** applied a genetic algorithm with real number encoding to identify the structural damage by minimizing the objective function, which directly compares the changes in the measurements before and after damage. Three different criteria are considered, namely, the frequency changes, the mode shape changes, and a combination of two. A laboratory tested cantilever beam and a frame are used to demonstrate the proposed techniques, Numerical results show that the damage elements can be detected by GA, even when the analytical model is not accurate.

Structural system identification within the linear regions has been well developed and many techniques have been applied to structural damage assessment. However, the question of whether a structure is still linear after the damage remains. This is very important because the dynamical behavior of a nonlinear system can be quite different from those of its associated linear system. Also if the structural system becomes nonlinear after damage, its dynamical characteristics cannot be estimated by using the linear system identification methods. **Wang and Chen (2000)** have made an attempt to develop methods for the identification of highly localized structural damage in weak nonlinear structures. The damage was defined as either a reduction of stiffness

or a change of restoring force characteristics. The location vector method (LVM) was applied to identify the location and type of damage. The Fast Fourier transform (FFT) and the least-squares method were used to quantify the damage. **Masri et al. (1993, 1996, and 2000)** employed the neural network to detect the changes in nonlinear systems. **Chong and Imregun (2000)** formulated a frequency-domain modal analysis technique that was applicable to weakly non-linear multi-degree of freedom systems. One of the advantages of the method was the ability to determine the response of the non-linear system at any level once its variable modal parameters had been identified at some reference force level. The authors also presented the experimental verification and the application to a representative engineering case. **Lin, Betti, Smyth, and Longman (2001)** presented an adaptive on-line parameter identification algorithm based on the variable trace approach for the identification of non-linear hysteretic structures. At each time step, this recursive least-square-based algorithm upgrades the diagonal elements of the adaption gain matrix by comparing the value of the estimated parameter between two consecutive time steps. The effectiveness and efficiency of the proposed algorithm was shown by considering the effects of excitation amplitude, of the measurement units, of larger sampling time interval and of measurement noise. **Kerschen and Golinval (2001)** investigated the vibrations of a clamped beam for two different kinds of non-linearity. Firstly, the beam showed a non-linear behavior characterized by a piecewise linear stiffness and secondly, the non-linearity came from a bilinear stiffness. They demonstrated the performance of the restoring force surface method and presented both numerical and experimental results. Obviously, the nonlinear system identification will be developed by many researchers in the not too far future.

When performing vibration tests on civil engineering structures, such as bridges, it is often unpractical and expensive to use artificial excitation (shakers, drop weights). Ambient excitation on the contrary is freely available (wind, traffic). This output-only system identification now becomes more and more important. **Peeters and Rock (1999)** proposed a stochastic subspace identification method. The proposed algorithm was validated with real vibration data from a steel mast excited by wind load. **Huang and Liu (2001)** applied a subspace approach cooperating with an instrumental variable concept to evaluate the coefficient matrices of a state-space model. The dynamic characteristics of a structure are determined from the coefficient matrices. The feasibility of the procedure is demonstrated through processing an in situ ambient vibration measurement of a five-story steel frame, an impulse response measurement of a three-span continuous bridge, and simulated earthquake responses of five-story steel frames from shaking table tests.

Although the regularization increased the popularity of parameter identification due to its capability of deriving a stable solution, the significant problem is that the solution depends upon the regularization parameters chosen. **Furukawa (2001)** presented a technique for deriving solutions without the use of the parameters and, further, an optimization method, which can work efficiently for problems of concern. Numerical examples show that the technique can efficiently search for appropriate solutions. **Zhang, et al. (2002)** developed a generalized model of differential hysteresis which contains 13 control parameters. Three identification algorithms are developed to estimate the control parameters for different classes of inelastic structure. These

algorithms are based upon the simplex, extended Kalman Filter, and generalized reduced gradient method. Novel techniques such as global search and internal constraints are incorporated to facilitate convergence and stability. Effectiveness of the devised algorithms is demonstrated through simulations of two inelastic systems with both pinching and degradation characteristics in their hysteretic traces.

In structural system identification, different mathematical models will introduce different explanations on the result of identification even with the same set of input/output data. The model inaccuracy in structural system identification can be categorized into two items: (1) the uncertainty due to nonlinear model; and (2) the completeness of model description (or extract description). Selecting the exact model becomes one of the important issues for identification.

2. 3.2.2 Model updating and Mode Selection

A common theme in using system identification for structural health monitoring and damage diagnosis is to use a model updating approach. Usually, highly accurate and detailed finite-element models (FEMs) are required to analyze and predict the dynamical behavior of complex structures during analysis and design. Once the finite-element model of a physical system is concentrated, its accuracy is often tested by comparing its modes of vibration and frequency response with those obtained from the physical system. If the correlation between the two is poor, then assuming that the experimental measurements are correct, the analytical model must be adjusted so that the agreement between the analytical predictions and the test results is improved. The updated model may then be considered a better representation of the physical structure than the initial analytical model. Any observed local decrease in the stiffness of the model is assumed to indicate the location and severity of damage in the monitored structure. The updated model can subsequently be used with reasonable accuracy to assess the stability and control characteristics and to predict the dynamical responses of the structure. The above process of correcting the system matrices is known as model updating.

The methods for FEM update that are used for NDE can be divided into in the following major categories: mode flexibility methods, optimal matrix update methods, sensitivity-based matrix update methods, eigen-structure assignment methods, changes in measured stiffness methods, and combined modal parameters methods, etc.. All of these FEM update techniques require that the user select a subset of the measured modes to be correlated with the corresponding modes of the FEM. Normally, the first few modes of the structure are used in the FEM correlation because they generally the best identified modes. However, in some situations the higher frequency modes are critical to the location of structural damage, and so it is necessary to include them in the set of modes for FEM correlation. Many modes that are below these in frequency do not undergo significant modification as a result of the damage, so that they contribute to the computational burden without contributing significantly to the location of the damage. The number of modes is limited not only by the computational burden, but also by the inherent ill conditioning and statistical bias associated with large-order update problems. Because of this limit, it is important to have systematic criteria for selecting which modes are most indicate of the structural damage. **Doebling, Hemez, et al. (1997)** utilized the MAC, mode

selection strategies and FE model update to detect damage. They found that a mode selection strategy based on maximum modal strain energy produced more accurate update results than a strategy based on minimum frequency. **Lardies and Larbi (2001)** also proposed a new method for model order selection and modal parameter estimation in time domain. The model selection is still a difficult problem to be studied.

2.3.2.3 Review of Damage Detection Methods

2.3.2.3.1 Statistical Analysis methods

FE modeling provides a complete set of analytical and theoretical modal parameters for a structure, but these parameters are usually of uncertainty accurate. The experimental data is accurate to some extent, but incomplete, and also intervolved by the noise. Any method to do modal updating must address the mismatch between the level of information in the detailed analytical FEM and the relatively sparse information. **Beck and Katafygiotis (1992 and 1997)** have presented a general Bayesian statistical approach, which treats the uncertainties that arise from measurement noise, modeling error, and possible non-uniqueness in the problem of updating the stiffness distribution. **Sohn and Law (1997 and 2000)** have recently extended this approach to multiple damage locations. **Vanik, Beck, and Au (2000)** used this approach to on-line monitoring, wherein specified modal parameters are identified on a regular basis and the probability of damage for each substructure is continually updated. **Philip and Lee (2000)** developed new approaches that used two set of measured frequency response data to update the analytical system mass and stiffness parameters in order to improve the agreement between the dynamical behaviors of the analytical and actual systems. The algorithm adjusted model without iteration.

Papadopoulos and Garcia (2001) presented a probabilistic approach, which examined the eigenvalue problem from a statistical standpoint by considering eigenvalue and eigenvector uncertainty, along with a correlated analytical stochastic finite element model to assess the damage. The effectiveness of the proposed technique was illustrated using simulated data on a three-degree-of- freedom spring-mass system and on an Euler-bernoulli cantilever aluminum beam. **Katafygiotis, Yuen, and Chen (2001)** adopted a Bayesian probabilistic framework for modal updating and proposed a new probabilistic approach that used the statistic properties of an estimator of the spectral density to obtain expressions for the updated probability density function (PDF) of the modal parameters. Examples of SDOF systems and MDOF systems using simulated data were presented to illustrate the proposed method. **Sohn and Law (1997 and 2000)** employed a similar method to identify multiple damage locations of multistory frame structures and reinforced-concrete bridge column.

Yeo, Shin, Lee and Chang (2000) presented a reliable damage detection algorithm for framed structures, of which the stiffness properties can be explicitly expressed with those of members, by introducing a regularization technique for system identification, a parameter grouping technique for locating damaged members and overcoming the sparseness of measured data, a data perturbation method for obtaining statistical distributions of system parameters with

a set of noise-polluted measured data, and a statistical approach by a hypothesis test for damage assessment. Unlike most references focused on the different methods for extracting damage-sensitive features from vibration response measurements, **Sohn, czarnecki, and Farrar (2000)** took a statistical pattern recognition paradigm to quantifying the observed changes in these features. They employed various projection techniques such as principal component analysis and linear and quadratic discriminate operators with the SPC in an effort to enhance the discrimination between features from the undamaged and damaged structures. The primary objective of their study is to identify the existence of damage. **Sayyer and Rao (2000)** presented a general methodology for structural fault detecting using fuzzy logic, based on the monitoring the static, eigenvalue, and dynamic response. Fuzzy logic coupled with principles of continuum damage mechanics was used to identify the location and extent of the damage. This methodology represented a unique approach to damage detection that can be applied to a variety of structures used in civil engineering, machine and aerospace applications.

Xia, et al. (2002) proposed a statistical method with combined uncertain frequency and mode shape data for structural damage identification. The finite element model is updated by comparing the measured vibration data before and after damage occurs. The effects of uncertainties in both the measured vibration data and the finite element model are considered as random variables in model updating. The statistical variations of the updated finite element model are derived with perturbation method and Monte Carlo technique. The probabilities of damage existence in the structural members are then defined. The results between the calculation and testing show that all the damages are identified correctly with high probabilities of damage existence.

Model updating within a statistical framework appears to be a promising general approach to damage diagnosis and structural health monitoring of large civil structures in view of the inescapable data and modeling uncertainties. But many aspects require further research, including optimal location of sensors, the type of damage, which can be reliably detected and reliably located using a giving array of sensors on a structure, strategies for making decisions about possible damage and determining the corresponding probabilities of false alarm and missed alarms, etc..

2.3.2.3.2 Damage index Methods

Cawley and Adams (1979) proved that the ratio of the model frequency change between any two models is the function of the damage location only. The ratios were then used as damage indicators, which were calculated from a candidate set of assumed possible damage scenarios. The structural damage was then localized by comparing the predicted ratios with the ratios computed based on measured modal frequencies. **Friwell et al. (1994)** improved this method by statistic tool. **Kaouk and Zimmerman (1994)** developed a Eigen-structure Assignment Technique for locating the damage and then quantified the damage with minimum rank perturbation theory in a space truss structure in the laboratory. **Lim and Kashangaki (1994)** presented the concept of the best achievable eigenvectors as a damage indicator, which was computed based on the candidate set of assumed damage cases. Damage in a full-scale truss

structure was located from the differences between the best achievable eigenvectors and the measured modes. **Wahab and Roeck (1999)** introduced a damage indicator called “mode curvature damage factor” to detect damage of a real prestressed concrete bridge.

The modal flexibility involves functions of both the natural frequencies and mode shapes. Some researchers **(Raghavendrachar and Aktan (1992), Pandey amd Biswas (1994), DeWolf and Zhao (1998))** have found experimentally that modal flexibility can be a more sensitive parameter than natural frequencies or mode shapes along for structural monitoring and damage detection in bridges. **Zhao and DeWolf (1999)** studied theoretically the sensitivity by comparing use of natural frequencies, mode shapes, and modal flexibilities for monitoring. The results demonstrated that modal flexibilities are more likely to indicate damage than either natural frequencies or mode shapes.

Ivanovic, Trifunac, and Todorovska (1999) discovered the changes of the system natural frequency tend to be small in the early stage of damage, and therefore may be difficult to quantify, even from accurately processed recorded motions. Other difficulties arise from the non-uniqueness in the model representation. Unless the model accounts for the soil-structure interaction, and it ahs been carefully validated and calibrated, it is very difficult to identify the true causes and sources of observed non-linearity in the response. They suggested that the formation of damaged zones in structures could be monitored or identified via the delay in travel times of seismic waves through these zones. A preliminary analysis indicated that this method (1) can lead to detectable changes in the travel times of the waves passing through the areas known to have experienced damage, and (2) in its simplest form does not to require detailed modeling or analysis of soil-structure interaction. This approach needs further development and testing.

Shi, et al. (1998, 2000, and 2002) proposed using the ratio of change in model strain energy in each element as another damage indicator. The approach requires only the elemental stiffness matrix, the analytical mode shapes, and the incomplete measured mode shapes. The effect of analytical mode truncation, incomplete measured mode, and measurement noise in the damage detection were discussed. Results from the modal simulation and experiment with a two-story partial steel frame indicated that the presented method is effective in localizing damage, but it is noise sensitive in the damage quantification to some extent. **Mak and Law (2000)** also assessed structural damage by elemental modal strain changes ratios. **Law, et al. (1998, 2000, and 2001)** also employed the modal strain energy and neural network to assess the damage. In addition, **Shi et al. (2000)** presented a sensitivity and statistical-based method to localize structural damage by direct use of incomplete mode shapes. The method was an extension of the multiple damage location assurance criterion (MDLAC), developed by **Messina, et al. (1998),** by using incomplete mode instead of model frequency. In general, the damage detection strategy is localize the damage sites first by using incomplete mode shapes, and then detect the damage sits and extent again by using measured natural frequencies, which have a better accuracy than mode shapes.

Liang and Lee (1991) presented a new modal parameter, the energy transfer ratio (ETR), based on the complex damping theory, and they proved theoretically that ETR indicator could be much more sensitive to structural damage. **Kong (1996)** carried out the testing of the model

bridge under ambient excitation and the experimental results showed that the energy transfer ratio was a sensitive indicator of structural damage. Furthermore, **Huang (1997)** proposed a new process of modal parameter identification based on complex modal energy measurement (including the ETR index). The damage growth measurement was performed by using the proposed diagnostic technique based on ETR in large scale structures. The ETR index has been investigated through real steel bridge as a sensitive damage indicator, but the ETR have not been applied the concrete bridge structures.

Lee (1995) and Caicedo, et al. (2000) proposed a method to identify the location of damage in civil engineering structures, which is based on changes in the component transfer functions of the structure, or the transfer functions between the floors of a structure. Multiple damage locations can be identified and qualified using the proposed approach. Experimental verification of this approach using a four-story frame structure in the Washington University Structural Control and Earthquake Engineering Lab was also provided.

Wang, et al. (2000) presented a comparative study of applying various mode-based indices to the structural damage detection of the Tsing Ma suspension bridge with a main span of 1377m and an overall length of 2160m. Five mode-based damage indices, including coordinate modal assurance criterion (COMAC), enhanced coordinate modal assurance criterion (ECOMAC), mode shape curvature (MSC), and modal strain energy index (MSEI), and modal flexibility index (MFI) are applied respectively for the damage location identification of various simulated damage scenarios in the bridge by 3D finite element method. The numerical simulation results show that the applicability and the performance of each index depend on the damage type concerned. Based on the performance evaluation, the preferred damage indices in accordance with different damage types were recommended.

Maeck, Wahab, and Peeters, et al. (2000) conducted different techniques and compared to derive from experimentally determined modal characteristics of a reinforced concrete beam its dynamic bending stiffness. The degradation of stiffness, due to cracking of the reinforced concrete, gives information on the position and severity of the damage that has occurred.

Gupta, Nielsen, and Kirkegaard (2001) estimated structural damage form a known increase in the fundamental period of a structure after an earthquake or prediction of degradation of stiffness and strength for a known damage. He proposed a modified Clough-Hohnston single-degree-of-freedom oscillator to establish reliable correlations between the response functions in the case of a simple elastic-plastic oscillator. The proposed model has been used to demonstrate that ignoring the effects of aftershocks in the case of impulsive ground motions may lead to unsafe designs.

Ren and Roeck (2002) proposed a damage identification technique at an element level. The element damage equations have been established through the eigen-value equations based on changes in frequencies and mode shapes of vibration. Several solution techniques are discussed and compared. Numerical results show that the non-negative least-squares method can lead to satisfactory results in most cases. An experimental program of the reinforced concrete beam under static and dynamic loading was used to demonstrate the identification scheme. In this paper, the adaptation of the finite element model is required.

Bernal (2002) presented a technique to localize damage in structures. Central to the approach is the computation of a set of vectors, designated as damage locating vectors (DLVs) that have the property of inducing stress field whose magnitude is zero in the damaged elements. The DLVs are associated with sensor coordinates and are computed systematically as the null space of the change in measured flexibility. Numerical simulations carried out with realistic levels of noise and modeling error illustrate the robustness of the technique. **Abdo and Hori (2002)** presented a numerical study of the relationship between damage characteristics and the changes in the dynamic properties. It is found that the rotation of mode shape is a sensitive indicator of damage. The numerical results clarify that the rotation of mode shape has the characteristic of localization at the damaged region even though the displacement modes are not localized. Also, the results illustrate that the rotations of modes are robust in locating multiple damage locations with different sizes in a structure. Furthermore, using the changes in the rotation of mode shape does not need very fine grid of measurements to detect and locate damage effectively.

There may be other damage indices to indicate the locations and extent of damage. For real civil structures, only one damage index may not be enough. Until now, the relationships between damage type and damage index are not clear. A lot of further studied are needed in this area.

2.3.2.3.3 Methods From Static Data

Static parameter estimation is based on measured deformations induced by static loads such as a slowing moving track on a bridge. There are many instances in which static loadings is more economical than dynamic loading. Many applications require only element stiffness for condition assessment. In these cases static testing and analysis can prove simple and more cost effective.

Hajela and Soeiro (1990) proposed the output error method and the use of static structural displacements as the measures response, which is departure from the standard practice of using eigen-modes alone for the identification problem. **Sanayei and Onipede (1991)** presented a method to identify the stiffness parameters for linear elastic structures subjected to static loads. Structural stiffness was identified at element level using applied forces and measured displacements at a subset of degree freedom used to define the structural model. **Sanayei, et al. (1990, 1992, and 1997)** used the preceding method to determine the effects of measurement error. Both static displacement and static strain measurements were used to successfully evaluate the unknown stiffness parameters of the structural components. They also presented a heuristic method to select a small subset of error tolerant force and displacement measurement locations.

Banan, et al. (1994a,b) set up an algorithm for estimating member constitutive properties of the finite-element model from measured displacements under a known loading. The algorithm was based on the concept of minimizing an index of discrepancy between the model and the measurements using the constrained least-squares minimization. **Sanayei and Saletnik (1996a,b)** developed a method for parameter estimation of linear-elastic structures using strain measurements and preserving structural connectivity. Numerical simulations on truss and frame structures demonstrated its system's ability to identify all or portion of structural cross-sectional

properties, including element failures. **Hjelmstad and Shin (1997)** proposed a damage detection algorithm based on a system identification method, where the output error estimator was implemented to estimate the parameters and the idea of group parameters was used in constructing models of structural systems.

Since the natural frequencies, mode shapes, and static responses of a structural system are functions of structural parameters, these parameters may be identified by comparing the dynamic and static characteristics predicted from the mathematical model to those values determined by test. One of the consequences of the development of damage is the decrease in local stiffness, which in turn results in changes in some of the responses. It is therefore necessary that the dynamic and static characteristics of the structure be monitored for damage detection and assessment. Based on the concept, **Oh and Jung (1998)** propose an improved method that can identify a finite-element model of a structure capable of providing structural characteristics that are consistent with those measured in static and dynamic tests (i.g., the curvature of mode and the static displacement data). The detection of damage in a member with stronger influence on the higher modes is more difficult. Thus, the use of static displacements obtained by a loading condition that simulate higher modes was proposed as a solution to this problem. **Cui, F. (2000)** presented a new method for parameter identification based on the strain and displacement data from static testing, in which Gauss-Newton, gradient, and Monte-Carlo formulas were compositely employed to solve the ill-condition and uncertainties. Furthermore, based on the formula of the algorithm of static responses, they also proposed a complex approach, where combined static strain and displacement with dynamic response (i.g., mode shape) to localize damage and identify the severity of damage. Several algorithms were compositely applied to improve the sensitivity of parameter identification and enhance the reliability of solution process. The static and dynamic responses were utilized to calibrate the confidence of identification.

Wang, Hu, et al. (2001) proposed a structural damage identification algorithm using static test data and changes in natural frequencies jointly. A proper definition of Measured Damage Signature (MDS) and Predicted Damage Signature (PDS) were presented and matched to detect the location of damage. After obtaining the possible damage location, an iterative estimation scheme for solving non-linear optimization programming problems, which is based on the quadratic programming technique, was used to predict the damage extent. A remarkable characteristic of the approach was that it could be directly applied in the cases of incomplete measured data. Two examples were presented and the results showed that the algorithm was efficient for the damage identification. **Jang, et al. (2002)** used the system identification (SI) method to identify structural parameters in a FEM by minimizing the error between measured and analytical computed responses. A regularization scheme is applied to alleviate the ill-posedness of an inverse problem by adding a regularization function to the primary error function. Two different algorithms depending on the type of measured response have been developed to assess damage. Static displacements from static loading and modal data from impact vibration were measured through laboratory experiments on a grid-type model bridge. Damage is simulated by saw-cutting the cross section with various depths and identified as the reduction in the structural stiffness of the elements around the crack. Through the experimental

works, the applicability of the SI-based damage assessment algorithms has been rigorously investigated.

Modal updating by finite element method is often used to identify the changes of damage using static testing data. Because the errors caused by finite element model may be greater than changes of damage, the finite element models should be firstly calibrated using the measured modal properties and experimental data. Only the finite element models are reliable, the results from modal updating by finite element methods are valuable.

2.3.2.3.4 Sub-structure Analysis Methods

In the model updating approach, it is common only to update stiffness correction factors for selected substructures rather than for individual structural members. The goal is to reduce the number of stiffness parameters to be updated so that the ill-conditioning and non-uniqueness are kept within tolerable levels. Having smaller substructures where damage has occurred is also desirable so that better localization and assessment of its severity can be performed. **Koh, et al. (1991)** proposed a sub-structural approach to estimate the stiffness and damping coefficients from the measurements of dynamic responses. The structures were decomposed into several smaller subsystems for which state and observation equations were formulated and solved by EKF method with a weighted global iteration algorithm. **Zhao, et al. (1995)** reported their work on the sub-structural identification in frequency domain for the identification of frequency dependent systems such as soil-structure interaction systems. **Yun and Lee (1997)** proposed a sub-structural identification method using auto-regressive and moving average with stochastic input (ARMAX) model and the sequential prediction error method. Since the damage locations are not known a priori, adaptive sub-structuring is useful. **Hjelmstad and Shin (1997)** developed a damage detection and assessment algorithm in this regard based on the parameter estimation with an adaptive parameter grouping scheme from static response.

Abdelghani, et al. (1997) have developed a system identification-based approach for analysis and diagnosis of structures under operating conditions. Of interest in their work is the separation of diagnosis into global damage alarm and damage detection. A simplified algorithm is presented for measurement of the statistical likelihood of damage. This statistical test does not attempt to quantify potential damage, but only provides an intelligent alarm, which takes into account all individual changes of modal frequencies and shapes and compares them to their confidence domain to evaluate whether the changes might be significant. The global alarm concept is perhaps more achievable than damage detection for complex and uncertain civil structures.

Park and Reich (1999) reviewed two complementary methods for model-based damage detection with applications, i.e., the sub-structural flexibility method and the sub-structural transmission zeros method. **Alvin, et al. (1995 and 1999)** presented a computational procedure for extracting substructure-by-substructure flexibility from global frequencies and mode shapes. The proposed procedure appears to be effective for structural applications such as damage localization and finite element model reconciliation. **Zhang, Q.W. (1999)** proposed a damage identification algorithm termed as constrained sub-matrix factor adjustment and extended the

algorithm by using both of static and dynamic measurements.

For damage detection and condition assessment of large and complex structural systems, substructural identification may be an effective way.

2.3.3 Neural Networks Approaches

The model updating approach described in the last subsection is based on a parametric structural model. Health monitoring techniques may rely on nonparametric system identification approaches, in which a priori information about the natural of the model is not needed. Nonparametric models can be used to detect damage, although it is more difficult to use them for localization of damage.

Among the nonparametric identification approaches that have been receiving growing attention recently are neural networks. Neural networks do not require information concerning the phenomenological nature of the system being investigated, and they also have fault tolerance, which makes them a robust means for representing model-unknown systems encountered in the real world. Neural networks do not require any prior knowledge of the system to be identified. It can treat both linear and nonlinear systems with the same formulation.

A number of investigators have evaluated the suitability and capabilities of these networks for damage detection purposes. **Ghaboussi, et al. (1991) and Wu, et al. (1992)** trained neural networks to recognize the frequency response characteristics of healthy and damaged structures in which the properties of individual members were adjusted to reflect varying levels of damage. **Elkordy, et al. (1993)** used a finite-element model to develop failure patterns that were used to train a neural network so that it can later diagnose damage in the reference structure. **Szewczy and Hajela (1994)** presented a neural network approach based on mapping the static equilibrium requirement for a structure in a finite-element formulation, with the assumption that structural damage is reflected in terms of stiffness reduction. All of these exploratory studies indicated that neural networks offer a powerful tool for assessing the condition of structures with inherent damage. But a study by **Masri, et al. (1996)** complements the work of other investigators by concentrating on a class of problems where knowledge of the failure states is not available. In other words, the potential failure modes of the test structure are so varied and so unpredictable that is not feasible to train the neural network by furnishing it with pairs of failure states and corresponding diagnostic response. By not postulating or searching among limited set of expected failure modes, the approach of this study can be applied equally well whether the underlying structural response is linear or not. However, such an approach has the disadvantage that detectable change in the signature of the analyzed response measure of the structure are not directly attributable to a specific failure mode, but simply indicate that damage has been sustained by an element or unit of a structure that has a dominant contribution to the response measure being analyzed

Levin and Lieven (1998) proposed a new method of dynamic finite-element model updating using neural networks. Because all practical experimental data will contain noise, so it is desirable to develop an updating method that is resistant to noise. It is widely known that

neural networks tend to be robust in the presence of noise and are able to distinguish between these random errors and the desired systematic outputs. Hence, it seems natural and appropriate to apply neural networks to this field. In this paper, the experimental data were firstly prepared by using modal analysis on the FRF's, and then the resulting model shapes and natural frequencies are assembled into an experimental vector. Another advantage of the proposed approach is the avoidance of the common-problem of co-ordinate incompleteness; i.e., the neural network updating method is capable of working with a limited number of experimentally measured DOF's and modes. The proposed updating method is tested on a simple cantilevered beam, with promising results. The main drawback is that this method is computationally expensive, and it will fail if FE model has repeated modes. However, it would seem that there is significant potential for this model updating method to work with practical structures. **Atalla and Inman (1998)** implemented FRF's to identify faults in finite-element models. **Marwala and Hunt (1999)** implemented modal properties and FRF's simultaneously to identify faults. **Zang and Imregun (2001)** used the measured frequency response functions (FRF's) as input data to artificial neural networks to detect structural damage. The results showed that, in all cases considered, it was possible to distinguish between the highway and changed states with good accuracy and repeatability.

Chang, Chang, and Xu (1999) proposed an adaptive neural network (NN) method for model updating and the damage detection. The NN model was first trained off-line and then retrained during iteration if needed. Numerical simulation of suspension bridge model updating demonstrated the effectiveness of the proposed method.

Marwala (2000) and Zang and Imregun (2001) presented a committee of neural networks technique, which employs frequency response function (FRF's), modal properties (natural frequencies and model shapes), and wavelet transformation (WT) data simultaneously to identify damage in structures. The committee approach assumed that the errors given by the three individual approaches were uncorrelated, a situation that became more apparent when using measured data rather than simulated data. The committee approaches were used in parallel to diagnose faults on a three-degree-of-freedom structure and a population of cylindrical shell. It is demonstrated that the committee procedure is more reliable than using each procedure individually. The disadvantage of the committee was that it required more than one trained network.

Masri et al. (2000) focused on evaluating the efficiency of model-unknown identification approaches such as neural networks for detecting modifications in the characteristics of the underlying physical systems. Such methods would be particularly useful in assessing intricate mechanical systems whose internal states are not accessible for measurements. In particular, these methods address the issue of low-sensor spatial resolution, unknown system topology, and measurement noise well. The system was tested in its " virgin" state as well as in "damaged " states corresponding to different degree of parameter changes. It is shown that the proposed method is robust procedure and a practical tool for the detection and overall quantification of changes in nonlinear structures whose constitutive properties and topologies are not known.

Ni, Ko, and Zhou (2001) developed multi-novelty indices to detect the damage region

based on vibration measurement. Firstly, a bridge is partitioned into a set of structural regions and it is assumed that there are vibration transducers at each region. For each region, a neural network based on novelty detector was formulated by using the global natural frequencies and the localized modal components. Then the modal flexibility values were used to trains an auto-associative neural network and to obtain a novelty index. The applicability of the proposed method for structural damage region identification was demonstrated by taking the Tsing Ma Bridge and the Ting Kou Bridge as examples.

The effectiveness of neural network methods is determined by the completeness of original data library and the reliability of algorithms. The neural network method may be effective for the on-line monitoring of large structures, such as cable-stayed bridges and suspension bridges.

2.4 SENSORS AND OPTIMUM PLACEMENT

One of the problems facing structural health monitoring is that very little is known about the actual stress and strains in a structure under external excitations. For example, the standard earthquake recordings are made of motions of the floors of the structure and no recordings are made of the actual stresses and strains in structural members. There is a need for special sensors to determine the actual performance of structural members.

Structural health monitoring requires integrated sensor functionality to measure changes in external environmental conditions, signal processing functionality to acquire, process, and combine multi-sensor and multi-measured information. Individual sensors and instrumented sensor systems are then required to provide such multiplexed information.

2.4.1 Sensor types

Housner et al. (1997) summarized sensor types in structural control and their applications in civil engineering. In general, there are kinds of sensors for on-line monitoring, such as piezoelectric transducer, optical fibre sensors, embedded brag grating sensors, etc.. The reliability and durability of these sensors have being testified in many large bridges and tall buildings. Unlike many mechanical systems, typical civil engineering structures are often large in size and therefore have very low natural frequencies. In addition, the vibration level of the structural responses is very often quite low except under strong earthquake. Therefore, the sensors of a monitoring system must be able to work in a very low frequency range and they must have a large dynamic measurement range. The industry has made great achievements in developing sensor and is still working forward.

2.4.2 Optimum Sensor Placement

The estimation of the parameter values involves uncertainties due to limitations of the mathematical models used to represent the behavior of the real structure, the presence of measurement error in the data, and insufficient excitation and response bandwidth. In particular, the choice of the number and the location of the sensor in the structure have a major influence on

the quality, or equivalently the uncertainty, of the model parameter estimation. Because complete modal data is impossible for a large flexible structure, measurements yield only partial mode shapes with respect to the total degree-of-freedom corresponding to the FEM, a common practice to bridge the gap is to expand the measured mode shapes or the reduction of freedom in FEM. Unfortunately, this process unavoidably introduces consequential errors and increases the difficulty in damage detection. One alternative method is to use the measured incomplete mode shapes to detect damage, then the relatively more information collected can be used advantageously for damage detection.

Methods have been developed to place sensors in an optimal fashion to address the identification and control of dynamic structures by **Udwadia and Garba (1985)**. **Kammer (1991)** proposed an effective independence algorithm based on the contribution of each sensor location to the linear independence of the identified modes. The initial candidate set of sensor locations was quickly reduced to the number of available sensors. **Hemez and Farhat (1994)** extended the effective independence method in an algorithm where sensor placement was achieved in terms of the strain energy contribution of the structure.

Penny, et al. (1994) proposed a methodology for optimum sensor locations for parameter identification in dynamic systems. **Udwadia (1994)** developed a rational statistical-based approach to the optimal location of sensor based on Fisher's information matrix for the model parameters. Using the expected Bayesian loss function involving the trace of the inverse of the Fisher information matrix, **Heredia and Esteva (1998)** have extended this work to treat the case of large model uncertainties expected in model updating. **Cobb and Liebst (1997)** have reported the optimal sensor placement for the purpose of detecting structural damage. The prioritization of sensor locations was based on an eigenvector sensitivity analysis of a finite element model of the structure. **Reynier and Hisham (1999)** proposed two method to determine the optimal or near optimal positioning of sensors. The optimal sensors location was proposed on the finite element model associated to the structure to be tested. The first method of location of sensors emphasized the minimization of the noise effect, the estimate of the modal coordinates was found in a least-squares sense. The second method was based on the observability gramian and the optimal sensors location had to ensure observability requirements.

Shi, Law, and Zhang (2000) presented a method in which the sensor locations were prioritized according to their ability to localize structural damage based on the eigenvector sensitivity method. Numerical examples and test results showed that this approach was effective for detecting structural damage directly using optimum and incomplete test modes. **Xia and Hao (2000)** proposed measurement selection in terms of two factors, namely the sensitivity of a residual vector to the structural damage, and the sensitivity of the damage to the measurement noise. The advantage of the proposed technique was that it was based on the undamaged state of structure and thus independent of the damaged configuration. Therefore, it was applicable in practice to determine the measurement selection prior to field testing and damage identification analysis.

Fu and Moosa (2000) proposed probabilistic advancing cross-diagnosis method to diagnosis-decision making for structural health monitoring. It was experimented in the laboratory

respectively using a coherent laser radar system and a CCD high-resolution camera. Results showed that this method was promising for field application. Another new idea is that neural network techniques are used to place sensors. For example, **Worden and Burrows (2001)** used the neural network and methods of combinatorial optimization to locate and classify faults.

The static and dynamic data are collected from all kinds of sensors which are installed on the measured structures. And these data will be processed and usable information will be extracted. So the sensitivity, accuracy, and locations, etc. of sensors are very important for the damage detections. The more information are obtained, the damage identification will be conducted more easily, but the price should be considered. That's why the sensors are determined in an optimal or near optimal distribution. In a word, the theory and validation of optimum sensor locations will still being developed.

2.5 EXAMPLES OF HEALTH MONITORING IMPLEMENTATION

In order for the technology to advance sufficiently to become an operational system for the maintenance and safety of civil structures, it is of paramount importance that new analytical developments are ultimately verified with appropriate data obtained from monitoring systems, which have been implemented on civil structures, such as bridges.

Overman, et al. (1987) instrumented the Sunshine Skywey bridge in Florida more than 500 sensors to verify design assumptions, monitor construction quality and the conditions in service. **Muria-Vila, et al. (1991)** initiated a monitoring program to study the dynamic properties of the total 1543m cable-stayed Tampico Bridge in Mexico. The main span is the 360m in length, 21 servo accelerometers were installed and ambient and pull-back tests were conducted. The resulting frequencies were good in agreement but the damping values were still estimated. **Alampalli, et.al (1994 and 2000)** were studying continuous monitoring of two steel bridges over the Conrail mainline tracks in Rochester, N.Y. These bridge were built in 1963. The monitoring system was included as a part of rehabilitation contracts. Altogether 5 inclinometers, 22 accelerometers, and 5 strain gauges were installed in these two bridges. All these were connected with circular to a remote host computer. Natural frequencies, mode shapes, damping ratios, modal assurance criteria, etc. were then computed for use in condition monitoring and assessment. **Westermo and Thompson (1995)** designed and evaluated structural monitoring system with solid-state sensors for installation in several bridges and buildings. They reported on a project to install fully automatic and tele-metered strain sensors on 10 bridges in Georgia.

Abe, Fujino, et al. (1999) studied the feasibility of health monitoring of a 720m span Hakucho Suspension Bridge in Japan by ambient vibration measurement. An identification scheme that made use of cancellation of randomness in data by shaking was employed to use the ambient vibration measurements with high accuracy. **Helmicki, Hunt, et al. (1999)** addressed the measurement and documentation of construction and service effects for a three-span continuous steel stringer bridge in the Cincinnati, Ohio area. A total 642 channels of sensor data were available for bridge monitoring. The measurements were used to check the design and the project is on going. **Catbas, et al. (1999)** designed and implemented a long-term continuously

operating health monitoring system for the Commodore Barry Bridge, with spans of 822+1644+822 ft. Over 80 channels of different sensor types were installed to collecting data such as temperature, wind speed and direction, strains, acceleration, etc. Several long span suspension bridges in China, such as Tsingma Birdge, Humen Birdge, and Jiangyin Yangzi Bridge etc., were also installed many types of sensors for health monitoring. **Foote P.D (1999)** introduced the programs within European nations and European collaboration programs for structural health monitoring.

Idriss (2001) designed an optical fiber monitoring system and installed it into a 3 span high performance prestressed concrete (HPC) highway bridge in Albuquerque, NM. The data were collected during the beam fabrication, bridge construction, and service phases and analyzed to determine the prestress losses and get a better understanding of the properties and behavior of HPC.

Mufti (2001) summarized the applications of SHM of Canadian bridge engineering, including fibre-reinforced polymers sensors, remote monitoring, intelligent processing, practical applications in bridge engineering, and technology utilization. Further study and applications are still being conducted now. **Fujino and Abe (2001)** introduced the research and development of SHM systems at the Bridge and Structural Lab of the University of Tokyo. They also presented the ambient vibration based approaches for Laser Doppler Vibrometer (LDV) and the applications in the long-span suspension bridges.

The extraction of the measured data is very hard work because it is hard to separate changes in vibration signature duo to damage form changes, normal usage, changes in boundary conditions, or the release of the connection joints.

New bridges offer opportunities for developing complete structural health monitoring systems for bridge inspection and condition evaluation from “cradle to grave” of the bridges. Existing bridges provide challenges for applying state-of-the-art in structural health monitoring technologies to determine the current conditions of the structural element, connections and systems, to formulate model for estimating the rate of degradation, and to predict the existing and the future capacities of the structural components and systems. Advanced health monitoring systems may lead to better understanding of structural behavior and significant improvements of design, as well as the reduction of the structural inspection requirements. Great benefits due to the introduction of SHM are being accepted by owners, managers, bridge engineers, etc..

2.6 RESEARCH AND DEVELOPMENT NEEDS

Most damage detection theories and practices are formulated based on the following assumption: that failure or deterioration would primarily affect the stiffness and therefore affect the modal characteristics of the dynamic response of the structure. This is seldom true in practice, because (1) Traditional modal parameters (natural frequency, damping ratio and mode shapes, etc.) are not sensitive enough to identify and locate damage. The estimation methods usually assume that structures are linear and proportional damping systems. (2) Most currently used damage indices depend on the severity of the damage, which is impractical in the field. Most

civil engineering structures, such as highway bridges, have redundancy in design and large in size with low natural frequencies. Any damage index should consider these factors. (3) Scaled modeling techniques are used in current bridge damage detection. A single beam/girder models cannot simulate the true behavior of a real bridge. Similitude laws for dynamic simulation and testing should be considered. (4) Many methods usually use the undamaged structural modal parameters as the baseline compared with the damaged information. This will result in the need of a large data storage capacity for complex structures. But in practice, there are majority of existing structures for which baseline modal responses are not available. Only one developed method (**Stubbs and Kim 1996**), which tried to quantify damage without using a baseline, may be a solution to this difficulty. There is a lot of research work to do in this direction. (5) Seldom methods have the ability to distinguish the type of damages on bridge structures. To establish the direct relationship between the various damage patterns and the changes of vibrational signatures is not a simple work.

Health monitoring requires clearly defined performance criteria, a set of corresponding condition indicators and global and local damage and deterioration indices, which should help diagnose reasons for changes in condition indicators. It is implausible to expect that damage can be reliably detected or tracked by using a single damage index. We note that many additional localized damage indices which relate to highly localized properties of materials or the circumstances may indicate a susceptibility of deterioration such as the presence of corrosive environments around reinforcing steel in concrete, should be also integrated into the health monitoring systems.

There is now a considerable research and development effort in academia, industry, and management department regarding global health monitoring for civil engineering structures. Several commercial structural monitoring systems currently exist, but further development is needed in commercialization of the technology. We must realize that damage detection and health monitoring for bridge structures by means of vibration signature analysis is a very difficult task. It contains several necessary steps, including defining indicators on variations of structural physical condition, dynamic testing to extract such indication parameters, defining the type of damages and remaining capacity or life of the structure, and relating the parameters to the defined damage/aging. Unfortunately, to date, no one has accomplished the above steps. Many further studies are needed.

Where to go from here? In order for the model-based damage detection methods to be adopted eventually for on-line health monitoring, the following should be addressed:

(1) The accurate definition of damage and new sensitive damage indices should be developed. These indices could distinguish not only the place and the extent of damage, but also the types of damage in a structure,

(2) Fast algorithms for system identification are needed, if possible, on a real-time basis. First of all, the identification of the basic characteristics of existing bridges must be accurate and reliable. This is the basis of the structural damage identification. Secondly, the objects of sensors arrangement must be clear, because there are amounts of data to be treated and the noise should be filtrated. Furthermore, a method for localized structural identification is highly desirable so

that not all of the sensor output is processed for online monitoring purposes. In this way, substructure identification method may be the direction.

(3) There are still considerable uncertainties in the testing, analysis, and environment for the purpose of damage detection. Sometimes, it is very difficult to sort out the uncertainties and pinpoint whether the lack of reliable results from modal analysis were due to the damage or due to an error in the considerably complicated procedures of modal analysis. At this point, it is concluded that a controlled study of a physical model in the laboratory would be an excellent method to understand the sources of uncertainties, and limits of confidence when modal analysis was used as a technology for condition assessment and damage identification. More research is needed on the analytical techniques for damage identification using available and realistic structural monitoring data, including the combination of static data and vibration testing information. This research should consider the uncertainties inherent in the materials and construction, the variability of structural properties due to environmental conditions, unknown modeling errors and assumption, etc.

(4) Although we have not discussed any non-model based damage detection methods, a robust online health monitoring system would require a hybridization of both non-model and model-based methods. Studies are needed to develop sensible hybrid damage detection methods that are easy to implement and robust. According to the existing study, one of the realistic methods may be the stochastic subspace identification method by using the environmental excitation data.

(5) Unfortunately, nearly all of the existing systems are not instrumented to get the responsible data. The data acquisition systems with multi-channel and signal processing system have being developed for structural health monitoring. Economical sensor placement and data collection methodologies, both onsite and remote, are needed in order for online health monitoring technologies to have practical benefits for national’s existing infrastructure and transportation systems.

(6) The reliability and durability of the entire SHM system should be studied. The interrelationship of structural behavior and the effect of each and all components of the monitoring system on the overall safety should be studied, including sensors and their optimal placements, communication, data acquisition, etc.

(7) The evaluation of serviceability and load-carrying capacity for existing highway bridges based on the damage identification and reliability theory should be studied. It is very important for the load rating, condition assessment, and decision making of repair, strengthening, and rehabilitation of existing highway bridges.

(8) Information techniques and imagine systems are needed to integrate field, theoretical and laboratory research for solving large system identification and condition assessments problems.

(9) New and innovative construction materials will enhance the strength and durability of the infrastructure system in the twenty-first century. Testing and evaluation methodologies need to be developed specific for characterization of these newer and high performance materials. Advanced condition monitoring technologies will enable detection of cracks, onset of failure,

extent of degradation, and location of damaged zones in structural elements.

(10) Standards and code for SHM, and how can structural health monitoring be better applied in practice? ----philosophies, cost, devices, efficiency……The Health Monitoring System of Bridge will be included in the scope of Bridge Management System (**Ryall, 2001**).

Chapter 3

Methods and Procedures for Bridge Damage Detection

3.1 General

Structural Health Monitoring and damage detection base on the technique of dynamic diagnostic, which is used to measure various modal parameters deriving from the dynamic characteristics of a system. Performing this technique requires several different approaches. Among those approaches, *measurement and signal processing* will be the major aspect and one of the foundations of experimental modal analysis. In this chapter, the components of typical dynamic data acquisition system and theoretical basis of correlation method in ambient signal processing will be briefly introduced.

The key issue in vibration-based damage detection and evaluation is to improve the signature-to-noise ratio. However, most of the currently used damage indices are not sensitive enough to bridge damages. In this chapter, a newly defined modal parameter, the modal energy transfer ratio (ETR) is introduced for this study. The modal energy transfer ratio, referred to as the ratio of energy transfer to total energies in the non-proportionally damped and multiple degree of freedom (MDOF) system, is based on the complex damping theory (Liang and Lee 1991). The complex damping theory therefore will be a significant essence for understanding the basic definition of ETR. Thus we will illustrate the complex damping theory and the definition of ETR from both physical and mathematical perspectives in this chapter.

Traditionally, civil engineers use both input and output to get free-decay signals, and the modal parameters are then identified through these free decay signals by using time domain or frequency domain system identification methods. This method is usually called the forced response technique. For large civil engineering structures, such as bridges, forced excitation may be impossible or impractical. Ambient excitation (environmental excitation or traffic vibration) seems to be the most practical approach for measurement in terms of acceptable performance, low costs, and easy operations. Because it is very difficult to measure the natural excitation exactly during the ambient testing, the traditional forced response technique can not be used directly to process ambient response data. In this chapter, modal identification methods both in frequency domain and in time domain are introduced. In frequency domain, Single-degree-of freedom identification method is illustrated based on the transfer function analysis. The cross-correlation of the ambient response is proved to have the decaying form, and this decaying signal has the same vibrational signatures as the original system. After that, the traditional system identification method in the time domain can be used to identify the modal parameters. The proposed methods are further verified by a field ambient bridge testing and associated finite element modeling.

3.2 Measurement and Signal Processing

3.2.1 Measurement

A typical measurement system consists of hardware and software implements. Careful pretest planning, including understanding and selecting transducers, arranging transducers, and implementing the data acquisition system, etc., can save time in making measurements and most useful information can be obtained from the test data.

The basic schematic for a typical dynamic data acquisition system is shown in Fig. 3.1. The first part of the system is transducers. A transducer is a device which converts shock or vibration motion into an optical, a mechanical, or, most commonly, an electrical signal that is proportional to a parameter of the experienced motion. Various transducers with different characteristics have been developed to measure different types of vibratory motion, such as acceleration, velocity, displacement, and force. Among those transducers, the accelerometer is most commonly used vibration measurement instrument due to its small size and large usable frequency range (see Appendix A). Amplifiers and AAF are to condition the signals from the structural system or elements picked up by transducers. The main purpose of this process is to avoid noise interferences. Meanwhile, the signals are still analog and change continuously with time. For conveniences, the analog

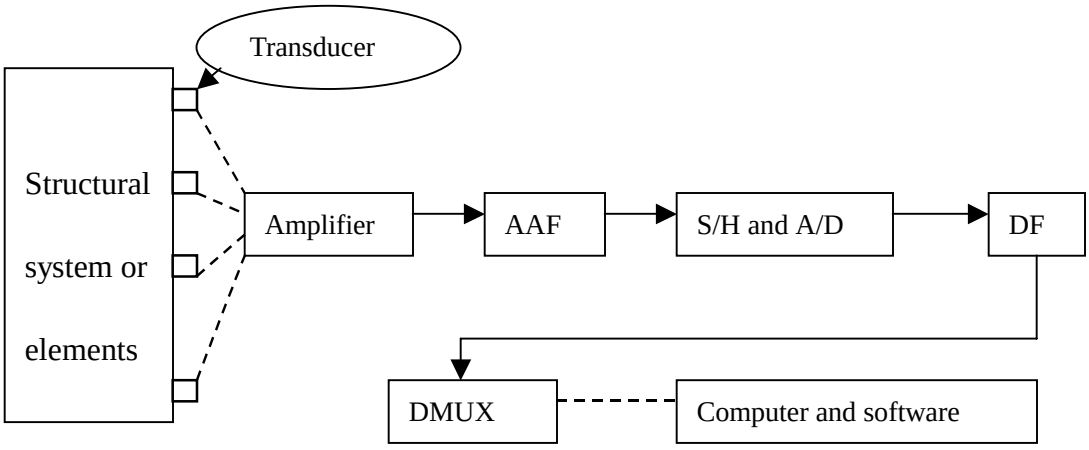

Note: AAF——Anti-aliasing filter; S/H——sampling holder;
A/D——Simulation converter; D/F——digital filter;
DMUX—— Multi-channels digital converter; ----- cables.

Fig. 3.1 Basic Schematic for a Typical Dynamic Data Acquisition System.

signals are converted to digital signals by A/D converter. Then the digital signals go through the digital filters and multi-channels digital converter and are stored in the computer. The control part, including computer hardware and software, is used to direct the whole system to accomplish the data sampling and analysis. The key part of the computer-based dynamic data

acquisition system is the A/D converter. The theory and design of various types of A/D converter are not included in this report, but there are two important parameters, sampling rate and sampling number, which are related to those characteristics and will be discussed as follows.

The dynamic data acquisition used in this research is shown in Fig. 3.2, which consists of the following parts: (a) 32 Channels A/D Converter, (b) Low-pass Filter, (c) P-III laptop computer, (d) relative data acquisition software and analysis software, (e) piezoelectric transducers (including accelerometers and velocity transducers). The main features of this data acquisition system include the data-acquisition and data-storage function, simulation of artificial input, segment data storage and display, window function selections, zoom functions, FFTs for data pre-evaluation, and data analysis and treatment, etc. Measurement Steps may follow *Shock and Vibration Handbook* (Harris 1995).

(a) Acquisition and Processing System.

(b) Accelerometer Sensors.

Fig. 3.2 Dynamic Data Acquisition System.

3.2.2 Signal Processing

In this section, the basic signal processing techniques, such as FFT, window function, and average analysis, will be specified firstly. After that, both forced excitation and ambient vibration signal processing methods will be briefly summarized.

3.2.2.1 Discrete Fourier Transformation and Fast Fourier Transformation

The basic relationships used to transform information from the time domain to the frequency domain, or vice versa, are the Fourier transform pair.

$$X(\omega) = \int_{-\infty}^{+\infty} x(t) e^{-j\omega t} dt \qquad (3.1a)$$

$$x(t) = \frac{1}{2\pi} \int_{-\infty}^{+\infty} X(\omega) e^{j\omega t} d\omega \qquad (3.1b)$$

In practical digital applications, $x(t)$ is known only for a finite time interval or record length T. That is to say, we have

$$X(\omega) = \int_0^T x(t) e^{-j\omega t} dt \qquad (3.2a)$$

$$x(t) = \frac{1}{2\pi} \int_0^T X(\omega) e^{j\omega t} d\omega \qquad (3.2b)$$

Data total of N equally spaced time intervals Δt apart and $\Delta t = \frac{T}{N}$. As a consequence of Shannon's theorem, $\Delta t \le \frac{1}{2 f_{\max}}$, and $f_{\max}$ is a maximum frequency., and then $\omega_{\max} = 2\pi f_{\max}$.

In time domain and frequency domain, the relative discrete variants are listed in the following

Time discrete variant: $t_n = n\Delta t = \frac{nT}{N}, \quad n = 0,1,2,....., N-1$

Time discrete signal: $\hat{x}(t_n) = \hat{x}(n\Delta t) = \hat{x}(n)$

Frequency discrete variant: $\omega_m = m\Delta\omega = \frac{2\pi m}{T}, \quad m = 0,1,2,....., N-1$

Frequency discrete signal: $\hat{X}(\omega_m) = \hat{X}(m\Delta\omega) = \hat{X}(m)$

Then the Discrete Fourier Transform (DFT) pair, equivalent to Eqs. (3.2a) and (3.2b), become

$$\hat{X}(m) = \Delta t \sum_{n=0}^{N-1} \hat{x}(n) e^{-j2\pi mn/N} \qquad (3.3a)$$

$$\hat{x}(n) = \frac{1}{N\Delta t} \sum_{m=0}^{N-1} \hat{X}(m) e^{j2\pi mn/N} \qquad (3.3b)$$

In order to keep the symmetric characteristics, we order $\hat{X}(\omega_m) = \frac{1}{\Delta t} \hat{X}(m)$ and $\hat{x}(n) = \hat{x}(t_n)$, then we have DFT form as follows

$$\hat{X}(\omega_m) = \sum_{n=0}^{N-1} \hat{x}(t_n) e^{-j2\pi mn/N} \qquad (3.4)$$

$$\hat{x}(t_n) = \frac{1}{N} \sum_{m=0}^{N-1} \hat{X}(\omega_m) e^{j2\pi mn/N} \qquad (3.5)$$

Because of large amount of data, the applications of DFT were limited, until **Cooley and Turkey (1965)** proposed a fast computation method, named *Fast Fourier Transform* (FFT). The

FFT is the key of signal processing. There are many extended methods of FFT and they are applied in many aspects (Details may be found in **Brigham, E.O. (1988)**).

3.2.2.2 Window Functions

One practical solution to the leakage problem involves the use of windowing and there is a range of different window functions for different classes of problems. Four commonly used functions are called rectangular, Hanning, Kaiser-Bessel, and flat-top for the stable signal problems, such as ambient or periodic signals. The Hanning window function is often chosen as a general purpose window for use with periodic or random signal analysis. For transient signal such as impulse input, the rectangular window function is recommended. Additionally, for the transient response signal, there is exponential window function, which can be expressed as:

$$w(t) = \begin{cases} 0 & 0 < t < t_0 \\ e^{-(t-t_0)/\tau_e} & t_0 < t < T \end{cases} \qquad (3.6)$$

where t_0 is the time while the window begins. τ_e is the window decay time constant. The main objective in using the exponential window is to overcome the filter leakage due to the signal truncation. However, this window function will affect modal damping since each mode's exponential damping term is multiplied by the window's exponential function. Therefore, from the measured damping ratio ξ_m, the window damping ratio ξ_w must be subtracted to obtain the real i^{th} mode's damping ratio ξ_i:

$$\xi_i = \xi_m - \xi_w \qquad (3.7)$$

and

$$\xi_w = \frac{1}{\tau_e \omega_i} \qquad (3.8)$$

where ω_i is the i^{th} natural frequency.

Furthermore, force window is used for the transient excitation signal. For example, if the input is the impulse signal, a rectangular window function, shown as follows, may be adopted.

$$w(t) = \begin{cases} 0 & 0 < t < t_0 \\ 1 & t_0 < t < T \end{cases} \qquad (3.9)$$

3.2.2.3 Averaging

The long period record has several important features and advantages. However, because of the limitation of hardware, sometimes, it is impossible to store a sufficient time history in digital memory. An alternative method is scan averaging. The random signals require a large

number of individual frequency spectra that must be averaged together in order to reduce spectral uncertainty. Even though the boarder bandwidth obtained by scan averaging might result in a loss of spectrum detail, it provides considerable improvement in the dynamic range of the result. Readers may find the details of averaging technique in several reference books, for example, "*Vibration Testing - Theory and Practice*"(by **McConnel, K.G., 1995**) and "*Modal Testing: Theory and Practice* " (by **Ewins, D.J., 1995**).

In order to more quickly obtain the averaged frequency spectrum, the data windows can be overlapped. Overlapping may be used with all window functions. In this research, Hanning window is ideally suited for this application. In this report, each impact can produce 1024 points and a total of 8 impacts may be conducted. The averaging spectrum normally can reduce the noise and has better performances in the dynamic range of the result.

3.2.2.4 Summary

In the previous Sections, the basic problems encountered in signal processing are discussed. There are two major signals, which would be dealt with in this report. One is obtained by the impulse input and the other is by the ambient input. The impulse input would be obtained by hammer impact, and the ambient input is by vehicle traveling. The signal processing will be summarized in Fig. 3.3.

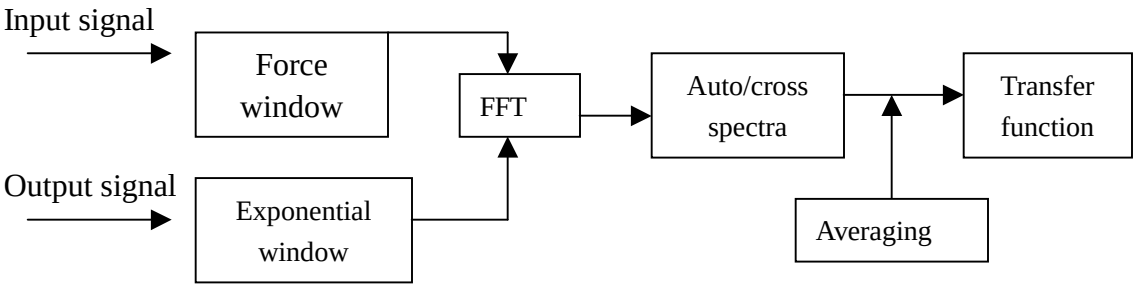

Fig. 3.3 (a) Flow-diagram of Impulse Signal Processing.

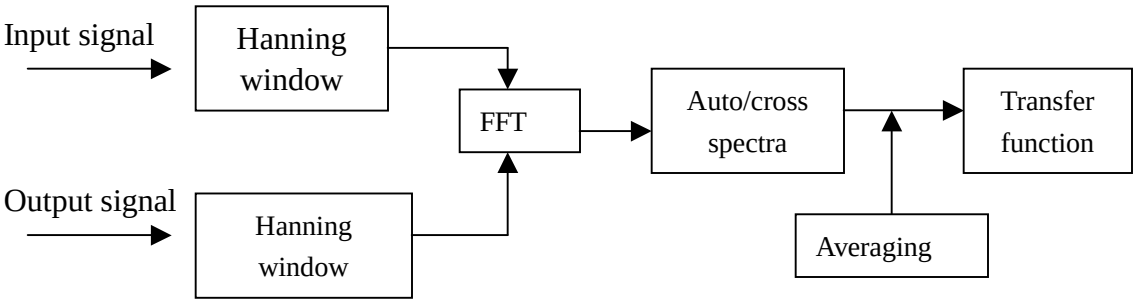

Fig. 3.3 (b) Flow-diagram of Ambient Signal Processing.

3.3 Energy Transfer Ratio (ETR)

3.3.1 Definition of Energy Transfer Ratio (ETR)

In non-proportionally damped structures, such as most civil engineering structures, there exists certain amount of energy transferred among vibration modes. The ratio of the modal energy transferred during a cycle and the total modal energy stored by the structure before the cycle is called modal energy transfer ratio (ETR), which was established by **Liang and Lee (1991)** who developed the theory of complex energy in structural dynamics. ETR is a quantitative description of the energy transfer, like the damping ratio which is a quantitative description of energy dissipation. The definition of ETR is shown in this section.

Consider only the homogeneous form of the equation of motion,

$$[M]\ddot{X}+[C]\dot{X}+[K]X=0 \qquad (3.10)$$

where $[M]$、$[C]$、$[K]$are respectively the mass, damping, and stiffness matrix. $\ddot{X}$, $\dot{X}$, and X are acceleration, velocity, and displacement, respectively. For convenience, the mass matrix is usually simplified into a unit matrix. In order to simplify the mass matrix and keep the other matrices symmetrical, pre-multiply $[M]^{-0.5}$ on both sides of Eq. (3.10), and let $Y=[M]^{0.5}X$. Then the new modified governing equation can be rewritten as:

$$\ddot{Y}+[\overline{C}]\dot{Y}+[\overline{K}]Y=0 \qquad (3.11)$$

where: $[\overline{C}]=[M]^{-0.5}[C][M]^{-0.5}$; $[\overline{K}]=[M]^{-0.5}[K][M]^{-0.5}$; $[\overline{C}]$, $[\overline{K}]$ are the new modified damping and stiffness matrices. $\ddot{Y}$, $\dot{Y}$, and Y are the acceleration, velocity, and displacement vectors in the new coordinate after transformation.

The general purpose of modeling here is to decouple and diagonalize the governing equation into a set of degree of freedom equations. For most of realistic systems, they are non-proportionally damped systems and cannot be decoupled easily. For this purpose, special treatment is needed. Here, we apply the state-space concept to decouple and diagonalize the governing equation. Therefore, the next step for modeling is to transfer the modified motion equation (Eq. 3.11) into a continuous state-space equation. Using Eq. (3.11), the state-space equation can be expressed as

$$[\overline{Z}]=[A][Z] \qquad (3.12)$$

where $$[Z]=\begin{bmatrix}\dot{Y}\\ Y\end{bmatrix} \qquad (3.13)$$

$$[A]=\begin{bmatrix} -[\overline{C}] & -[\overline{K}] \\ I & 0 \end{bmatrix} \tag{3.14}$$

Where $[A]$ is called the continuous state matrix and $[Z]$ is called the state vector. The continuous state matrix $[A]$ can be eigen-decomposed into the following form:

$$[A]=[P][\Lambda][P]^{-1} \tag{3.15}$$

Where $[P]$ is the eigen-vector of the continuous state matrix and $[\Lambda]$ is the eigen-value matrix of the continuous state matrix. They can be interpreted into the following formulas by the complex model shape and the complex frequency:

$$[P]=\begin{bmatrix} P_1\Lambda_1 & P_1^*\Lambda_1^* \\ P_1 & P_1^* \end{bmatrix} \tag{3.16}$$

$$[\Lambda]=\begin{bmatrix} \Lambda_1 & 0 \\ 0 & \Lambda_1^* \end{bmatrix} \text{ and } [\Lambda_1]=diag(\lambda_i)_{n\times n} \tag{3.17}$$

Where P_1 is the complex mode shape matrix, $\lambda_i=-\xi_i\omega_i \pm j\sqrt{1-\xi_i^2}\omega_i$ is the i^{th} eigen-value of generally damped system, or is called the **complex frequency**, and the superscript * refers to the complex conjugate operation. The subscript i refers to the modal order. By using the same idea, the modified stiffness matrix $[\overline{K}]$ in Eq. (3.11) can also be eigen-decomposed and its eigenvector Q can be obtained. The relationship of the stiffness matrix $[\overline{K}]$ and its eigenvector Q is shown as:

$$Q^T[\overline{K}]Q=diag(\omega_{ni}^2) \tag{3.18}$$

Where ω_{ni} are the i^{th} natural frequencies in the system. For a proportionally damped system, Eq. (3.11) can be diagonalized easily into a set of single degree freedom equations only by pre-multiplying eigenvector Q^T. However, for a non-proportionally damped system, the coupling pairs in the damping matrix will exist if we only pre-multiply Q^T, and Eq. (3.11) cannot be diagonalized. In order to decouple the non-proportionally damped system and obtain a more general decoupled form, the generalized Rayleigh quotient should be applied. The generalized Rayleigh quotient includes the eigenvector Q, the couple mode shape P_1, and the

modified damping matrix $[\overline{C}]$. It is shown as

$$\Psi = \frac{Q^T [\overline{C}] P_1}{Q^T P_1} \tag{3.19}$$

Applying the generalized Rayleigh quotient, **Liang et al.** (1991) decoupled and diagonalized Eq. (3.11) into the following set of single degree freedom equations.

$$\ddot{\varpi}_i + 2\vartheta_i \omega_i \dot{\varpi}_i + \omega_{ni}^2 \varpi_i = 0 \tag{3.20}$$

$$\vartheta_i = \xi_i + j\zeta_i = \frac{\Psi_{ii}}{2\omega_i} \tag{3.21a}$$

and

$$\omega_i = \omega_{ni} \exp(\zeta_i) \tag{3.21b}$$

where $\ddot{\varpi}$, $\dot{\varpi}$, and ϖ are the acceleration, velocity, and displacement in the i^{th} mode after decoupling and $j = \sqrt{-1}$. ϑ_i, ξ_i, and ζ_i are the complex damping ratio, dissipation damping ratio, and energy transfer ratio (ETR) in the i^{th} modal, respectively. ω_i and ω_{ni} are the i^{th} natural frequencies of the non-proportionally and the corresponding proportionally damped system., respectively. Eq. (3.20) is a more general decoupled form and it satisfies both proportionally and non-proportionally damped systems. In the proportionally damped system, the Rayleigh quotient is in real number form. That means the energy transfer ratio (ETR) doesn't exist in the proportionally damped system. Otherwise, the Rayleigh quotient will be in complex number form and ETR exists. According to Eqs. (3.10)-(3.20), the modal parameters, including conventional parameters (natural frequencies and dissipation damping ratio) and energy transfer ratios (ETR), are defined theoretically.

3.3.2 Energy Phenomena in Both Proportionally and Non-proportionally Dynamic System

According to the complex damping theory of **Liang and Lee** (1991), the existence of ETR depends on whether the system is proportionally or non-proportionally damped. The ETR's influences on both systems will be the major concern in this section. We can use the proportionally damped criterion introduced by **Caughey and O'Kelley (1965)**, which is shown as follows, to verify a system:

$$CM^{-1}K = KM^{-1}C \tag{3.22}$$

where $[M]$, $[C]$, and $[K]$ are demonstrated as Eq. (3.10). If a system satisfies Eq. (3.22), the system is proportionally damped, otherwise, it is non-proportionally damped. The two simple 2-DOF proportionally damped and non-proportionally damped systems with the same typical modal parameters (frequencies, dissipation damping ratio, and mode shapes) would be presented as examples in the following.

SYSTEM 1: Proportionally Damped System

$$M = \begin{bmatrix} 1 & 0 \\ 0 & 1 \end{bmatrix},\ C_1 = \begin{bmatrix} 0.7221 & -0.7826 \\ -0.7826 & 2.2873 \end{bmatrix},\ K = \begin{bmatrix} 80 & -5 \\ -5 & 90 \end{bmatrix}$$

SYSTEM 2: Non-proportionally Damped System

$$M = \begin{bmatrix} 1 & 0 \\ 0 & 1 \end{bmatrix},\ C_2 = \begin{bmatrix} 2 & -1 \\ -1 & 1 \end{bmatrix},\ K = \begin{bmatrix} 80 & -5 \\ -5 & 90 \end{bmatrix}$$

According to the theory developed above, the complex damping ratios and frequencies in both systems are summarized in Table 3.1.

Table 3.1 Modal Parameters in both Given Systems

System No.	Frequency (Hz)	Dissipation Damping Ratio	Energy Transfer Ratio (ETR)
SYSTEM 1 Proportionally Damped System	1.4050 1.5272	0.0226 0.1361	0.0 0.0
SYSTEM2 Non-Proportionally Damped System	1.4050* 1.5272*	0.0335 0.1262	-0.027 0.027

*: not modified according to Eq. (3.21b)

According to the above results, both systems have the same frequencies and very close dissipation damping ratio. But the energy transfer ratios are different. There is energy transfer in the non-proportionally damped system.

In order to discuss energy phenomena in quantity for a dynamic system, the response of the system should be considered first. The traditional approach for the response is to assume the solution in each mode as the following format.

$$\varpi_i = G_i e^{\lambda_i t} \qquad (3.23)$$

where G_i is an arbitrary complex constant and $e^{\lambda_i t}$ denotes the exponential function. Eq. (3.23) is then substituted into Eq. (3.20) and the characteristic equation can be obtained.

$$\lambda_i^{\,2} + 2\vartheta_i\omega_i\lambda_i + \omega_{ni}^{\,2} = 0 \qquad (3.24)$$

With both non-proportionally and lightly damping assumptions, the process of approximating the solution of the characteristic equation was depicted in Appendix B, and the roots of the Eq. (3.28) can be expressed as follows.

$$\lambda_i = -\xi_i e^{\mu\zeta_i}\omega_{ni} \pm j\sqrt{1-\xi_i^{\,2}}\,e^{\mu\zeta_i}\omega_{ni} \qquad (3.25a)$$

and

$$\omega_i = \omega_{ni}\exp(\zeta_i) \qquad (3.25b)$$

Then the response can be found by substituting Eq. (3.25) into Eq. (3.23). Using the response function, the inertial, damping, and spring force F_{mi}, F_{ci}, F_{ki} in each mode can be obtained and they are in complex number form.

$$\left.\begin{aligned} F_{mi} &= \ddot{\varpi} = G_i\lambda_i^{\,2}e^{\lambda_i t} \\ F_{ci} &= 2\vartheta_i\omega_{ni}\dot{\varpi} = 2\vartheta_i\omega_{ni}(G_i\lambda_i e^{\lambda_i t}) \\ F_{ki} &= \omega_{ni}^{\,2}\varpi = \omega_{ni}^{\,2}(G_i e^{\lambda_i t}) \end{aligned}\right\} \qquad (3.26)$$

The work done by these forces during one cycle of motion, with period of $T = \dfrac{2\pi}{\omega_{ni}}$, can then be integrated by force and response.

$$\left.\begin{aligned} W_{mi} &= \int_0^T F_{mi}\,d\varpi_i = \frac{\lambda_i^{\,2}G_i}{2}(e^{2\lambda_i T} - 1) \\ W_{ci} &= \int_0^T F_{ci}\,d\varpi_i = \vartheta_i\omega_{ni}G_i\lambda_i(e^{2\lambda_i T} - 1) \\ W_{ki} &= \int_0^T F_{ki}\,d\varpi_i = \frac{\omega_{ni}^{\,2}G_i}{2}(e^{2\lambda_i T} - 1) \end{aligned}\right\} \qquad (3.27)$$

where W_{mi}, W_{ci}, W_{ki} are the work done by the inertial, damping, and spring forces in each mode. Then we can adopt another modified complex plane to transform these formulas by dividing a coordinate transformation factor ($\eta = G_i\lambda_i(e^{2\lambda_i T} - 1)$).

$$\left.\begin{aligned} \overline{W}_{mi} &= \frac{\eta\lambda_i}{2} = \frac{1}{2}\omega_{ni}e^{\zeta_i}(-\xi_i + j\sqrt{1-\xi_i^{\,2}}) \\ \overline{W}_{ci} &= \vartheta_i\omega_{ni} = (\xi_i + j\zeta_i)\omega_{ni} \\ \overline{W}_{ki} &= \frac{\omega_{ni}^{\,2}}{2\lambda_i} = \frac{1}{2}\omega_{ni}e^{\zeta_i}(-\xi_i - j\sqrt{1-\xi_i^{\,2}}) \end{aligned}\right\} \qquad (3.28)$$

Thus the energy representation in the modified plane can be listed as the above form. Where

$\overline{W}_{mi}, \overline{W}_{ci}, \overline{W}_{ki}$ are the work done by the inertial, damping, and spring forces after coordinate transformation. The work in Eq. (3.28) is the complex number form, and the real and imaginary part can be interpreted as energy dissipation and transfer, respectively. For the un-damped system ($\vartheta = 0$), there will be no real part existed in Eq. (3.28). Obviously, only energy transfer will exist between the inertial and spring forces. For the proportionally damped system whose damping is real and $\zeta = 0$, the work done by inertial and spring force is also real. Then the damping absorbs energy from the inertial and spring forces. However, energy transfer still exists between the inertial and spring forces. Because damping dissipates the energy, the response will delay. On the other hand, for the non- proportionally damped system, the damping is also complex, and the energy phenomena will be even more intricate. Energy dissipation and transfer occur among inertial, damping, and spring forces simultaneously.

In conclusion, the real part of the complex damping is the ratio of the dissipating energy and the geometric sum of the complex done by the inertial and spring forces. The imaginary part of the complex damping is the ratio of energy transfer to the geometric sum of complex work done by the inertial and spring forces. These ratios are mathematically shown as

$$\xi_i = \frac{\mathrm{Re}(\overline{W}_{ci})}{2\sqrt{\overline{W}_{mi}\overline{W}_{ki}}} \qquad (3.29)$$

$$\zeta_i = \frac{\mathrm{Im}(\overline{W}_{ci})}{2\sqrt{\overline{W}_{mi}\overline{W}_{ki}}} \qquad (3.30)$$

3.3.3 Extraction of ETR from Experimental Data

The modal parameters and associated eigenvectors may be identified through modal testing techniques to get the mass, stiffness, and damping matrices. However, we have to select certain degrees of freedom and then build up the matrices through identified eigenvectors. This process is called modal truncation. Based on the complex energy measurement (**Liang and Lee**, 1991), the extraction of ETR is developed and will be illustrated as follows.

Firstly, the complex eigen-values and eigenvectors of the continuous-time state matrix would be restored by computing the complex frequencies and complex mode shapes of a system. Because there are couples of conjugate pairs, only one pair would be necessary for calculation. Based on this consideration, the complex frequencies, Λ_1, and complex mode shapes, P_1 can be assembled as the following matrix formation.

$$\Lambda_1 = \begin{bmatrix} \lambda_1 & 0 & ... & 0 \\ & \lambda_2 & ... & 0 \\ ... & ... & ... & ... \\ 0 & 0 & ... & \lambda_r \end{bmatrix}, \qquad P_1 = \begin{bmatrix} \Phi_1 & \Phi_2 & ... & \Phi_r \end{bmatrix} \tag{3.31}$$

Secondly, once the complex frequencies and complex mode shapes have been found, the new eigenvalues and eigenvectors can be calculated according to the following equations.

$$[\Lambda] = \begin{bmatrix} \Lambda_1 & 0 \\ 0 & \Lambda_1^* \end{bmatrix}, \text{ and } \quad [P] = \begin{bmatrix} P_1\Lambda_1 & P_1^*\Lambda_1^* \\ P_1 & P_1^* \end{bmatrix} \tag{3.32}$$

Based on the theory described in Section 2.3.1, the continuous-time similar state matrix can be computed by using the new eigenvalues and eigenvectors in Eq. (3.15). The new similar continuous-time state matrix, $\overline{A_c}$ is shown as follows.

$$\overline{A_c} = [P]\Lambda[P]^{-1} = \begin{bmatrix} -\tilde{C} & -\tilde{K} \\ I & 0 \end{bmatrix} \tag{3.33}$$

Thirdly, the state matrix $\overline{A_c}$ can be divided into four parts: the damping matrix, the stiffness matrix, the unit matrix, and zero matrix. For ETR estimation, the first two part of matrices, the damping matrix $\tilde{C}$ and the stiffness matrix $\tilde{K}$, are most important and should be extracted individually. Normally, the damping matrix should be symmetrical and the off-diagonal elements are negative. However, the estimated damping separated from the estimated state matrix does not satisfy the above conditions due to errors of numerical calculation. For this consideration, the square root average should be applied to modify the state matrix. The formulas to symmetrize the damping are shown in the following.

$$\tilde{D}_{ij} = \begin{cases} C_{ij} & i = j \\ -\sqrt{\left|\tilde{C}_{ij}\tilde{C}_{ji}\right|} & i \neq j \end{cases} \tag{3.34}$$

After the modified damping matrix has been calculated, the estimated state matrix can be modified using the modified damping matrix and the estimated stiffness separated from Eq. (3.33). The new modified state matrix is shown as follows.

$$\hat{A}_c = \begin{bmatrix} -\tilde{D} & -\tilde{K} \\ I & 0 \end{bmatrix} \tag{3.35}$$

Fourthly, the natural frequencies can be obtained by computing the complex frequencies of the new state matrix. On the other hand, the new complex mode shape matrix, $\hat{P}_1$ can be found by computing the eigenvector of the new modified state matrix. Also the eigenvector matrix Q of

the estimated stiffness matrix $\tilde{K}$ can be obtained by eigensystem operation. By substituting both new complex mode shape matrix $\hat{P}_1$ and eigenvector matrix Q into the Rayleigh quotient (Eq. (3.19)), the complex damping ratios can be obtained as:

$$2\omega_i \vartheta_i = \frac{Q_i^T \tilde{D} \hat{P}_{1i}}{Q_i^T \hat{P}_{1i}} \tag{3.36}$$

Because ω_i is very close to ω_{ni}, so the value of $\frac{\omega_{ni}}{\omega_i}$ is very close to 1. ω_i in the Eq. (3.36) may be replaced by ω_{ni}. The damping ratios are divided from the real part of the complex damping ratios. On the other hand, the energy transfer ratios are the imaginary part of the complex ratios.

The whole process can produce not only the typical modal parameters, such as natural frequencies, damping ratios, and mode shapes, but also the newly modal parameters, energy transfer ratios (ETR). The extraction process is summarized as a flowchart and shown in Fig. 3.4.

3.3.4 Previous Results of Using ETR on Damage Detection

It can be shown that ζ_i is the ratio of energy transferred during one cycle to 4π times of the energy of the mode before the cycle. ζ_i can be measured by several methods either locally or globally. Local ETR can detect damage in a small region and global ETR indicates a change of the bridge physical conditions.

Suppose there exists a generally damped structure and a corresponding proportionally damped system with the same mass, and stiffness matrices, all the same damping ratios can always be found. Denoted the i^{th} natural frequency of such a system by ω_{ni}, we have the following relationship:

$$\omega_i = \omega_{ni} \exp(\zeta_i) \tag{3.37}$$

Now, suppose a damage breaks out in a structure. It often does not significantly affect the value of mass, damping, and stiffness. Therefore, both the undamaged structure and the damaged structure can be seen as variants from their corresponding proportionally damped system. Denote the i^{th} natural frequency of the undamaged and the damaged systems by ω_{i0} and ω_{ij} (j demonstrates different damage extent or damage condition), we can write as follows.

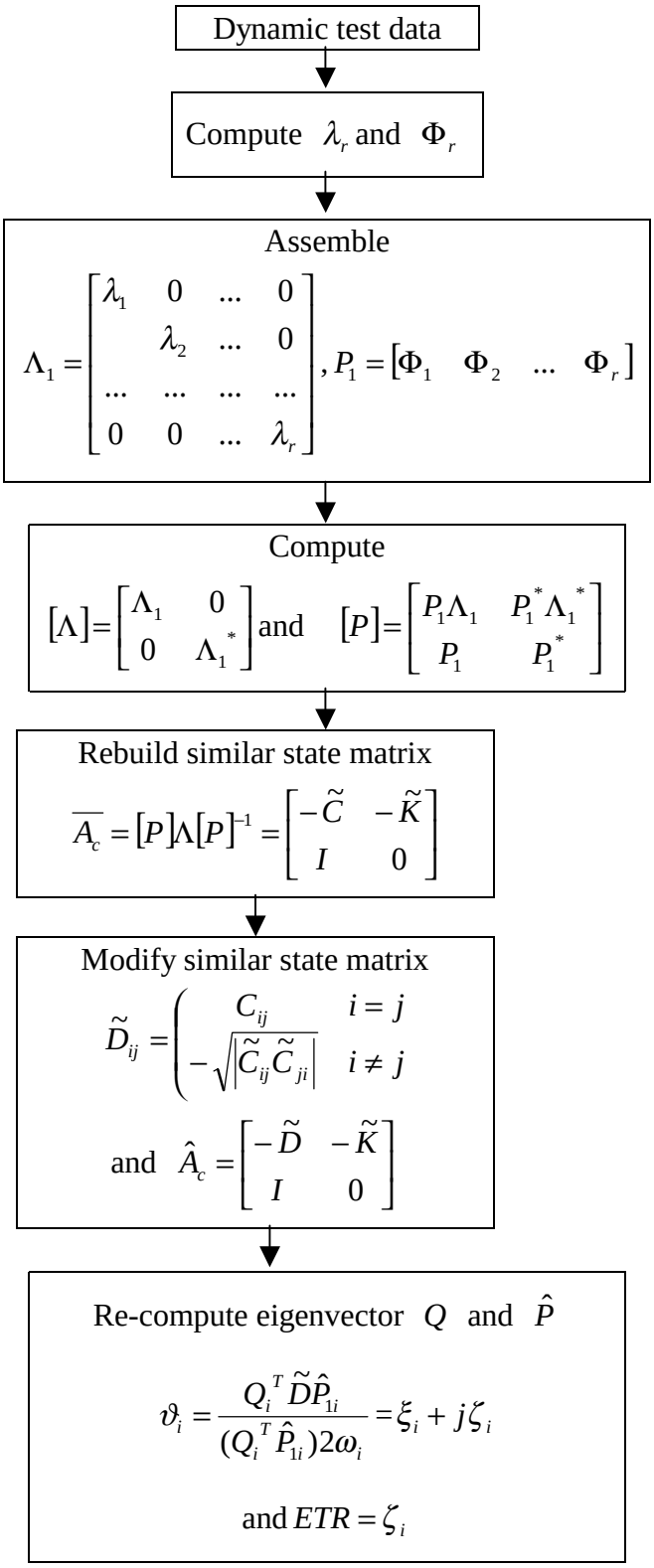

Fig. 3.4 Summary of ETR Extraction Procedures.

$$\omega_{i0} = \omega_{ni} \exp(\zeta_{i0}) \qquad (3.38a)$$

$$\omega_{ij} = \omega_{ni} \exp(\zeta_{ij}) \qquad (3.38b)$$

Now suppose the damage creates a change between ω_{i0} and ω_{ij} by the factor 0.1%, that is to say:

$$\omega_{ij} - \omega_{io} = \frac{\exp(\zeta_{ij}) - \exp(\zeta_{i0})}{\exp(\zeta_{i0})} = 0.1\%$$

If $\zeta_{i0} = 0.001$, then: $\qquad \dfrac{\zeta_{ij} - \zeta_{i0}}{\zeta_{i0}} = 100\%$

It can be seen that the result will be 1000 times more sensitive than the change of natural frequencies due to the damage. Extensive studies (**Lee and Liang** 1999) reveal that the change of ETR is close to 200 percent if a 5% local change of stiffness occurs. The changing of stiffness is used to simulate the "damage", which can only cause about 2% change in natural frequencies, 6% change in damping ratios and 7.5% change in mode shapes. Also ETR can denote the damage location. It has been theoretically demonstrated that ETR is more sensitive to structural damage.

Additionally, **Kong (1996)** demonstrated that ETR was very sensitive to the simulated bearing failure and the deterioration of a girder of a 1:6 scaled composite bridge model. In order to verify and compare the modal energy measurement with other methods, three bridges were measured under ambient and impact excitation by **Lee and Liang (1999).** One was the Peace Bridge (steel bridge) on Niagara River between Buffalo, New York and Fort Erie, Ontario, Canada. The second was a highway bridge on Route 400, New York. The third was a 3-span prestressed concrete box girder bridge on Audubon Parkway, New York. Since there was no real damage existed in these bridges, there were no notable changes in the measured and the baseline signatures. These field tests were intended to establish good measurements repeatability in ETR extraction.

ETR is a modal parameter related to energy dissipation and transfer. Real engineering system belongs to non-proportionally systems. Therefore, energies are not only absorbed by damping but also transferred to damping and ETR exists in real world systems. Estimation of ETR requires frequencies, damping and mode shapes mathematically. In addition, ETR will include energy phenomena and local properties in physical terms. Since ETR is a local and energy parameter, it cannot only identify energy-related damage but also locate damage.

Numerical examples reveal that the ETR is well acceptable under 5% noise (including 5%). Noise effects of real system are not avoided. The ETR may be a good and sensitive damage index. However, since uncertainties in a real system exist, it is impossible to have a perfect simulation to represent a real test. Real challenges for the identification method will be performing the method for real experimental tests, which are problem-dependent. Actual

experimental tests and the applications for damage probes will be presented in the following chapters.

Despite the complex damping theory, structural damage diagnosis by using vibration signatures will be another major concern in this study. A sensitive parameter is an important consideration for this damage approach. For example, modeling and identifying the system, interpreting the relationships between the parameters and dynamic behaviors, and understanding the characteristics of the modal parameters are all necessary to achieve the final results.

Although previous studies have established the possibility that the change of ETR may be used for damage assessment of highway bridges, to establish a direct relationship between various damage patterns and changes of vibrational signatures is not a simple task. Other problems include the ability of ETR to detect non-predetermined damage, the application of ETR approach to concrete slabs and concrete bridges, the identification of severity of bridge damage, etc. There is still a lot to be accomplished to enlarge the ETR applications.

3.4 Modal Analysis Identification Methods

3.4.1 Brief Introduction of Modal Analysis Identification Methods

Once the pre-processing, measurement and signal processing, has been done, the next step for evaluating dynamic characteristics of a system is to perform modal parameters estimation from the measured data. The primary purpose of parameter estimation is to calculate modal parameters, such as natural frequencies, damping ratios, and mode shapes associated with the system to be measured. Many modal analysis packages tend to be mostly black boxes with automatic. However, it is necessary to understand how a black box works. The typical estimation methods are performed in the frequency domain and in the time domain.

In the frequency domain, the objective of parameter estimation is to measure the modal parameters with respect to each resonant peak of the frequency response function. The techniques to extract modal parameters in the frequency domain have been developed for thirty years. Among them, there are half-power points, circle fitting, and polyreference -frequency-domain algorithms, Global rational fraction polynomial method, etc., which can be found in several literatures or papers **(Ewins 1995, Allemang and Brown 1995, as well as Maia and Silva 1997)**. Most of these methods work well provide that there are no closely spaced frequencies or high damping effects to be accounted for. But problems associated with frequency resolution, leakage, and high modal densities led researches to start looking at time domain methods as a promising alternative. In the time domain, the force and response histories are used directly to extract modal parameters. Among those well-known techniques, there are ITD (**Ibrahim time domain)(Ibrahim, 1973, 1976, 1977)**, complex exponential methods **(Brown et. al. 1979)**, Polyreference **(Vold and Rocklin 1982),** the Eigensystem Realization Algorithm (ERA) (**Juang and Pappa, 1985, 1987, 1994**), and Polyreference Complex Exponential method (PRCE) (**Vold, 1982 and Deblauwe 1985**). In general, these methods require high level of computational capacity since they identify vibrational signatures by using

all the data at one time. These methods are referred as off-line time domain identification methods.

Instead of using all the data at one time to estimate vibrational signatures, several recursive (on-line) identification methods were developed by using small fraction of the data each time. After initial estimation is assumed, the estimation begins by using first fraction of data. The estimated results from first running are then used as the initial estimation for the second fraction of data. Theoretically, the estimation will converge to the correct value when more and more data are used. There are six widely used recursive identification methods, namely, Recursive Least Squares Methods, Recursive Instrumental Variable Methods, Vector Autoregressive Moving Average (VARMA (p,q)) model method (**Lardies and Larbi (2001)),** Generalized Least Squares Methods, Prediction Error Method, and Maximum Likelihood Method. Recursive identification methods are more useful for on-line monitoring when longer data record is available, especially, for systems with time-varying parameters or non-stationary characteristics.

In very general terms, time domain models tend to provide the best results when a large frequency range or large number of modes exist in the data, whereas frequency domain models tend to provide the best results when the frequency range is limited and the number of modes is relatively small. However, time domain methods have a major disadvantage in that they can only estimate modes inside the frequency range of analysis, and take no account of the residual effects of modes that lie outside that range. That's the reason, some years ago, people returned to frequency domain techniques, which could improve the accuracy of the results by accounting for residual terms or by increasing the order of the model. On the other hand, people are exploring the feasibility of combining of frequency domain and time domain to identify modal parameters. For example, **Bellizzi, Guillemain, et al. (2001)** presented a new method based on time-frequency representations for identifying the non-linear modal parameters of a multi-degree-of-freedom non-linear lightly damped mechanical system.

In this report, the frequency domain methods and time domain methods are employed to estimate the modal parameters. The methods will be introduced in detail in the following section.

3.4.2 Principles of SDOF Modal Identification Method in Frequency Domain

One way of deriving the dynamic response of a system under any type of excitation, including obviously the periodic and harmonic ones, is by means of the Laplace Transform method. Basically, the Laplace Transform method converts differential equations into algebraic ones that are easier to manipulate. Another great advantage of the method is that it can treat discontinuous functions and automatically take into account the initial conditions. The Laplace Transform of a function $x(t)$, denoted as $X(s)$ is defined as

$$X(s) = \int_0^\infty e^{-st} x(t) dt \qquad (3.39)$$

where is, in general, a complex quantity known as the Laplace variable.
Consider the generalized form of the equation of motion of MDOF systems,

$$[M]\ddot{X}+[C]\dot{X}+[K]X=[f(t)] \tag{3.40}$$

where $[M]$, $[C]$, and $[K]$ are $n\times n$ respectively the mass, damping, and stiffness matrix. $\ddot{X}$, $\dot{X}$, and X are $n\times 1$ vector of time-varying acceleration, velocity, and displacement, respectively, and $[f(t)]$ is an $n\times 1$ vector of time-varying external excitation forces.

Taking the Laplace Transform on each side of Eq. (3.39), and we obtain:

$$\begin{aligned}&[M]\left[s^2X(s)-sx(0)-\bar{x}(0)\right]+[C][sX(S)-x(0)]+[K]X(s)\\&=([M]s^2+[C]s+[K])X(s)-[M]s\,x(0)-[M]\bar{x}(0)-[C]x(0)\\&=F(s)\end{aligned} \tag{3.41a}$$

or

$$([M]s^2+[C]s+[K])X(s)=F(s)+[M]\bar{x}(0)+([M]s+[C])x(0) \tag{3.41b}$$

where $x(0)$ and $\bar{x}(0)$ are the initial displacement and velocity respectively and the right hand side of Eq. (3.41b) can be regarded as a generalized transformed excitation. If the initial conditions are zero, the ratio of transformed response to the transformed excitation can be expressed as follows.

$$H(s)=\frac{X(s)}{F(s)} \tag{3.42a}$$

$$H(s)=\frac{1}{Z(s)}=\frac{1}{[M]s^2+[C]s+[K]} \tag{3.42b}$$

where is known as the system transfer function. If we order $s=j\omega$ in Eq. (3.42a), then we have

$$X(\omega)=H(\omega)F(\omega) \tag{3.43}$$

where $X(\omega)$ and $F(\omega)$ are the response vector and excitation vector in the frequency domain respectively, and $H(\omega)$ is the frequency response function matrix. Its element is shown as

$$H_{ij}(\omega)=\frac{X_i(\omega)}{F_j(\omega)} \tag{3.44}$$

which is the ratio of response value at i coordinate to excitation force at j excitation only.

Similarly, we order $s = j\omega$ in Eq. (3.42b),

$$Z(\omega) = ([K] - \omega^2[M]) + j\omega[C] \qquad (3.45)$$

The real matrix, which satisfies the symmetric property, posses special and very important properties known as the orthogonality properties.

$$\Phi^T[M]\Phi = \begin{bmatrix} \ddots & & \\ & m_r & \\ & & \ddots \end{bmatrix} \qquad (3.46a)$$

and

$$\Phi^T[K]\Phi = \begin{bmatrix} \ddots & & \\ & k_r & \\ & & \ddots \end{bmatrix} \qquad (3.46b)$$

where $\Phi = [\phi_1 \quad \phi_2 \quad \ldots \quad \phi_n]$ is known as the mode shape matrix, k_r and m_r are modal stiffness and modal mass of r^{th} mode (also called generalized stiffness and mass), respectively. We assume that the damping matrix $[C]$ also satisfies the orthogonality properties.

$$\Phi^T[C]\Phi = \begin{bmatrix} \ddots & & \\ & c_r & \\ & & \ddots \end{bmatrix} \qquad (3.46c)$$

and then substitute Eqs. (3.46a), (3.46b), and (3.46c) into Eq. (3.45):

$$Z(\omega) = \Phi^{-T} \begin{bmatrix} \ddots & & \\ & z_r & \\ & & \ddots \end{bmatrix} \Phi^{-1} \qquad (3.47a)$$

where

$$z_r = (k_r - \omega^2 m_r) + j\omega c_r \qquad (3.47b)$$

So the transfer function may be as follows.

$$H(\omega) = Z^{-1}(\omega) = \Phi \begin{bmatrix} \ddots & & \\ & z_r & \\ & & \ddots \end{bmatrix} \Phi^T \qquad (3.48a)$$

and its element may be

$$H_{ij}(\omega)=\sum_{r=1}^{n}\frac{\phi_{ri}\phi_{rj}}{m_r[(\omega_r{}^2-\omega^2)+j2\xi_r\omega_r\omega]} \qquad (3.48b)$$

and

$$\omega_r{}^2=\frac{k_r}{m_r},\quad \xi_r=\frac{c_r}{2m_r\omega_r} \qquad (3.48c)$$

where ω_r, ξ_r and ϕ_r are natural frequency, damping ratio, and mode shape vector of r^{th} mode.

It is not hard to discover that the frequency response of a system with n DOF's equals the linear accumulation of frequency response of n systems with single degree of freedom. The tasks of modal analysis are to measure the elements of frequency response function matrix and to identify the modal model parameters and physical model parameters.

The result that the product of an eigenvector with a scalar multiple is also an eigenvector leads to the important question of scaling or ***normalization*** of eigenvectors. A common and useful approach is to arrange the eigenvector to be normalized such that,

$$\Phi^T[M]\Phi=I_{n\times n} \qquad (3.49a)$$

and

$$\Phi=[\phi_1\quad\phi_2\quad ...\quad\phi_n] \qquad (3.49b)$$

This means that the n generalized masses are all set to unity and have the effect that

$$\Phi^T[K]\Phi=\Lambda \qquad (3.50a)$$

where

$$\Lambda=diag(\lambda_j),\qquad j=1,2,...n \qquad (3.50b)$$

The modal vectors arising from the normalization process are generally called ***normal modes***.

If each modal frequency is not closely spaced, based on Eq. (3.48b), the frequency response function (FRF) can be represented as follows:

$$H_{ij}(\omega)=\sum_{r=1}^{n}{}_rH_{ij}(\omega)\approx{}_rH_{ij}(\omega) \qquad (3.51a)$$

and

$${}_rH_{ij}(\omega)=\frac{\phi_{ri}\phi_{rj}}{m_r[(\omega_r{}^2-\omega^2)+j2\xi_r\omega_r\omega]} \qquad (3.51b)$$

where ${}_rH_{ij}(\omega)$ is the contribution of r^{th} mode to frequency response function. The frequency response function of complex mode is listed in the following:

$$ {}_rH_{ij}(\omega) = \frac{{}_rU_{ij} + j\,{}_rV_{ij}}{2j[\sigma_r + j(\omega - \nu_r)]} - \frac{{}_rU_{ij} - j\,{}_rV_{ij}}{2j[\sigma_r + j(\omega + \nu_r)]} \qquad (3.52) $$

In this part, we will discuss the identification of parameters, such as ν_r, σ_r, ${}_rR_{ij}$, ${}_rU_{ij}$, and ${}_rV_{ij}$, firstly under complex mode condition. In the next section, the identification of mode shapes, and modal mass will be presented.

The frequency response function is listed in Eq. (3.52). Among the range of frequencies where the circle-fitting method is applied, Eq. (3.52) may be similarly presented as follows:

$$ \begin{aligned} {}_rH_{ij}(\omega) &= \frac{{}_rU_{ij} + j\,{}_rV_{ij}}{2j[\sigma_r + j(\omega - \nu_r)]} \\ &= \frac{1}{2}\left[\frac{{}_rU_{ij}(\nu_r - \omega) + {}_rV_{ij}\sigma_r}{\sigma_r{}^2 + (\nu_r - \omega)^2} - j\frac{{}_rV_{ij}(\nu_r - \omega) - {}_rU_{ij}\sigma_r}{\sigma_r{}^2 + (\nu_r - \omega)^2}\right] \\ &= \frac{{}_rR_{ij}e^{j\alpha_r}}{2}\left[\frac{\nu_r - \omega}{\sigma_r{}^2 + (\nu_r - \omega)^2} - j\frac{\sigma_r}{\sigma_r{}^2 + (\nu_r - \omega)^2}\right] \\ &= \frac{e^{j\varphi'}}{\sqrt{\sigma_r{}^2 + (\nu_r - \omega)^2}}\frac{{}_rR_{ij}}{2}e^{j\alpha_r} \end{aligned} \qquad (3.53a) $$

where

$$ \varphi' = \arctan\left(\frac{-\sigma_r}{\nu_r - \omega}\right) \qquad (3.53b) $$

$$ \alpha_r = \arctan\left(\frac{{}_rV_{ij}}{{}_rU_{ij}}\right) \qquad (3.53c) $$

There are several conclusions from the above formulation:

(1) The diameter of complex mode's circle is proportional to the peak value of parameter ${}_rR_{ij}$. It is not located below the real axle, but it rotates an angle α_r (show in Fig. 3.5).

(2) The curves of real and imaginary part in the frequency response function are not similar with those in real mode condition. The values of ν_r and σ_r will not be determined based on these frequency response curves.

(3) The peak amplitude of frequency response curve is related to the value of ν_r. The

value of σ_r may be determined according to the frequencies ω_1 and ω_2, which are relative to the half-power points (see Fig. 3.6a).

(4) When $\omega = \nu_r$, the maximum value of $\frac{ds}{d\omega}$ may be obtained (see in Fig 3.6b).

In general, there are two methods that may be employed to determine the parameters, such as ν_r, σ_r, ${}_rR_{ij}$. One is the peak amplitude method, and the other is the circle-fitting method.

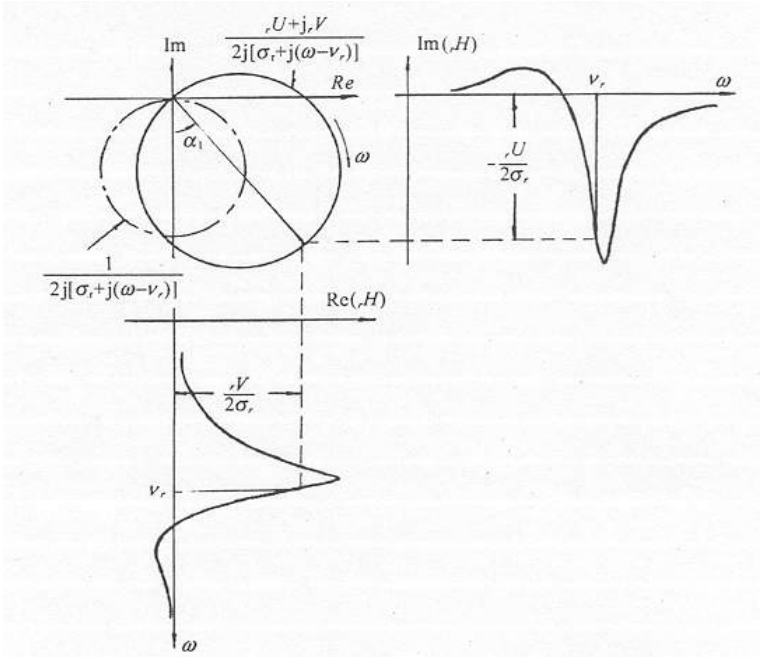

Fig. 3.5 Circle of Complex Mode and Curves of Real and Imaginary Part of FRF.

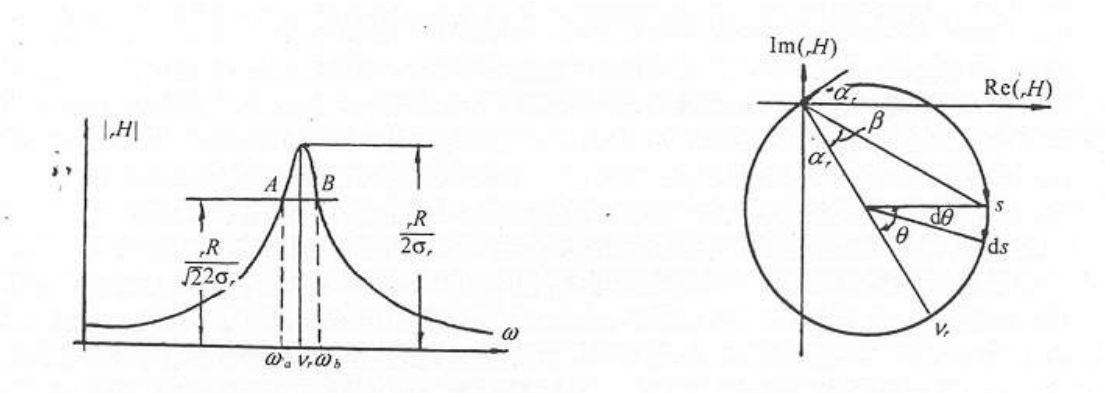

(a) Curve of FRF. **(b) Circle of Complex Mode.**

Fig. 3.6 Curve and Circle.

3.4.3 Modified SDOF Modal Identification Method

In the above section, the effects of other modes on the identified mode were not included. Sometimes, in order to improve the accuracy of the identification, this kind of effects should be considered properly.

According to Eqs. (3.51a) and (3.52), near the value of ν_r, we may obtain:

$$H_{ij} = {}_rH_{ij} - j\frac{{}_rL_{ij}}{\omega} + {}_rZ_{ij} \tag{3.54}$$

where the second part represents the effects of each mode before r^{th} mode, and the third represents the effects of each mode after r^{th} mode. Where there is the narrow range of frequency near ν_r, the change of frequency ω is very small, and the second part in Eq. (3.54) does not change with that of frequency ω.

$$\begin{aligned} H_{ij} &= {}_rH_{ij} + {}_rZ_{ij} - j\,{}_rB_{ij} \\ &= \frac{{}_rR_{ij}e^{j\alpha_{rij}}}{2j[\sigma_r + j(\nu_r - \omega)]} + {}_rZ_{ij} - j\,{}_rB_{ij} \end{aligned} \tag{3.55}$$

For the real mode condition, there is $\alpha_{rij} = 0$, and the peak amplitude method may be employed to extract the parameters, such as ν_r, σ_r, and ${}_rR_{ij}$. For the complex mode condition, only the circle-fitting method may be applied. The details will be presented as follows.

Ⅰ. The Circle-Fitting Method

In general terms, the center of circle is assumed at $(\frac{-a}{2}, \frac{-b}{2})$, and the circle may not go through the original point of coordinate system. Then the formula of circle is:

$$(x + \frac{a}{2})^2 + (y + \frac{b}{2})^2 = d^2 \tag{3.56a}$$

or

$$x^2 + y^2 + ax + by + c = 0 \tag{3.56b}$$

where

$$d^2 = (\frac{a}{2})^2 + (\frac{b}{2})^2 - c \tag{3.57c}$$

Just like the above section, the least square method is employed and we may obtain that:

$$\begin{bmatrix} a \\ b \\ c \end{bmatrix} = \begin{bmatrix} \sum_{i=1}^{m} x_i^2 & \sum_{i=1}^{m} x_i y_i & \sum_{i=1}^{m} x_i \\ \sum_{i=1}^{m} x_i y_i & \sum_{i=1}^{m} y_i^2 & \sum_{i=1}^{m} y_i \\ \sum_{i=1}^{m} x_i & \sum_{i=1}^{m} y_i & m \end{bmatrix}^{-1} \begin{bmatrix} -\sum_{i=1}^{m} (x_i^3 + x_i y_i^2) \\ -\sum_{i=1}^{m} (x_i^2 y_i + y_i^3) \\ -\sum_{i=1}^{m} (x_i^2 + y_i^2) \end{bmatrix} \tag{3.58}$$

where i represents the measurements while $\omega = \omega_i$, and m represents the measured points in the circle.

Ⅱ. Extraction of Parameters v_r, σ_r, and ${}_r R_{ij}$

We may determine the value of v_r according to the principle that $\frac{ds}{d\omega}$ taken as maximum value. Once v_r is determined, the value α_r may be determined by connecting a line from the location of v_r through the center of the circle. The angle between the line and the vertical axle is α_r. Furthermore, several measured points may be selected before and beyond the point v_r to calculate the σ_r, based on the following formula:

$$\sigma_r = \frac{\omega_2 - \omega_1}{\tan\frac{\beta_1}{2} + \tan\frac{\beta_2}{2}} \tag{3.59}$$

More attention should be paid on the accuracy and stability of σ_r. If errors among the values of α_r from different points are smaller than 4 to 5%, the results are acceptable. The value of ${}_r R_{ij}$ may be determined as follows

$${}_r R_{ij} = 2\sigma_r d \tag{3.60}$$

3.5 Theoretical Basis of Correlation Method in Ambient Signal Processing

The cross-correlation function between two response measurements which result from an unknown white excitation has a decaying form and this decaying signal has the same vibrational signatures as the original system. After the cross-correlation functions of ambient

responses are obtained, the traditional time domain system identification techniques, such as Polyreference method (see Appendix C) can be used on these free-decaying cross-correlation functions to estimate the vibrational signatures of the original system.

Consider a general n-DOF, linear time-invariant system, with equation of motion written as follows:

$$[M]\ddot{X}(t+\tau)+[C]\dot{X}(t+\tau)+[K]X(t+\tau)=f(t+\tau) \tag{3.61}$$

Pre-multiplying Eq. 3.61 by $x_1(t)$, a reference coordinate, integrating from 0 to T, and taking the limit as T trends to infinity:

$$\begin{aligned}&\lim_{T\to\infty}\frac{1}{T}\int_0^T x_1(t)[M]\ddot{X}(t+\tau)dt+\lim_{T\to\infty}\frac{1}{T}\int_0^T x_1(t)[C]\dot{X}(t+\tau)dt\\&+\lim_{T\to\infty}\frac{1}{T}\int_0^T x_1(t)[K]X(t+\tau)dt=\lim_{T\to\infty}\frac{1}{T}\int_0^T x_1(t)f(t+\tau)dt\end{aligned} \tag{3.62}$$

Theoretically, differentiation and integration can be interchanged if the integrals in Eq. (3.62) converge uniformly. In practice, we have found that under regularly controlled testing conditions, the signals picked up from field tests and lab experiments will roughly satisfy the interchange requirements.

$$\begin{aligned}&[M]\frac{d^2}{d\tau^2}\lim_{T\to\infty}\frac{1}{T}\int_0^T x_1(t)X(t+\tau)dt+[C]\frac{d}{d\tau}\lim_{T\to\infty}\frac{1}{T}\int_0^T x_1(t)X(t+\tau)dt\\&+[K]\lim_{T\to\infty}\frac{1}{T}\int_0^T x_1(t)X(t+\tau)dt=\lim_{T\to\infty}\frac{1}{T}\int_0^T x_1(t)f(t+\tau)dt\end{aligned} \tag{3.63}$$

Eq. (3.63) can be written in the compact form

$$[M]\ddot{R}_{x_1X}(\tau)+[C]\dot{R}_{x_1X}(\tau)+[K]R_{x_1X}(\tau)=R_{x_1f}(\tau) \tag{3.64}$$

where $R_{x_1X}(\tau)$ and $R_{x_1f}(\tau)$ are cross-correlation functions, and list as follows.

$$R_{x_1X}(\tau)=\lim_{T\to\infty}\frac{1}{T}\int_0^T x_1(t)X(t+\tau)dt \tag{3.65}$$

$$R_{x_1f}(\tau)=\lim_{T\to\infty}\frac{1}{T}\int_0^T x_1(t)f(t+\tau)dt \tag{3.66}$$

Performing a ***Laplace transform*** on Eq. (3.64), we have

$$(S^2[M]+S[C])+[K])S_{x_1X} = S_{x_1f} \tag{3.67}$$

After that we order $[H]$ as the transfer function.

$$[H]=\frac{1}{S^2[M]+S[C])+[K]}=\frac{S_{x_1X}}{S_{x_1f}} \tag{3.68}$$

Where S_{x_1f} and S_{x_1X} are the output and input functions, respectively. Furthermore, we can write the detailed form:

$$S_{x_1f} = \begin{bmatrix} S_{x_1f_1} \\ S_{x_1f_2} \\ \cdots \\ S_{x_1f_n} \end{bmatrix} = \begin{bmatrix} H^*_{11}S_{f_1f_1} \\ H^*_{12}S_{f_2f_2} \\ \\ H^*_{1m}S_{f_mf_m} \end{bmatrix} \tag{3.69}$$

and

$$S_{x_1X} = \begin{bmatrix} S_{x_1X_1} \\ S_{x_1X_2} \\ \cdots \\ S_{x_1X_n} \end{bmatrix} = \begin{bmatrix} H_{11} & H_2 & \cdots & H_{1m} \\ H_{21} & H_{22} & \cdots & H_{2m} \\ \cdots & \cdots & \cdots & \cdots \\ H_{n1} & H_{n2} & \cdots & H_{nm} \end{bmatrix} \begin{bmatrix} H^*_{11}S_{f_1f_1} \\ H^*_{12}S_{f_2f_2} \\ \\ H^*_{1m}S_{f_mf_m} \end{bmatrix} \tag{3.70}$$

and we have

$$S_{x_1X_i} = \sum_{j=1}^{m} H_{ij}H^*_{ij}S_{f_jf_j}\,, \qquad i=1,2,.....,n \tag{3.71}$$

If the excitation force $f(\tau)$ is white noise, by definition

$$S_{f_jf_j} = S_{jj} = Cons\tan t = C_{jj} \tag{3.72}$$

then

$$S_{x_1X_i} = \sum_{j=1}^{m} H_{ij}H^*_{ij}C_{jj}\,, \qquad i=1,2,.....,n \tag{3.73}$$

We apply inverse Laplace transform to Eq. (3.73)

$$R_{x_1X_i}(\tau) = \lim_{T\to\infty}\frac{1}{T}\sum_{j=1}^{m}\int_0^T C_{jj}h_{ij}(t)h_{ij}(t+\tau)dt \qquad i=1,2,.....,n \tag{3.74}$$

Where $h(t)$ is the impulse response function. Since the integration of the impulse response function has a free decaying form, the cross-correlation functions in Eq. (3.74) between two

measurements will have the decaying form. The traditional system identification methods, like the Polyreference method, can be used to extract modal parameters. In the above analysis, the signal in channel 1, $x_1(t)$, is selected as reference. Multiple channel data can be processed into auto/cross-correlation function by selecting any channel reference. In cases when $f(t+\tau)$ is not white noise, usable data can still be obtained if the magnitude of responses due to non-white part in $f(t+\tau)$ is sufficiently small compared to the response of the initial condition, $R(0)$.

Chapter 4

Model Bridge Testing

To substantiate and apply the theory of modal energy transfer in civil engineering structures, such as bridges, there are two big issues that need to be considered. First, it is necessary to choose one type of bridge in order to carry out the experimental study and further verify the proposed method for bridge damage detection. Based on the study of bridge type and associated damage patterns, the single span slab-on-girder type of highway bridges is selected as our study object. The second issue is to link the vibrational signature to various types of bridge damages. Building and testing a model bridge in the laboratory will provide an opportunity to eliminate the problem of environmental disturbances (for example, temperature, and humidity). At the same time, if a model bridge is used, it will be much easier to control the damage type introduced and its development. This makes it convenient to find the direct relationships between the damage indices and damage patterns.

4.1 Experimental Objectives

The main objective of this experimental program is to study the possible linkage among the bridge damage patterns and the changes of ETR, other indices through vibration testing and static testing of the modal bridge and vibrational signature analysis techniques, as well as parameter identification techniques. Other objectives include: (1) investigation of the possibility of parameter identification according to the measured data; (2) verification of the various damage identification algorithm and computer programs; and (3) engineering application of the proposed damage indices. A 1:6 scale model bridge (a simple span slab-on-girder bridge) was designed and manufactured in the laboratory. The complete set of vibrational signatures was firstly extracted from ambient response signals. This provided the baseline for later damage identification. Then several artificial damage situations were introduced into the model bridge, and the changes of vibrational signatures (including ETR) and static data (including displacement and strain) would be obtained. The combination of static and dynamic response data would be used to validate the proposed methodology of damage detection.

4.2 Bridge Type and Damage Pattern

The National Bridge Inventory contains about 570,000 highway bridges. If we exclude culverts and tunnels for the moment, the inventory still includes about 470,000 bridges. The proportions by superstructure type are shown in Fig. 4.1. Steel bridges outnumber any other types. Steel is followed by concrete, prestressed concrete, and timber. There are a few other types of bridges, such as masonry, iron, and aluminum. Fig. 4.2 presents data about these bridges by type and age. There have been two bridge-building booms one in the post-depression era and the

second in the period when the interstate system was constructed. We also see that the majority of bridges built prior to 1970 were steel bridges (including composite bridges) and that the proportion of prestressed concrete bridges has been increasing steadily. There have also been a small, but steady, number of timber bridges built over the years.

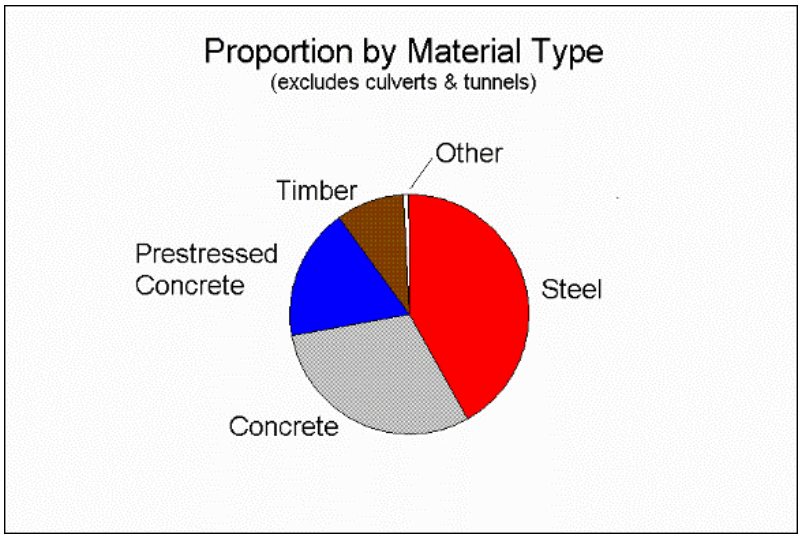

Fig. 4.1 Proportion by Material Type (Excludes Culverts and Tunnels).

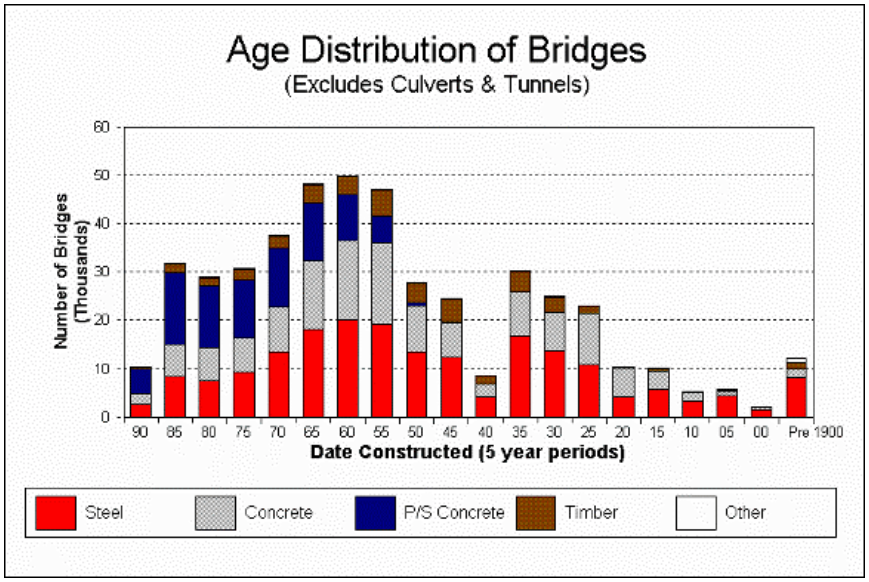

Fig. 4. 2 Age Distributions of Bridges (Excludes Culverts and Tunnels).

Fig. 4.3 shows what the most critical problems are. We can see the proportion by type of all bridges compared to the proportion by type for structurally deficient bridges. A bridge is classified as structurally deficient when it has a poor or worse rating for the condition of the deck, superstructure, or substructure or when its load-carrying capacity is significantly below

minimum standards. This classification includes the most serious types of deterioration.

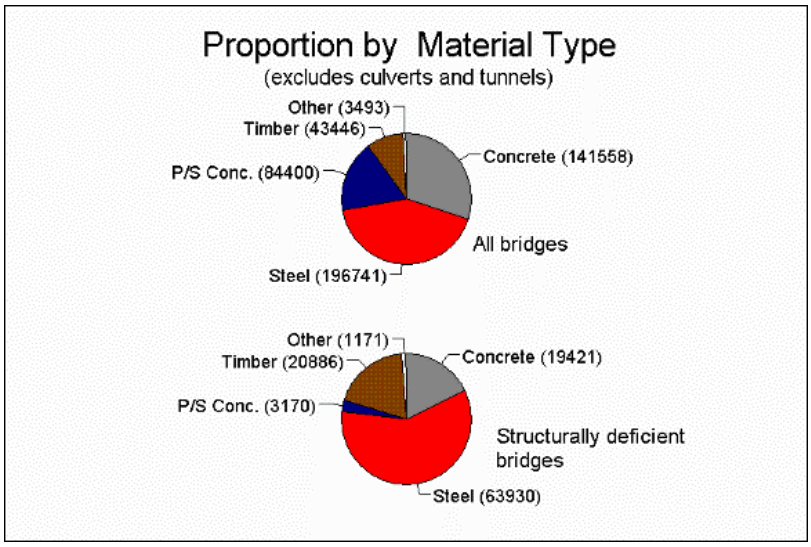

Fig. 4.3 Proportion by Material Type (Excludes Culverts and Tunnels).

There are about 110,000 structurally deficient bridges in the inventory. While steel bridges represent about 40 percent of the overall bridge total, they include about 60 percent of the structurally deficient bridges. The number of structurally deficient reinforced concrete bridges is not comparatively high in the comparison of proportions, and only a relatively small proportion of the prestressed concrete bridges are structurally deficient. Timber bridges, while representing only 9 percent of the entire number of bridges, represent 20 percent of the structurally deficient bridges. About half of the nation's timber bridges are classified as structurally deficient.

Fig. 4.4 indicates this analysis one step further and shows why the bridges of different types are classified as structurally deficient. The primary reason that steel and timber bridges are classified as structurally deficient is a low structural adequacy rating. This means the bridge has a very low load rating. It is also worth noting that steel bridges are structurally deficient more in substructures than in superstructures or decks.

Fig. 4.5 shows the nation's 576,000 bridges, including large culverts and tunnels, by date of original construction. It has the same general shape as figure 2. The black line on the chart shows the percentage of each age group that is classified as structurally deficient or functionally obsolete. The number of deficient bridges steadily increases with age, with 80 percent of those bridges built between 1905 and 1910 classified as deficient. About 1 percent (5,000 bridges) becomes deficient each year.

Today, about 187,000 bridges are classified as deficient. This figure has been reduced somewhat over the past few years, but only after federal bridge funding was increased to approximately 3 billions per year. From the above, we can see that steel girder bridges are commonly used in the United States and are the most vulnerable to deterioration. Steel bridges are more susceptible to aging, thus the need for inspection and maintenance becomes increasingly important. Therefore, in this study, a simple-span slab-on-girder bridge was selected for the purpose of damage

identification.

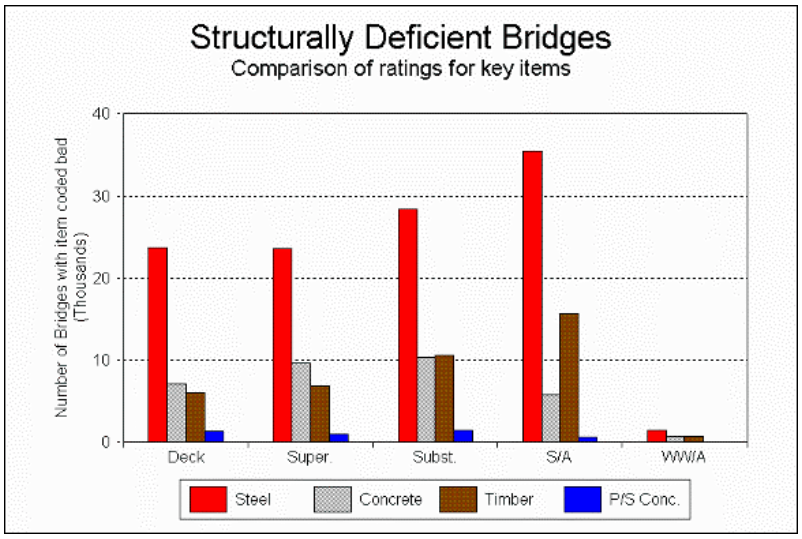

Fig. 4.4 Structurally Deficient Bridges (Comparison of Ratings for Key Items).

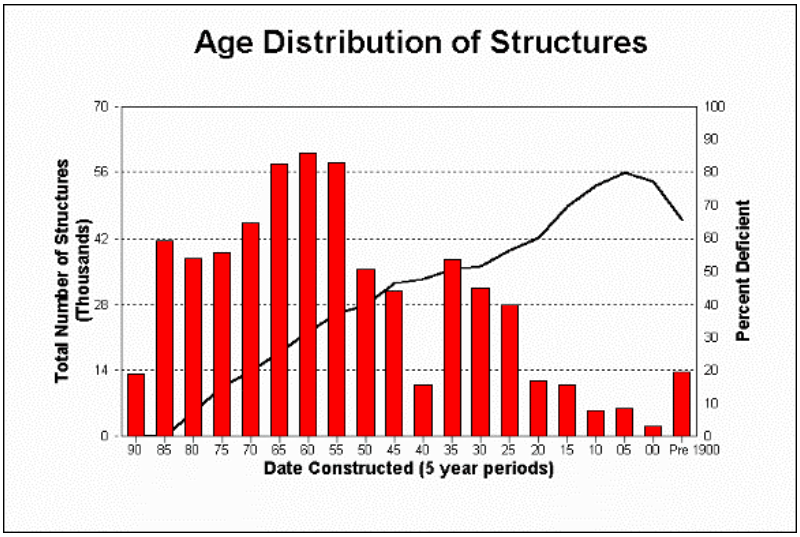

Fig. 4.5 Age Distributions of Structures.

4.3 Design and Modeling of Slab-on-Girder Bridge

4.3.1 Similitude Laws

An experimental scale model must satisfy the necessary similitude requirements. Similitude requirements in the static testing include the physical condition similitude, the geometrical condition similitude, and boundary condition similitude. Besides these three requirements, the dynamic model should satisfy the following two requirements: (a) the similitude of equilibrium equation of the point motion; and (2) the similitude of original condition of the motion. Some

researchers have validated that the factor of strain similitude should equal 1 ($S\varepsilon = 1$) while studying the nonlinear geometric and material problems, seismic and dynamic stability problems, etc. When the model and the experiment could satisfy $S\varepsilon = 1$ and other similitudes, the experimental results of model structure could be prototype structure. All other requirements must be adjusted to satisfy certain relevant scale factors (see Table 4.1).

These requirements would represent a true-scale model in which all length quantities are scaled to the geometric scale factor S_l; materials of the same properties are used in model and prototype ($S_E = 1$ and $S_\upsilon = 1$). The time scale will be $\sqrt{S_l}$, which means that the sample points maintain the same and the interval becomes smaller while the dynamic load being thrown to the model. On the other hand, the effective mass density of the model material must be artificially increased to the value of $1/S_l$.

Non-dimensional material properties, such as Poison's ratio and the damping factor, also have to be considered. Their values should be kept equal in model and prototype if they have a significant effect on the response. Clearly, damping is influential in any dynamic problem, requiring $S_\xi = 1$. This again calls for the use of the same basic materials in model and prototype bridges.

4.3.2 Model Bridge Design

A real single slab-on-girder bridge was selected to be the prototype bridge. The bridge is 60ft long and 30ft-6.5in wide. It is covered by 8in high reinforced concrete deck (pulsing 0.5in wearing surface) and is supported by 4 pieces of W36×150 steel I-beam (E_s=29,000kips/in^2) at the interval of 8ft each (the size of cover steel plate at the bottom flange is 7.3125ft×0.3125ft) (Fig. 4.6). The channel type of diaphragms was placed at the one-third of span and the ends of the girders, totally 4 diaphragms.

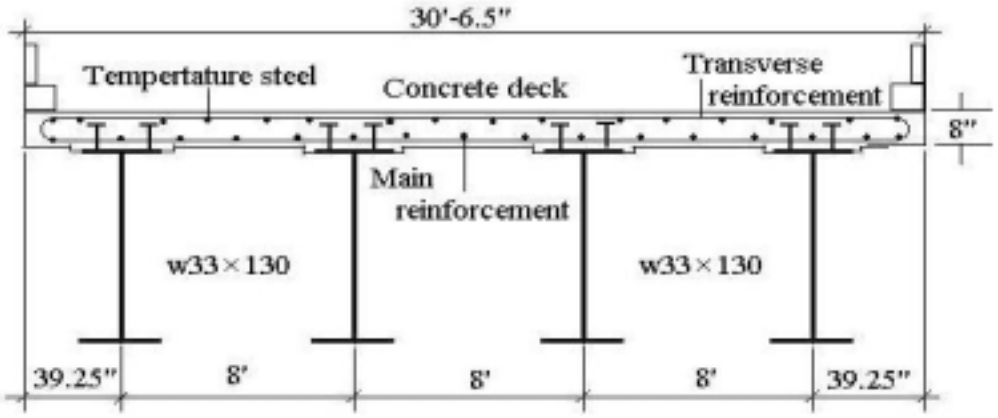

Fig. 4.6 Detailed Transverse Cross-Section of the Prototype Bridge.

Table 4.1 Similitude Theory for Dynamic Testing

Type	Physical Properties	Similitude Relationship	Specification
Material	Strain (ε) Stress (σ) Modulus of Elasticity (E) Poison's ratio (υ) Density of mass (ρ)	$S\varepsilon = 1$ $S_\sigma = S_E$ $S_E = 1$ $S_\upsilon = 1$ $S_\rho = S_\sigma / S_l$	Control parameters in model design
Geometric	Length (l) Displacement (x) Angle (β) Area (A)	S_l $S_x = S_l$ 1 $S_A = S_l^2$	Control parameters in model design
Load	Concentrated load and shear (P) Line load (W) Surface load (q) Moment (M)	$S_P = S_l^2$ $S_W = S_\sigma S_l$ $S_q = S_\sigma$ $S_M = S_\sigma S_l^3$	
Dynamic	Mass (m) Stiffness (K) Damping (C) Time (t) Frequency (ω) Velocity (v) Acceleration (a) Gravity (g) Damping ratio (ξ)	$S_m = S_\rho S_l^3$ $S_K = S_E S_l$ $S_C = S_m / S_t$ $S_t = \sqrt{S_m / S_K} = \sqrt{S_l}$ $S_\omega = 1 / \sqrt{S_l}$ $S_v = S_x / S_t$ $S_a = S_x / S_t^2 = 1$ $S_g = 1$ $S_\xi = S_C / \sqrt{S_K S_m}$	s_m : control parameters in model design s_t 、s_g or s_a : control parameters while dynamic loading

For the slab-on-girder bridge, the placement of the main reinforcement was perpendicular to the direction of the traffic. No. 6 bars at 9 in spacing were selected for the main reinforcement of the slab, and No. 5 bars at 9 in spacing were selected for distribution steel and No. 4 temperature steel reinforcing should be provided at 18in spacing for longitudinal reinforcement. The detailed reinforcement plan is shown in Table 5.2.

The main considerations in selecting the length scale factor were the space availability of the laboratory, the minimum thickness of model concrete deck, the web thickness to accommodate the normal steel plate and the sizes of reinforcing steel wires, and the data acquisition capacity, etc. In this experimental program, the length scale factor is 1:6. The resulting scaled factors, which finally used to build modal bridge, are as follows:

$$S_l = \frac{1}{6};\ S_t = \frac{1}{2.45};\ S_g = 1;\ S_P = \frac{1}{36}; S_\omega = 2.45; S_m = \frac{1}{36}; S_\rho = \frac{1}{6}$$

The steel wires were chosen to simulate the prototype steel reinforcement inside the slab of the prototype bridge. Typically, $\phi 6.5$ bars were used in the scaled concrete slab. The cross-section of scaled modal bridge is demonstrated in Fig. 4.7. The details of diaphragm and the connection of girders are shown in Fig. 4.8.

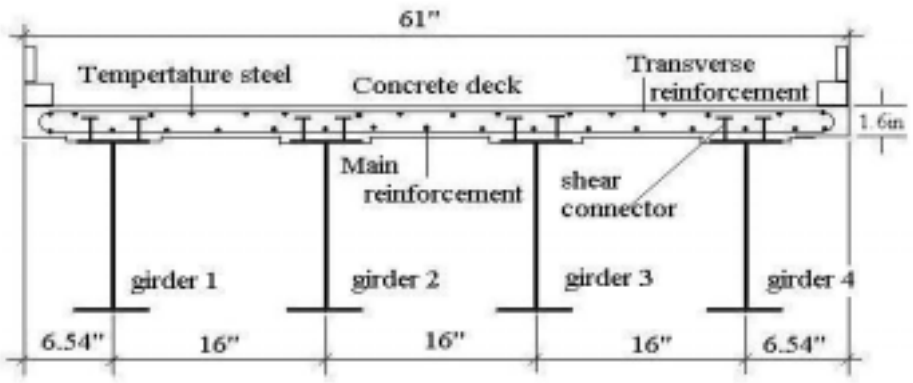

Fig. 4.7 Detailed Transverse Cross-Section of the Model Bridge.

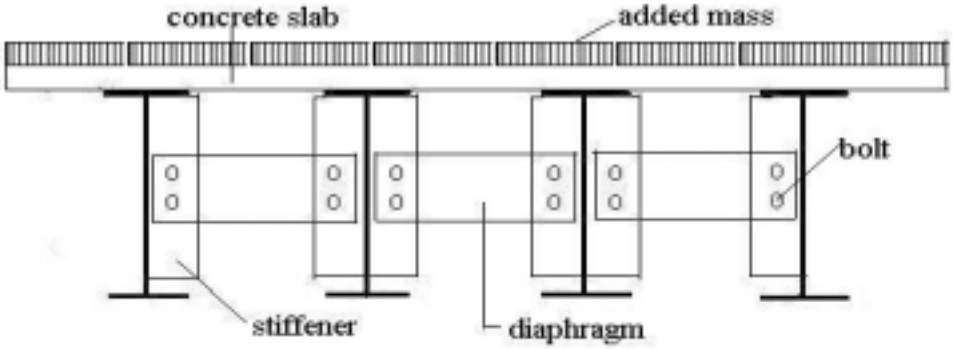

Fig. 4.8 Diaphragm-Girder Connection of the Model Bridge.

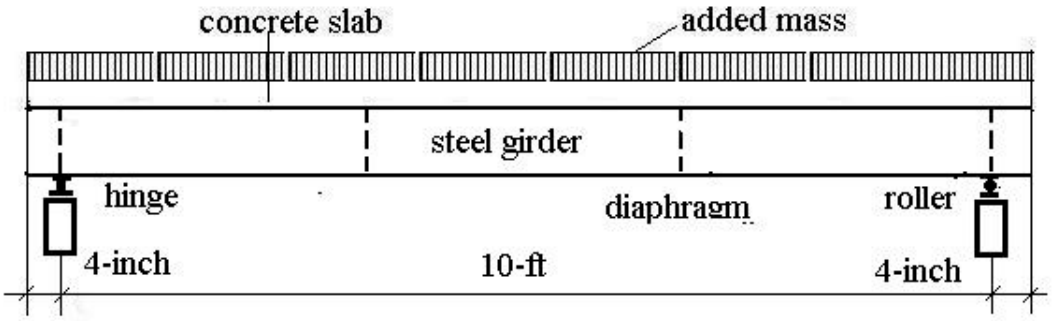

Fig. 4.9 1:6 Scaled Model Bridge.

Table 4.2 Summary of Model Bridge Design

		Prototype	1:6 actual model	Remark
Total length		60 ft	10ft	1. **Shear connector:** Because of thin concrete, the shear connector may be made of reinforcement of G16 with a length of 1 in. 2. **Stiffener:** steel plate with a size of $4.5\times1.8\times0.12$-in. 3. **bolt:** diameter of 12 mm.
Concrete slab		366.5in×8in	61.1in×1.6in	
Steel girder		W33×130	W5.5×4.53	
Cross -section	I_{xx}	6710	6.4913	
	I_{yy}	218	0.241	
	S_{xx}	406	2.225	
	S_{yy}	37.9	0.241	
Diaphragm		C 15×33.9	C2.76×2.32	
Cross -section	I_{xx}	315	0.8293	
	I_{yy}	8.13	0.0823	
	S_{xx}	42	0.600	
	S_{yy}	3.11	0.174	
Interval of girder		8ft	16 in	
Mass		217704.6lb	1315.4lb *	
Concrete strength		C40	C40	
Main reinforcement		No.6 bars	ϕ6.5 bars	
Transverse reinforcement		No.5 bars	ϕ6.5 bars	
Temperature Steel		No.4 bars	ϕ6.5 bars	
Cross-sections of steel girder and diaphragm in the modal bridge		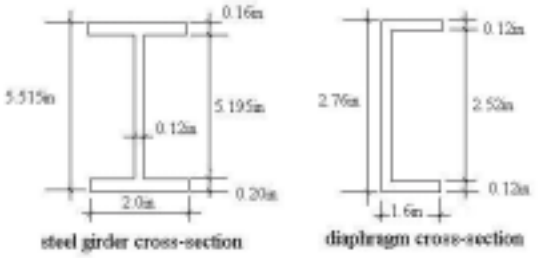		

Note: *: To maintain the mass similitude, the mass of the model was increased to 6 times its self-weight by adding iron or lead blocks.

The whole modal bridge is schematically shown in Fig. 4.9. The properties of the actual model and the prototype bridge are summarized in Table 4.2. The sizes of steel girder are larger than those of the theoretical model because of construction reasons. The cover steel plate at the bottom of lower flange was fused to the lower bottom. To maintain the mass similitude, the mass of model should be increased to 6 times its self-weight (based on the prototype concrete deck and girder) by adding lead or iron blocks.

4.3.3 Damage Simulation for the Model Bridge

There are many types of bridge failure in the field. Bearing failure is quite common after a several earthquake or the settlement of bridge bents. Another failure is the cracking or out-of-plane buckling near the diaphragm and plane plate welding in the steel girders under the normal operational environment. Two types of artificial damages were introduced in the model bridge. The first one was to simulate the loss of a bearing after a severe earthquake or the settlement of bents. The loss of a bearing was simulated by taking a central roller (at girder 2) off, while the other three rollers still remain in their original positions. Another purpose of this study is to investigate the effect of boundary constraint to the changes of modal parameters. The second type of artificial damage is the out-of-plane buckling and cracking of the steel girders near the one-third span where the transverse diaphragm of the modal bridge is connected by welding stiffeners. It is simulated by cutting one exterior girder (girder 1) and one inner girder (girder 3) to 1/2 height of the web from the lower flange by using electric saw near the one-third span (girder 1) and two-third span (girder 3). At the beginning, the cracks were recovered by the cover plates and bolts. Then the extent of damage was simulated by loosening the different number of bolts. The detail of this artificial damage is demonstrated in Fig. 4.10. The combination of damage conditions is shown in Table 4.3.

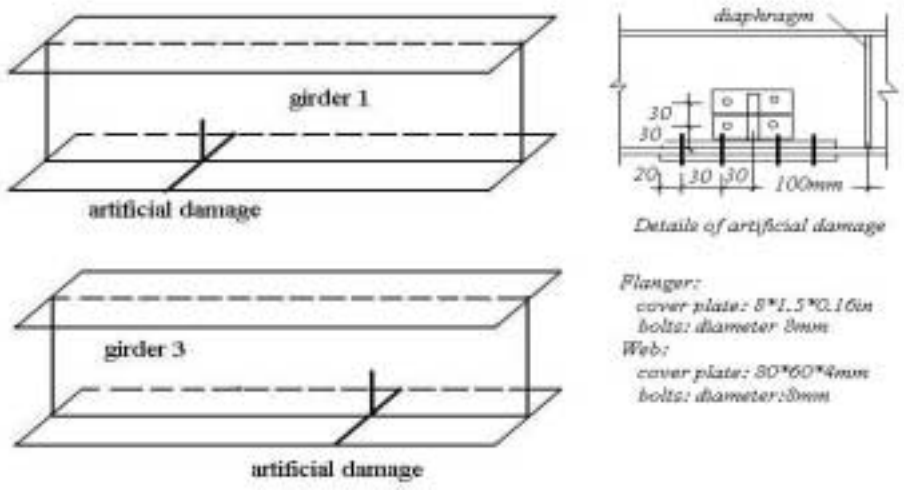

Fig. 4.10 Artificial Damage to Simulate Girder Crack.

Table 4.3 Combination of Damage Condition

Combination	Damage condition	Remarks
Comb1	**Bearing damage**	1. Bolts of Girder 1 were removed firstly and bolts of girder 3 were loosened one by one.
Comb2	**Girder 1 damage**	
Comb2.1	(a) Loosen the bolts in flange	
Comb2.2	(b) Loosen a couple of bolts at web	
Comb2.3	(c) Loosen two couple of bolts at web	
Comb3[1]	**Girder 1 and 3 damage**	
Comb3.1	(a) Loosen the bolts in flange	
Comb3.2	(b) Loosen a couple of bolts at web	
Comb3.3	(c) Loosen two couple of bolts at web	
Comb4	**Bearing and girder 3 damage**	
Comb4.1	(a) Loosen the bolts in flange +bearing	
Comb4.2	(c) Loosen two couple of bolts at web+ bearing	
Comb5	**Bearing, girder 1 and 3 damage**	
	Girder 1 and 3, as well as bearing have complete damage	

4.4 Construction of Slab-on-Girder Bridge Model

4.4.1 Steel Girder

All steel plate should be selected from the same steel materials. They were cut by automatic cutter and then welded by auto-welding machine. The hammer impact on the plate to modify the residue deformation was habited. The dimension of steel girders should be accurate and prefixed at the factory. The stud connectors were welded on the upper flange of steel girder. The bearing plates with dimension of 3x2x0.20-in were not welded to each end of beam. Figs. 4.11 and 4.12 showed the steel frame girders and the reinforcement of the model bridge. Fig. 4.13 showed the details of artificial damage in the model bridge.

Fig. 4.11 Steel Frame Girders.

Fig. 4.12 Reinforcement of the Model.

Fig. 4.13 Details of the Artificial Damage.

4.4.2 Concrete Deck

Because the deck was thin, the holding and installation may be very difficult. So the support system was prepared firstly and then the concrete deck was casted on the steel frame girders. The following showed the casting concrete slab and the model of bridge.

Fig. 4.14 Casting Concrete Slab. **Fig. 4.15 Model of Slab-on-girder Bridge.**

4.4.3 Material Properties

According to the relative national material standards and material testing codes, the concrete cube ($150\times150\times150$-mm^3) strength at 40 days and mechanical properties of steel were summarized in Tables 4.4 and 4.5.

4.5 Experimental Set-up and Data Acquisition System

4.5.1 Testing Content

The dynamic response of a bridge structure under vehicular excitation is a complex phenomenon

due to the interaction between the bridge and vehicles. This kind of interaction is influenced by many parameters, including characteristics of the vehicle and the bridge structure, the vehicle speed, pavement roughness, the number of vehicles and travel paths, etc. The research has revealed that most of the energy associated with traffic load is confined to the frequency range 0-30Hz (for real bridges). In this study, vibration testing (including the ambient excitation and the impulse impact excitation) and static testing were applied on the model bridge. Firstly, special considerations for vibration testing were given to the following factors, namely, the distribution effect of the added mass, the effect of vehicle speed, the effect of selection of window functions, and the effect of excitation locations. Some parameters were then determined for the normal testing. The content of normal testing was summarized in the following:

(1) Vibration testing: the frequency, mode shape, damping ratio. and ETR values.

(2) Static testing: the displacement and strains.

Table 4.4 Mechanical Properties of Concrete

Concrete	Compressive strength (MPa)		Tensile Strength (MPa)		Modulus of Elasticity ($\times 10^4$ MPa)	
	Mean	Std. Dev.	Mean	Std. Dev.	Mean	Std. Dev.
C40	54.4	0.7778	3.54	0.1710	3.004	0.0416

Table 4.5 Mechanical Properties of Steel

Steel Type	Yield Strength (Mpa)		Ultimate Strength (Mpa)		Modulus of Elasticity ($\times 10^5$ MPa)	
	Mean	Std. Dev.	Mean	Std. Dev.	Mean	Std. Dev.
0.12in	252.83	2.5658	382.03	1.4093	2.02	0.0361
0.16in	301	1.7321	444.26	2.3188	2.09	0.0206
0.20in	316.04	0.7805	490.48	1.2071	2.05	0.0227

4.5.2 Measuring Positions

In experimental modal testing, the measurement locations chosen have a major influence on the quality of the results and furthermore influence the reliability of damage identification. Some researchers have proposed optimal sensor locations strategies. Here we made the selection of measurement positions according to experiences.

1 Vibrational Measuring Positions

A total of 25-26 measuring positions were selected to pick up the acceleration response of the model bridge (each condition included the vertical and horizontal arrangement). Position 25

at the girder 1 bearing was selected to be the reference point for all records under cart excitation in order to determine the phase angels and the corresponding mode shape. Under the hammer impact excitation, the energy hammer has a special load cell, which can be connected to the data acquisition system, and it acts as a start switch and the reference point. Meanwhile, the accelerator at reference point can be moved to the bearing damage position. Accelerometers were mounted on the lower flange of each steel girder in the vertical direction and on the web near the lower flange while in the horizontal direction. The instrumentation is shown in Figs. 4.16 and 4.17.

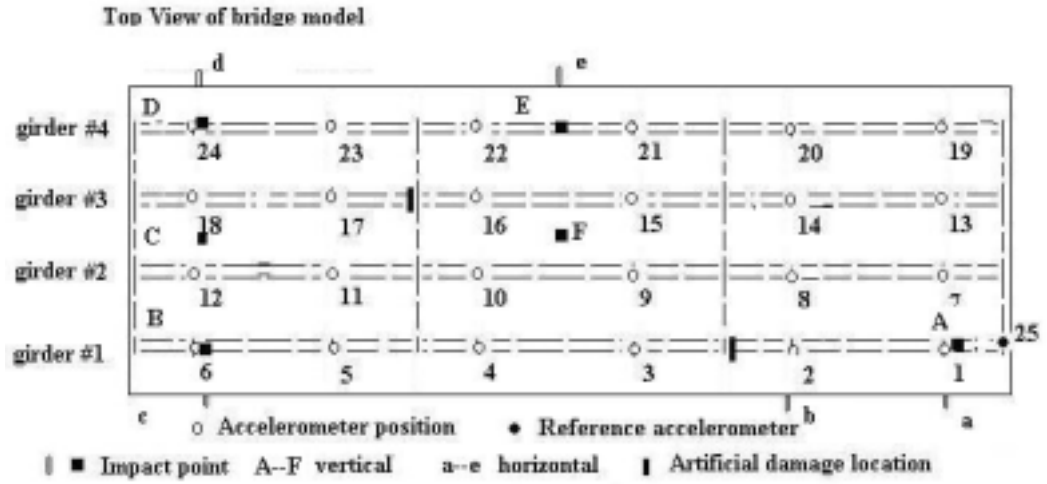

Fig. 4.16 Location of Accelerometers.

(a) Vertical Arrangement **(b) Horizontal Arrangement**

Fig. 4.17 Arrangement of Accelerator.

2 Static Measuring Positions

In order to obtain the static response of the model bridge, deflection and strain were

measured. The deflections at the ends, 1/4 span, mid-span, and 3/4 span of each girder were measured using electronic deflection gages. The strains of cross-sections at 1/4 span and mid-span were also measured by strain gages. The measured positions of deflection and strain are shown in Figs. 4.18 and 4.19.

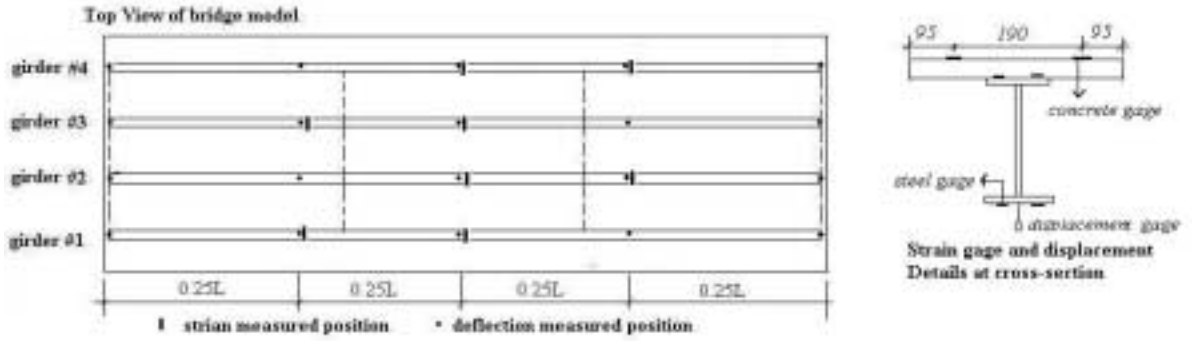

Fig. 4.18 Measured Positions of Deflection and Strain.

Fig. 4.19 Deflection and Strain Measurement of the Model Bridge.

4.5.3 Loading Equipments and Data Acquisition System

1. Loading Equipments

The ambient vibration environment was utilized as the major excitation for bridge condition diagnostics, which would allow field tests to be conducted while the bridge is in service. A model cart was manufactured in the laboratory, which is 1:6 scaled and represents a typical 4-wheel car. The ambient excitation was produced by pulling the cart back and forth across the model bridge to simulate the traffic excitation environment in the real situation (Fig. 4.20). Two bars with guard gear wheel were placed at the end of the steel frame to control the movement path of the cart. The pull and control system included the engine, speed controller, and switch which can control the cart forth and back (Fig. 4.21).

An impact hammer named the energy hammer was used to produce impact excitation. A soft tip was tied on the head of the hammer to minimize the local damage on the model bridge, which could be affected by the impact (Fig. 4.22). The impact hammer included a load cell whose capacity was 125 kN. The maximum impact load of the hammer was 50 kN.

(a) Scaled Cart.

(b) Sided Traffic Line.

Fig. 4.20 Cart Excitation and Traffic Line.

(a) Engine Machine.

(b) Control System.

Fig. 4.21 Pull System and Control System.

(a) Hammer.

(b) Impact at the Center of Bridge.

Fig. 4.22 Hammer.

The static loading on the model bridge was carried by using MTS Loading System with ±250kN capacity actuator (Fig. 4.23). The maximum loading is about 80-100kN at the mid-span. The increment of loading is 10kN. After all tests were finished based on all damaged conditions, the static loading was conducted until the model bridge failed. The load points located the center lines of four girders, that's to say, the model bridge was loaded at four points on the center span.

(a) Control Room of MTS.

(b) Power Station of MTS.

(c) Static Loading on the Model Bridge.

Fig. 4.23 MTS Loading System and Static Loading on the Model Bridge.

2. Data Acquisition System

The dynamic data acquisition was done by INV-series Data Acquisition System (in Fig. 4.24 (a)), which consists of the following parts: (a) 32 Channels A/D Converter, (b) Low-pass Filter, (c) P-III book-computer, (d) and relative data acquisition software and analysis software.

The main features of this data acquisition system include the data-acquisition and data-storage function, simulation of artificial input, segment data storage and display, window function selections, zoom functions, FFTs for data pre-evaluation, and data analysis and treatment, etc. It has been widely used in civil engineering. The accuracy and reliability of this system have been proved by many engineering examples.

The static response data was collected by the 3595 Series IMPs Data Acquisition System, including 200 strain channels (Fig. 4.24 (b)). The whole experiment set-up of the model bridge is shown in Fig. 4.25.

(a) INV Dynamic Acquisition System. **(b) IMP Static Data Acquisition System.**

Fig. 4.24 Data Acquisition System.

Fig. 4.25 Whole Experiment Set-up of the Model Bridge.

4.6 Testing Procedure and Conditions

The vibration testing results combined with relative static data should be used to assess the damage at the same extent of damage for all tests.

4.6.1 Testing Procedure

4.6.1.1 Pre-testing

In order to minimize the errors from the testing process and determine the relative coefficients, it is essential to consider the effects of several factors, for example, the distribution of added mass, vehicular speed, the method and locations of excitation, etc. in vibration testing. On the other hand, the preloading in static testing is necessary for the checking of loading system and data acquisition system. The pre-testing was conducted on the non-damaged model bridge.

1. Distribution of Added Mass

According to the similitude requirements for dynamic testing, certain extra mass was added on the surface of the concrete slab so that the model bridge would have the same stress-strain relationships as the prototype bridge. From this point of view, it would be better to uniformly spread the added mass (iron block) on the concrete slab. Under this situation, the tires of the model cart touched the surface of the lead or iron block, which was covered by cement mortar to smooth the surface, instead of the concrete deck (Fig. 4.25). On the other hand, a non-uniformly distributed mass was spread over the deck in order to simulate the real situation where the tires of the vehicle contact directly on the surface of the concrete deck. In this case, two sides of the deck undertook more weight than the central area (Fig. 4.25 (a)). Then we decided which distribution of added mass would be used for the normal testing.

2. Vehicle Speed

Four different speeds (V=0.34m/s, 0.82m/s, 1.06m/s, and 1.32m/s) were selected to study the effect of speed on the estimation of model parameters. According to results from the vibration testing at different speeds, we determined the vehicle speed for the normal testing.

3. Excitation Locations and Type

In order to control the excitation location under ambient vibration testing, a special guard system was used to force the cart to move along a fixed path. The guardrail was first placed along the centerline of the slab. Because of the iron block on the side of the model bridge, the sided excitation was impossible. But in the formal testing, the excitation locations would include the center and the sided lines. The distance between the centerline and sided line was 470 mm.

Similar tests were conducted using impact excitation to verify the above ambient testing results. The positions at Fig. 4.16 were the impact excitation positions used individually for each impact test.

4. Data Processing

There are many factors related to data processing, which will affect the testing results, such as the type of window function, the length of the window, and the sampling rate, etc. Usually, the sampling rate will not affect the test results significantly if the rate is three to four times higher than the highest frequency to be evaluated. The length of the window can also be determined after the signal resolution (inverse of the sampling rate) and the highest interesting frequency are known. Therefore, only the effect of window functions is studied in this test. Two types of window functions, the rectangular window and the Hanning window functions, which are among the most widely used in practice, were selected as study objects.

5. Static Preloading

After the vibration pre-testing was over, the static preloading was conducted. The maximum preloading is about 80kN. Deflections and strains should be collected. Totally, two preloadings were carried out. The control system and the oil-pressure power system of MTS, as well as data acquisition system should be checked carefully. The data of deflection and strains should also be compared with each other and with the calculation from the elastic-theory.

The pre-testing was conducted from May 8 to 31, 2001.

4.6.2 Normal Testing Conditions

After the necessary coefficients were determined from the pre-testing, the normal testing would be performed. According to the combinations of damage, the static testing was generated first, followed by vibration testing for each testing condition. First of all, the testing was conducted on the non-damaged model bridge, then the damaged model bridge. The tests were conducted in the sequences in Table 4.6 under each testing condition. The normal testing conditions were shown in Table 4.7.

Table 4.6 Sequence of Loading under Each Testing Condition

Date	Sequence	Testing contents	Name of data file	Note
	1. Redistribution of inner force	Removed the bolts or support of bearing		
	2. Static loading	4 points loading at the center of span		Maximum load is 60-80kN
	3. Cart excitation	Sided line		Horizontal arrangement of accelerator
	4. Cart excitation	Center line		
	5. Impact	Horizontal impact		
	6. Impact	Vertical impact		Vertical arrangement of accelerator
	7. Cart excitation	Center line		
	8. Cart excitation	Sided line		

Table 4.7 Conditions of Normal Testing

Experiment	Damage Condition of Model Bridge	Remarks
Expt1	**Non-damage**	
Expt2	**Bearing damage**	*: Bolts of Girder 1were removed firstly and bolts of girder 3 were loosened one by one
Expt3	**Girder 1 damage**	
Expt3.1	(a) Loosen the bolts in flange	
Expt3.2	(b) Loosen a couple of bolts at web	
Expt3.3	(c) Loosen two couple of bolts at web	
Expt4*	**Girder 1 and 3 damage**	
Expt4.1	(a) Loosen the bolts in flange	
Expt4.2	(b) Loosen a couple of bolts at web	
Expt4.3	(c) Loosen two couple of bolts at web	
Expt5	**Bearing, girder 1 and 3 damage**	
	Girder 1, 3 and bearing have complete damage	
Expt6	**Recovery and non-damage**	
Expt7	**Bearing and girder 3 damage**	
Expt7.1	(a) Loosen the bolts in flange +bearing	
Expt7.2	(c) Loosen two couples of bolts at web+ bearing	

4.7 FE Modeling of Slab-on-Girder Bridge Model

The major objectives of FE modeling are in the following: (1) to study the changes of frequencies before and after damages; (2) to study the relationships between the changes of frequencies and the types of damages (bearing damage and girder deterioration); (3) to study the relationships between the changes of frequencies and the single damage or multiple damages; (4) to study the relationships between the changes of frequencies and the extent of damage.

The program **ANSYS 5.5**, a finite element analysis software package, was used to create a detailed three-dimensional analytical model to capture the dynamic behavior of the model bridge. The superstructures were modeled in detail to capture the dynamic of the structure. The shell elements with membrane and plate bending behavior were utilized to model the flange and web of I-beam, the channel diaphragms and girder stiffeners. The block elements were used to model the added iron block because iron blocks were connected to the concrete slab with cement mortar. The mass per unit volume for shell and block element is used respectively. The steel girder bearings were simulated using the “constraint command” in the **ANSYS 5.5** program packages. The material parameters, such as the moduli of elasticity of concrete and steel, were determined according to the material testing results. The calculated frequencies and mode shapes for the undamaged and some damaged model are shown in the following.

4.7.1 FE Model of Intact Condition

The mode shapes are shown in Fig. 4.26.

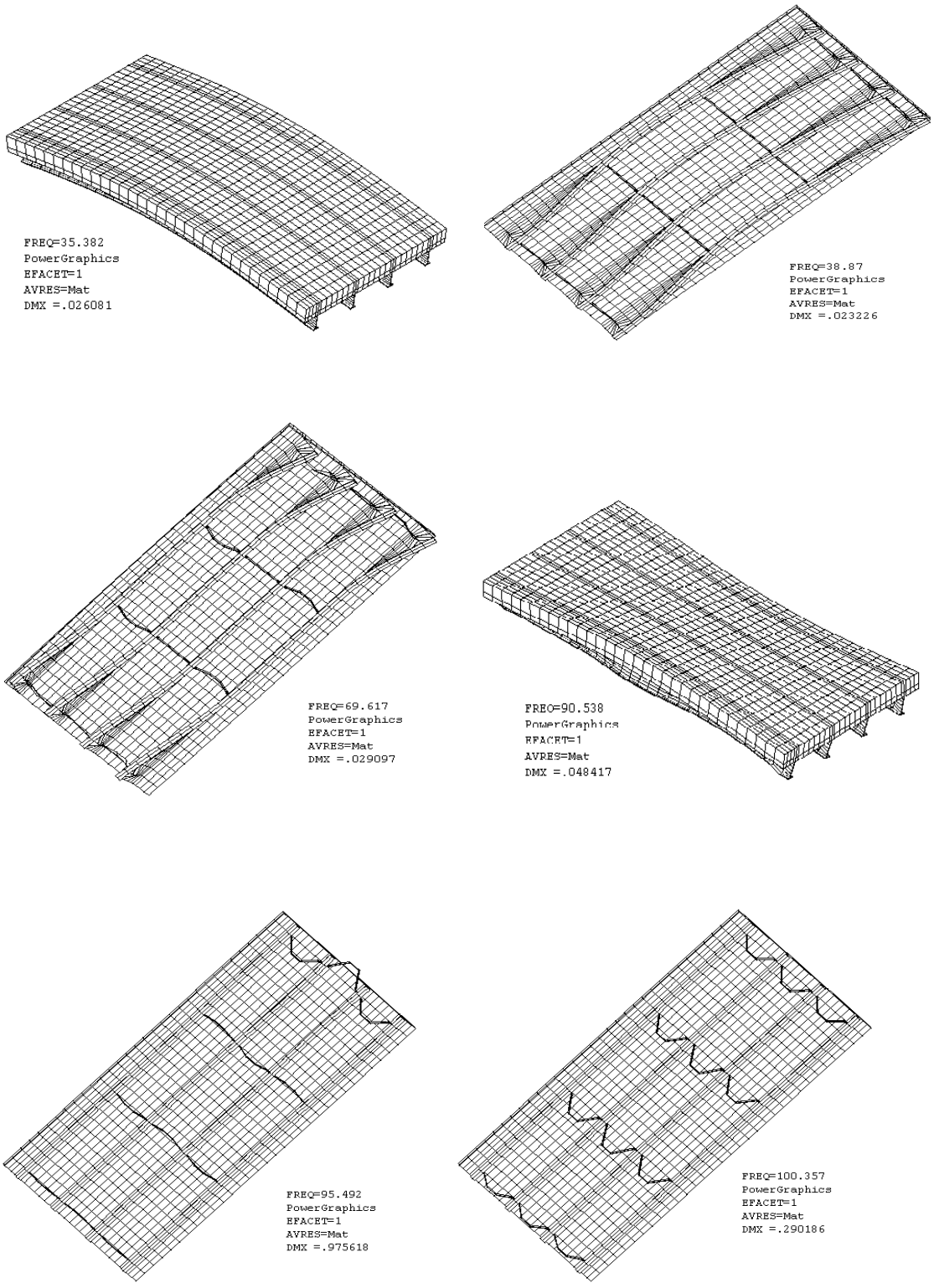

Fig. 4.26 FEM Modeling of Intact Condition Using ANSYS 5.5 Program.

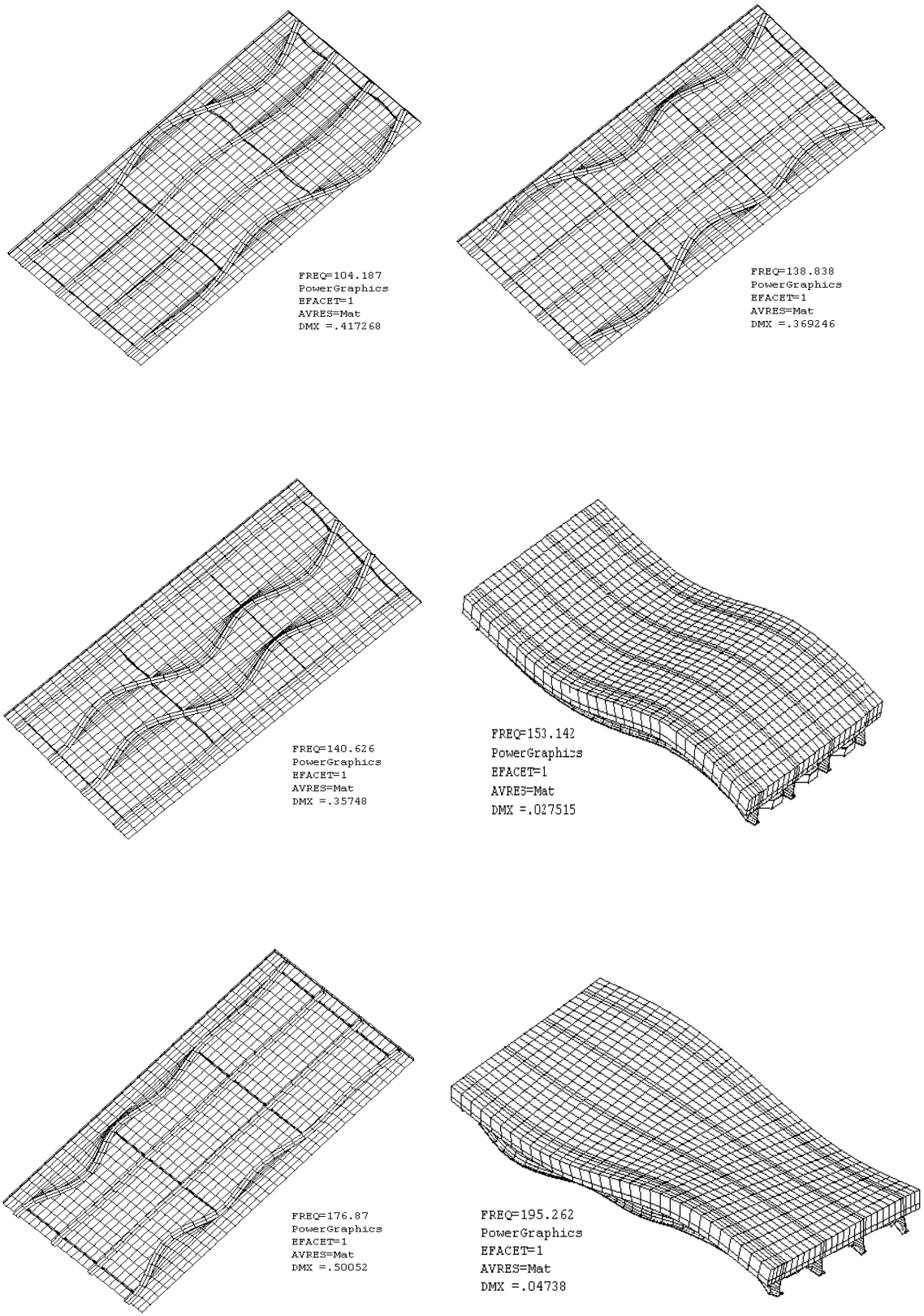

Fig. 4.26 FEM Modeling of Intact Condition Using ANSYS 5.5 Program (continued).

4.7.2 FE Model of Bearing Damage

The bearing damage is simulated such that only the central roller at girder 2 is considered to be seriously damaged, while other bearings are in good condition. The damaged bearing is not restricted, but the intact bearings are modeled by using the constraint command in **ANSYS 5.5** program packages. The mode shapes are shown in Fig. 4.27. The changes in natural frequencies before and after induced bearing damage are listed in Table 4.8. It can be seen that the second and the seventh natural frequencies have experienced much bigger changes before and after bearing damage, while other natural frequencies only have minor changes.

Table 4.8 Frequency Changes before and after Bearing Damage

Mode No.	Frequency at intact condition	Frequency with bearing damage	Differences
No.1	35.382 Hz	35.207 Hz	0.495%
No.2	38.870 Hz	35.891 Hz	8.305%
No.3	69.617 Hz	66.718 Hz	4.164%
No.4	90.538 Hz	87.719 Hz	3.114%
No.5	95.492 Hz	95.078 Hz	0.434%
No.6	100.357 Hz	104.191 Hz	3.820%
No.7	104.187 Hz	117.844 Hz	13.108%
No.8	138.838 Hz	138.844 Hz	0.004%
No.9	140.626 Hz	140.686 Hz	0.043%
No.10	153.142 Hz	157.255 Hz	2.686%
No.11	176.870 Hz	176.880 Hz	0.006%
No.12	195.262 Hz	193.020 Hz	1.148%

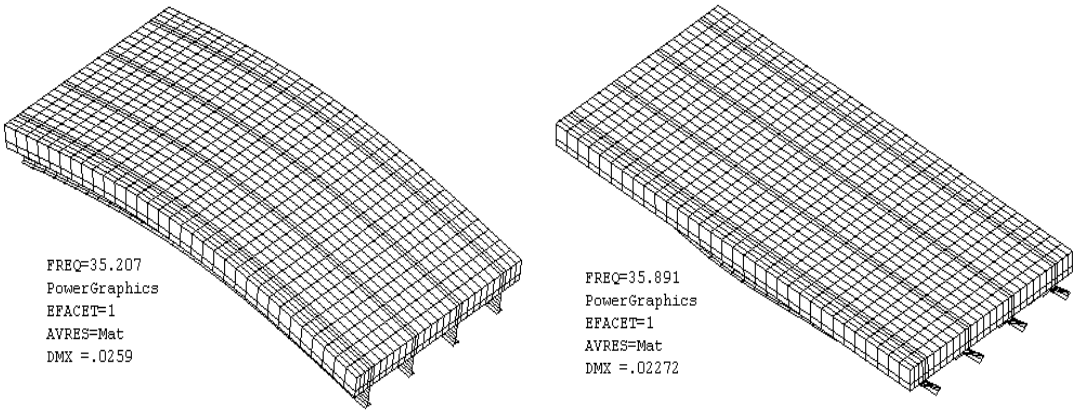

Fig. 4.27 FEM Modeling of Bearing Damage Using ANSYS 5.5 Program.

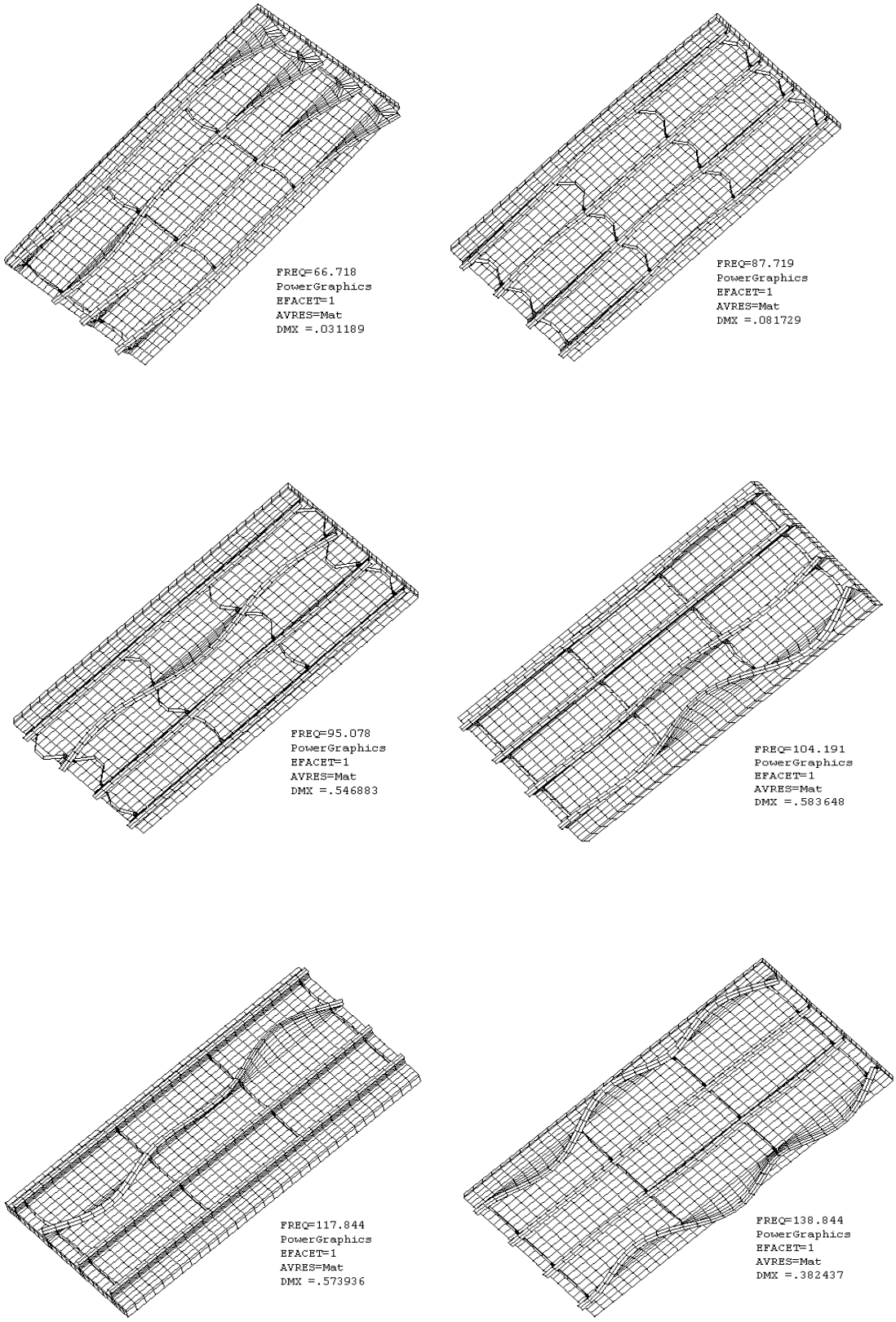

Fig. 4.27 FEM Modeling of Bearing Damage Using ANSYS 5.5 Program (Continued).

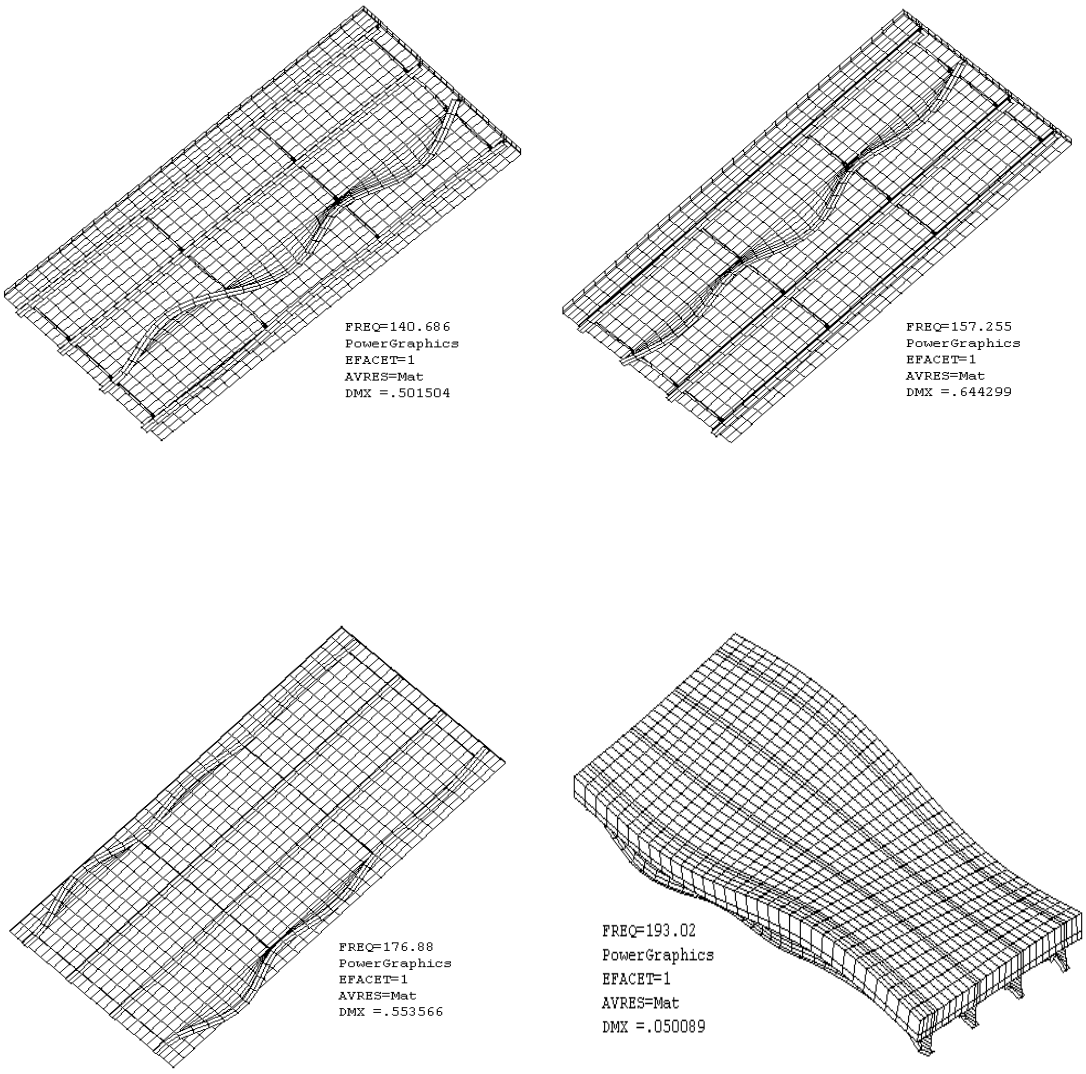

Fig. 4.27 FEM Modeling of Bearing Damage Using ANSYS 5.5 Program (Continued).

4.7.3 FE Model of Girder 1 Cracking in the Modal Bridge

The finite element modeling is to study the changes of natural frequencies before and after girder deterioration. It is well known that natural frequencies are directly proportional to stiffness. The crack damage in the girders is modeled by cutting apart web and flange, and the stiffness of girder is weakened. In the program ANSYS 5.5, the girder is modeled by a number of three-dimension shell elements. The place where the girder is cut is modeled in detail in Fig. 4.28.

The FE modeling results of mode shapes are shown in Fig. 4.29. The FE modeling results of frequency are listed in Table 4.9. It is found that when girder deterioration occurs, the seventh, the eighth, the ninth, and the eleventh natural frequencies have much larger changes, while other frequencies have minimal changes.

Fig. 4.28 the FE Model of Crack in the Girder (under Vibration).

Table 4.9 Frequency Changes before and after Girder 1 Cracking

Mode No.	Frequency at intact condition	Frequency at Girder 1 cracking	Differences
No.1	35.382 Hz	35.296 Hz	0.243%
No.2	38.870 Hz	38.860 Hz	0.026%
No.3	69.617 Hz	69.141 Hz	0.684%
No.4	90.538 Hz	89.489 Hz	1.157%
No.5	95.492 Hz	95.980 Hz	0.511%
No.6	100.357 Hz	100.17 Hz	0.186%
No.7	104.187 Hz	109.23 Hz	4.841%
No.8	138.838 Hz	129.30 Hz	6.869%
No.9	140.626 Hz	134.12 Hz	4.626%
No.10	153.142 Hz	152.73 Hz	0.269%
No.11	176.870 Hz	166.12 Hz	6.078%
No.12	195.262 Hz	192.10 Hz	1.619%

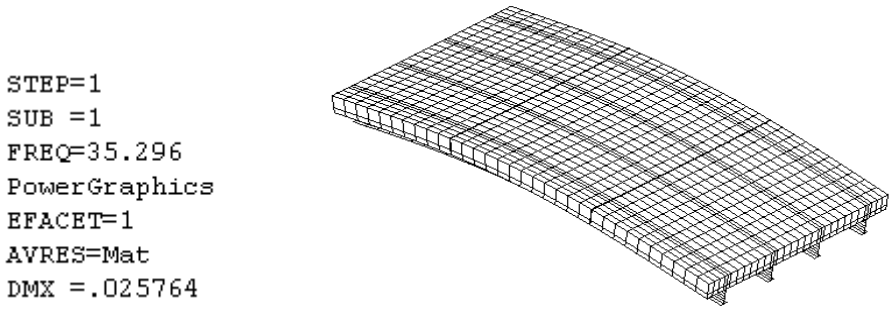

Fig. 4.29 FEM Modeling of Girder 1 Damage Using ANSYS 5.5 Program.

STEP=1
SUB =2
FREQ=38.86
PowerGraphics
EFACET=1
AVRES=Mat
DMX =.020418

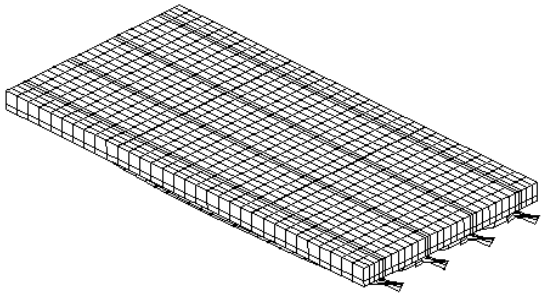

STEP=1
SUB =3
FREQ=69.141
PowerGraphics
EFACET=1
AVRES=Mat
DMX =.028526

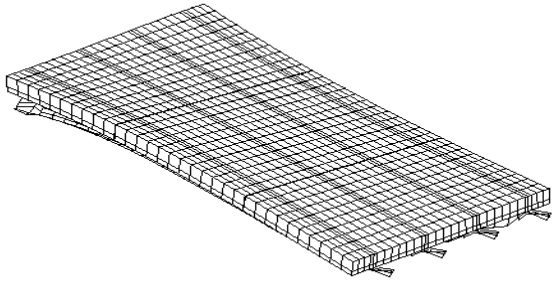

STEP=1
SUB =4
FREQ=89.489
PowerGraphics
EFACET=1
AVRES=Mat
DMX =.04777

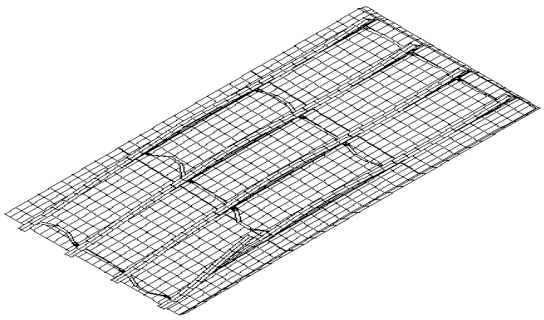

STEP=1
SUB =5
FREQ=95.98
PowerGraphics
EFACET=1
AVRES=Mat
DMX =.965531

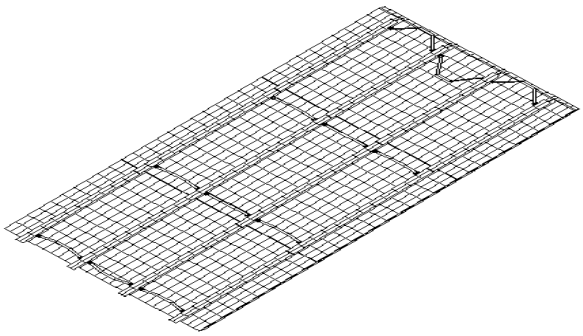

Fig. 4.29 FEM Modeling of Girder 1 Damage Using ANSYS 5.5 Program (Continued).

FREQ=100.17
PowerGraphics
EFACET=1
AVRES=Mat
DMX =.30966

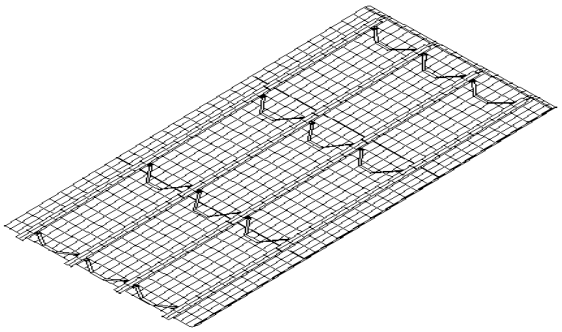

STEP=1
SUB =18
FREQ=109.228
PowerGraphics
EFACET=1
AVRES=Mat
DMX =1.148

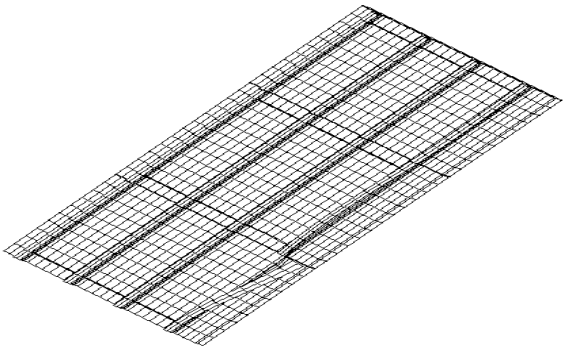

STEP=1
SUB =19
FREQ=129.296
PowerGraphics
EFACET=1
AVRES=Mat
DMX =.598944

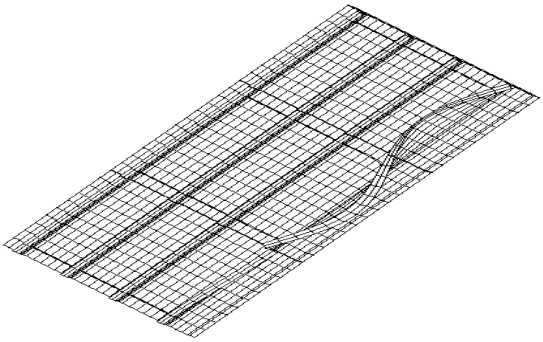

STEP=1
SUB =20
FREQ=134.12
PowerGraphics
EFACET=1
AVRES=Mat
DMX =.661924

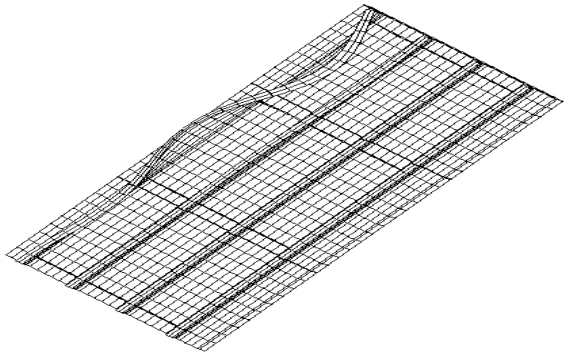

Fig. 4.29 FEM Modeling of Girder 1 Damage Using ANSYS 5.5 Program (Continued).

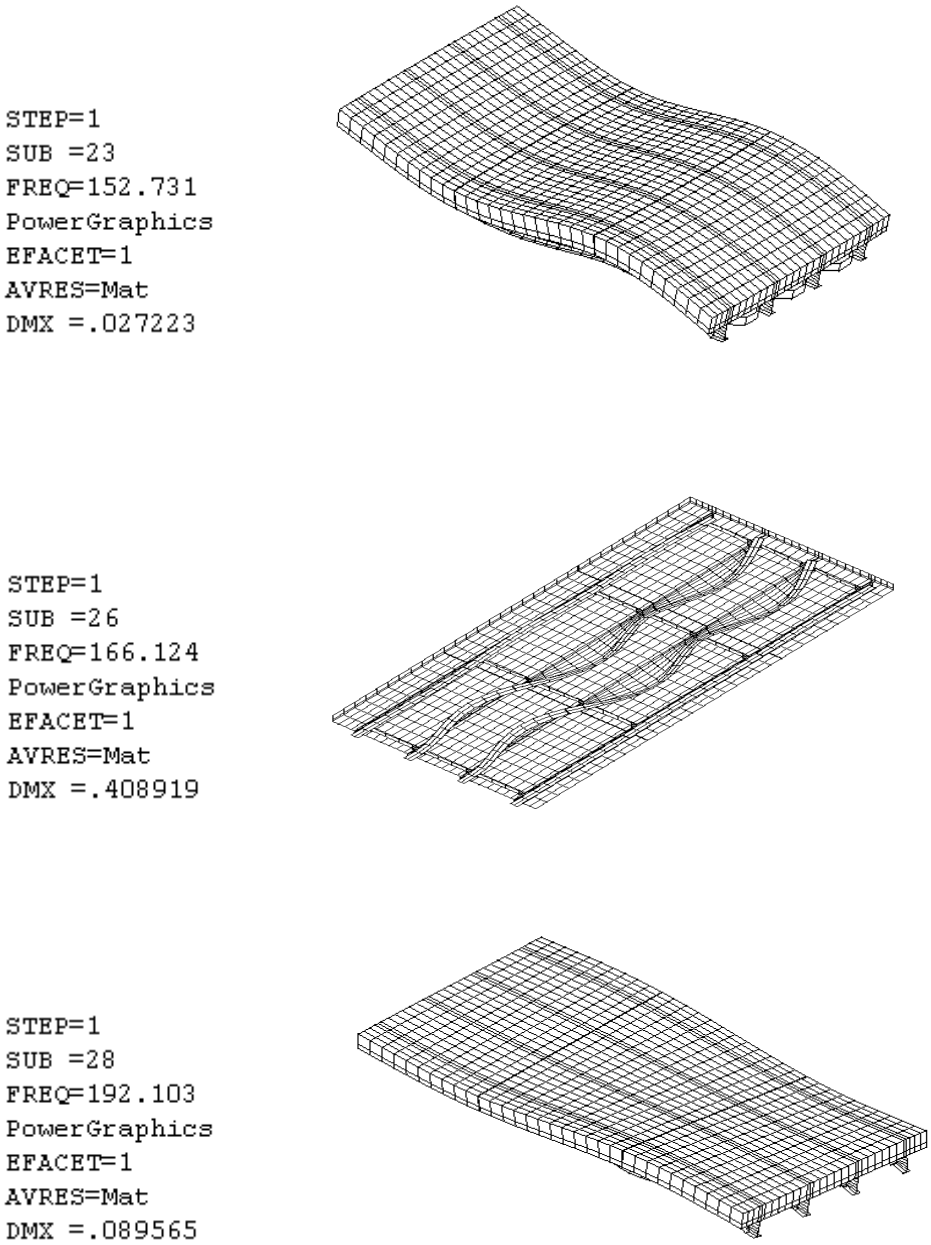

Fig. 4.29 FEM Modeling of Girder 1 Damage Using ANSYS 5.5 Program (Continued).

4.7.4 FE Model of Girder 1 and 3 Damage in the Modal Bridge

When damages in girders 1 and 3 occurred simultaneously, the FE modeling results of natural frequency are listed in Table 4.10 and the FE modeling results of mode shapes are shown in Fig. 4.30. The changes of frequencies are similar with those only due to girder 1 damage, but the changing values are larger than those only due to girder 1 damage.

Table 4.10 Frequency Changes before and after Girders 1 and 3 Cracking

Mode No.	Frequency at intact condition	Frequency at Girders 1and 3 cracking	Differences
No.1	35.382 Hz	35.103 Hz	0.789%
No.2	38.870 Hz	38.856 Hz	0.036%
No.3	69.617 Hz	69.120 Hz	0.714%
No.4	90.538 Hz	89.468 Hz	1.182%
No.5	95.492 Hz	93.794 Hz	1.778%
No.6	100.357 Hz	100.02 Hz	0.336%
No.7	104.187 Hz	109.23 Hz	4.841%
No.8	138.838 Hz	129.30 Hz	6.869%
No.9	140.626 Hz	134.12 Hz	4.626%
No.10	153.142 Hz	152.20 Hz	0.269%
No.11	176.870 Hz	164.24 Hz	7.141%
No.12	195.262 Hz	191.88 Hz	1.732%

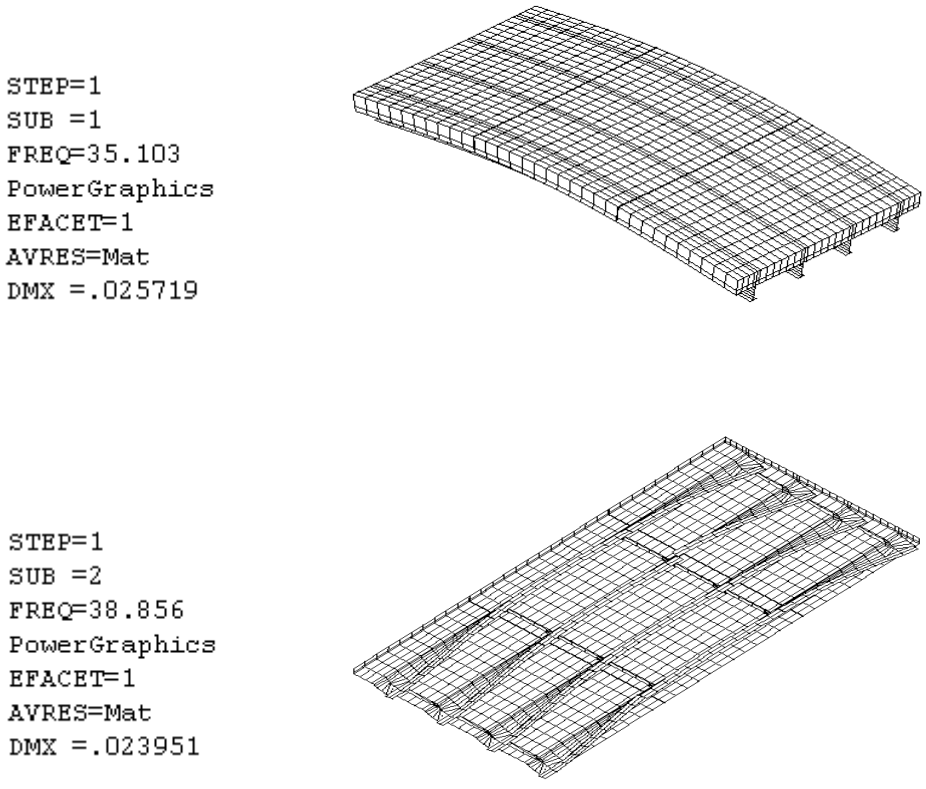

Fig. 4.30 FEM Modeling of Girders 1 and 3 Damage Using ANSYS 5.5 Program.

STEP=1
SUB =3
FREQ=69.12
PowerGraphics
EFACET=1
AVRES=Mat
DMX =.040791

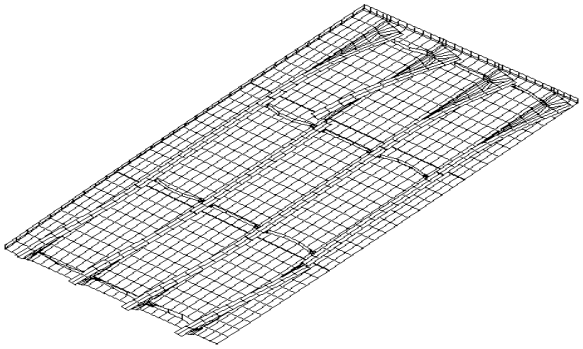

STEP=1
SUB =4
FREQ=89.468
PowerGraphics
EFACET=1
AVRES=Mat
DMX =.047773

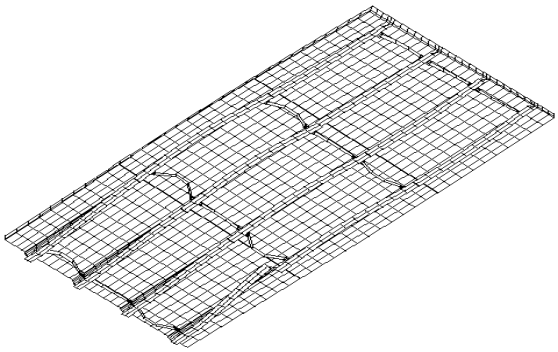

STEP=1
SUB =5
FREQ=93.794
PowerGraphics
EFACET=1
AVRES=Mat
DMX =.93278

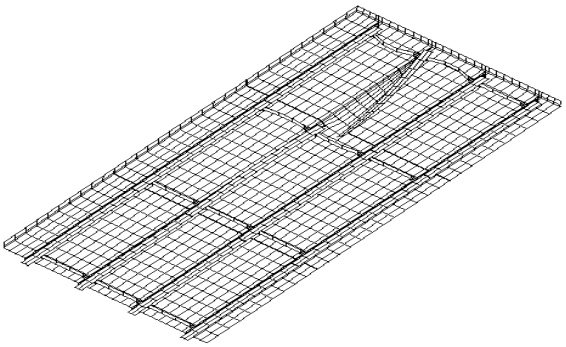

STEP=1
SUB =18
FREQ=100.021
PowerGraphics
EFACET=1
AVRES=Mat
DMX =.32274

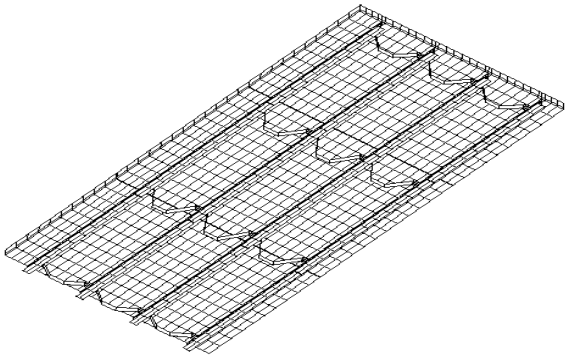

Fig. 4.30 FEM Modeling of Girders 1 and 3 Damage Using ANSYS 5.5 Program (continued).

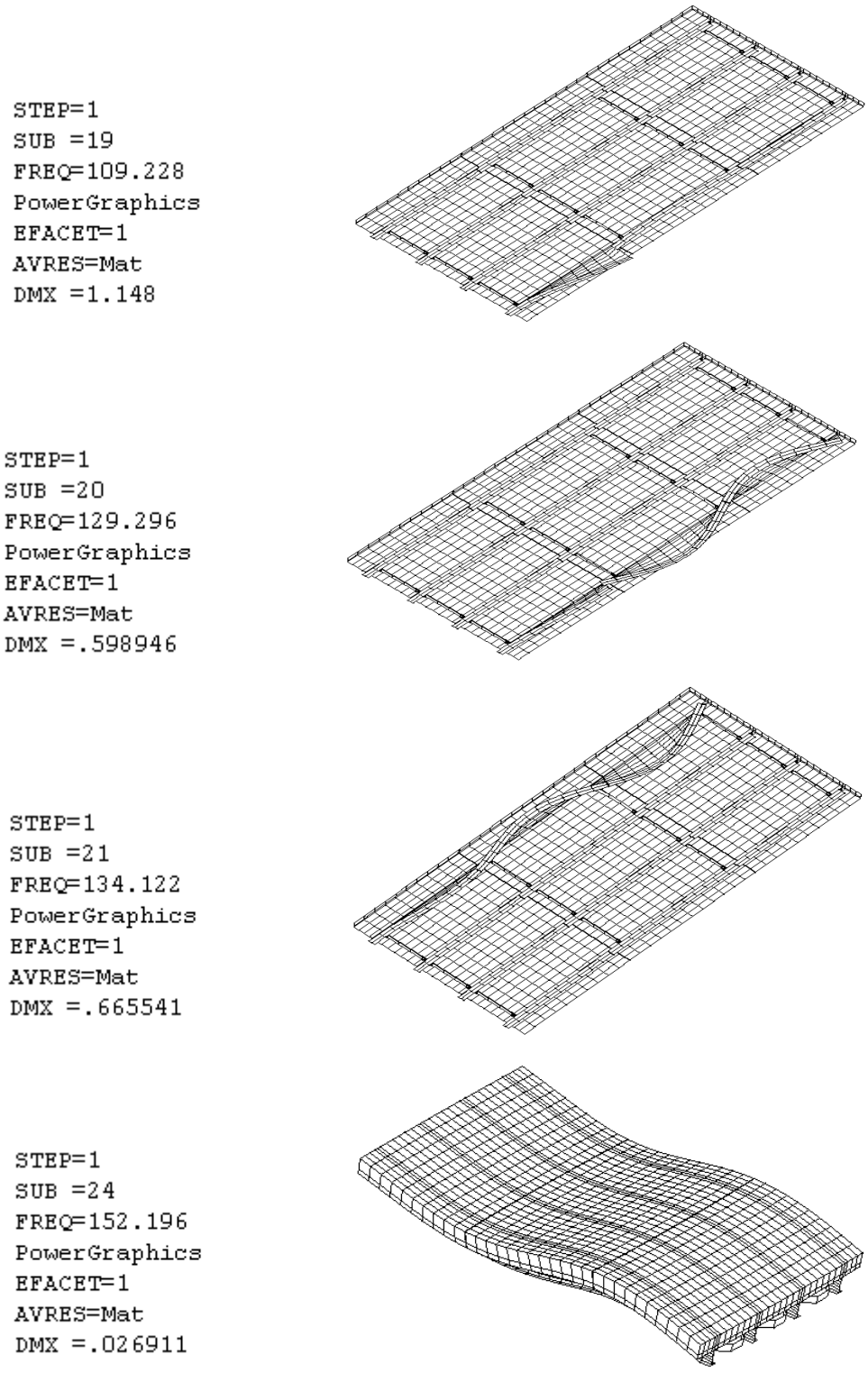

Fig. 4.30 FEM Modeling of Girders 1 and 3 Damage Using ANSYS 5.5 Program (continued).

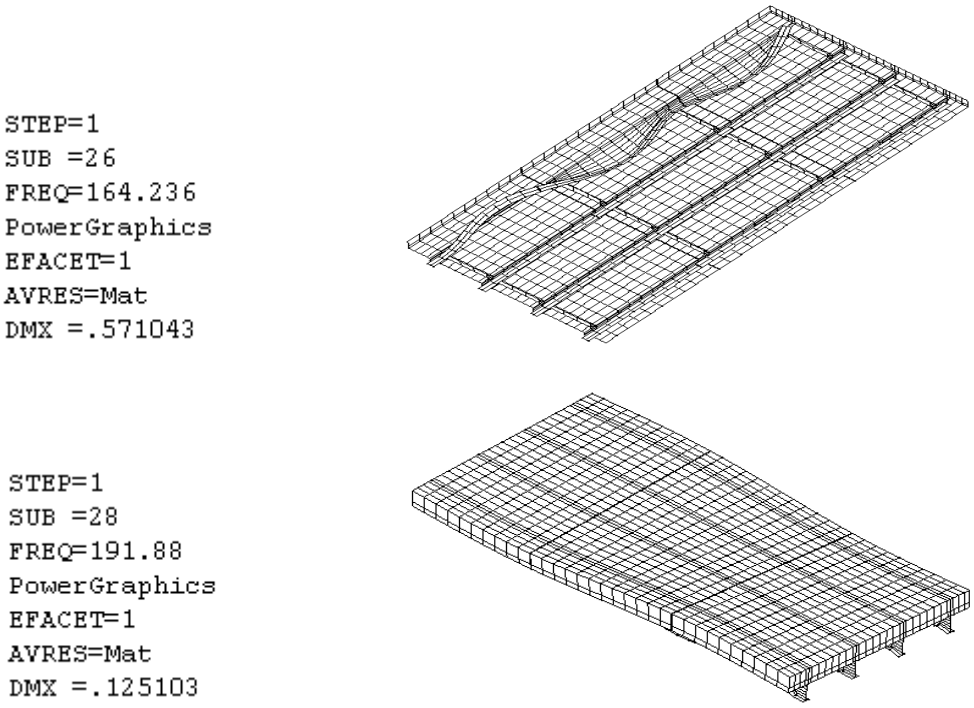

Fig. 4.30 FEM Modeling of Girders 1 and 3 Damage Using ANSYS 5.5 Program (continued).

4.7.5 FE Model of Girder 1 Cracking and Bearing Damage in the Modal Bridge

When damages in the girder 1 and bearing of girder 2 occurred simultaneously, the FE modeling results of natural frequency are listed in Table 4.11, and the FE modeling results of mode shapes are shown in Fig. 4.31. The changes of frequencies are similar those due to girders 1 and 3 damage, but the changing values are larger than those due to girders 1 and 3 damage.

Table 4.11 Frequency Changes before and after Girder 1 and Bearing Damage

Mode No.	Frequency at intact condition	Frequency at Girder 1and bearing damage	Differences
No.1	35.382 Hz	35.116 Hz	0.752%
No.2	38.870 Hz	35.867 Hz	7.726%
No.3	69.617 Hz	66.278 Hz	4.796%
No.4	90.538 Hz	86.494 Hz	4.467%
No.5	95.492 Hz	91.408 Hz	4.277%
No.6	100.357 Hz	98.079 Hz	2.270%
No.7	104.187 Hz	109.23 Hz	4.841%
No.8	138.838 Hz	128.20 Hz	7.662%
No.9	140.626 Hz	134.12 Hz	4.626%
No.10	153.142 Hz	145.39 Hz	5.062%
No.11	176.870 Hz	164.23 Hz	7.146%
No.12	195.262 Hz	190.37 Hz	2.505%

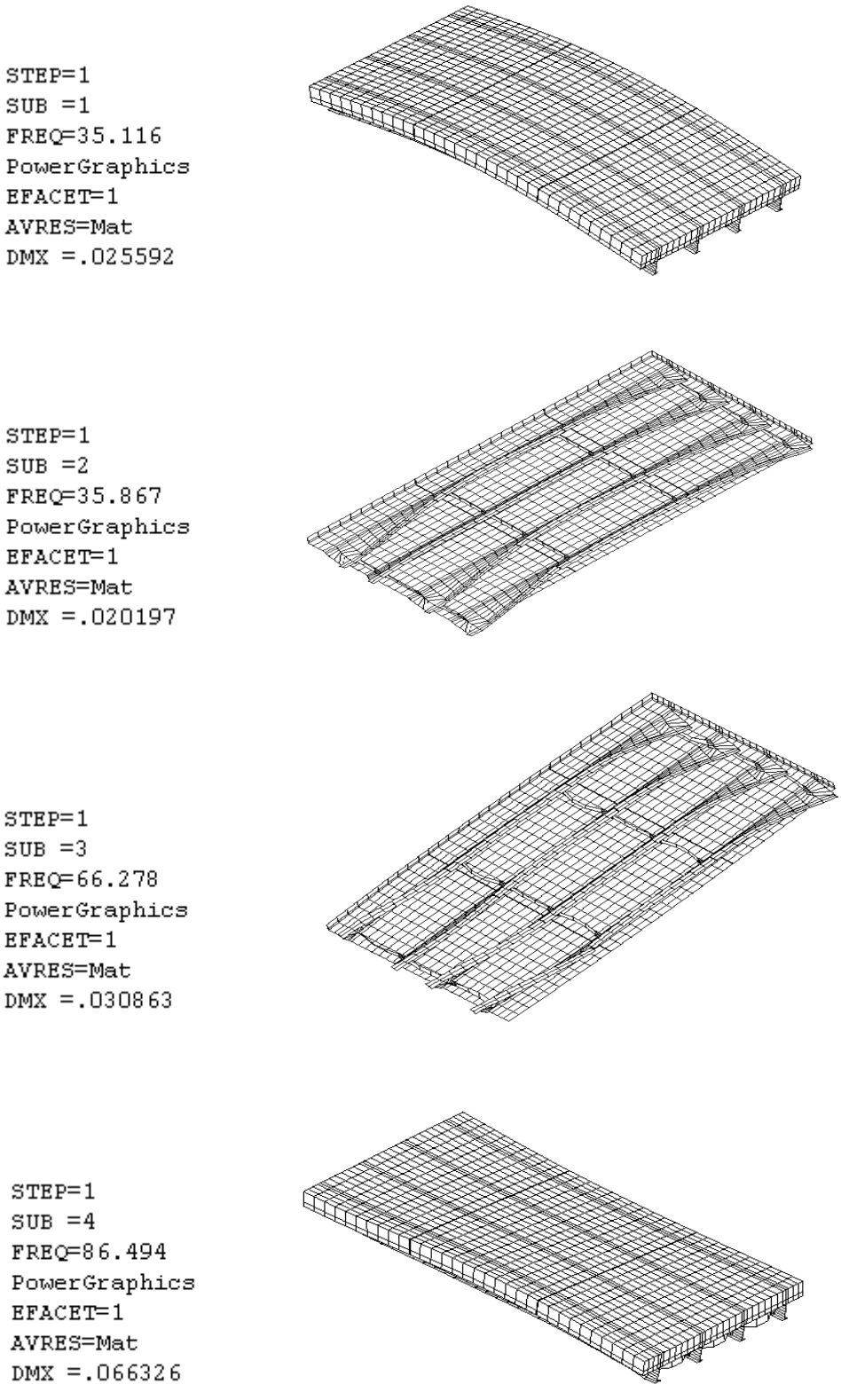

Fig. 4.31 FEM Modeling of Girder 1 and Bearing Damage Using ANSYS 5.5 Program.

STEP=1
SUB =5
FREQ=91.408
PowerGraphics
EFACET=1
AVRES=Mat
DMX =.141403

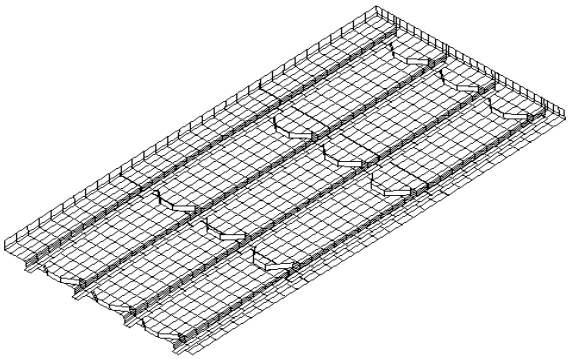

STEP=1
SUB =17
FREQ=98.079
PowerGraphics
EFACET=1
AVRES=Mat
DMX =.598217

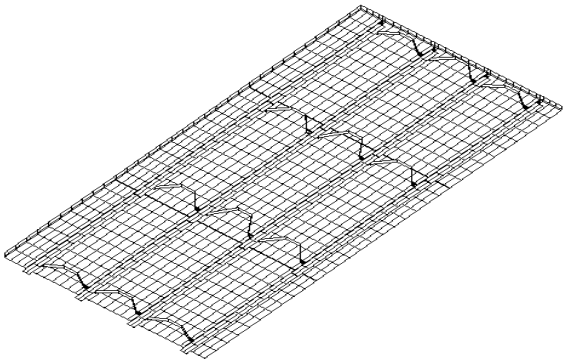

STEP=1
SUB =18
FREQ=109.225
PowerGraphics
EFACET=1
AVRES=Mat
DMX =1.148

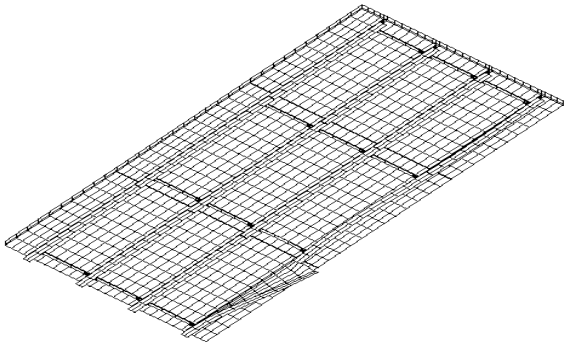

STEP=1
SUB =20
FREQ=129.295
PowerGraphics
EFACET=1
AVRES=Mat
DMX =.598858

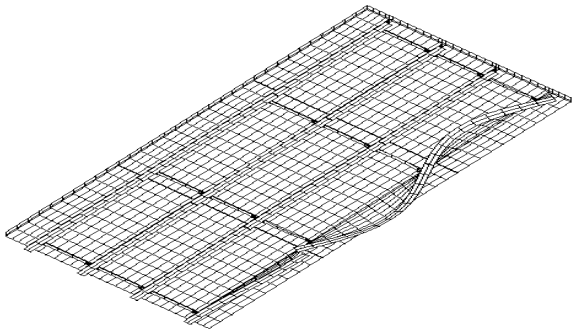

Fig. 4.31 FEM Modeling of Girder 1 and Bearing Damage Using ANSYS 5.5 Program (Continued).

STEP=1
SUB =21
FREQ=134.122
PowerGraphics
EFACET=1
AVRES=Mat
DMX =.665491

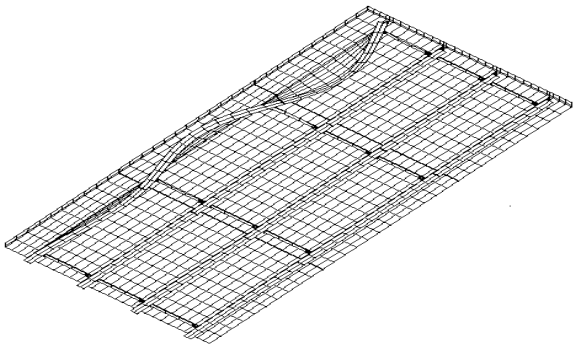

STEP=1
SUB =24
FREQ=145.389
PowerGraphics
EFACET=1
AVRES=Mat
DMX =.622433

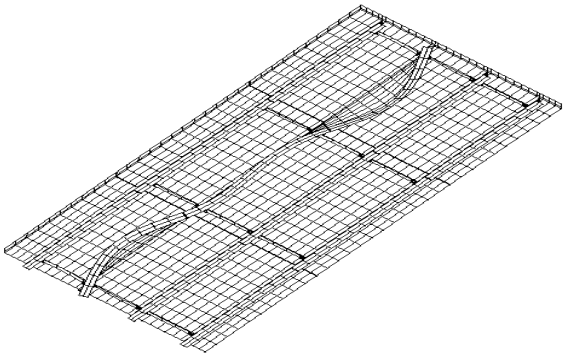

STEP=1
SUB =26
FREQ=164.234
PowerGraphics
EFACET=1
AVRES=Mat
DMX =.570884

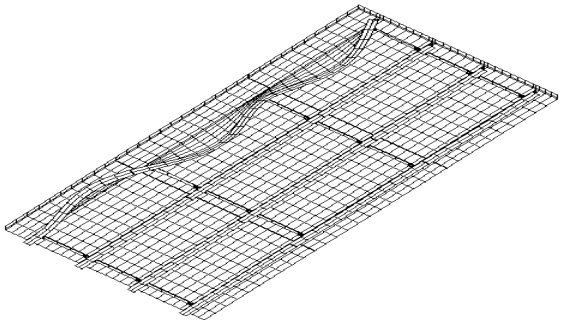

STEP=1
SUB =29
FREQ=190.371
PowerGraphics
EFACET=1
AVRES=Mat
DMX =.060735

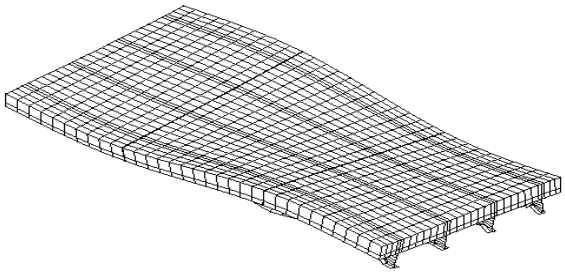

Fig. 4.31 FEM Modeling of Girder 1 and Bearing Damage Using ANSYS 5.5 Program (Continued).

4.7.6 FE Model of Girder 1 and 3 Cracking and Bearing Damage in the Modal Bridge

When damages in the girders 1 and 3 as well as in the bearing of girder 2 occurred simultaneously, the FE modeling results of natural frequency are listed in Table 4.12 and the FE modeling results of mode shapes are shown in Fig. 4.32. The changes of frequencies are similar with those due to girder 1 and bearing damage, but the changing values are larger than those due to girder 1 and bearing damage.

Table 4.12 Frequency Changes before and after Girder 1 and Bearing Damage

Mode No.	Frequency at intact condition	Frequency at Girders 1 and 3, and bearing damage	Differences
No.1	35.382 Hz	34.932 Hz	1.272%
No.2	38.870 Hz	35.865 Hz	7.731%
No.3	69.617 Hz	66.307 Hz	4.755%
No.4	90.538 Hz	86.300 Hz	4.467%
No.5	95.492 Hz	91.378 Hz	4.308%
No.6	100.357 Hz	98.076 Hz	2.273%
No.7	104.187 Hz	109.30 Hz	4.908%
No.8	138.838 Hz	128.20 Hz	7.662%
No.9	140.626 Hz	134.12 Hz	4.626%
No.10	153.142 Hz	143.54 Hz	6.270%
No.11	176.870 Hz	163.26 Hz	7.675%
No.12	195.262 Hz	190.25 Hz	2.567%

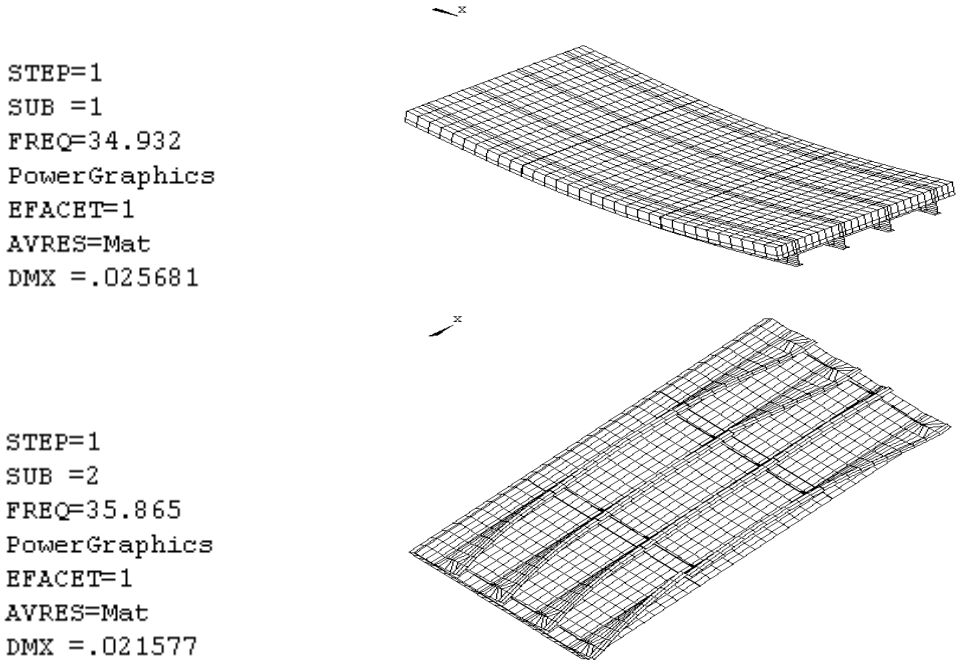

Fig. 4.32 FEM Modeling of Girder 1, Girder 3, and Bearing Damage Using ANSYS 5.5 Program.

STEP=1
SUB =3
FREQ=66.307
PowerGraphics
EFACET=1
AVRES=Mat
DMX =.042967

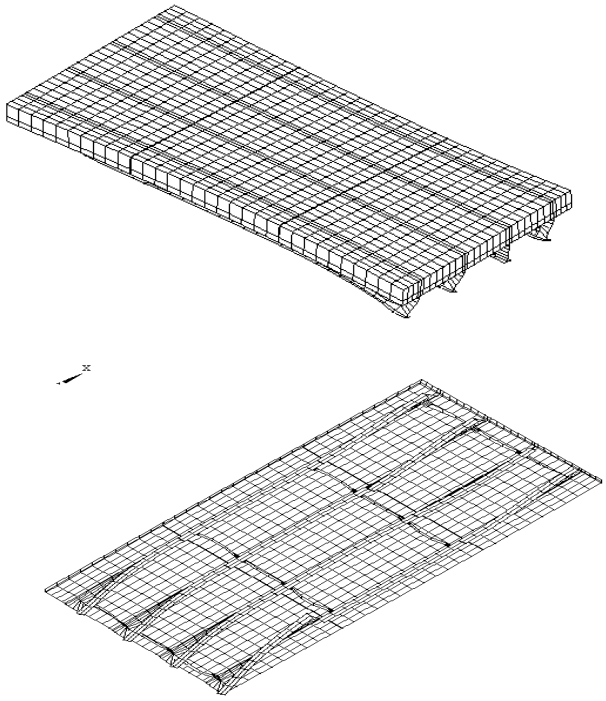

STEP=1
SUB =4
FREQ=86.3
PowerGraphics
EFACET=1
AVRES=Mat
DMX =.065713

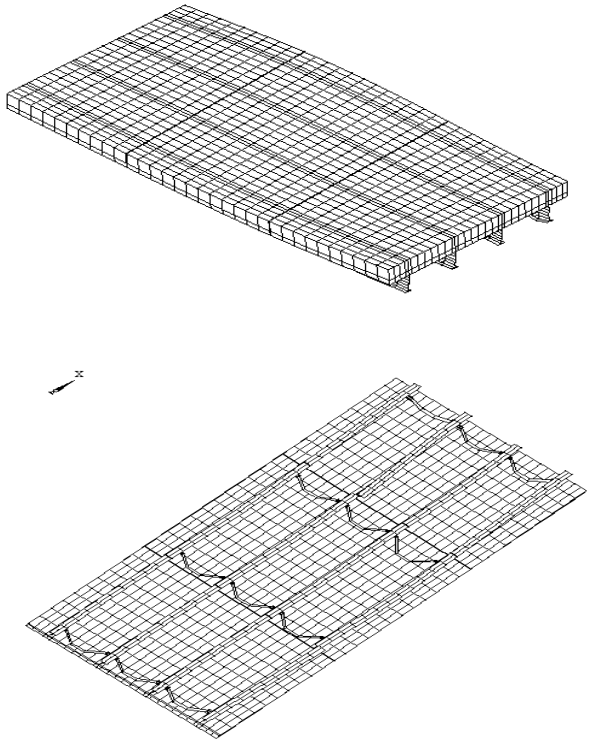

Fig. 4.32 FEM Modeling of Girder 1, Girder 3, and Bearing Damage Using ANSYS 5.5 Program (Continued).

STEP=1
SUB =5
FREQ=91.378
PowerGraphics
EFACET=1
AVRES=Mat
DMX =.139412

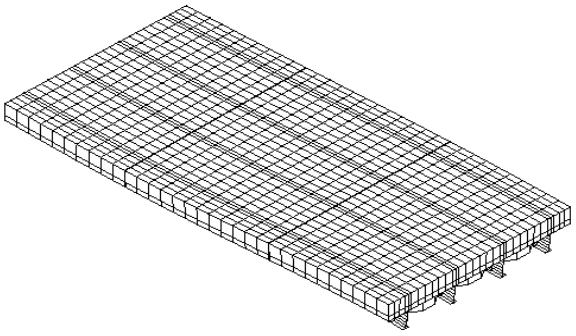

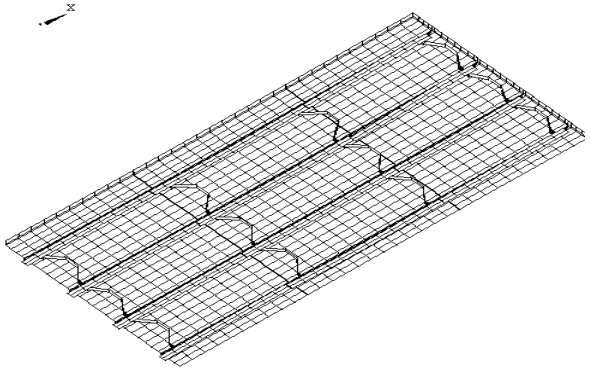

STEP=1
SUB =18
FREQ=98.076
PowerGraphics
EFACET=1
AVRES=Mat
DMX =.606595

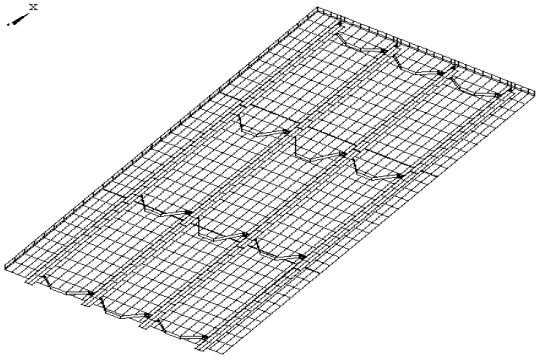

STEP=1
SUB =19
FREQ=109.299
PowerGraphics
EFACET=1
AVRES=Mat
DMX =1.147

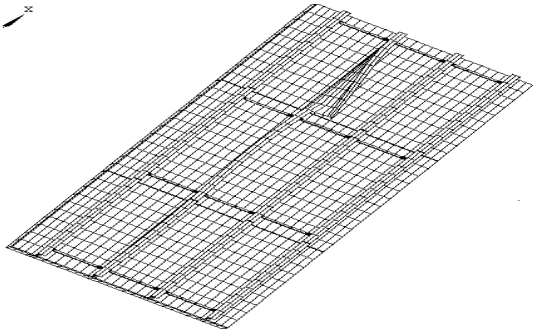

Fig. 4.32 FEM Modeling of Girder 1, Girder 3, and Bearing Damage Using ANSYS 5.5 Program (Continued).

STEP=1
SUB =20
FREQ=128.204
PowerGraphics
EFACET=1
AVRES=Mat
DMX =.533281

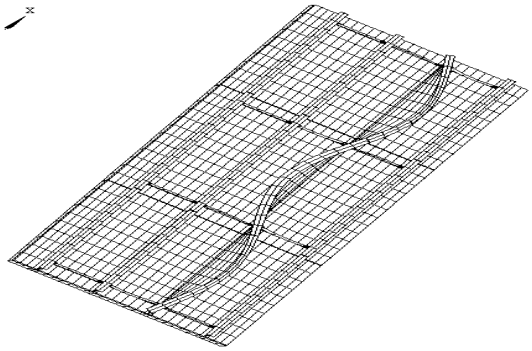

STEP=1
SUB =22
FREQ=134.121
PowerGraphics
EFACET=1
AVRES=Mat
DMX =.665051

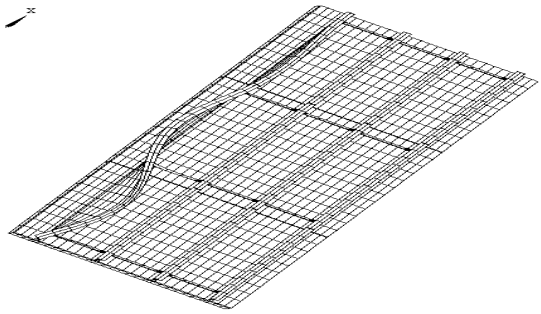

STEP=1
SUB =24
FREQ=143.542
PowerGraphics
EFACET=1
AVRES=Mat
DMX =.0414

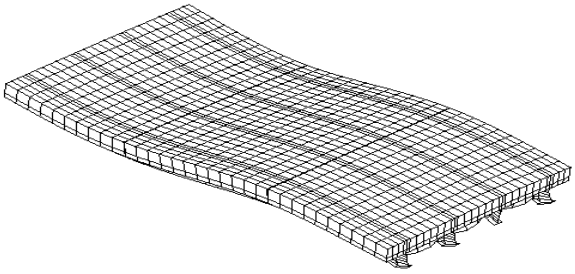

STEP=1
SUB =26
FREQ=163.26
PowerGraphics
EFACET=1
AVRES=Mat
DMX =.603071

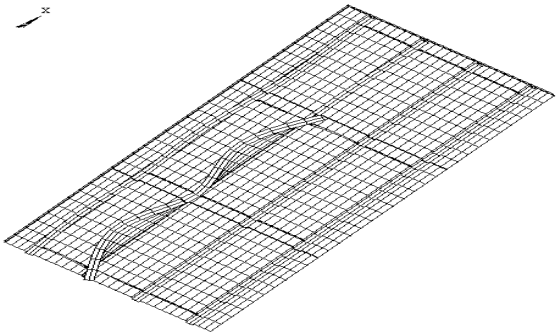

Fig. 4.32 FEM Modeling of Girder 1, Girder 3, and Bearing Damage Using ANSYS 5.5 Program (Continued).

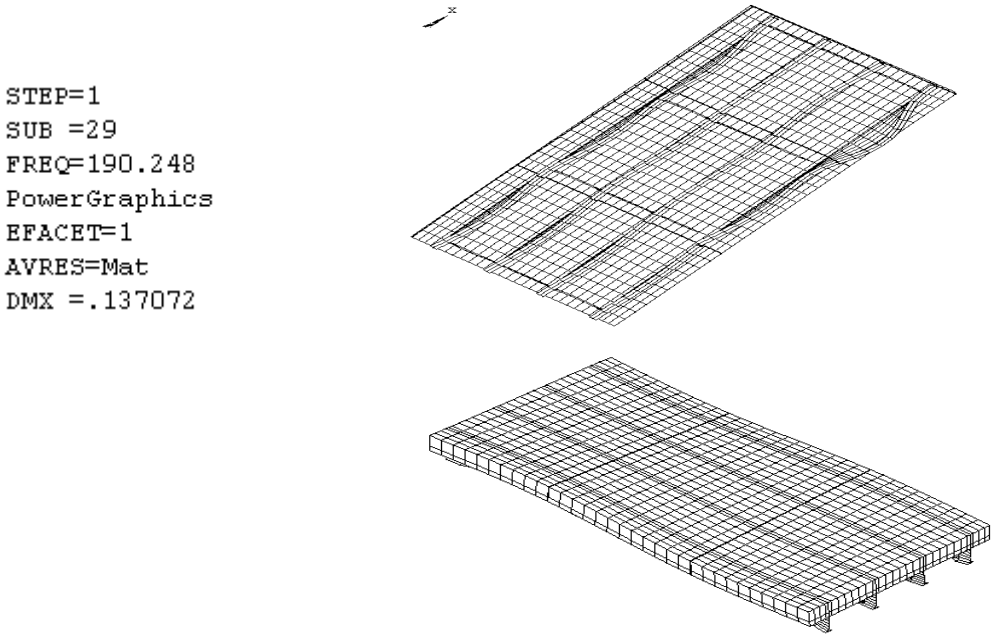

Fig. 4.32 FEM Modeling of Girder 1, Girder 3, and Bearing Damage Using ANSYS 5.5 Program (Continued).

4.7.7 Summary of FE Modeling Damage

From the above calculation and comparison, the trends of frequency change with the damage conditions are shown in Fig. 4.33. As the extent of girder damage increases, the changes of frequency also increase, but the changes of frequency are not sensitive to the girder damage. On the other hand, the changes of frequency don't reveal the extent of bearing damage. Sometimes, the changes of frequency increase, and sometimes they decrease.

The frequency and damping ratio are the parameters that indicate the whole properties of structures, but the damage always develops in the local area in the structures. To some extent, the frequency is not the best damage index.

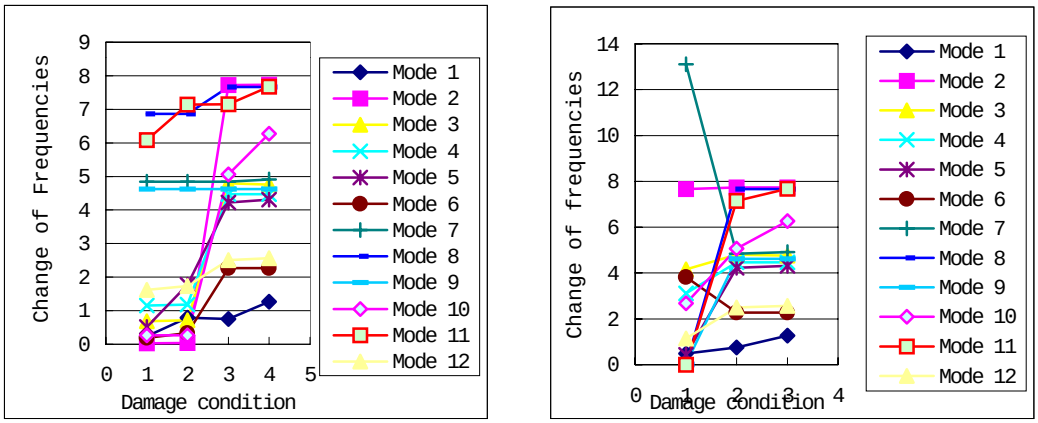

(a) Damage Trends in the Girders **(b) Damage Trends at Bearing**

Fig. 4.33 Trends of Damage Changes.

Chapter 5

Testing Results and Damage Identification

The building and study of a model bridge and the development of the theoretical base for ambient analysis have paved the way to experimentally verify the proposed method for bridge damage identification. The pre-testing is discussed in the first part of this chapter. Special considerations for ambient testing are given to the following factors: namely, the distribution effect of the added mass, the effect of the vehicular speed, the effect of window functions, and the effect of excitation locations and method. On the other hand, the results of static loading are also included in the first part.

Since typical modal parameters may not be sensitive enough to detect minor damage, it is necessary to find a more sensitive index to implement this technique. The second part of this chapter presents the experimental results of bridge damage detection and localization through the changes of ETR and other vibrational signatures before and after damages are introduced. In this part, by performing dynamic testing and modal parameter identification for the model, two main concerns for damage identification, detecting and locating damage, are investigated.

The growth of damage in terms of size and /or severity in structures is referred to damage dynamics. A practical and acceptable diagnostic technique is capable of not only identifying damage location and sensitivity but also tracing the deterioration tendencies, since damage in the structures grows from small defects. Further efforts to perform experimental and numerical damage analysis are the main concern in the third part of this chapter. The damage development of the model bridge in detail and simulate the method are proposed in chapter 3. Lastly, we summarize the work and state the important conclusions of the testing and calculation results.

5.1 Results of Pre-testing of the Model Bridge

The pre-testing was conducted on the non-damaged model bridge. Except for the non-uniformly distributed mass, the effects of other factors were analyzed according to the intact condition of the model bridge with uniformly distributed mass. Typical response spectrum was obtained through time history signals transferred by FFT-FT and averaged.

5.1.1 Effect of Excitation Locations

To study the effect of load location, the ambient excitation and hammer impact were used. Location of accelerometers was shown in Fig. 4.16.

5.1.1.1 Ambient Excitation Test

The bridge is symmetric and the added mass is uniformly distributed over the concrete slab. To minimize any possible torsion effect of the model bridge, the cart was firstly pulled along the

central line of the model (Fig. 5.1a). When the accelerators were arranged in the vertical direction and the speed of the cart is $0.34m/s$, the typical frequency response spectrum (from auto-spectrum analysis) at some points is shown in Figs. 5.2.1-5.2.16. It was found that, along the girders, the modes near two ends of the model bridge (for example, points 1 and 6) are more apparent than those near the center of span (for example, points 3 and 4), especially those modes between 96 and 170Hz. But across the girders (for example, points 1, 7, 13, 19), the frequency responses are similar symmetric. The cart was then moved to one side of the model bridge (Fig. 5.1b) and the speed of the cart is $0.35m/s$. It was found that the frequency responses under one-sided excitation are similar with those under central excitation. From these figures, we may conclude that (1) the frequency response of the model bridge at different points is also different. (2) The difference of frequency response caused by excitation locations is not very clear. Similar conclusions are obtained while accelerometers were arranged in the horizontal direction.

(a) At the Center Line

(b) At One Side of the Slab

Fig. 5.1 Ambient Excitation Locations.

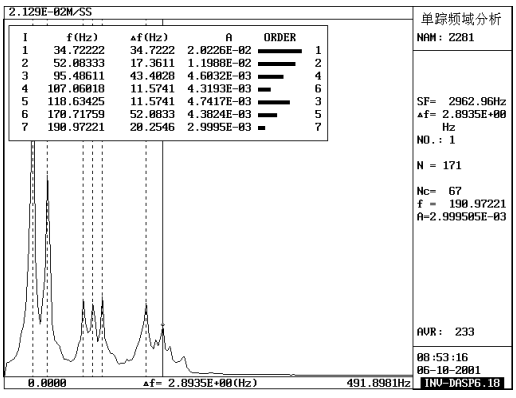

Fig. 5.2.1 Position 1.

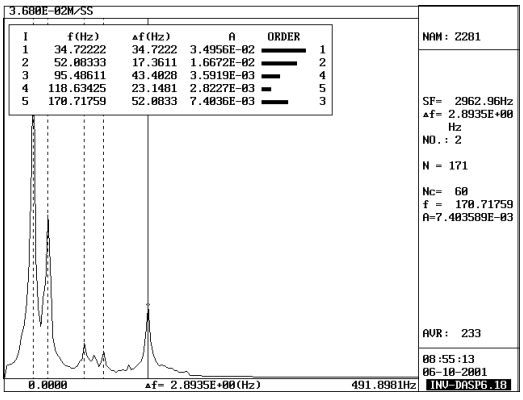

Fig. 5.2.2 Position 2.

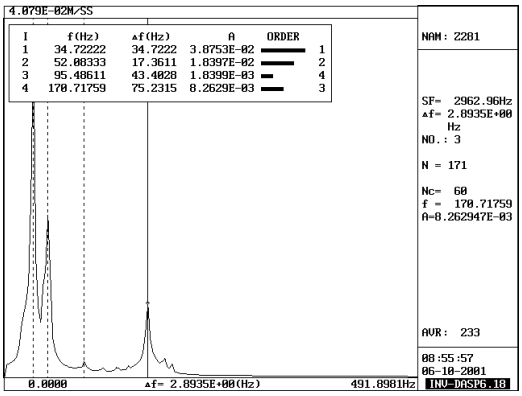

Fig. 5.2.3 Point 3.

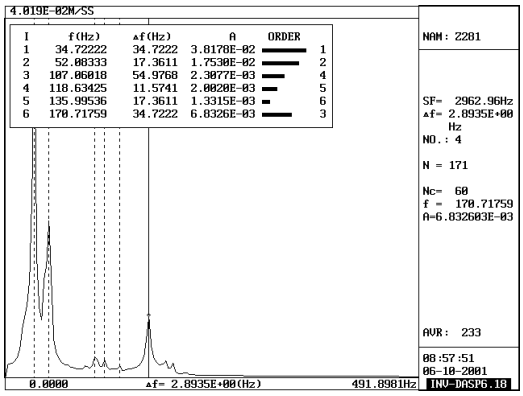

Fig. 5.2.4 Point 4.

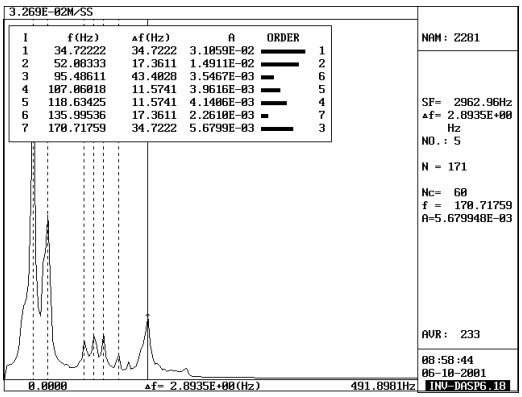

Fig. 5.2.5 Point 5.

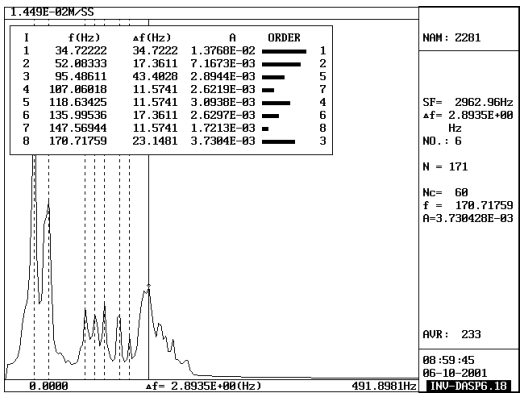

Fig. 5.2.6 Point 6.

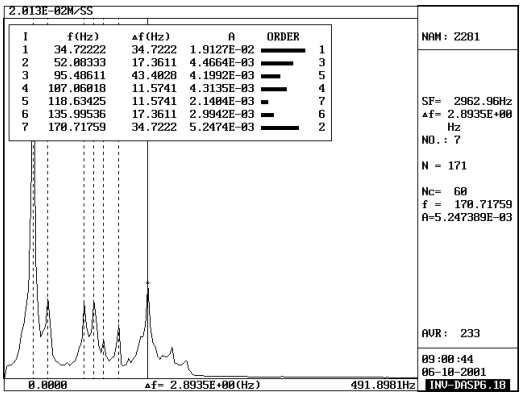

Fig. 5.2.7 Point 7.

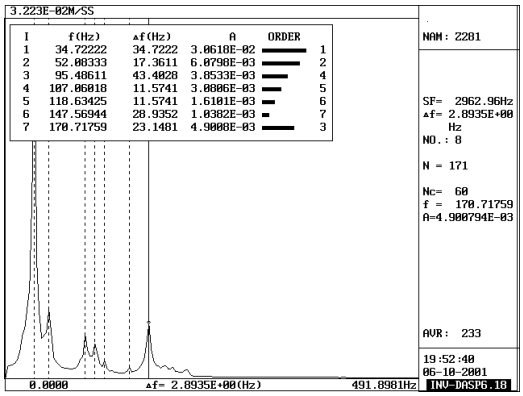

Fig. 5.2.8 Point 8.

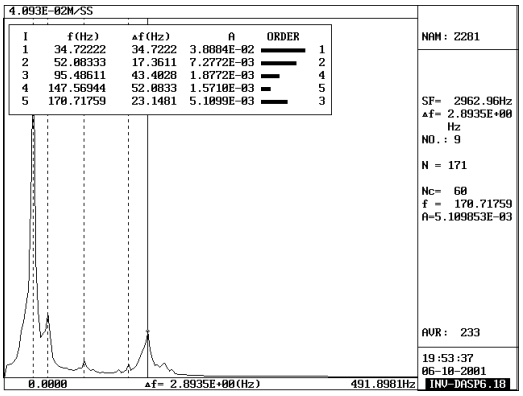

Fig. 5.2.9 Point 9.

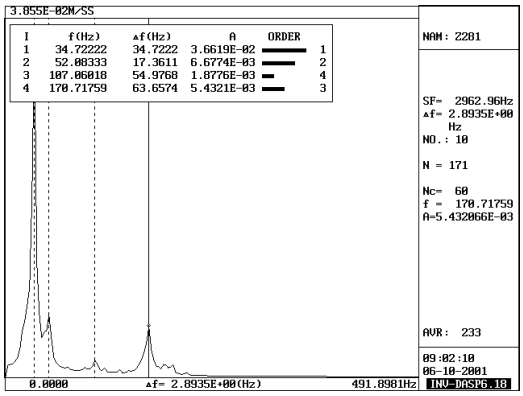

Fig. 5.2.4 Point 10.

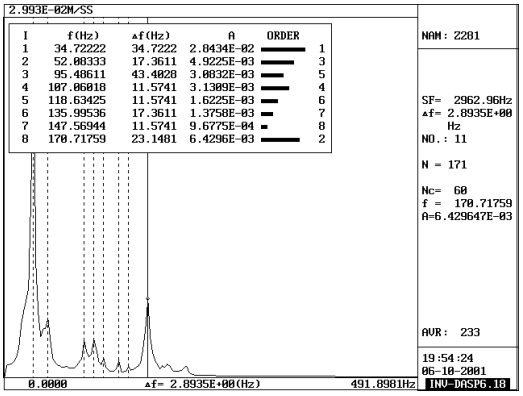

Fig. 5.2.11 Point 11.

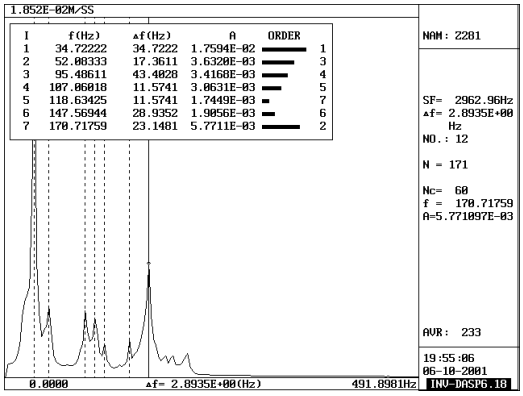

Fig. 5.2.12 Point 12.

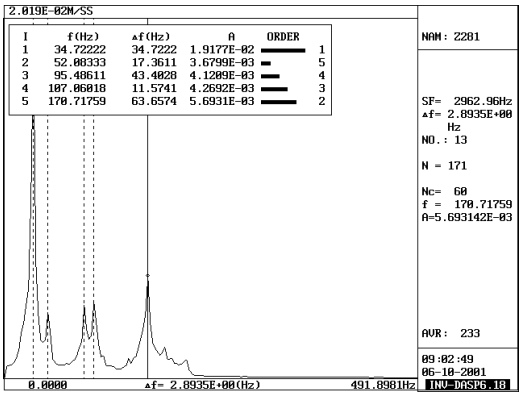

Fig. 5.2.13 Point 13.

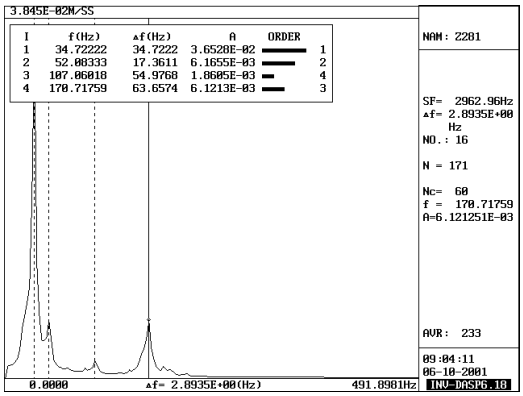

Fig. 5.2.14 Point 16.

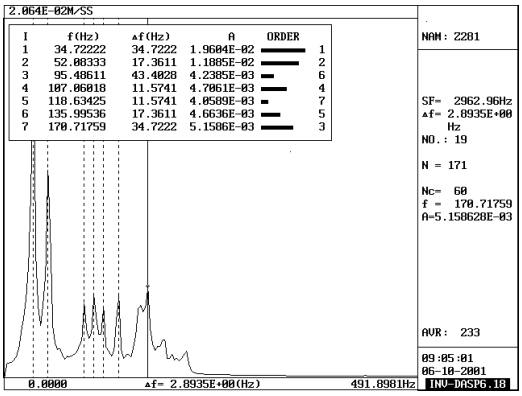

Fig. 5.2.15 Point 19.

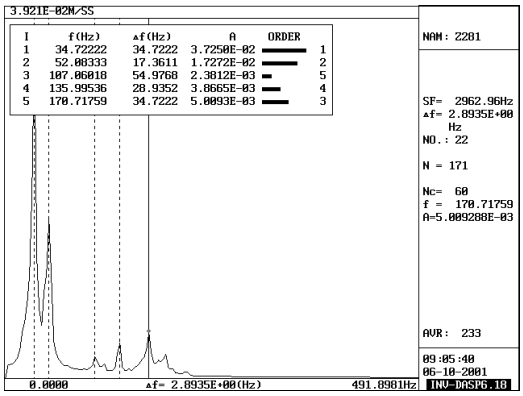

Fig. 5.2.16 Point 22.

Fig. 5.2 Frequency Response Spectrums under Central Excitation.

On the other hand, from cross-power spectrum analysis at some points (Fig. 5.3), there are obvious differences between the central excitation and one-sided excitation. The cross-power spectrum at one point was relative to that of the reference point at the girder 1 bearing. This demonstrates that the excitation locations will have a strong effect on the modes of the model bridge, even though the bridge is typically symmetric.

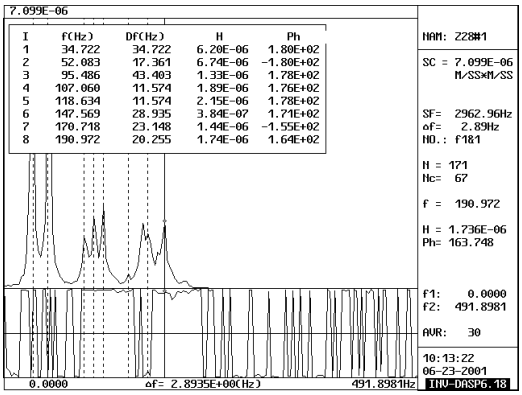

(a) Under Central Excitation

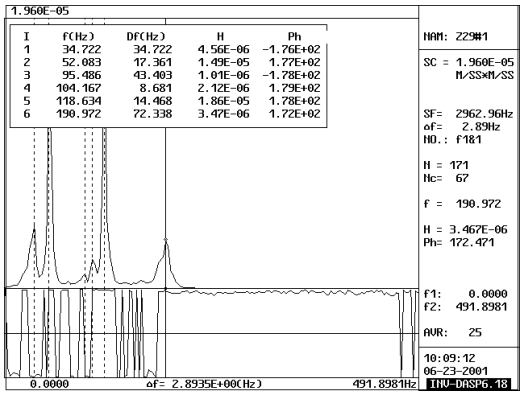

(b) Under One-sided Excitation

Fig. 5.3.1 Point 1.

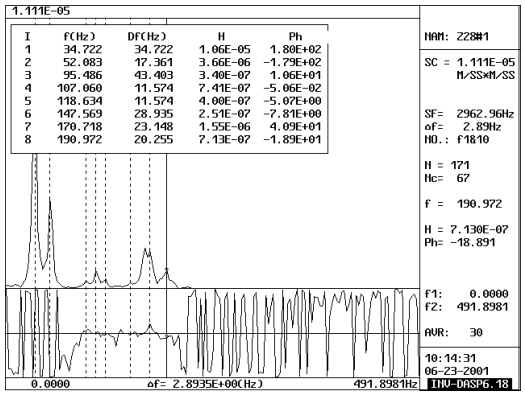

(a) Under central excitation

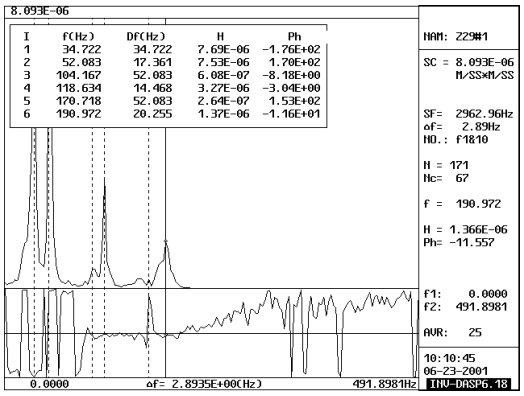

(b) Under one-sided excitation

Fig. 5.3.2 Point 10.

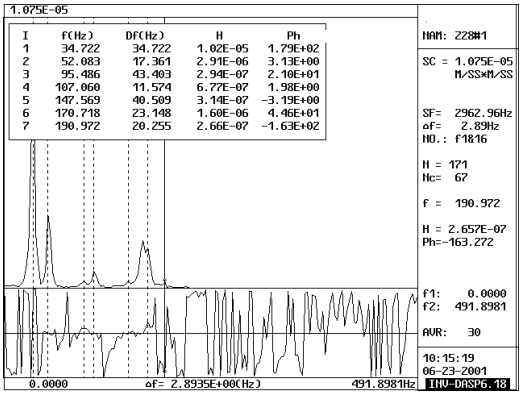

(a) Under central excitation

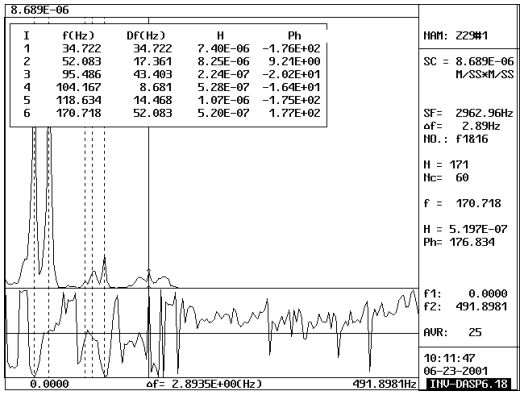

(b) Under one-sided excitation

Fig. 5.3.3 Point 16.

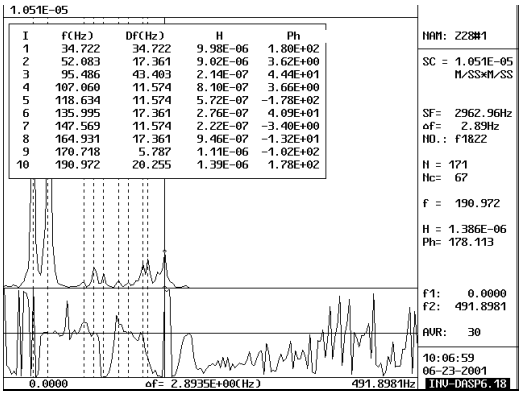

(a) Under central excitation

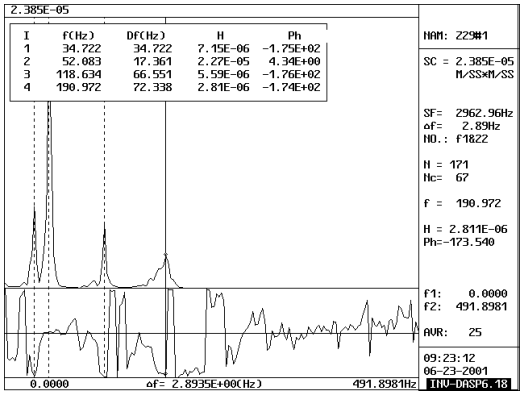

(b) Under one-sided excitation

Fig. 5.3.4 Point 22

Fig. 5.3 Cross-power Spectrums under Different Excitation Locations. (Accelerator Vertical Arrangement)

Table 5.1 Identified Frequencies and Damping Ratios

Table 5.1 (a) Under Central Excitation

Identified frequencies and dampings ratios
FIT METHOD : MONOFREEDOM(C)
TEST NAME : Z281#
RESPONSE TYPE : ACCELERATION

MODE No.	FREQUENCY		Damping		
	Hz	Radius	%	½BW(Hz)	Radius
1	34.037	213.858	0.0008	0.001	0.004
2	48.155	302.565	0.0062	0.006	0.037
3	89.795	564.195	15.3060	27.488	172.712
4	134.002	841.959	0.0285	0.076	0.480
5	169.437	1064.605	0.0415	0.140	0.883

Table 5.1 (b) Under One-sided Excitation

Identified frequencies and dampings ratios
FIT METHOD : MONOFREEDOM(C)
TEST NAME : Z291#
RESPONSE TYPE : ACCELERATION

MODE No.	FREQUENCY		Damping		
	Hz	Radius	%	½BW(Hz)	Radius
1	33.723	211.889	0.0003	0.000	0.001
2	50.100	314.787	0.0228	0.023	0.144
3	87.577	550.262	0.1128	0.197	1.241
4	103.162	648.186	0.8634	1.781	11.193
5	170.194	1069.358	0.3222	1.097	6.891

Note: Accelerators were arranged in the vertical direction in Table 5.1.

The natural frequencies and damping ratios are identified using transfer function analysis methods. The first 5 modes (the speed of $0.35m/s$ or so) under central excitation and one-sided excitation are listed in Table 5.1(a) and Table 5.1(b). The transfer function analysis approves that excitation locations have a strong effect on the modes of the model bridge.

When accelerators were arranged in the horizontal direction and the speed of the cart was $0.35m/s$, the cross-power spectrum at some points under the central excitation and one-sided excitation are shown in Fig. 5.4. Those modes between 28 and 144Hz were well separated under central excitation, but were omitted under one-sided excitation. The results (see Table 5.2) from transfer function analysis also reiterate this conclusion.

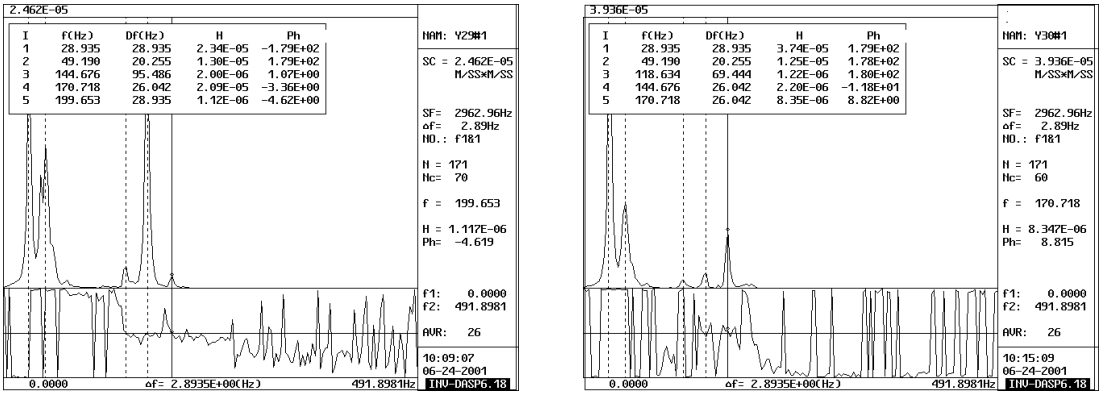

(a) Under central excitation (b) Under one-sided excitation

Fig. 5.4.1 Point 1.

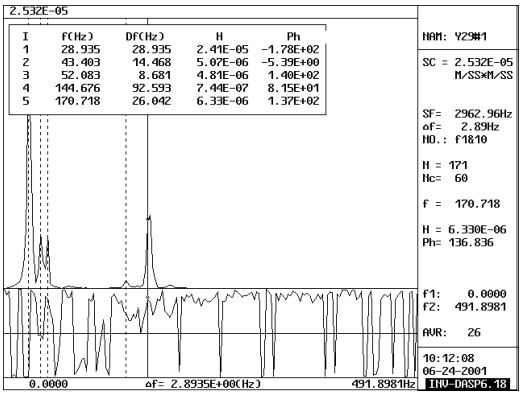

(a) Under central excitation

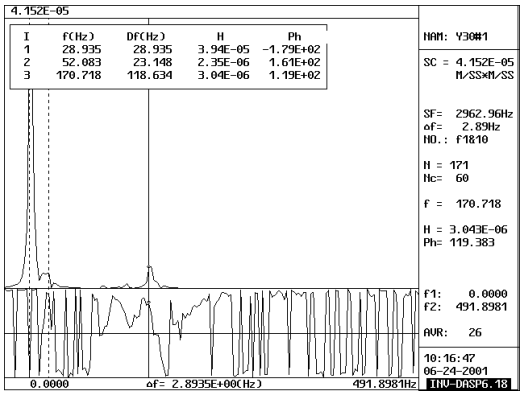

(b) Under one-sided excitation

Fig. 5.4.2 Point 10.

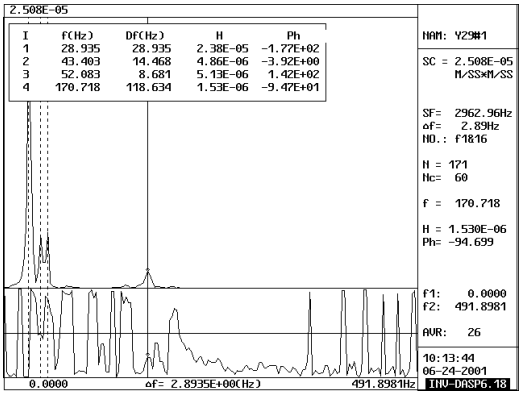

(a) Under central excitation

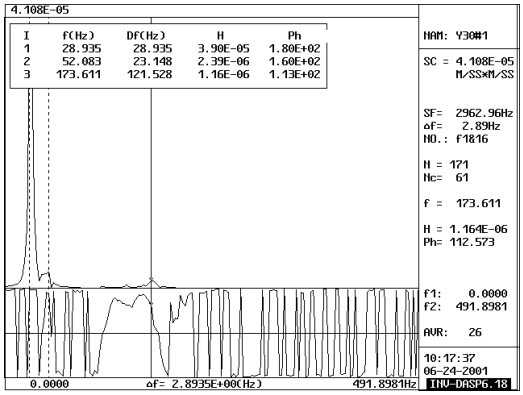

(b) Under one-sided excitation

Fig. 5.4.3 Point 16.

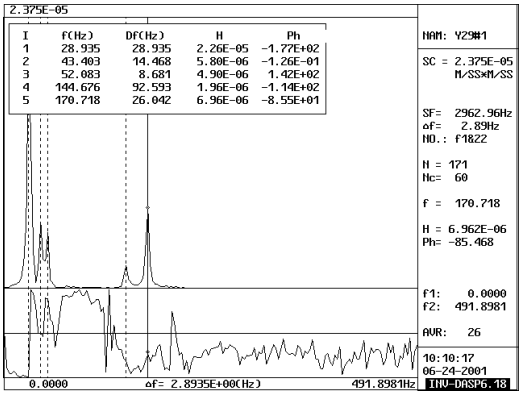

(a) Under central excitation

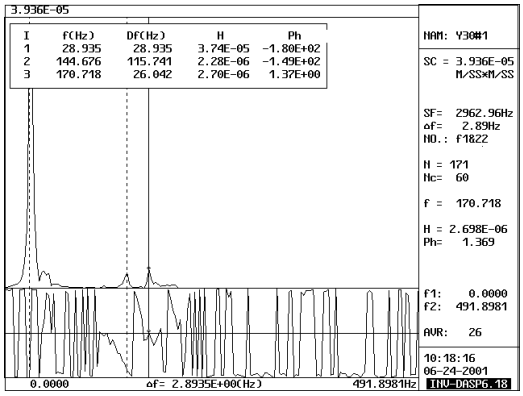

(b) Under one-sided excitation

Fig. 5.4.4 Point 22.

Fig. 5.4 Cross-power Spectrums under Different Excitation Locations (Accelerator Horizontal Arrangement).

Table 5.2 Identified Frequencies and Damping Ratios

Table 5.2 (a) Under Central Excitation

Identified frequencies and dampings ratios
FIT METHOD : MONOFREEDOM(C)
TEST NAME : Y291#
RESPONSE TYPE : ACCELERATION

MODE No.	FREQUENCY		Damping		
	Hz	Radius	%	½BW(Hz)	Radius
1	26.712	167.837	45.5333	24.326	152.843
2	50.338	316.283	0.6877	0.692	4.350
3	77.846	489.122	0.3027	0.471	2.962
4	144.267	906.458	0.0001	0.000	0.003
5	170.316	1070.129	0.1150	0.392	2.462
6	197.129	1238.598	0.6079	2.397	15.059

Table 5.2 (b) Under One-sided Excitation

Identified frequencies and dampings ratios
FIT METHOD : MONOFREEDOM(C)
TEST NAME : Y301#
RESPONSE TYPE : ACCELERATION

MODE No.	FREQUENCY		Damping		
	Hz	Radius	%	½BW(Hz)	Radius
1	27.859	175.041	0.2513	0.140	0.880
2	119.735	752.319	0.3681	0.882	5.539
3	144.981	910.944	0.0001	0.000	0.003
4	171.528	1077.740	0.5303	1.819	11.431
5	197.938	1243.679	0.3041	1.204	7.564

Note: Accelerators were arranged in the horizontal direction in Table 5.2.

5.1.1.2 Hammer Impact Test

Similar tests were conducted using impact excitation (see Fig. 5.5) to verify the above arguments. The positions A, B, C, D, E, F and a, b, c, d, e at Fig. 4.16 are impact excitation points used individually for each impact test. When accelerator were arranged in the vertical direction, it has been found that, for possible excitation locations, such as A, the frequency response spectrum will have well separated modes which are shown in Fig5.6 (a). For central excitation points, such as positions E and F, the modes between 53 and 190Hz can not be well separated (see in Fig. 5.6 (c) and (d)). While accelerators were arranged in the horizontal direction, for central excitation points, such as e, the modes between 53 and 167Hz can not be well separated (see in Fig. 5.7 (e)). The frequencies and damping ratios identified from transfer function analysis are listed in Table 5.3 (vertical) and Table 5.4 (horizontal). The impact testing results support our conclusions obtained from ambient testing that excitation locations do affect the mode distribution.

Fig. 5.5 (a) Vertical Impact.

Fig. 5.5 (b) Horizontal Impact.

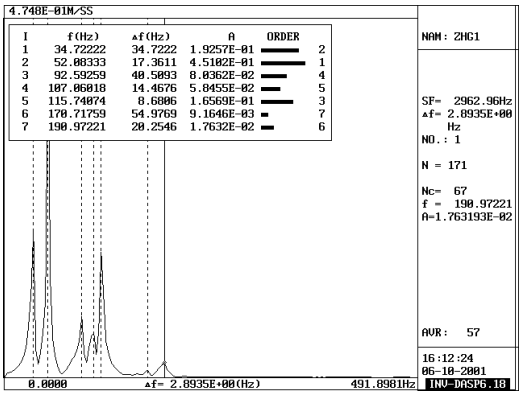

Fig. 5.6 (a) Under Impact at Point A.

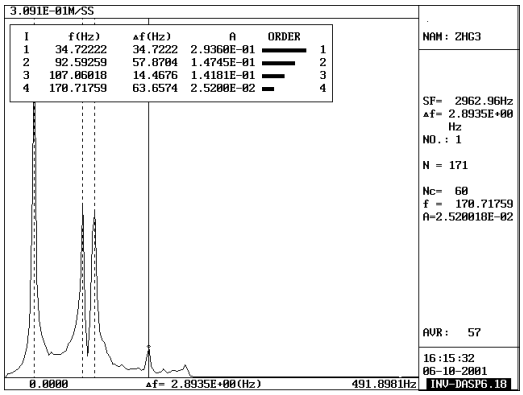

Fig. 5.6 (b) Under Impact at Point C.

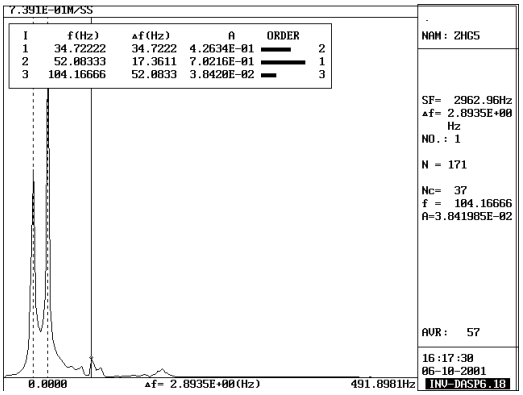

Fig. 5.6 (c) Under Impact at Point E.

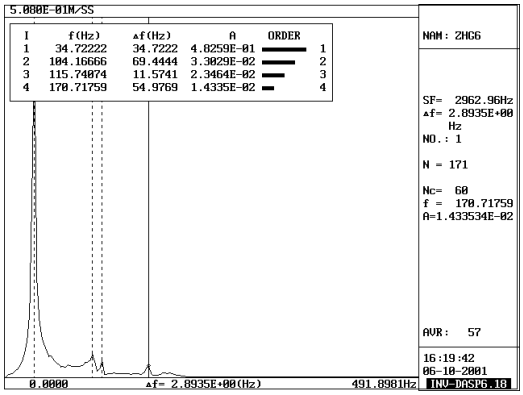

Fig. 5.6 (d) Under Impact at Point F.

Fig. 5.6 Frequency Responses at Point 1 under Different Impact Points (Accelerator Vertical Arrangement).

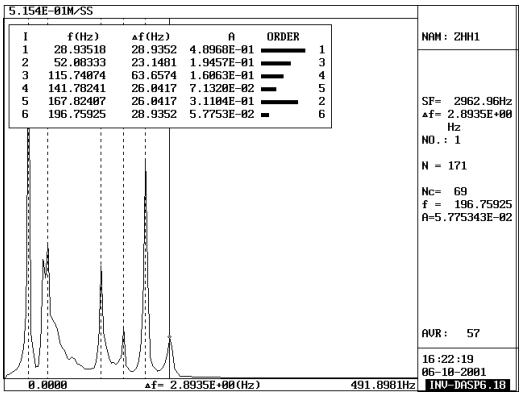

Fig. 5.7 (a) Under Impact at Point a.

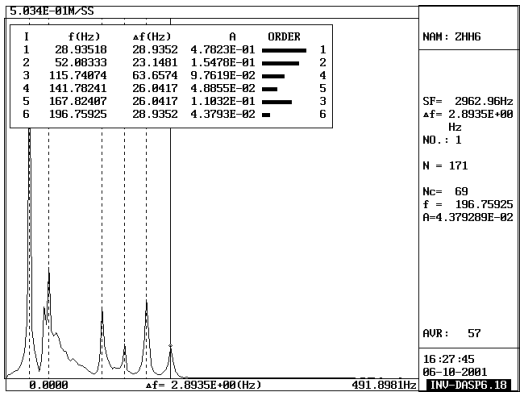

Fig. 5.7 (b) Under Impact at Point b.

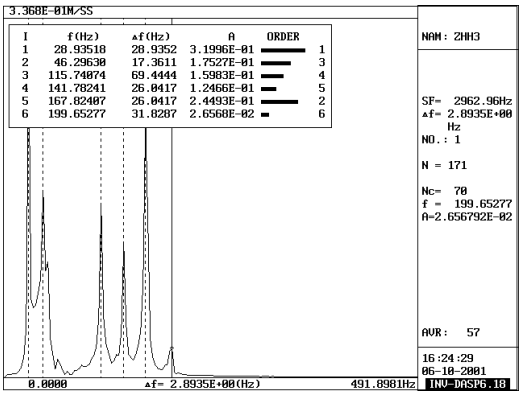

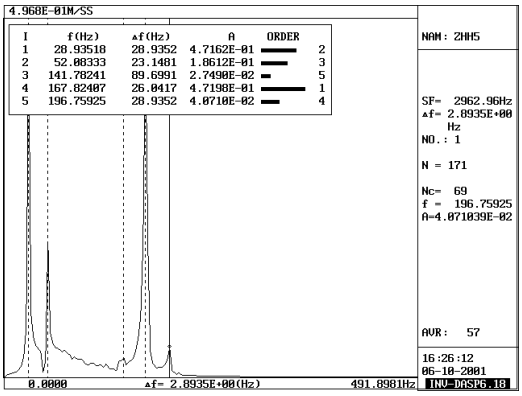

Fig. 5.7 (c) Under Impact at Point d **Fig. 5.7 (d) Under Impact at Point e**

Fig. 5.7 Frequency Responses at Point 1 under Different Impact Points (Accelerator Horizontal Arrangement).

Table 5.3 Identified Frequencies and Damping Ratios

Table 5.3 (a) Impact at Point A

Identified frequencies and dampings ratios
FIT METHOD : MONOFREEDOM(C)
TEST NAME : ZHC1#
RESPONSE TYPE : ACCELERATION

MODE No.	FREQUENCY		Damping		
	Hz	Radius	%	½BW(Hz)	Radius
1	33.805	212.403	1.0454	0.707	4.441
2	52.664	330.898	1.2836	1.352	8.495
3	93.250	585.908	1.7555	3.274	20.572
4	115.474	725.542	0.8967	2.071	13.012
5	140.516	882.886	3.0321	8.521	53.541
6	169.174	1062.948	0.7698	2.605	16.366
7	185.429	1165.088	1.7754	6.584	41.370

Table 5.3 (b) Impact at Point C

Identified frequencies and dampings ratios
FIT METHOD : MONOFREEDOM(C)
TEST NAME : ZHC3#
RESPONSE TYPE : ACCELERATION

MODE No.	FREQUENCY		Damping		
	Hz	Radius	%	½BW(Hz)	Radius
1	33.860	212.749	1.0097	0.684	4.296
2	93.270	586.036	1.7514	3.267	20.528
3	105.705	664.161	1.1006	2.327	14.620
4	169.243	1063.387	0.7759	2.626	16.501
5	188.713	1185.716	1.5658	5.910	37.131

Table 5.3 (c) Impact at Point E

Identified frequencies and dampings ratios
FIT METHOD : MONOFREEDOM(C)
TEST NAME : ZHC5#
RESPONSE TYPE : ACCELERATION

MODE No.	FREQUENCY		Damping		
	Hz	Radius	%	½BW(Hz)	Radius
1	33.722	211.880	1.1939	0.805	5.059
2	52.278	328.470	1.3892	1.452	9.126
3	104.241	654.967	0.8058	1.680	10.556
4	168.786	1060.511	0.0733	0.247	1.554

Table 5.3(d) Impact at Point F

Identified frequencies and dampings ratios
FIT METHOD : MONOFREEDOM(C)
TEST NAME : ZHC6#
RESPONSE TYPE : ACCELERATION

MODE No.	FREQUENCY		Damping		
	Hz	Radius	%	½BW(Hz)	Radius
1	33.749	212.048	1.0590	0.715	4.491
2	105.724	664.280	1.5895	3.361	21.117
3	169.235	1063.333	1.2795	4.331	27.210

Note: Accelerators were arranged in the vertical direction in Table 5.3.

Table 5.4 Identified Frequencies and Damping Ratios

Table 5.4*(a) Impact at Point a

Identified frequencies and dampings ratios
FIT METHOD : MONOFREEDOM(C)
TEST NAME : ZHH1#
RESPONSE TYPE : ACCELERATION

MODE No.	FREQUENCY		Damping		
	Hz	Radius	%	½BW(Hz)	Radius
1	28.794	180.917	2.2113	1.273	8.001
2	49.282	309.648	3.8216	3.767	23.667
3	115.512	725.785	0.9166	2.118	13.306
4	144.346	906.956	0.3958	1.143	7.179
5	169.294	1063.703	0.2824	0.956	6.007
6	195.959	1231.244	1.1033	4.324	27.170

Table 5.4*(b) Impact at Point d

Identified frequencies and dampings ratios
FIT METHOD : MONOFREEDOM(C)
TEST NAME : ZHH3#
RESPONSE TYPE : ACCELERATION

MODE No.	FREQUENCY		Damping		
	Hz	Radius	%	½BW(Hz)	Radius
1	29.149	183.149	2.3208	1.353	8.501
2	51.319	322.450	0.5412	0.555	3.490
3	114.980	722.443	1.2412	2.854	17.934
4	143.970	904.591	0.1867	0.537	3.377
5	169.759	1066.628	0.1537	0.522	3.279
6	199.635	1254.342	0.4447	1.776	11.156

Table 5.4*(c) Impact at Point e

Identified frequencies and dampings ratios
FIT METHOD : MONOFREEDOM(C)
TEST NAME : ZHH5#
RESPONSE TYPE : ACCELERATION

MODE No.	FREQUENCY		Damping		
	Hz	Radius	%	½BW(Hz)	Radius
1	29.079	182.708	1.6260	0.946	5.942
2	51.933	326.304	1.2429	1.291	8.112
3	142.540	895.607	0.2364	0.674	4.235
4	170.097	1068.754	0.1712	0.582	3.659
5	196.871	1236.977	0.6155	2.424	15.228

Table 5.4*(d) Impact at Point b

Identified frequencies and dampings ratios
FIT METHOD : MONOFREEDOM(C)
TEST NAME : ZHH6#
RESPONSE TYPE : ACCELERATION

MODE No.	FREQUENCY		Damping		
	Hz	Radius	%	½BW(Hz)	Radius
1	28.966	181.999	1.7212	0.997	6.265
2	51.016	320.540	2.7093	2.764	17.369
3	115.657	726.695	0.8337	1.928	12.117
4	143.798	903.510	0.2919	0.839	5.274
5	169.301	1063.751	0.3654	1.237	7.775
6	196.259	1233.132	1.2179	4.781	30.037

***Note: Accelerators were arranged in the horizontal direction in Table 5.4.**

5.1.2 Effect of Vehicle Speed

Four different speeds (V=0.34m/s, 0.82m/s, 1.06m/s, and 1.32m/s) were selected to study the effect of speed on the estimation of model parameters. Fig. 5.8 demonstrates the frequency response spectrum of the same location (point 4) at different vehicle speeds under the central excitation.

It is found that the number of modes does not change with the increase of vehicle speed, but the damping ratios, especially those associated with higher modes, have significant changes (see Table 5.5). This can be explained by the fact that, the damping ratios are strongly dependent on the response level. For a linear system, the response level is directly proportional to the excitation level, and in this case, the excitation level is directly related to the vehicle speed.

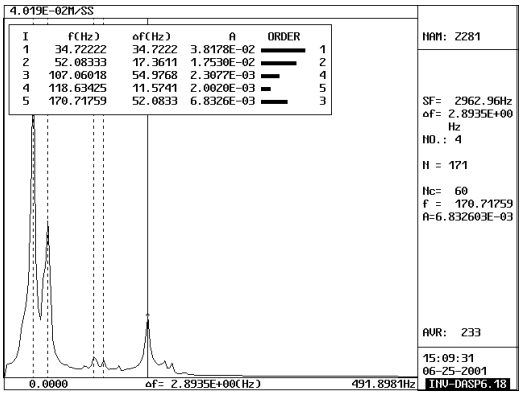

Fig. 5.8(a) Under V=0.34 m/s.

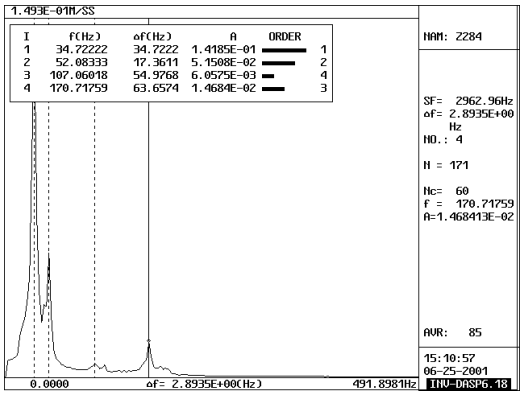

Fig. 5.8(b) Under V=0.82 m/s.

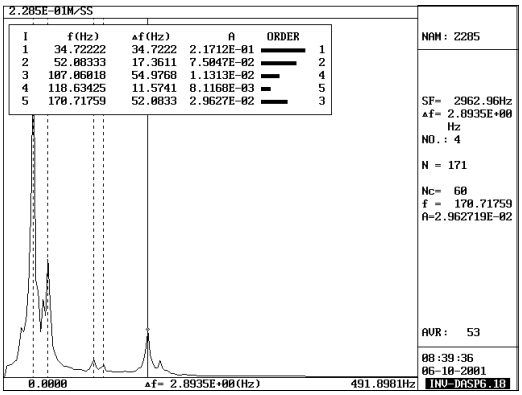

Fig. 5.8(c) Under V=1.32 m/s.

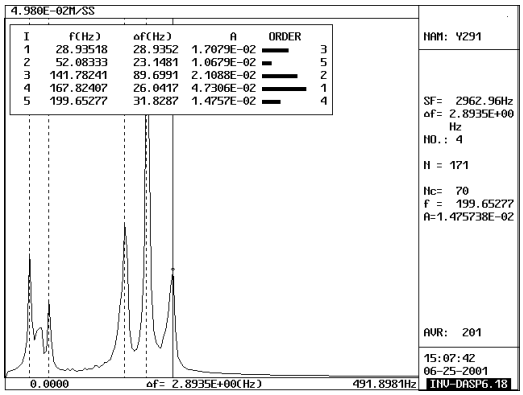

Fig. 5.8(d) Under V=0.34 m/s.

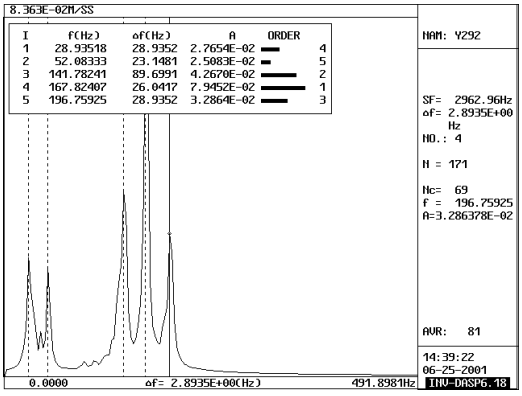

Fig. 5.8(e) Under V=0.84 m/s.

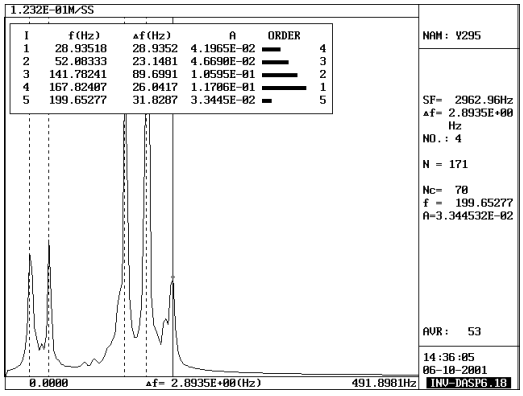

Fig. 5.8(f) Under V=1.34 m/s.

Fig. 5.8* Frequency Responses under Different Vehicle Speeds.

***Note: Accelerator vertical arrangement in Fig.5.8 (a)-(c) and horizontal arrangement in Fig. 5.8 (d)-(f).**

Table 5.5 Identified Frequencies and Damping Ratios

Table 5.5*(a) Under V=0.34 m/s

Identified frequencies and dampings ratios
FIT METHOD : MONOFREEDOM(C)
TEST NAME : Z281#
RESPONSE TYPE : ACCELERATION

MODE No.	FREQUENCY		Damping		
	Hz	Radius	%	½BW(Hz)	Radius
1	33.598	211.104	0.0004	0.000	0.002
2	89.608	563.024	11.3500	20.341	127.807
3	169.566	1065.414	0.0564	0.191	1.203

Table 5.5*(b) Under V=0.82 m/s

Identified frequencies and dampings ratios
FIT METHOD : MONOFREEDOM(C)
TEST NAME : Z284#
RESPONSE TYPE : ACCELERATION

MODE No.	FREQUENCY		Damping		
	Hz	Radius	%	½BW(Hz)	Radius
1	32.107	201.731	0.0001	0.000	0.000
2	87.936	552.517	0.7775	1.367	8.592
3	170.196	1069.372	0.0037	0.013	0.080

Table 5.5*(c) Under V=1.32 m/s

Identified frequencies and dampings ratios
FIT METHOD : MONOFREEDOM(C)
TEST NAME : Z285#
RESPONSE TYPE : ACCELERATION

MODE No.	FREQUENCY		Damping		
	Hz	Radius	%	½BW(Hz)	Radius
1	33.571	210.934	0.0001	0.000	0.001
2	91.686	576.079	0.2494	0.457	2.874
3	170.539	1071.526	0.0001	0.000	0.002

Table 5.5*(d) Under V=0.34 m/s

Identified frequencies and dampings ratios
FIT METHOD : MONOFREEDOM(C)
TEST NAME : Y291#
RESPONSE TYPE : ACCELERATION

MODE No.	FREQUENCY		Damping		
	Hz	Radius	%	½BW(Hz)	Radius
1	28.794	180.921	0.2734	0.157	0.989
2	144.324	906.815	0.0001	0.000	0.003
3	170.316	1070.129	0.1150	0.392	2.462
4	197.129	1238.598	0.6079	2.397	15.059

Table 5.5*(e) Under V=0.84 m/s

Identified frequencies and dampings ratios
FIT METHOD : MONOFREEDOM(C)
TEST NAME : Y292#
RESPONSE TYPE : ACCELERATION

MODE No.	FREQUENCY		Damping		
	Hz	Radius	%	½BW(Hz)	Radius
1	27.757	174.403	0.0498	0.028	0.174
2	143.741	903.153	0.0221	0.064	0.399
3	169.472	1064.826	0.0807	0.274	1.719
4	196.611	1235.345	0.4464	1.755	11.029

Table 5.5*(f) Under V=1.34 m/s

Identified frequencies and dampings ratios
FIT METHOD : MONOFREEDOM(C)
TEST NAME : Y295#
RESPONSE TYPE : ACCELERATION

MODE No.	FREQUENCY		Damping		
	Hz	Radius	%	½BW(Hz)	Radius
1	26.664	167.532	12.7944	6.823	42.870
2	145.824	916.240	0.0002	0.001	0.004
3	170.239	1069.641	1.0320	3.514	22.076
4	196.780	1236.408	0.0036	0.014	0.089

***Note: Accelerator vertical arrangement in Table 5.5 (a)-(c) and horizontal arrangement in Table 5.5 (d)-(f).**

5.1.3 Effect of Data Processing

There are many factors related to data processing, which will affect the testing results. Examples are the type of window function, the length of the window, and the sampling rate, etc. Usually, the sampling rate will not affect the testing results significantly if the rate is four times higher than the highest frequency to be evaluated. The length of the window can also be determined after the signal resolution (inverse of the sampling rate) and the highest interesting

frequency are known. Therefore, only the effect of window functions was studied in this section.

Two types of window functions, rectangular window and the Hanning window functions, which are among the most widely used in practice, are selected as study objects. For a given ambient response signal (for example, point 1 under cart excitation), the time history was averaged by a rectangular window and a Hanning window respectively. Their corresponding frequency response spectrum is shown in Fig. 5.9 (a)-(d). It can be seen that the magnitude of the spectrum evaluated with a rectangular window is larger than that obtained by using Hanning window.

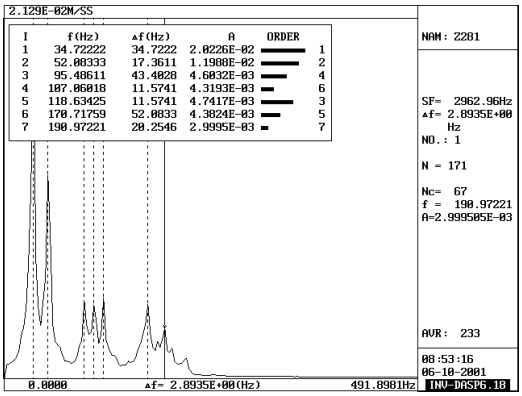

Fig. 5.9 (a) Using Rectangular Window.

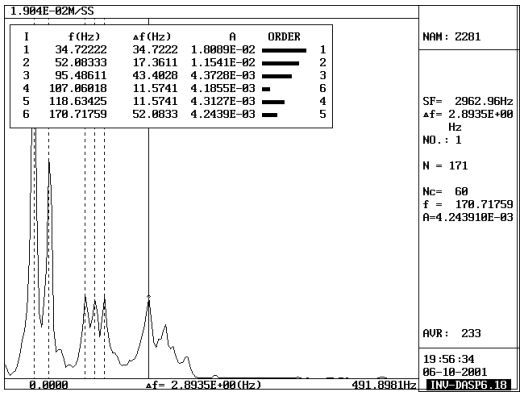

Fig. 5.9 (b) Using Hanning Window.

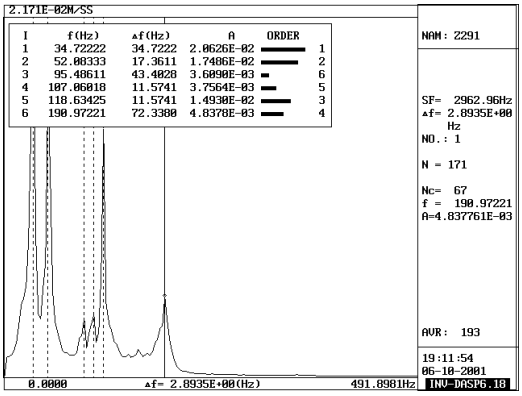

Fig. 5.9 (c) Using Rectangular Window.

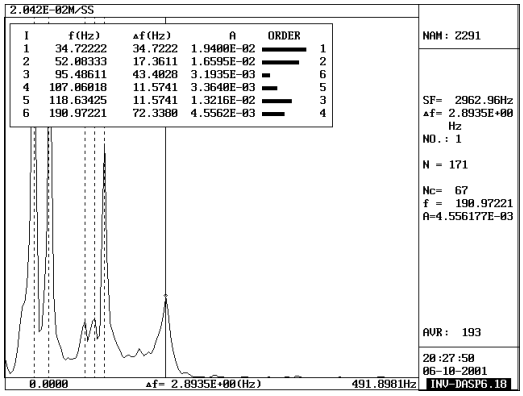

Fig. 5.9 (d) Using Hanning Window.

Fig. 5.9 Frequency Response Spectrums at Point 1 Using Different Window Functions.

The peaks in the spectrum averaged by Hanning window are much smoother than those averaged by using rectangular window from the auto-power density function at points 1(in Fig. 5.10 (a) and (b)) and 16 (in Fig. 5.10 (c) and (d)) under cart excitation. This can be explained by the fact that when a rectangular window is used, more energy will be concentrated in the range of dominant frequencies. There are no other obvious discrepancies caused by using various window functions.

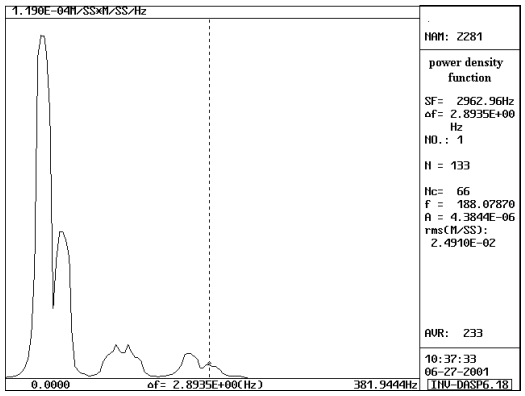

Fig. 5.10 (a) Using Rectangular Window.

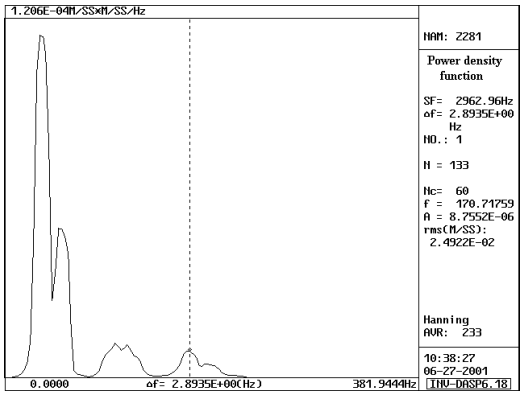

Fig. 5.10 (b) Using Hanning Window.

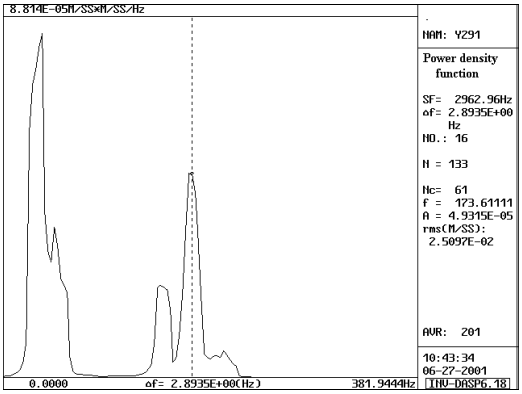

Fig. 5.10 (c) Using Rectangular Window.

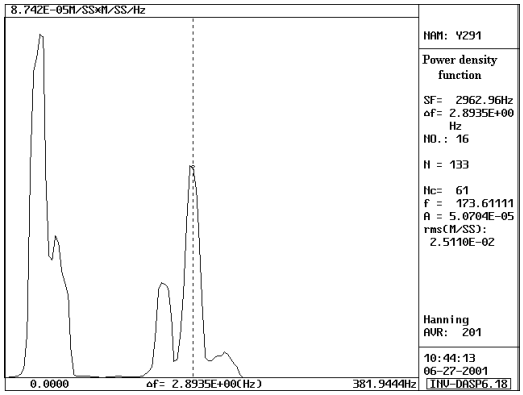

Fig. 5.10 (d) Using Hanning Window.

Fig. 5.10 Auto-power Density Functions at Points 1 and 16 Using Different Window Functions.

5.1.4 Effect of Distribution of Added Mass

Two types of distribution of added mass were considered in the testing. In the uniformly distributed mass (see Fig. 5.11 (b)), the ambient excitation was simulated by pulling the cart back and forth along the surface of the slab. The tires of the cart were directly touched the surface of the iron block instead of the deck surface. The other was non-uniformly distributed mass (see Fig. 5.11 (a)). In this case, two sides of the deck undertook more weight than the central area. Due to the inappropriate construction process, cement mortar was used to cover the iron block. This operation was convenient for cart driving and the static loading, but it increased greatly the rigidity of the model bridge (the total mass meets the similitude requirements). The first frequency of the model bridge with uniformly distribution of added mass was about twice that of the model bridge with non-uniformly distribution of added mass, but other frequencies remained the same. Another problem was that the added iron blocks took part in loading. The concrete deck was in the tension condition when the external static loading was implemented. Though these problems existed, they did not affect the damage detection and identification.

(a) Non-uniformly distributed mass

(b) Uniformly distributed mass

Fig. 5.11 Distribution of Added Mass.

Fig. 5.12 is the typical auto-power density function at point 1 with different distribution masses. There are two modes existing with non-uniform distribution (in Fig. 5.12 (a)), but four modes with uniform distribution mass (in Fig. 5.12 (b)) while accelerators are in the vertical direction. The auto-power density function was contrast while accelerators were in the horizontal direction (in Fig. 5.12 (c) and (d)). From the above results shown in Fig. 5.13, it can be concluded that the distribution manner of the added iron mass strongly affects the dynamic behavior of the model bridge. The natural frequencies and damping ratios of model bridge with non-uniform mass under hammer impact are listed in Table 5.6 (a) and (c), and Table 5.6 (b) and (d) are those of model bridge with uniform mass under hammer impact. The changes of transverse vibration are smaller than those of vertical vibration, because the changes of transverse rigidity were smaller than those of vertical rigidity.

The detailed calculation analysis has also demonstrated that the manner of added mass distribution strongly affects the dynamic behavior of the model bridge. The first frequency was 11.195 Hz when the mass of the model bridge distributed among each member, that's to say, each material has 6 times its self-weight by amplifying its specific gravity to satisfy the similitude law. When the iron blocks were distributed uniformly and the added mass was concentrated on the concrete slab (the iron blocks and concrete slab were treated as same material, but the mass was identical and the specific gravity was changed), the first frequency was 20.312 Hz.

The calculation results of experimental model bridge agree well with testing results. The first frequency of experiment was 33.86 Hz, and that of calculation was 35.382 Hz.

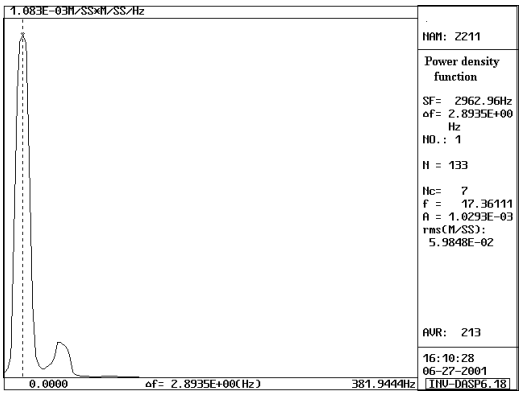

Fig. 5.12 (a) With Non-uniformly Mass.

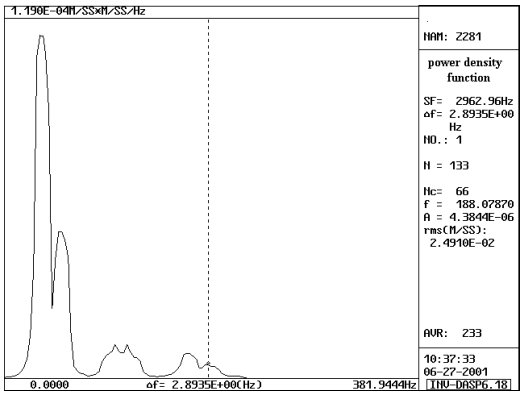

Fig. 5.12 (b) With Uniformly Mass.

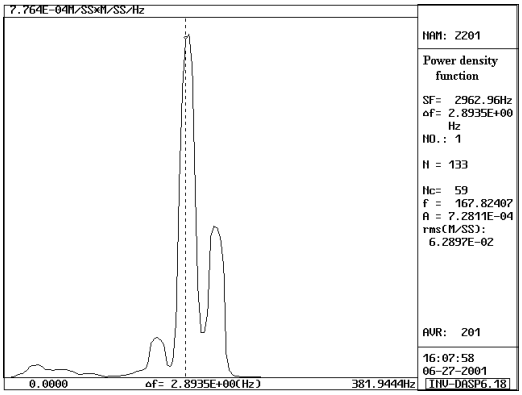

Fig. 5.12 (c) With Non-uniformly Mass.

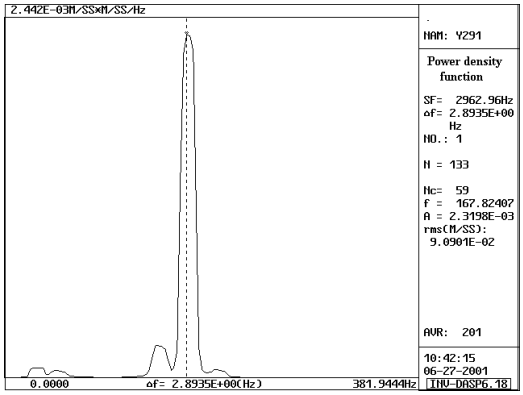

Fig. 5.12 (d) With Uniformly Mass.

Fig. 5.12 Auto-power Density Function with Different Distribution of Mass.

*Note: Accelerator vertical arrangement in Fig. 5.12 (a)-(b) and horizontal arrangement in Fig. 5.12 (c)-(d).

Table 5.6 Identified Frequencies and Damping Ratios

Table 5.6 (a) Impact at Point C

Identified frequencies and dampings ratios
FIT METHOD : MONOFREEDOM(C)
TEST NAME : Z143#
RESPONSE TYPE : ACCELERATION

MODE No.	FREQUENCY		Damping		
	Hz	Radius	%	½BW(Hz)	Radius
1	16.467	103.464	1.2004	0.395	2.484
2	52.995	332.980	1.9557	2.073	13.024
3	85.977	540.207	5.3037	9.120	57.302
4	104.466	656.380	1.6867	3.524	22.142
5	140.551	883.109	1.3237	3.721	23.379
6	156.635	984.167	0.4306	1.349	8.476
7	194.237	1220.427	2.1456	8.335	52.371

Table 5.6 (b) Impact at Point C

Identified frequencies and dampings ratios
FIT METHOD : MONOFREEDOM(C)
TEST NAME : ZHC3#
RESPONSE TYPE : ACCELERATION

MODE No.	FREQUENCY		Damping		
	Hz	Radius	%	½BW(Hz)	Radius
1	33.860	212.749	1.0097	0.684	4.296
2	93.270	586.036	1.7514	3.267	20.528
3	105.705	664.161	1.1006	2.327	14.620
4	169.243	1063.387	0.7759	2.626	16.501
5	188.713	1185.716	1.5658	5.910	37.131

Note: Accelerators were arranged in the vertical direction in Table 5.6(a) and (b).
Table 5.6 (a) is for non-uniform mass and Table 5.6(b) is for uniform mass.

Table 5.6(c) Impact at Point a

Identified frequencies and dampings ratios
FIT METHOD : MONOFREEDOM(C)
TEST NAME : 2151#
RESPONSE TYPE : ACCELERATION

MODE No.	FREQUENCY		Damping		
	Hz	Radius	%	½BW(Hz)	Radius
1	29.857	187.596	13.1017	7.823	49.156
2	56.557	355.355	1.4190	1.605	10.085
3	105.903	665.405	3.9855	8.441	53.039
4	141.798	890.942	0.4458	1.264	7.944
5	170.329	1070.209	0.5310	1.809	11.365
6	195.619	1229.110	0.0001	0.000	0.003

Table 5.6(d) Impact at Point a

Identified frequencies and dampings ratios
FIT METHOD : MONOFREEDOM(C)
TEST NAME : ZHH1#
RESPONSE TYPE : ACCELERATION

MODE No.	FREQUENCY		Damping		
	Hz	Radius	%	½BW(Hz)	Radius
1	28.794	180.917	2.2113	1.273	8.001
2	49.282	309.648	3.8216	3.767	23.667
3	115.512	725.785	0.9166	2.118	13.306
4	144.346	906.956	0.3958	1.143	7.179
5	169.294	1063.703	0.2824	0.956	6.007
6	195.959	1231.244	1.1033	4.324	27.170

Note: Accelerators were arranged in the horizontal direction in Table 5.6 (c) and (d).
Table 5.6 (c) is for non-uniform mass and Table 5.6(d) is for uniform mass.

5.1.5 Results of Static Loading

Because of the construction of concrete casting and iron block arrangement, some points were destroyed or their strains became unstable. These points would not be considered. The setup of static loading is shown in Fig. 5.13. At the center of span, the load-strain relationships at the bottom of flange demonstrate the linear relationships (See in Fig. 5.14 (a)). The difference between girders 1 and 2 is small. The same conclusion was also obtained from the load-deflection relationships at the center of span of the model bridge (See in Fig. 5.14 (b)). The distribution of deflection along the length of girder 2 reveals that the model bridge is flexible under static loading at the center of span (See in Fig. 5.14 (d)). On the concrete slab, the strain distribution along the cross direction conforms to that of real structures. Other data were saved as the reference of damaged conditions. There is an important aspect to be declared, that’s to say; all static loading was restricted in the elastic range. Because the material non-linearity affects the damage detection and thus the results of the finite element calculation will become inaccurate. This problem is very complicated and beyond the study of this project.

Fig. 5.13 Static Loading Setup of the Model Bridge.

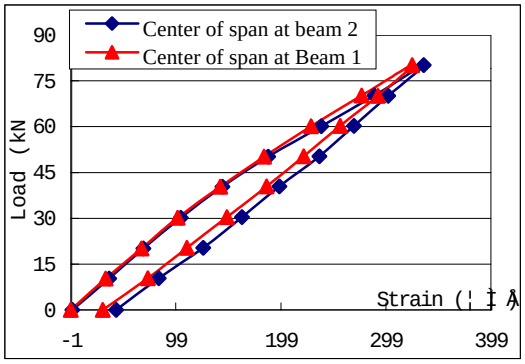

Fig. 5.14 (a) Load-strain Relationships.

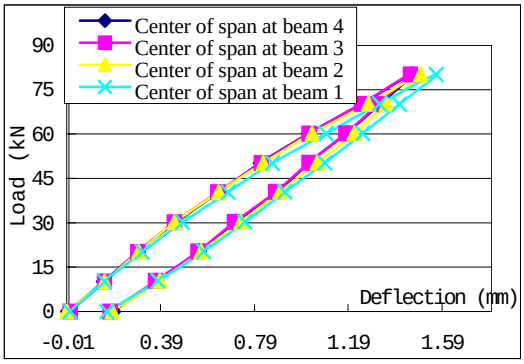

Fig. 5.14 (b) Load-deflection Relationships.

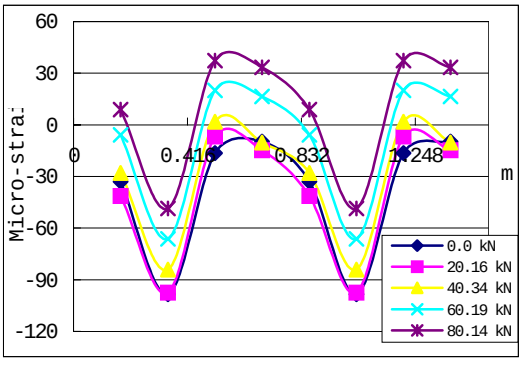

Fig. 5.14 (c) Strain Distribution.

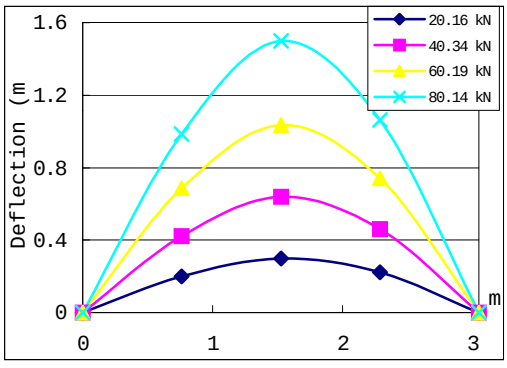

Fig. 5.14 (d) Deflection Distribution.

5.1.6 Summary of Pre-testing

Suggested by the characterization test results, uniformly distributed mass was spread over concrete slab, and the vehicle speed was about 1.32m/s for ambient excitation testing. Total 6 excitation points were selected to excite the structure from location A (a) to F (f). Hanning window function was used during signal processing to limit leakage. The sampling rate was 3000Hz, and the cut-off frequency was 200Hz. Moving window average technique was used to enhance the signal-to-noise ratio. The power density functions or frequency response spectrum was calculated after 57 averages with 87.5% overlap. The overlap allows for a more optimal use of the time history.

The comparison of the frequencies and damping ratios of the model bridge with uniformly distribution mass under two different excitations is summarized in Table 5.7. Reasonably good agreements have been achieved except the third natural frequency and damping ratios in Table 5.7 (a) and (b).

Table 5.7(a) Comparison of Ambient and Impact Test Results

	Comparison of Natural Frequency		Comparison of Damping Ratio	
Mode No.	Ambient Test	Impact Test	Ambient Test	Impact Test
No.1	33.723hz	33.722hz	0.0003%	1.1939%
No.2	50.100hz	52.664hz	0.0228%	1.2836%
No.3	89.795hz	93.250hz	15.3060%	1.7555%
No.4	103.16hz	105.724hz	0.8634%	1.5895%
No.5	134.082hz	140.516hz	0.0285%	3.0321%
No.6	169.437hz	169.243hz	0.0415%	0.7759%
No.7	185.492hz	188.713hz	1.7645%	1.5658%

*Note: Accelerators were arranged in the vertical direction in Table 5.7 (a).

Table 5.7(b) Comparison of Ambient and Impact Test Results

	Comparison of Natural Frequency		Comparison of Damping Ratio	
Mode No.	Ambient Test	Impact Test	Ambient Test	Impact Test
No.1	27.859hz	28.966hz	0.2513%	1.7212%
No.2	50.338hz	51.319hz	0.6877%	0.5412%
No.3	119.735hz	115.512hz	0.3681%	0.9166%
No.4	144.267hz	143.798hz	0.0001%	0.2919%
No.5	170.316hz	169.759hz	0.1150%	0.1537%
No.6	197.129hz	196.871hz	0.6079%	0.6155%

*Note: Accelerators were arranged in the horizontal direction in Table 5.7 (b).

5.1.7 Comparison between Testing and FEM Calculation at Intact Condition

The frequency comparison between testing and FEM calculation was listed in Table 5.8. Some frequencies are good agreement, but others have great differences, which were explained by the following reasons. (1) The added mass in FEM was treated as rigid connection with the concrete slab, but actually, the added iron blocks were attached to the slab by cement mortar. On the other hand, some iron blocks were uniformly distributed, but FE model was treated as uniform distribution. So there are great difference of the second and the third frequencies between the testing and the calculation. (2) The arrangement of accelerators was uniformly distributed on the four girders. Under car ambient excitation and hammer impact excitation, some mode shapes could not be measured out. (3) While the signal was treated and the modal parameters were identified, the modified SDOF modal identification method could not identify the closed mode shapes. (4) The effects of supported condition, especially the piers of bridge, were not considered in the FEM calculations. But the testing results contained all effects of all kinds of factors, also including the environmental noise, car, and engine noise, etc.

In general, there are errors among the testing results, but there are no changes in the basic characteristics. The FEM calculation must be checked out by the testing data and then the results may be used, because many assumptions are employed while the FE model is setup.

Table 5.8 Frequency Comparison of Testing and FEM Calculation at Intact Condition

Mode No.	Frequency of calculation	Frequency of testing
No.1	35.382 Hz	33.722 Hz
No.2	38.870 Hz	28.966 Hz
No.3	69.617 Hz	52.644 Hz
No.4	90.538 Hz	93.250 Hz
No.5	95.492 Hz	--*
No.6	100.357 Hz	105.724 Hz
No.7	104.187 Hz	115.512 Hz
No.8	138.838 Hz	140.516Hz
No.9	140.626 Hz	143.798 Hz
No.10	153.142 Hz	169.243Hz
No.11	176.870 Hz	188.713 Hz
No.12	195.262 Hz	196.187 Hz

*: This frequency was not measured out.

5.2 Damage Identification from Static Data

Usually, static parameter estimation is based on measured deformation and strain induced by static loads. Using a finite-element model of the structure, measured and analytical responses are compared. Parameters that define the model at the elemental level are then updated to minimize the difference between the measured and analytical responses. Then the revised model can serve as a baseline for model updating and condition assessment. The key problem is that this method is often troubled by non-uniqueness and non-continuity of the solutions when the measured data are polluted with noise. But this is definitely the direction of development.

In this section, deflections and strains will be extracted from the experimental data to identify the damage. The changes of deformation before and after damage may indicate presence of damage. Because of time limit, FEM updating method and parameters estimation will be conducted in the next phase. The damage conditions are listed in Table 5.9. The damage position and measured points of model bridge are shown in Fig. 5.15.

Table 5.9 Damage Conditions

Conditions	Content	Note
Intact	No damage	
Damage I	Bearing damage	At girder 2
Damage II	Only girder 1 damage	Cut off bottom flange and part of web
Damage III	Both girder 1 and 3 damage	Cut off bottom flange and part of web
Damage IV	Bearing damage, and girder 1 and 3 damage	

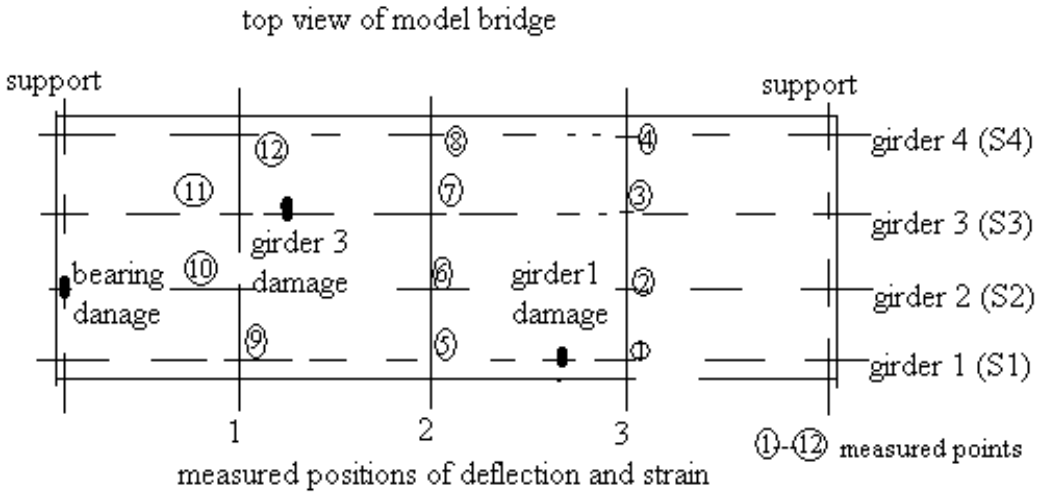

Fig. 5.15 Measured Positions and Damage Positions.

5.2.1 Bearing Damage (Damage I)

The changes of deflection and strain under different loading via positions due to bearing damage are shown in Fig. 5.16. The following conclusions may be obtained from these figures.

(1) The bearing damage at girder 2 caused more deflection change at near measured position than at other positions in Fig. 5.16(a). But similar condition doesn't occur in Fig. 5.16 (b). This indicates that deflection is more sensitive than strain to bearing removal.

(2) The bearing removal may cause the redistribution of the whole model bridge. The strain values caused by self-weight and bearing damage are shown in Fig. 5.16 (c). We couldn't conclude where the damage occurred from Fig. 5.16 (c). After bearing damage occurs and girder is also damaged, the strain value caused by self-weight near girder 3 damage position is larger than that at any other positions (Fig. 5.16 (d)). It may indicate that the strain is more sensitive than deflection to girder cracking (damage).

(3) We may conclude that bearing damage occurred at the roller of girder 2, which is near the largest deflection position.

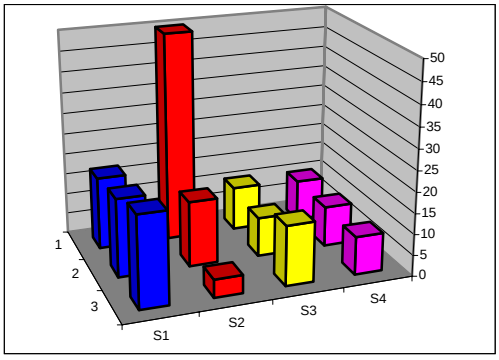

Fig. 5.16 (a) Deflection Changes (%) with 10kN External Load.

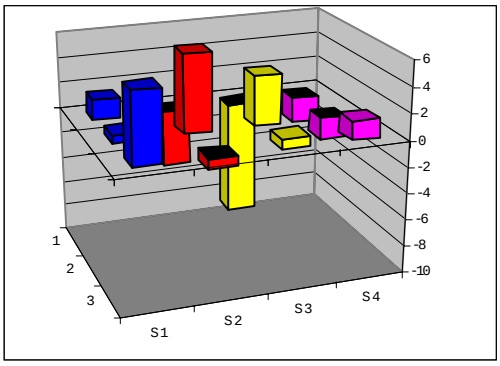

Fig. 5.16 (b) Strain Changes (%) with 60 kN External Load.

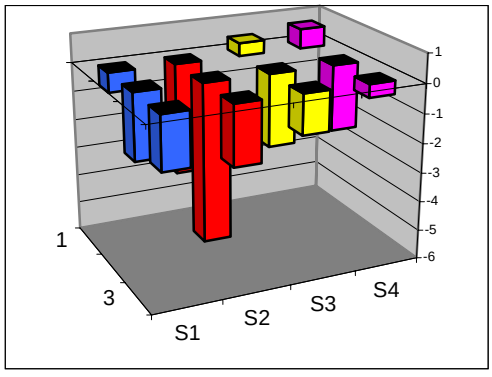

Fig. 5.16 (c) Strain Values Caused by Self-weight.

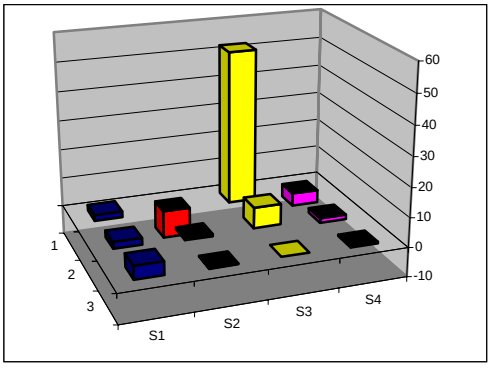

Fig. 5.16 (d) Strain Values Caused by Self-weight, Bearing Damage, and Girder 3 Damage.

Fig. 5.16 Deflection and Strain Changes via Positions due to Bearing Damage.

5.2.2 Only Girder Damage (Damage II)

Due to girder damages, the changes of deflection and strain under different loading via positions are shown in Fig. 5.17. The following conclusions may be obtained from these figures.

(1) The damage of girder 1 caused larger deflection changes at most of the measured positions in Fig. 5.17(a), not only nears the damage position. But similar condition doesn't occur in Fig. 5.17 (b). The strain change near damage position in girder 1 is greater than that at any other positions. It indicates that strain is more sensitive than deflection to girder cracking.

(2) The girder cracking may cause the redistribution of the whole model bridge. The strain values caused by self-weight and damages occurred in girders 1 and 3, respectively, are shown in Fig. 5.17 (c) and Fig 5.17 (d). We can conclude that the damage occurred near the measured position from Fig. 5.17 (c) and (d). It may indicate the strain is sensitive to girder cracking (damage).

(3) It is not possible to know exactly where the damage occurred. We can only obtain that the damage occurred around measured positions where the largest strain occurred.

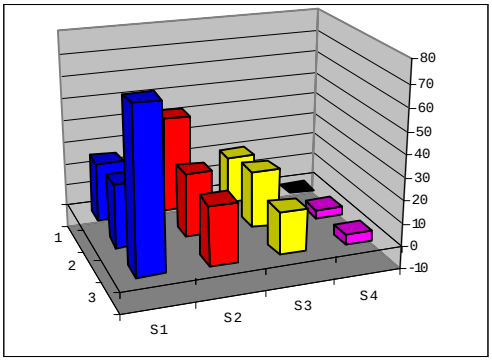

Fig. 5.17 (a) Deflection Changes (%) with 10kN External Load.

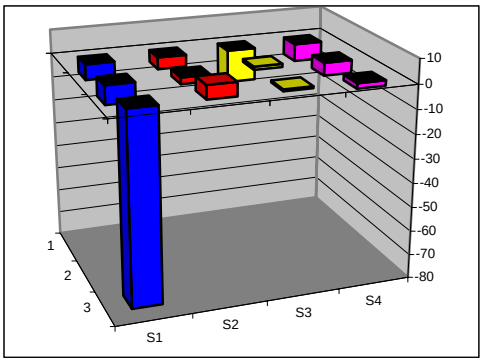

Fig. 5.17 (b) Strain Changes (%) with 60 kN External Load.

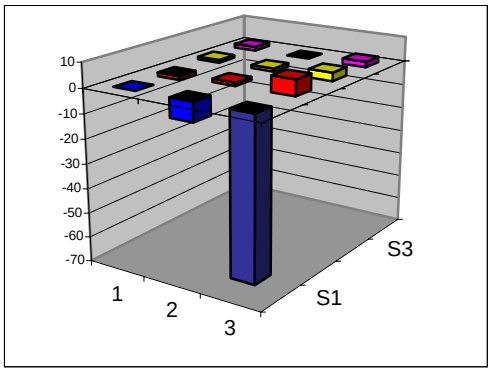

Fig. 5.17 (c) Strain Values Caused by Self-weight and Girder 1 Damage.

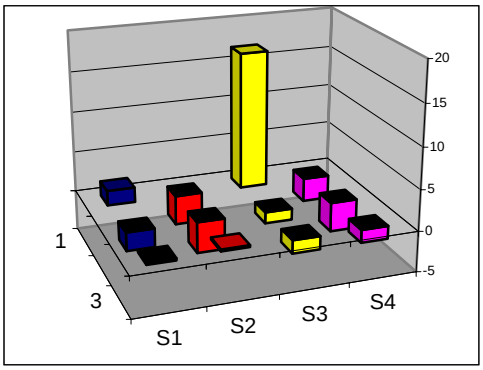

Fig. 5.17 (d) Strain Values Caused by Self-weight and Girder 3 Damage.

Fig. 5.17 Deflection and Strain Changes via Positions due to Girder Damages.

5.2.3 Girders 1 and 3 Damage (Damage III)

Due to damages occurred in girders 1 and 3, the changes of deflection and strain under different loading via positions are shown in Fig. 5.18. The following conclusions may be obtained from these figures.

(1) In Fig. 5.18 (a), we may not indicate where damages occurred from the deflection changes caused by damages occurred in girders 1 and 3. For example, the deflection near damage position in girder 1 changes drastically, but it changes slightly near damage position in girder 3. Though bearing of girder 2 is not damaged, the deflection changes greatly near the bearing. The measuring error exists definitely. It also indicates that deflection is not sensitive to girder cracking.

(2) The girder cracking may cause the redistribution of the whole model bridge. The strain values caused by self-weight and damages occurred in girders 1 and 3 are shown in Fig. 5.18 (c). We can conclude that the damage occurred near the measured position from Fig. 5.18(c). When external load is 60 kN, strain changes due to damages occurred in girders 1 and 3 are shown in Fig. 5.18(b). The strain changes near the two damage positions gain the largest values. This indicates that the strain is sensitive to different girder cracking (damages).

(3) If damages occur in girders 1 and 3 and the bearing is also damaged, the strain values increase a little due to the bearing damage. We can obtain this conclusion from the Fig. 5.18 (d).

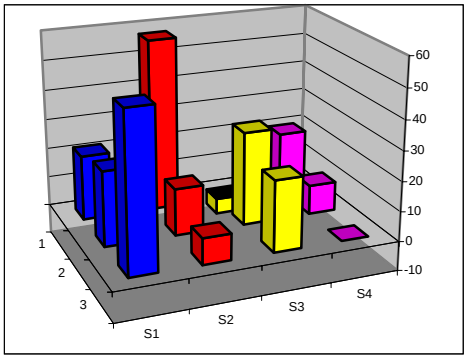

Fig. 5.18 (a) Deflection Changes (%) With 10 kN External Load.

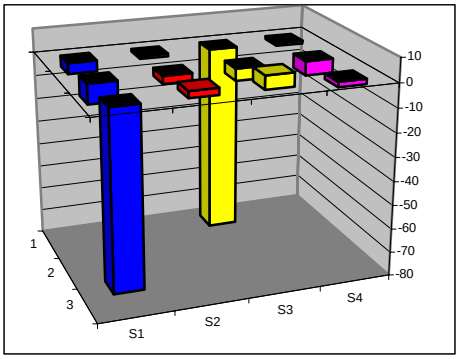

Fig. 5.18 (b) Strain Changes (%) with 60 kN External Load.

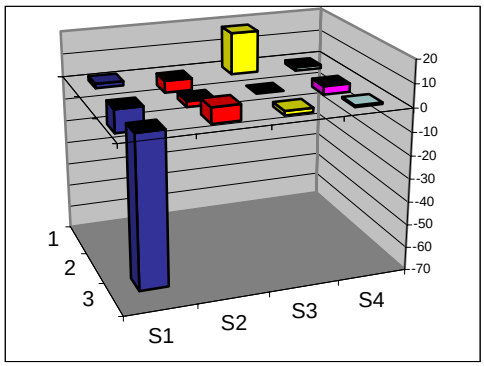

Fig. 5.18 (c) Strain Values Caused by Self-weight.

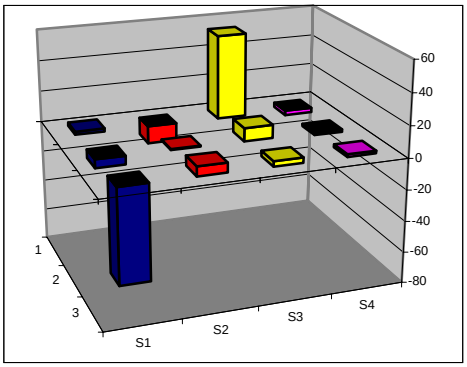

Fig. 5.18 (d) Strain Values Caused by Self-weight and all Damages.

Fig. 5.18 Deflection and Strain Changes via Positions due to Damages Occurred in Girders 1 and 3.

5.2.4 Girder 1, Girder 3, and Bearing Damages (Damage IV)

The changes of deflection and strain under different loading via positions due to all damages are shown in Fig. 5.19. The following conclusions may be obtained from these figures.

(1) We may not find where damage occurred from the deflection changes causes by all damages in Fig. 5.19 (a), though bearing of girder 2 was damaged, the deflection changes greatly near the bearing. In Fig. 5.19(b), bearing damage caused very little change of strain near the bearing position. But girder cracking at girders 1 and 3 produces very large changes of strain near these two damaged positions. It indicates that strain is sensitive to the composite damage of girder cracking.

(2) If damages of girders 1 and 3 occur and the bearing is also damaged, the strain values increase a little due to the bearing damage. We can conclude that strain is not sensitive to bearing damage from Fig. 5.19 (c).

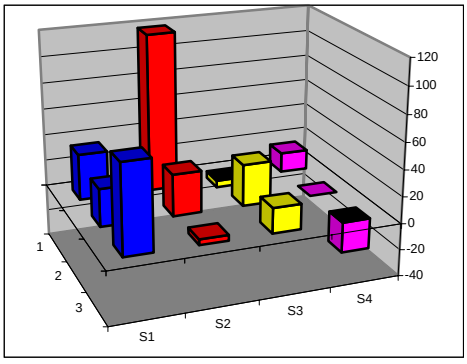

Fig. 5.19 (a) Deflection Changes (%) With 10 kN External Load.

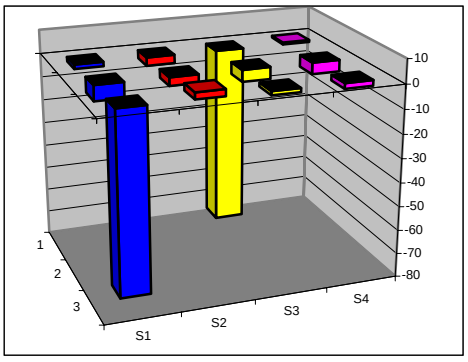

Fig. 5.19 (b) Strain Changes (%) With 60 kN External Load.

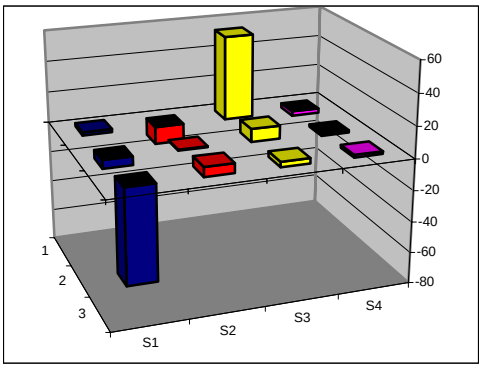

Fig 5.19 (c) Strain Values Caused

by Self-weight.

Fig. 5.19 Deflection and Strain Changes via Positions due to all Damages.

5.2.5 Damage Identification from Load-strain Relationship

Because the tests were conducted in the lab and the environmental factors were well controlled and compensated while strains and deflections were measured, it was concluded that the changes of strain and deflection were due to damages mainly. The testing indicates that the deflection changes very slightly under self-weight after the damages occurs, but strains at different points change greatly and obviously. Deflection and strain are varied depending on locations, but deflections indicate the whole deformation of bridge structures. In general, deflection is a global static signature and strain is a local static signature.

The relationships between load via deflection and load via strain may be extracted from the ordinary static testing. Usually, these relationships are used to assess the strength and capacity of a structure. It is important that this kind of results be used to assess the different types of damage for the damage detection of existing bridges, provided that the baseline model of the bridge exists. In this section, we will compare the measured deflections and strains under external loading before and after damage. Only those points, which are close to damage positions, are selected, because the deflection and strain values at these points are larger than those of other points due to damage. The measured points are listed in Fig. 5.15. Only those measured points, which are very close to the damage positions, are selected. The relationships between load-deflection and load-strain are shown in Figs. 5.20 and 5.21, respectively.

The typical relationship of load-deflection is shown in Fig. 5.20 (c). The measured point is located at the mid-span of girder 1. The load-deflection relationships are still linear after damages occurred. Some conclusions may be obtained from Fig. 5.20:

(1) The values at the original presented the changes of deflection under self-weight after the damages and the values are much smaller. This is different from that of strain changes under self-weight, which values changed a lot. On the other hand, though the deflection is small, we can see that the deflection changes greater due to bearing removal than that due

to cracking of girders. This may indicate that deflection is more sensitive to bearing damage than to girder cracking.

(2) The differences of curves between the intact and different kinds of damage are small, but the differences can indicate the happening of damage and/or condition changes of bridge structure.

(3) The load-deflection curves at different measured points are very similar. They cannot be used to locate the positions of damage and/or condition changes.

(4) Furthermore, the deflection is a global static signature and it presents the whole bending or torsion behavior of a structure, though it is dependent on the measured positions. That means different damages may cause the same change of deflection at one point. So load-deflection curves may indicate the strength or capacity of a structure, but they are difficult to be applied to assess the damages.

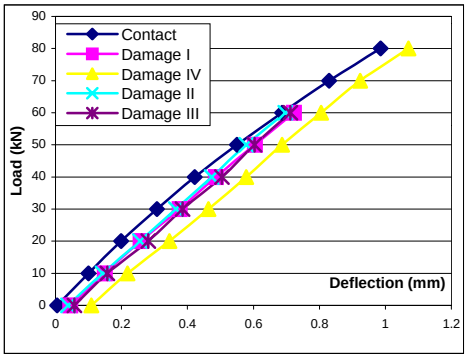

Fig. 5.20 (a) At Measured Point 10.

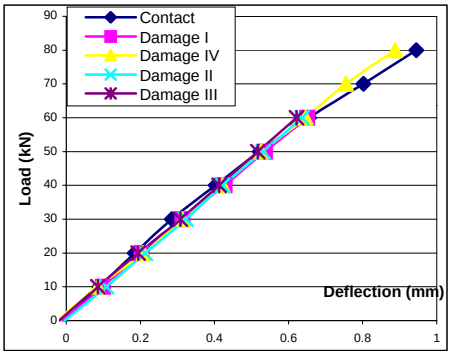

Fig. 5.20 (b) At Measured Point 11.

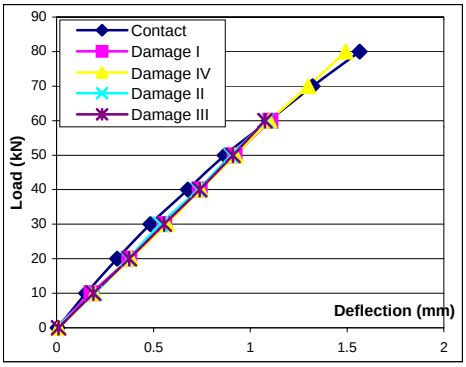

Fig. 5.20 (c) At Measured Point 5.

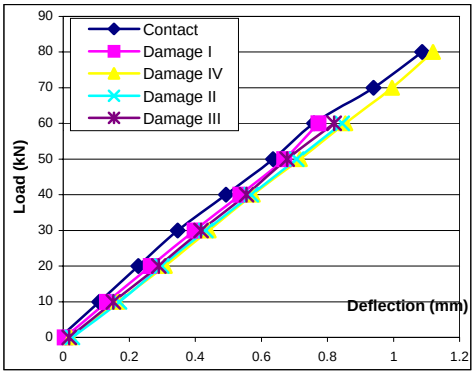

Fig. 5.20 (d) At Measured Point 1.

Fig. 5.20 Load-deflection Curves before and after Damages Occurred.

The typical relationship of load-strain is shown in Fig. 5.21 (c). The measured point is located at the mid-span of girder 1. The load-strain relationships are still linear after damages

occurred. There are some differences between the deflection curves and strain curves. Some conclusions may be obtained from Fig. 5.21:

(1) The strain changes very little due to bearing removal, even at the points where it is very close to the bearing damage position. This may indicate that the strain is not sensitive to bearing removal.

(2) The load-strain curves change greatly due to the cracking at girder 1 or girder 3, or both, from Fig. 5.21 (b) and (d). These two points are very close to the girder damage positions. We cannot only conclude that the damage occurs from the load -strain curves, but also locates where the damages are close to. This means that the load-strain curves may be used to detect the damage.

(3) Because the strain is not sensitive to bearing damage, the composite of different damages is hard to be identified from the load-strain curves. But it can be used to identify the composite of the same girder damages.

(4) Strain is strongly dependent on the measured positions, so it is a local static signature. It can be used to locate the damage.

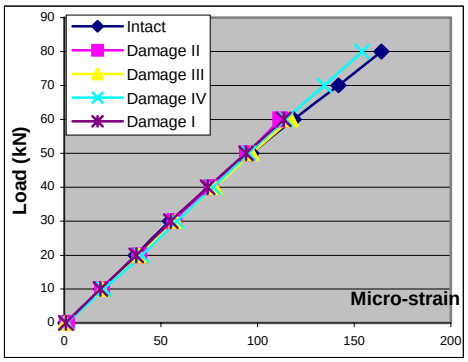

Fig. 5.21 (a) At Measured Point 10.

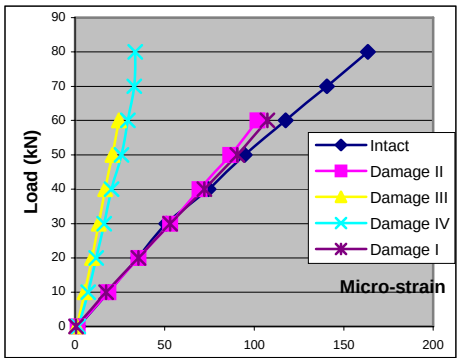

Fig. 5.21 (b) At Measured Point 11.

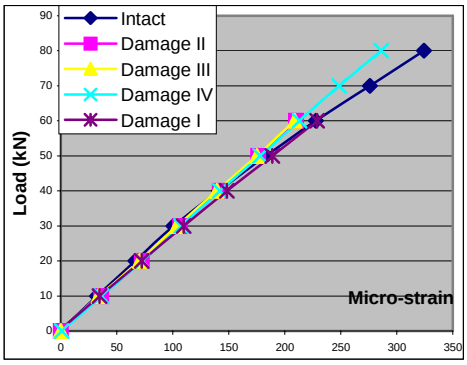

Fig. 5.21(c) At Measured Point 5.

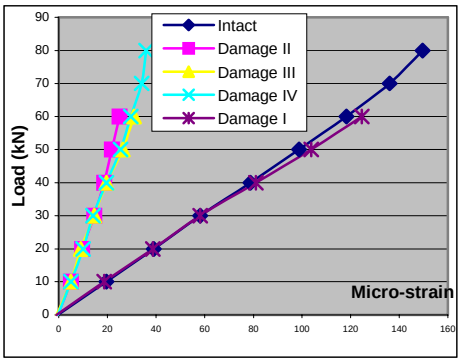

Fig. 5.21 (d) At Measured Point 1.

Fig. 5.21 Load-strain Curves before and after Damages Occurred.

5.2.6 Summary

From the above analysis, several important conclusions may be obtained:

(1) The deflection is sensitive to the bearing damage, but not to girder cracking damage.
(2) The strain is sensitive to girder cracking damage, but not to the bearing damage.
(3) Deflection is a global static signature and strain is a local static signature. Changes of deflection or strain may indicate the happening of damage and location of damage. But these indications strongly rely on the measured positions. If the measured points are very close to the damage positions, the indications are clear. Finding the accurate location may still need to be developed.
(4) The load-deflection relationships and the load-strain relationships still keep the linearity after the damages occurred, under the extent of external loading. That means the non-linearity caused by damage is very small.
(5) The ordinary load-deflection curves are hard to be used to detect the damage, but the load-strain curves may be used to identify the damage, if the baseline model of intact condition of a structure exists.
(6) One damage index is insufficient to detect the damages.

5.3 Damage Diagnosis by Using SDOF Modal Identification Method in Frequency Domain

Existence of structural damage leads to modification of the vibration modes. These modifications are manifested as changes in modal parameters (natural frequencies, mode shapes, and modal damping ratios) that can be obtained from results of dynamic testing. The existing study has presented that changes in the modal parameters may not be the same for each mode since the changes depend on the nature, location, and severity of the damage. This effect offers the possibility of using data from dynamic testing to detect, locate, and quantify damage. In this section, the frequencies and damping ratios identified by using SDOF modal identification method under various damage conditions are compared with those at intact condition, and damage will be diagnosed from the changes of these parameters.

5.3.1 Bearing Damage

The frequencies and damping ratios of the model bridge before and after bearing damage (damage I) were listed in Tables 5.10 and 5.11. From Table 5.10, we can see that bearing damage causes the changes of frequencies, but the values are small. In the vertical vibration, the first, third, and the fifth modal frequencies change larger than the rest. In the transverse vibration, only the second modal frequency changes largely. The bearing damage causes the decrease of frequencies of the lower vibration modes, but also causes the increase of the frequencies of some higher vibration modes. These demonstrate that different modes have different sensitivities to

bearing damage. The phenomena are found to correlate well with that of calculation (see §4.7.7). In the horizontal vibration, the bearing damage causes smaller changes of frequencies. It is because the changes of horizontal stiffness of the model bridge are smaller than that of vertical stiffness by removing the bearing.

Table 5.10.1 Vertical Frequency Changes before and after Bearing Damage Occurred

Mode No.	Frequency at intact condition	Frequency with bearing damage	Differences
No.1	33.805 Hz	32.261 Hz	-4.567%
No.2	52.664 Hz	51.502 Hz	-2.206%
No.3	93.250 Hz	98.749 Hz	5.897%
No.4	115.474 Hz	114.765 Hz	-0.614%
No.5	140.516 Hz	152.374 Hz	8.439%
No.6	169.174 Hz	167.247 Hz	-1.139%
No.7	185.429 Hz	187.733 Hz	1.243%

Table 5.10.2 Transverse Frequency Changes before and after Bearing Damage Occurred

Mode No.	Frequency at intact condition	Frequency with bearing damage	Differences
No.1	28.966 Hz	28.671 Hz	-1.018%
No.2	51.016 Hz	47.026 Hz	-7.821%
No.3	115.657 Hz	114.944 Hz	-0.616%
No.4	143.798 Hz	143.869 Hz	0.062%
No.5	169.301 Hz	169.070 Hz	-0.049%
No.6	196.259 Hz	196.045 Hz	0.109%

Natural frequencies change with the development of damage (in Fig. 5.22). It is shown that frequency changes of vertical vibration mode of composite damage (damage IV) are the same as those of only bearing damage (damage I) except for the seventh vibration mode. Changes of frequencies of composite damage (damage IV) under horizontal vibration mode have obvious difference as compared with those of bearing damage (damage I).

From Table 5.11, we can see that the changes of damping ratio are larger than those of frequencies due to bearing damage. This demonstrated that the damping ratio is more sensitive than the natural frequency to bearing damage. In the relative vibration direction, the mode at which the damping ratio has the biggest change is not necessarily the same as the mode where the natural frequency has the biggest change. On the other hand, damping ratios are affected by several factors, including inspection method, noise, etc. It is hard to obtain accurate damping ratios of the bridge structures. That is to say, only damping ratio index is insufficient to be used to detect and locate the damage.

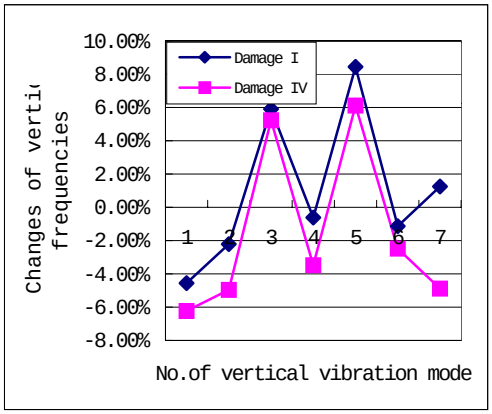

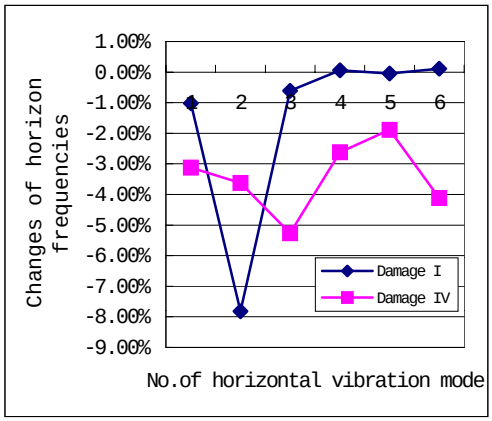

(a) Vertical Vibration. **(b) Horizontal Vibration.**

Fig. 5.22 Changes of Frequencies under Bearing Damage Conditions.

Table 5.11.1 Damping Ratio Changes (Vertical Mode Shape) before and after Bearing Damage Occurred

Mode No.	Damping Ratio at intact condition (%)	Damping Ratio with bearing damage (%)	Differences
No.1	1.0454	0.9785	-6.399%
No.2	1.2836	0.9199	-28.334%
No.3	1.7555	1.0418	-40.655%
No.4	0.8967	0.7060	-21.267%
No.5	3.0321	2.4268	-19.963%
No.6	0.7698	3.5309	358.677%
No.7	1.7754	1.7534	-1.239%

Table 5.11.2 Damping Ratio Changes (Transverse Mode Shape) before and after Bearing Damage Occurred

Mode No.	Damping Ratio at intact condition (%)	Damping Ratio with bearing damage (%)	Differences
No.1	1.7212	1.7240	0.163%
No.2	2.7093	1.2897	-52.397%
No.3	0.8337	0.7352	-11.791%
No.4	0.2919	0.0094	-96.780%
No.5	0.3654	0.5614	53.640%
No.6	1.2179	0.6513	-46.523%

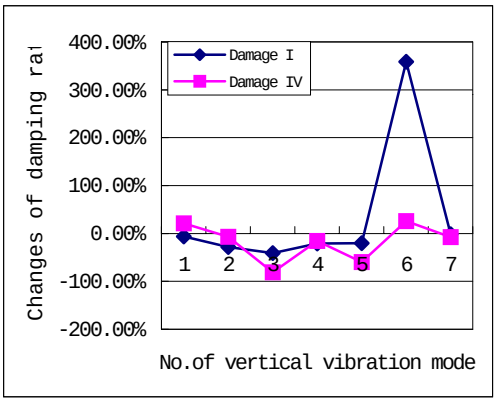

(a) Vertical Vibration.

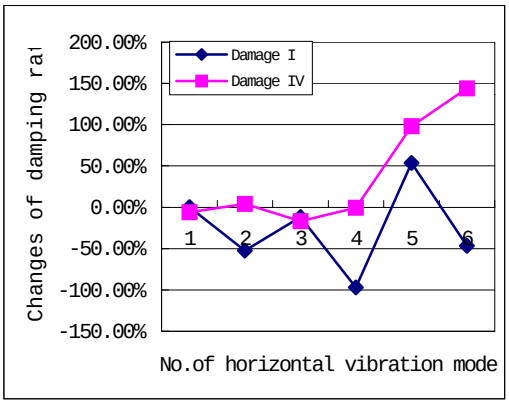

(b) Horizontal Vibration.

Fig. 5.23 Changes of Damping Ratios under Bearing Damage Conditions.

Based on the bearing damage, if damage of girders occurs, the changes of damping ratios of vertical vibration mode are greater than those of frequencies. The change of damping ratio of the sixth vibration mode under damage I is greater than that of other modes. But under damage IV, the changes are close to the average values for all modes. Under the horizontal vibration mode, the change of damping ratio of the fourth vibration mode under damage I is the greatest, but that of the sixth vibration mode under damage IV is the largest.

5.3.2 Girder Damage

The frequencies and damping ratios of the model bridge before and after girder 1 damage (damage II) were listed in Tables 5.12 and 5.13. From Table 5.12, we can see that the first natural frequency in the vertical vibration has the biggest changes due to girder damage. That is different from the result due to bearing damage. In the transverse vibration, the second and the fifth natural frequencies have larger changes, also different from that due to bearing damage. The cracking damage of girder also causes the decrease of frequencies in the lower vibration modes.

Table 5.12.1 Vertical Frequency Changes before and after Girder 1 Damage Occurred

Mode No.	Frequency at intact condition	Frequency at girder 1 damage	Differences
No.1	33.805 Hz	32.067 Hz	-5.141%
No.2	52.664 Hz	51.785 Hz	-1.669%
No.3	93.250 Hz	92.365 Hz	-0.949%
No.4	115.474 Hz	113.338 Hz	-0.614%
No.5	140.516 Hz	144.543 Hz	2.866%
No.6	169.174 Hz	167.724 Hz	-0.857%
No.7	185.429 Hz	182.386 Hz	-1.641%

Table 5.12.2 Transverse Frequency Changes before and after Girder 1 Damage Occurred

Mode No.	Frequency at intact condition	Frequency at girder 1 damage	Differences
No.1	28.966 Hz	29.605 Hz	2.206%
No.2	51.016 Hz	47.679 Hz	-6.541%
No.3	115.657 Hz	112.645 Hz	-2.604%
No.4	143.798 Hz	146.620 Hz	1.962%
No.5	169.301 Hz	169.451 Hz	0.089%
No.6	196.259 Hz	186.899 Hz	-4.769%

Different modes have different sensitivities to girder damage. The changes of frequencies under damage III and damage IV were shown in Fig. 5.24. The trends of frequency changes are the same as those of damage II. Among them, changes of frequencies under vertical vibration mode are greater than those under horizontal vibration mode.

The girder cracking damage just like bearing damage also causes larger changes of damping ratios (see Table 5.13). With different vibration mode shapes, damping ratios increase at some mode shapes, and decrease at other mode shapes under damage II. With the development of damage, the damping ratios under vertical vibration mode decrease, but increase under horizontal vibration mode (see Fig. 5.25).

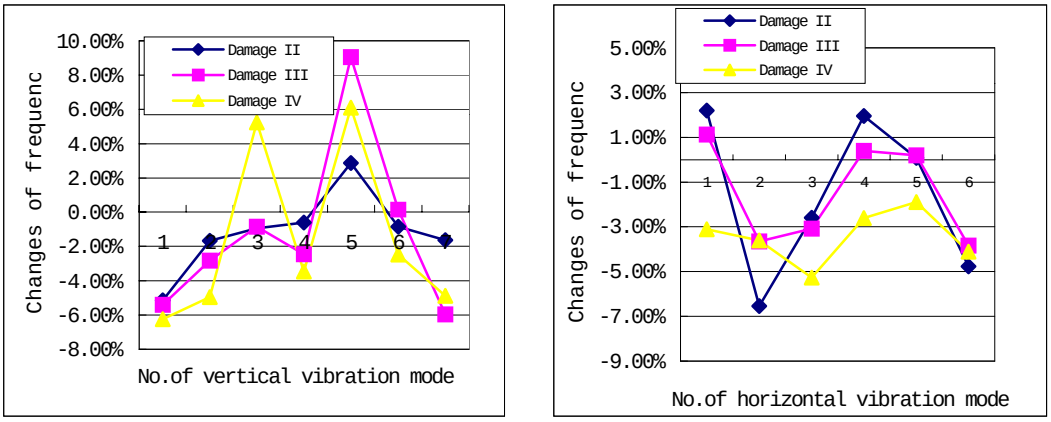

Fig. 5.24 Changes of Frequencies under Girder Damage Conditions.

Table 5.13.1 Damping Ratio Changes (Vertical Mode Shape) before and after Girder 1 Damage Occurred

Mode No.	Damping Ratio at intact condition (%)	Damping Ratio with girder 1 damage (%)	Differences
No.1	1.0454	1.0470	0.153%
No.2	1.2836	2.5970	102.322%
No.3	1.7555	1.1906	-32.179%
No.4	0.8967	1.0574	17.921%
No.5	3.0321	1.4825	-51.107%
No.6	0.7698	1.5596	102.598%
No.7	1.7754	0.5598	-68.469%

Table 5.13.2 Damping Ratio Changes (Transverse Mode Shape) before and after Girder 1 Damage Occurred

Mode No.	Damping Ratio at intact condition (%)	Damping Ratio with girder 1 damage (%)	Differences
No.1	1.7212	1.9765	14.833%
No.2	2.7093	2.0383	-24.767%
No.3	0.8337	0.5075	-39.127%
No.4	0.2919	0.0874	-70.058%
No.5	0.3654	0.5573	52.518%
No.6	1.2179	0.5772	-52.607%

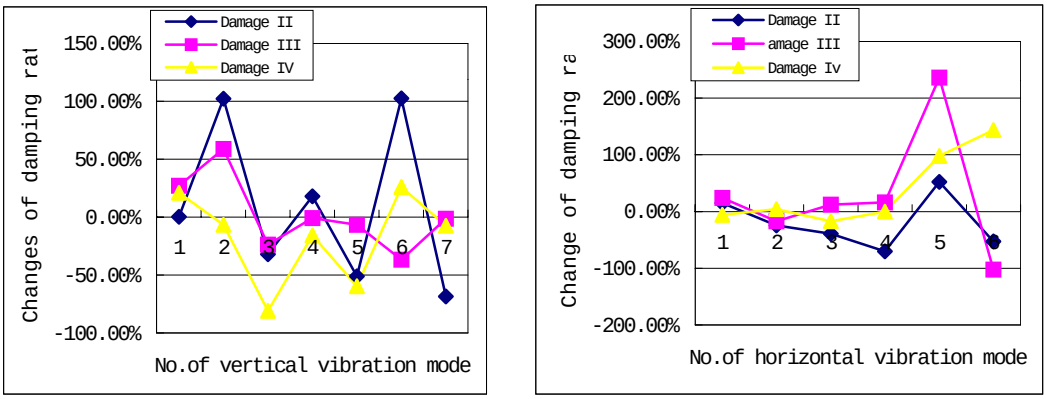

Fig. 5.25 Changes of Damping Ratios under Girder Damage Conditions.

5.3.3 Summary

From the above observation, we can conclude that:

(1) Different damage types may cause different changes in the modal parameters.
(2) Not all modes are sensitive to the same kind of damage. From the changes of modal parameters, we can only conclude that some damages may occur, but we couldn't identify what kind of damage occurred.
(3) We couldn't locate the damage from the modal parameters, except from mode shapes.
(4) The identification of composite damage (such as damage IV) is more difficult than that of singular damage.

5.4 Damage Diagnosis by Using ETR in the time Domain

The first two types of artificial damages were introduced in this research in order to verify the proposed methodology for bridge damage identification. One is the bridge bearing failure; and the other is the simulation of girder 1 cracking. In this section, the frequencies, damping ratios, and ETR index identified by using the correlation method and Polyreference method under these two damage conditions are compared with those at intact condition, and damage will be diagnosed from the changes of these parameters.

5.4.1 Bearing Damage

Bridge bearings are one of the most vulnerable parts of bridge structures under lateral earthquake loading. The behavior of bridge bearing depends on the magnitude of lateral excitation. A bridge bearing may experience minor damage under a small magnitude of lateral ground motion. And may be destroyed completely under a severe earthquake. In this study, it was assumed that only the roller at the girder 2 is seriously damaged, and other rollers are in good condition. The changes of natural frequencies and damping ratios for the first three models before and after bearing failure are summarized in Table 5.14. It can be inferred from the results that the bearing failure affects the second bending mode (mode 3) the most. The first torsion mode (mode 2) also has significant change after bearing is removed. All damping ratios increase after central bearing is damaged. Therefore, the natural frequency and damping ratio are indicators for the damage and/or condition changes. This conclusion is the same as that from the SDOF identification method.

Table 5.14 Changes of modal parameters before and after bearing damage

Mode Number	Natural frequency			Damping Ratio		
	Intact	Damaged	Changes	Intact	Damaged	Changes
Mode 1	34.63	32.65	5.72%	10.202%	6.287%	38.37%
Mode 2	53.25	57.74	8.43%	5.989%	10.422%	74.02%
Mode 3	79.86	74.82	6.31%	3.136%	7.008%	123.47%

Since natural frequencies are global parameters, we cannot locate the damage through the change of natural frequencies. A certain amount of damage at two different locations may cause the same amount of frequency change of structures **(Pandey, et al. 1994)**. Based on the same theory, damping ratios cannot be used to locate the damage either.

In the theory of ETR extraction in chapter 3, it indicates that ETR can be extracted through any 3-position measurements. Previous results demonstrated that ETR was sensitive to the bearing failure **(Kong, et al. 1996)**. However, the main objective of this study is to locate the damage through the changes of ETR before and after damage is introduced. To achieve this goal, the ETR is calculated transversely by using the response data from those accelerometers along the cross-section of the model bridge (see Fig. 5.26).

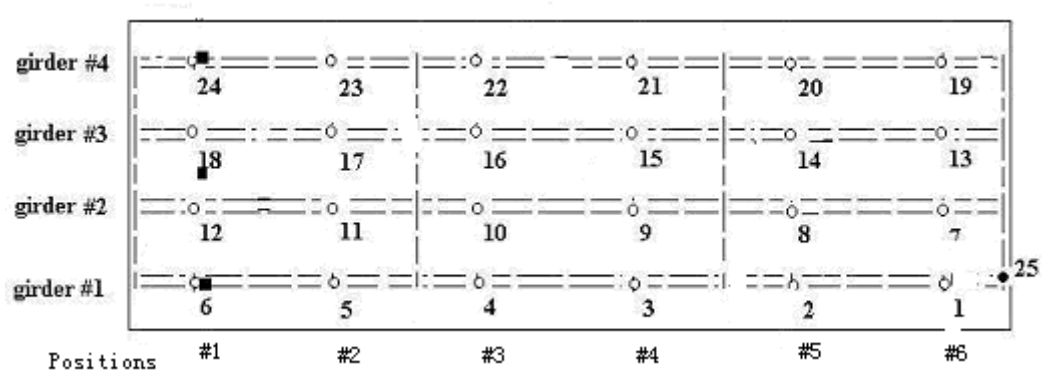

Fig. 5.26 Positions for ETR extraction along the transverse direction.

Table 5.15 and Fig. 5.27 demonstrate the change of ETR's among the first three modes after bearing damage is introduced. It was found that, although the ETR's at all positions have certain changes after the bearing damage is introduced, only the ETR of mode 3 at position 1 has a remarkable change. Referring to the artificial damage definition in chapter 3, it is found that position 1 is the place where the central roller was removed.

Table 5.15 Changes of ETR index before and after bearing damage

Mode Number	Change of ETR index					
	Position 1	Position 2	Position 3	Position 4	Position 5	Position 6
Mode 1	592.5%	75.13%	100%	96.91%	124.2%	87.48%
Mode 2	81.73%	1478%	938.3%	27.62%	31.59%	46.01%
Mode 3	4524%	18.78%	128.1%	55.14%	10.48%	32.72%

The following conclusions may be obtained from the above results:

1. ETR is very sensitive to the bearing removal. The biggest change of ETR before and after

bearing removal is around 4500%, and the smallest change of ETR is above 18%. It can be concluded that the change of ETR can be used to indicate the damage and /or condition changes of bridge structures.

2. The position where the biggest change of ETR occurs can indicate the location of damage. In our case, the roller near position 1 was removed and the biggest change of ETR in Table 5.15 is also around position 1. This observation is first obtained in this study and is very promising for ETR to be used to locate damage and condition changes.

3. Through the current ETR extraction strategy and interpretation methodology, it is not possible to identify exactly which roller was removed. There are totally 4 rollers at position 1. From the test results shown in Table 5.15, we can conclude that the damage occurred around position 1, but we cannot discern which roller at position 1 is damaged.

4. Natural frequencies and damping ratios are global vibration signatures and can well indicate the happening of damage and/or condition change of bridge structures. But they cannot be used to locate the position of damage and/ or condition change. They should be used together with ETR for the purpose of damage and/or condition changes. They should be used together with ETR for the purpose of bridge damage detection.

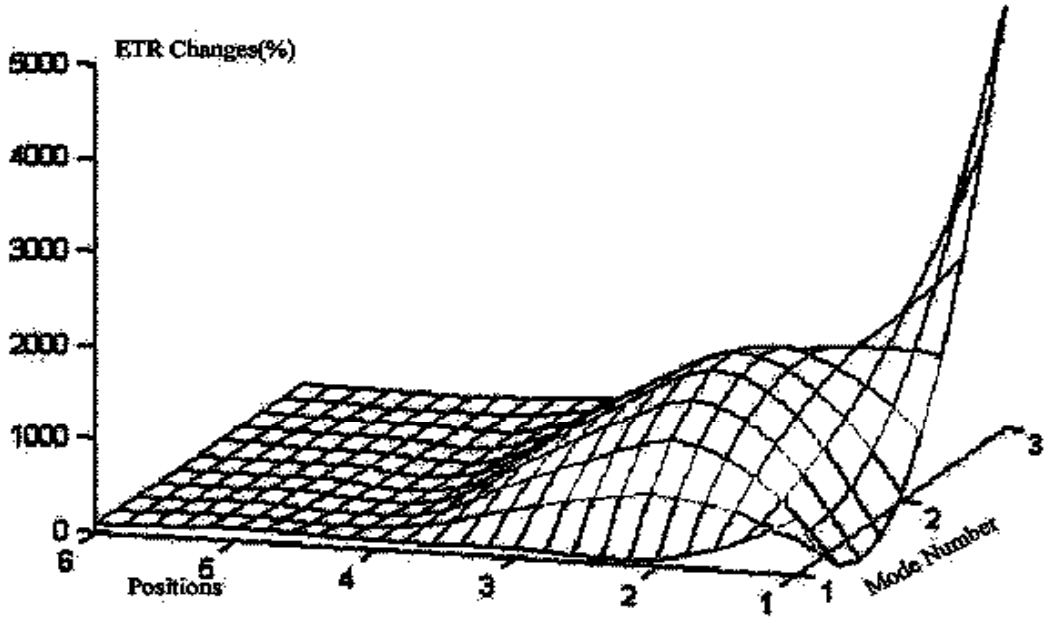

Fig 5.27 ETR Changes by Bearing Damage

5.4.2 Girder cracking

Girder deterioration is one of the most common damage patterns in slab-on girder type of bridges. Usually, this kind of damage occurs either near a support (bearing) of the bridge, or near the middle-span of the bridge, where a transverse diaphragm is connected by welded plates.

Previous studies on girder deterioration near the bridge support demonstrated that the natural frequency and damping ratio are not sensitive enough to locate the damage **(Farrar et al 1995).** In the research, the girder deteriorations around the one-third span are used to rate the ETR as a damage indicator and the damage is modeled by introducing a cut in one of the exterior girders (girder 1) from the bottom flange to 1/2 of the girder length from the pin support.

Changes of natural frequencies and damping ratios of the first three modes are summarized in Table 5.16. It can be seen that the natural frequency of mode 1 decreases substantially while the natural frequencies of the last two modes have just slight changes. At the same time, however, all damping ratios increase after girder cracking is introduced.

Table 5.16 Changes of modal parameters before and after girder 1 damage

Mode Number	Natural frequency			Damping Ratio		
	Intact	Damaged	Changes	Intact	Damaged	Changes
Mode 1	34.63	32.05	7.45%	10.202%	10.335%	1.30%
Mode 2	53.25	54.73	2.78%	5.989%	10.017%	67.26%
Mode 3	79.86	82.69	3.54%	3.136%	3.729%	18.91%

The ETRs of the first three modes after girder crack simulation are extracted transversely based on the same strategy described in the previous section. By using the ETR at the intact condition as baseline, the changes of ETR before and after girder deterioration are shown in Table 5.17 and Fig. 5.28.

Table 5.17 Changes of ETR index before and after girder 1 damage

Mode Number	Change of ETR index					
	Position 1	Position 2	Position 3	Position 4	Position 5	Position 6
Mode 1	100.0%	100.1%	62.93%	1614.7%	288.9%	99.08%
Mode 2	86.92%	214.3%	100.3%	820.2%	99.79%	99.63%
Mode 3	23.35%	34.03%	32.66%	68.21%	63.89%	42.24%

The following conclusions may be obtained from the test results:

1.ETR is sensitive to a simulated girder cracking. From the result shown in Fig. 4.34, the biggest change of ETR is 1614%, and the smallest change is 23%, which is much larger than the change of natural frequencies and damping ratios. For this case, the changes of ETR can be used to indicate the damage and/or condition changes.

2. The location where the damage was introduced is also the place where the ETR has the biggest change. In our study, the girder crack was introduced around the positions 4 and 5, and both mode 1 and mode 2 have the biggest changes of ETR. This shows good agreement between the biggest change of ETR and the location of damage.

3. The ETR's at both mode 1 and mode 2 are very sensitive to girder damage, while the ETR at mode 3 is less responsive.

4. The natural frequencies and damping ratios have different responses from ETR for the bearing failure case. In the bearing failure case, the second and the third modes have bigger changes in both natural frequencies and damping ratios, while in the girder cracking case, the first mode has the biggest change in natural frequencies and damping ratios.

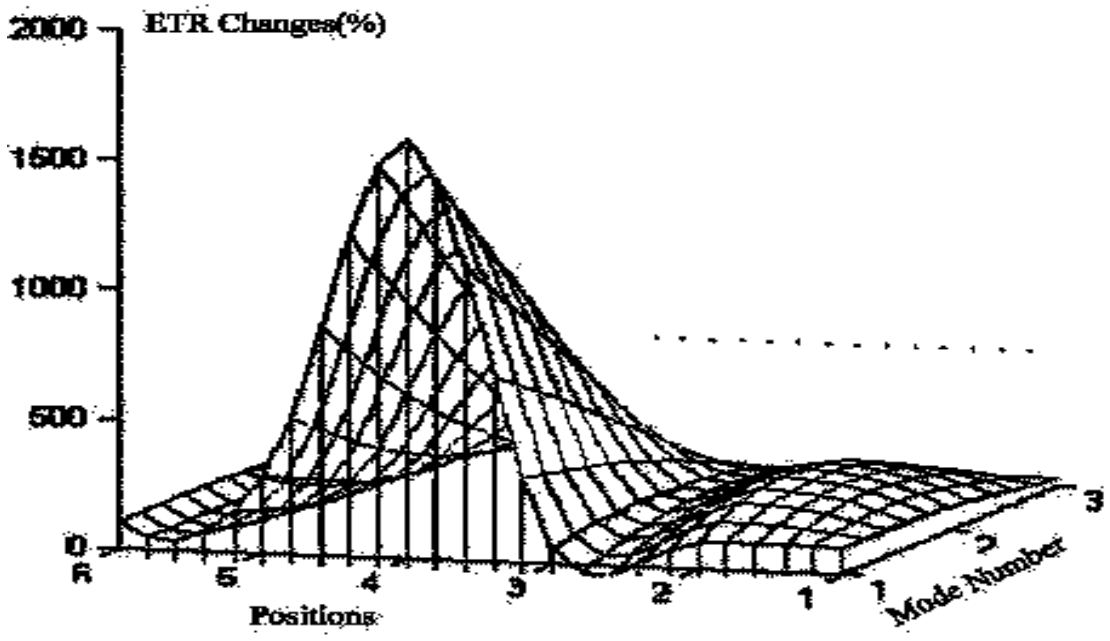

Fig 5.28 ETR Changes by Girder Cracking

5.4.3 Sensitivity Analysis

The above bridge damage diagnostic studies have demonstrated that the ETR is very sensitive to both types of bridge damage. At the same time, however, we don't know how other vibration signatures will respond under the same type of damage. Due to the limited time and experimental data, only natural frequencies, damping ratios, and ETR's of the first 3 modes are compared.

The sensitivity analysis was conducted by comparing the changes of vibration signatures of the first 3 modes after certain damage was introduced in the model bridge. More specifically, natural frequency, damping ratio, and model energy transfer ratio (ETR) are selected for the purpose of sensitivity analysis.

Tables 5.18 and 5.19 summarize the comparison results for both types of damage and the following conclusions may be obtained from the results:

1. ETR is much more sensitive to the introduced bridge damage than natural frequencies and damping ratios. For the bearing failure case, the biggest changes of natural frequency, damping ratio, and ETR are 8.43%, 123.4%, and 4524%, respectively. For the girder cracking case, the biggest changes of natural frequencies, damping ratios, and ETR are 7.45%, 67.26% , and 1614.7%, respectively.

Table 5.18 Sensitivity analysis results before and after bearing damage

Mode Number	Natural frequency Changes	Damping Ratio Changes	Change of ETR index
Mode 1	5.72%	38.37%	592.5%
Mode 2	8.43%	74.02%	81.73%
Mode 3	6.31%	123.4%	4524%

Table 5.18 Sensitivity analysis results before and after girder 1 damage

Mode Number	Natural frequency Changes	Damping Ratio Changes	Change of ETR index
Mode 1	7.45%	1.30%	1614.7%
Mode 2	2.78%	67.26%	820.2%
Mode 3	3.54%	18.91%	68.21%

2. The mode at which the ETR has the biggest change is not necessarily the same as the mode where the natural frequency and/or damping ratios have the biggest change. For the bearing removal case, mode 2 has the biggest change in natural frequencies while the biggest ETR change occurs at mode 3.

3. Comparatively, ETR is more sensitive to the damage due to bearing removal than to the simulated girder cracking. This is partly a result of the fact that the removing of the roller actually released the boundary condition constraint, which will certainly permit energy transfer more freely and easily.

4.Not all modes and associated ETR’s are sensitive to damage. In the bearing removal case, for example, only ETR at mode 3 shows large changes around the damage zone, while in the girder cracking case, ETR’s at both mode 1 and 2 are sensitive to damage.

5.4.4 Engineering Interpretation of ETR and Summary

Physically speaking, any structure can be represented in the terms of mass matrix [M], damping matrix [C], and stiffen matrix [K]. For the purpose of damage detection, it would be convenient to assume the mass of the structure remains unchanged before and after certain damages happen. This is usually the case for most types of structural damage, except at some special cases where significant mass of the structure is removed during the developing process of

damage. Numerous experimental results demonstrated that the vibration signatures (including ETR) will experience certain changes after damage occurs. Since the vibration signatures are obtained through structural response, the change in vibration signatures will directly reflect the changes of the structural response. The change in structural response will further reflect the change of stiffness and damping properties locally.

The change of local stiffness and damping properties will cause the redistribution of stiffness matrix [K] and damping matrix [C]. Since ETR comes directly from the complex damping theory and is directly related to the distribution of damping matrix, the ETR will change according to the type of damage.

It is widely believed that, as a result of damage, there would be a reduction in stiffness and decrease in the free energy stored in the body. Since each vibration mode has a different energy distribution, any localized damage will affect each mode differently depending on the location and severity of the damage (Change et al. 1993). Physically, in engineering sense, the damage will change the energy transfer path and therefore cause the energy redistributed.

If a system is isotropic and linear, vibration signatures including ETR will be the same everywhere. However, the damage will change the isotropic and linear properties of the structure and cause the vibration signatures including ETR locally.

Generally speaking, bridge is not isotropic, and therefore the damage usually just changes the linearity and ETR in certain area and/or certain direction. For a bridge, although it has a complete set of modes, physically, due to the limitation of excitation (magnitude and position), certain modes either cannot be excited under traditional excitation or may be the only measurable mode when unusual excitation applied. The issue of signature validity is important and may need further investigation.

From the above, it was found that ETR was sensitive to both types of damage: bearing damage and girder cracking. Modal energy transfer occurs among different locations. Therefore, ETR should be different on various locations. That means that ETR can be expressed as a local parameter, which may indicate the location of damage. The calculations verify the conclusion. On the other hand, it is found that ETR is sensitive to signal-to-noise ratio from the calculation. The diagnostic technique with the capability of tracing damage tendency will be more convenient for engineering practice.

Another important issue is that the identification parameters, including ETR in the time domain under ambient vibration, should be updated.

Chapter 6

Conclusion and Suggestion for Future Study

6.1 Conclusion

The principal focus of this study is to develop a diagnostic technique to probe damage conditions in a structure utilizing static parameter identification and energy-based modal parameter identification. Contributions of present work mainly include summary of structural health monitoring system, theoretical base of measurement and signal treatment, theoretical studies on energy transfer ratio (ETR), establishment of wide-range measurement system, ambient and impact analysis, parameter identification and estimation, finite element calculation, and experimental verification.

1. The ambient and impact signal processing techniques were studied to implement the bridge monitoring. It was shown that the cross-correlation function between two response measurements under white noise excitation has a decaying form, and therefore a traditional system identification method can be used to estimate vibration signatures of the structures. The time-domain poly-reference identification method and SDOF identification method were adopted to identify the vibration signatures. A full-scale ambient survey of a 3-span suspension bridge was conducted and the testing results have good agreements with FE modeling results. Thus, this study has established the possibility of developing an on-line bridge monitoring system based on the cross-correlation analysis method.

2. In order to verify and ensure the corresponding application of proposed vibrational signature, the slab-on-girder type of highway bridges was selected as the study object due to its popularity and vulnerability to aging. A 1:6 scaled signal span model bridge was manufactured in the laboratory. Similitude laws for static and dynamic modeling were satisfied. An ambient vibration environment was simulated by pulling a scaled car back and forth along the model bridge, as well as by hammering impact on different points on the bridge. Special attentions were given to the distribution effect of added mass, effect of vehicle speed, effect of window functions, and effect of excitation locations. The dynamic properties of the model bridge were identified through ambient testing and impact testing. Good agreement was achieved between these two tests. It was found that the linkage between the “controlled damage” of bridge and the vibrational signatures existed. Frequencies comparison between testing and FE calculation indicates that the majority of frequencies are in good agreement, except one or two.

3. The frequencies and damping ratios identified by using SDOF modal identification method under various damage conditions were compared with those under intact condition. It was found that different damage indices have different sensitiveness to different types of damage and extent.

Modal parameters, such as frequency and damping ratio, are not sensitive to the bearing damage or girder cracking. Other conclusions are as follows:

(1) Not all modes are sensitive to the same kind of damage. From the changes of modal parameters, we can only conclude that some damage may occur, but we cannot identify the kind of damage that occurred.
(2) We cannot locate the damage from modal parameters, except from mode shapes.
(3) The identification of composite damage (such as damage IV) is more difficult than that of singular damage.

4. Static parameters, such as deflections and strains were extracted from the experimental data to identify the damage. We obtained the following remarks:

(1) The deflection is sensitive to the bearing damage, but not to girder cracking damage.
(2) The strain is sensitive to girder cracking damage, but not to the bearing damage.
(3) Deflection is a global static signature, while strain is a local static signature. Changes of deflection or strain may indicate the happening of damage and location of damage. But these indications strongly rely on the measured positions. If the measured points are very close to the damage positions, the indications are clear. Finding the accurate location may still need to be developed.
(4) Under the extent of external loading, the load-deflection relationships and the load-strain relationships still remain linear after the damages occurred. That means the non-linearity caused by damage is very small.
(5) It is difficult to apply the ordinary load-deflection curves to detect the damage. However, the load-strain curves may be used to identify the damage, if the baseline model of intact condition of a structure exists.

5. The primary studies indicate that ETR index is heavily affected by the signal-to-noise ratio. Main conclusions are summarized as follows:

(1) ETR is much more sensitive to the introduced bridge damage than to natural frequencies and damping ratios.
(2) The location where the biggest change of ETR occurs can approximately indicate the location of damage. But it is not possible to know exactly where damage occurs.
(3) Natural frequencies and damping ratios are global vibrational signatures and can well indicate the happening of damage and/or condition change of bridge structures. But they cannot be used to locate the position of damage and/ or condition change. They should be used together with ETR for the purpose of damage and/or condition changes. They should be used together with ETR for the purpose of bridge damage detection.
(4) Not all modes associated ETR’s are sensitive to damage. In the bearing removal case, for example, only ETR at mode 3 shows large changes around the damage zone, while in the girder cracking case, ETR’s at both modes 1 and 2 are sensitive to damage.

6.2 Suggestion for Future Study

This research is just the initiative of utilizing vibrational signatures (ETR, etc.) and static parameters compositely in the laboratory. However, it is impossible to obtain perfect test specimen to represent a real system. For example, damages of the testing model bridges are known before testing and so detecting damage can be considered as a forward process. On the contrary, damages in the real structures are unknown and thus damage detection becomes an inverse process. The inverse process will be much more difficult than the forward process because they are problem-dependent and therefore with uncertainties. Future study needs include:

(1) ETR index has the solid theoretical base, but the extraction of ETR from the large amount of measured data is very onerous and the method still needs to be improved and updated, especially under the natural ambient excitation testing. The ability of ETR to detect non-predetermined damage, for example, concrete bridge damage, will be the next challenge.

(2) Finite element model updating and identification is the approach to identify the bridge damages by using dynamic and static measured information compositely. The key issues are the establishment of FE baseline model and identification arithmetic.

(3) Only using one damage index is insufficient to detect the damages. More understanding on the relationship between damage index (including ETR) and damage type is need.

(4) Advanced diagnosis techniques, including NDE, expect to be applied in the bridge damage detection.

(5) More studies on the optimal excitation locations for ambient vibration survey are needed. The sensor placement is also very important in order to get a stable signal with high signal-to-noise ratio.

(6) Regular detections are necessary to collect enough data for bridge condition evaluation.

Appendix A

Calibration of Accelerometer

The 9818-II of type piezoelectric accelerometers used in this research had a nominal sensitivity of 10^{-3}-10^{-4} g, and a frequency range from 0.1Hz to 2KHz. They were all calibrated before used in the test. The calibration results were listed in **Table A.1**.

Table A.1 Calibration Results of Model 9818 Industrial Accelerometers

Accelero meter ***No.***	Sensitivity (pC/ms^2)	Maximum Ratio of Transverse Sensitivity	Accelero meter ***No.***	Sensitivity (pC/ms^2)	Maximum Ratio of Transverse Sensitivity
009	143.9	1.4%	017	144.5	1.2%
022	147.1	2.9%	029	134.2	1.2%
031	146.7	2.2%	0101	141.9	1.2%
0102	142.8	3.0%	0104	134.6	1.4%
0110	133.6	4.4%	0113	134.7	5.0%
0116	136.6	2.0%	0117	136.0	1.0%
0121	138.5	2.4%	0123	142.0	4.6%
0124	135.6	2.8%	0126	132.0	1.2%
0127	141.8	2.4%	0130	142.2	1.8%
0133	111.6	2.2%	851	147.9	0.6%
865	135.9	1.6%	877	141.6	4.4%
880	141.2	3.4%	883	133.6	1.6%
900	5.23	1.5%			

Appendix B

Complex Frequency Approach

The characteristic equation for the non-proportionally damped system from Eq. (3.20) or Eq. (3.24) is shown as follows

$$\lambda_i^{\,2} + 2(\xi_i + j\zeta_i)\omega_i\lambda_i + \omega_{ni}^{\,2} = 0 \tag{B.1}$$

Then, solve the equation and roots can be obtained as

$$\begin{aligned}\lambda_i &= -(\xi_i + j\zeta_i)\omega_i \pm \sqrt{(\xi_i + j\zeta_i)^2\omega_i^{\,2} - \omega_{ni}^{\,2}} \\ &= -(\xi_i + j\zeta_i)\omega_i \pm \sqrt{(\xi_i + j\zeta_i)^2 - (\frac{\omega_{ni}}{\omega_i})^2}\omega_i\end{aligned} \tag{B.2}$$

Because ω_i is very close to ω_{ni}, so the value of $\frac{\omega_{ni}}{\omega_i}$ is very close to 1. Then Eq. (B.2) may become as follows:

$$\begin{aligned}\lambda_i &= -(\xi_i + j\zeta_i)\omega_i \pm (\sqrt{(\xi_i + j\zeta_i)^2 - (\frac{\omega_{ni}}{\omega_i})^2})\omega_i \\ &= -(\xi_i + j\zeta_i)\omega_i \pm (\sqrt{(\xi_i + j\zeta_i)^2 - 1})\omega_i \\ &= j\omega_{ni}\{j(\xi_i + j\zeta_i) \pm \sqrt{[j(\xi_i + j\zeta_i)]^2 + 1}\}\end{aligned} \tag{B.3}$$

Because of the assumption of light damping ($\left|j(\xi_i + j\zeta_i)\right| << 1$), the second part of Eq. (B.3) can be approximated by Taylor series expression and shown as:

$$\sqrt{[j(\xi_i + j\zeta_i)]^2 + 1} \approx 1 + \frac{1}{2}[j(\xi_i + j\zeta_i)]^2 \tag{B.4}$$

First, consider the positive part of Eq. (B.3). By substituting Eq. (B.4) into Eq. (B.3), the positive part of the roots can be:

$$\begin{aligned}\lambda_i &= j\omega_{ni}\{j(\xi_i + j\zeta_i) \pm \sqrt{[j(\xi_i + j\zeta_i)]^2 + 1}\} \\ &= j\omega_{ni}\{j(\xi_i + j\zeta_i) + 1 + \frac{1}{2}[j(\xi_i + j\zeta_i)]^2\} \\ &\approx j\omega_{ni}\exp[j(\xi_i + j\zeta_i)] \\ &= j\omega_{ni}\exp(j\xi_i)\exp(-\zeta_i)\end{aligned} \tag{B.5}$$

In Eq. (B.5), the first exponential equation can be approximated by Taylor series expression and shown as

$$\exp(j\xi_i) \approx 1 + j\xi_i - \frac{1}{2}\xi_i^{\,2} \approx 1 + \sqrt{1 - \xi_i^{\,2}} \tag{B.6}$$

Substitute Eq. (B.6) into Eq. (B.5) and the positive part of the roots can be approximated as:

$$\begin{aligned}\lambda_i &= j\omega_{ni}\exp(j\xi_i)\exp(-\zeta_i)\\ &= j\omega_{ni}(j\xi_i+\sqrt{1-\xi_i^2})\exp(-\zeta_i)\\ &= -\omega_{ni}\exp(-\zeta_i)\xi_i + j\sqrt{1-\xi_i^2}\omega_{ni}\exp(-\zeta_i)\end{aligned} \qquad \text{(B.7)}$$

The same idea can be used to approach the negative part of the roots and show as

$$\lambda_i = -\omega_{ni}\exp(\zeta_i)\xi_i - j\sqrt{1-\xi_i^2}\omega_{ni}\exp(\zeta_i) \qquad \text{(B.8)}$$

Eqs. (B.7) and (B.8) are the same with Eq. (3.29a), and if we order that

$$\omega_i = \omega_{ni}\exp(\mu\zeta_i) \qquad \text{(B.9)}$$

We can obtain the similar formula with that of the proportionally damped system:

$$\lambda_i = -\xi_i\omega_i \pm j\sqrt{1-\xi_i^2}\omega_i \qquad \text{(B.10)}$$

Also, Eqs. (B.7) and (B.8) satisfy the normal proportional damped system ($\zeta_i = 0$) and the roots will be

$$\lambda_i = -\xi_i\omega_{ni} \pm j\sqrt{1-\xi_i^2}\omega_{ni} \qquad \text{(B.11)}$$

The roots of the characteristic Eqs. (B.7) and (B.8) are also called the complex frequencies.

Then frequencies of non-proportionally and proportionally systems may be calculated as in Table B.1:

Table B.1 Comparison of Frequencies of Two Types of Damping System

ζ_i	0.00	± 0.01	± 0.02	± 0.03	± 0.04	± 0.05	± 0.06
$\frac{\omega_i}{\omega_{ni}}$	*1.000	1.010	1.020	1.030	1.041	1.051	1.062
	1.000	0.990	0.980	0.9704	0.9608	0.9512	0.9417

*: The value is relevant to the positive values of ζ_i

Generally, the ETR values of light damping systems, such as steel or concrete structures, are about 0.00-0.01. So the approximating of the process is acceptable.

Appendix C

Polyreference Identification Method in Time Domain

The polyreference identification method, also called the polyreference complex exponential method (PRCE), developed by **Vold** (1982), and originally used for multi-input excitation, has been continuously improved by other researchers, for example, **Deblauwe and Allemang** (1985). Apart from being a more general way of structural dynamical analysis, this overcomes the problems that sometimes occur when using a single input and multi-output method, where one mode of vibration may not be excited because the excitation may be located close to a mode of the structure.

Consider the generalized form of the equation of motion of N-DOF systems,

$$[M]\ddot{X}+[C]\dot{X}+[K]X=[f(t)] \qquad \text{(C.1)}$$

where $[M]$, $[C]$, and $[K]$ are the $n\times n$ mass, damping, and stiffness matrix, respectively. $\ddot{X}$, $\dot{X}$, and X are $n\times 1$ vector of time-varying acceleration, velocity, and displacement, respectively, and $[f(t)]$is an $n\times 1$ vector of time-varying external excitation forces. An ancillary equation may be developed as follows

$$I\dot{X}-I\dot{X}=0 \qquad \text{(C.2)}$$

then we may construct a new equation:

$$\begin{bmatrix}[M] & 0\\ 0 & I\end{bmatrix}\begin{Bmatrix}\ddot{X}\\ \dot{X}\end{Bmatrix}+\begin{bmatrix}[C] & [K]\\ 0 & -I\end{bmatrix}\begin{Bmatrix}\dot{X}\\ X\end{Bmatrix}=\begin{Bmatrix}[f(t)]\\ 0\end{Bmatrix} \qquad \text{(C.3a)}$$

we order $Y=\begin{Bmatrix}\dot{X}\\ X\end{Bmatrix}$, then

$$\hat{A}\dot{Y}+\hat{B}Y=\begin{Bmatrix}[f(t)]\\ 0\end{Bmatrix}$$

$$\dot{Y}=-\hat{A}^{-1}BY+\hat{A}^{-1}\begin{Bmatrix}[f(t)]\\ 0\end{Bmatrix}=AY+B\begin{Bmatrix}[f(t)]\\ 0\end{Bmatrix} \qquad \text{(C.3b)}$$

where

$$A=-\hat{A}B=\begin{bmatrix}-[M]^{-1}[C] & -[M]^{-1}[K]\\ I & 0\end{bmatrix} \qquad \text{(C.3c)}$$

$$B = \hat{A}^{-1} \tag{C.3d}$$

If the system has free vibration, $[f(t)] = 0$, then we have

$$\overline{Y} = AY \tag{C.4a}$$

at the initial condition: $Y\big|_{t=0} = Y(0)$, then the solution of Eq. (C.4a) is:

$$Y = e^{At} Y(0) \tag{C.4b}$$

If the state space matrix has non-repeated eigen-values, and under the light daming conditions, we have

$$AU = U\Lambda_1 \tag{C.5a}$$

where U is the eigenvector matrix, and $\Lambda_1 = diag\left[\lambda_1 \quad ... \quad \lambda_N \quad \lambda_1^* \quad ... \quad \lambda_N^*\right]$, and

$$A = U\Lambda_1 U^{-1} \tag{C.5b}$$

we rewrite Eq. (C.5b):

$$Y = e^{U\Lambda_1 U^{-1} t} Y(0) \tag{C.6a}$$

Eq. (4.53a) may be rewritten as:

$$\begin{aligned} Y &= e^{U\Lambda_1 U^{-1} t} Y(0) \\ &= (\sum_{i=0}^{\infty} \frac{1}{i!} (U\Lambda_1 U^{-1})^i t^i) Y(0) \\ &= U(\sum_{i=0}^{\infty} \frac{1}{i!} \Lambda_1^{\,i} t^i) U^{-1} \\ &= U e^{\Lambda_1 t} U^{-1} Y(0) \end{aligned} \tag{C.6b}$$

In the frequency domain, the relationship between the mode coordinate vector Z and physical coordinate Y is shown in the following:

$$Y = UZ \tag{C.7a}$$

Corresponding to the initial condition $Y(0)$, we have:

$$Z = U^{-1} y(0) \tag{C.7b}$$

where Z is the initial condition vector of complex modal coordinates.

The time-domain identification methods work with the corresponding impulse response function (IRF), obtained from Eq. (3.51) by an inverse Fourier transform. Assuming

that the frequency response function matrix $[H]_{m\times k}$ was obtained where there are k excitation points and m collection points, the IRF h_{ij} can be obtained from the element of matrix $[H]_{m\times k}$ by inverse Fourier transform. We may order that $X_l(i)$ be the unit impulse at the l point and at the time iT, we may obtain the k dimension vector:

$$X_l(i) = [h_{1l}(iT) \quad h_{2l}(iT) \quad ... \quad h_{kl}(iT)] \tag{C.8}$$

where T is the sampling time.

We may order $z = e^{\Lambda_1 T}$, according to Eqs. (C.6b) and (C.7), and we may obtain:

$$Y(i) = Uz^i Z \tag{C.9}$$

After the interview equation being input,

$$\begin{aligned} Y(i) &= Uz^i Z \\ X_l(i) &= GY(i) \end{aligned} \tag{C.10}$$

where G is the interview matrix. When the output is the displacement, we have $G = [1 \quad 0]$, and

$$\underset{(p+1)k\times 1}{\begin{Bmatrix} X_l(0) \\ X_l(1) \\ ... \\ X_l(p) \end{Bmatrix}} = \underset{(p+1)k\times 2N}{\begin{Bmatrix} GU \\ GUz \\ ... \\ GUz^p \end{Bmatrix}} Z_{2N\times 1} = \overset{)}{G}Z \tag{C.11a}$$

$$\overset{)}{G} = \underset{(p+1)k\times 2N}{\begin{Bmatrix} GU \\ GUz \\ ... \\ GUz^p \end{Bmatrix}} = \begin{Bmatrix} FI \\ Fz \\ ... \\ Fz^p \end{Bmatrix} \tag{C.11b}$$

where $F = GU$, and it is $k\times 2N$ dimension matrix. If p is the integer, and there is formula: $k\times p \geq 2N$, then G has at least k more rows than columns. There must exist a full rank $k\times k(p+1)$ matrix $\overset{)}{Q}$,such that

$$\hat{Q}\hat{G} = 0 \qquad \text{(C.12a)}$$

that is to say, there is a formula as follows

$$(\hat{Q})_{k\times k(p+1)}(\hat{G})_{(p+1)k\times 2N} = (\hat{Q}\hat{G})_{k\times 2N} = 0 \qquad \text{(C.12b)}$$

where $\hat{Q}$ may be portioned into square sub-matrices:

$$\hat{Q} = \begin{bmatrix} B(p) & B(p-1) & \dots & B(1) & I \end{bmatrix} \qquad \text{(C.13)}$$

Substituting equation (C.11b) and equation (C.12b) into equation (C.12a), we may have

$$\sum_{j=0}^{p} B(j)Fz^{p-j} = 0 \qquad \text{(C.14a)}$$

and we may obtain the formula from Eqs. (C.11a) and (C.14a) as follows

$$\sum_{j=0}^{p} B(j)X_l(p-j) = (\sum_{j=0}^{p} B(j)Fz^{p-j})Z = 0 \qquad \text{(C.14b)}$$

In order to determine the coefficient $B(l), l = 1,2,..., p-1, p$, let n be the origin of the time series; and we can multiply the response at time t_0 by $B(p)$, the response at time t_1 by $B(p-1)$,……, the response at time t_{p-1} by $B(1)$,and the summation may take the form:

$$\sum_{j=1}^{p} B(j)X_l(p-j+n) = X_l(p+n) \qquad \text{(C.15)}$$

which is independent of n or response location l.

By varying the response location l and the origin of the time series n in the above equation, such as $l = 1,2,......, m, m > k$; $n = 1,2,......, \bar{n}$, we order that $B = \begin{bmatrix} B(1) & B(2) & \dots & B(p-1) & B(p) \end{bmatrix}_{k\times pk}$, then the following equation is obtained:

$$(B)_{k\times pk} = \begin{bmatrix} T_1 & T_2 & \dots & T_l & \dots & T_m \end{bmatrix}_{kp\times m\bar{n}} = -\begin{bmatrix} R_1 & R_2 & \dots & R_l & \dots & R_m \end{bmatrix}_{k\times m\bar{n}} \qquad \text{(C.16)}$$

where,

$$(T_l)_{kp\times\bar{n}} = \begin{bmatrix} X_l(p-1) & X_l(p) & \dots \\ X_l(p-2) & X_l(p-1) & \dots \\ \dots & \dots & \dots \\ X_l(0) & X_l(1) & \dots \end{bmatrix}_{kp\times\bar{n}}$$

$$R_l = [X_l(p) \quad X_l(p+1) \quad ...]$$

Eq. (C.16) indicates that there is a excitation point l, and there is a corresponding equation $BT_l = -R_l$. The matrix B can be calculated in the meaning of least square:

$$B(\sum_{l=1}^{m} T_l T_l^T) = -\sum_{l=1}^{m} R_l T_l^T \qquad \text{(C.17a)}$$

$$B = -\sum_{l=1}^{m} R_l T_l^T (\sum_{l=1}^{m} T_l T_l^T)^{-1} \qquad \text{(C.17b)}$$

and then the order of the system can be determined.

According to Eq. (C.14a) and the following formula: $F = GU$, $z^{p-j} = e^{\Lambda_1 T(p-j)}$, and $\Lambda_1 = diag[\lambda_i \quad \lambda_i^*]$, $i = 1,2,.....,N$, we should calculate z firstly in order to get the complex frequency λ_i. We order the unit vector $e_i = I_i$, where the i^{th} element of the unit vector is 1. Multiply the unit vector into Eq. (C.14a), we may have:

$$(\sum_{j=0}^{p} B(j) F z^{p-j}) e_i = \sum_{j=0}^{p} B(j)_{k\times k} z_i^{p-j} (F_i)_{k\times 1} = 0 \qquad \text{(C.18)}$$

where $z_i^{p-j} = e^{\lambda_i T(p-j)}$ is the i^{th} element of matrix z^{p-j}.If we order $Z_i = e^{\lambda_i T}$, we have $z^{p-j} = e^{\lambda_i T(p-j)} = Z_i^{p-j}$, then we may rewrite Eq. (C.18) as follows:

$$P(Z_i) F_i = (\sum_{j=0}^{p} B(j)_{k\times k} Z_i^{p-j}) F_i = 0 \qquad \text{(C.19)}$$

where Z_i is the unknown parameter, which will be determined. If the value of Z_i is nonzero, then we have

$$\det(P(Z_i)) = 0 \qquad \text{(C.20)}$$

we may solve the equation by either Polyeig command at MATLAB or other methods and obtain the values of Z_i ($i = 1,2,.....,p$), and then we obtain the values of λ_i from Z_i according to $Z_i = e^{\lambda_i T}$:

$$\lambda_i = \frac{1}{T} \ln Z_i = a_i + jb_i \qquad \text{(C.21)}$$

The natural frequency and damping ratio may be found by the following formulations:

$$\omega_i \xi_i = -\frac{\ln(a_i^{\,2} + b_i^{\,2})}{2\Delta T}$$
$$\omega_i \sqrt{1-\xi_i^{\,2}} = \frac{\tan(\frac{b_i}{a_i} + k\pi)}{\Delta T} \qquad \text{(C.22)}$$

the k can be determined by trial and error until reasonable damping ratios are reached. The eigenvectors may be obtained from Eq. (C.19). Details may be referred to **Vold** (1982).

Appendix D

Identified Modal Parameters under Different Damage Conditions

D.1 Damage III

Table D.1.1 Vertical Frequency Changes before and after Damages Occurred in Girders 1 and 3

Mode No.	Frequency at intact condition	Frequency for damages of girders 1 and 3	Differences
No.1	33.805 Hz	31.976 Hz	-5.410%
No.2	52.664 Hz	51.170 Hz	-2.837%
No.3	93.250 Hz	92.446 Hz	-0.862%
No.4	115.474 Hz	112.642 Hz	-2.453%
No.5	140.516 Hz	153.226 Hz	9.045%
No.6	169.174 Hz	169.444 Hz	0.160%
No.7	185.429 Hz	174.354 Hz	-5.973%

Table D.1.2 Transverse Frequency Changes before and after Damage Occurred in Girder 1 and 3

Mode No.	Frequency at intact condition	Frequency for damages of girders 1 and 3	Differences
No.1	28.966 Hz	29.294 Hz	1.134%
No.2	51.016 Hz	49.150 Hz	-3.658%
No.3	115.657 Hz	112.084 Hz	-3.089%
No.4	143.798 Hz	144.372 Hz	0.399%
No.5	169.301 Hz	169.637 Hz	0.198%
No.6	196.259 Hz	188.715 Hz	-3.844%

Table D.1.3 Damping Ratio Changes (Vertical Mode Shape) before and after Damages Occurred in Girders 1 and 3

Mode No.	Damping Ratio at intact condition (%)	Damping Ratio for damages of girders 1 and 3 (%)	Differences
No.1	1.0454	1.3293	27.158%
No.2	1.2836	2.0391	58.858%
No.3	1.7555	1.3373	-23.822%
No.4	0.8967	0.8904	-0.703%
No.5	3.0321	2.8320	-6.599%
No.6	0.7698	0.4868	-36.763%
No.7	1.7754	1.7499	-1.436%

Table D.1.4 Damping Ratio Changes (Transverse Mode Shape) before and after Damages Occurred in Girders 1 and 3

Mode No.	Damping Ratio at intact condition (%)	Damping Ratio for damages of girder 1 and 3 (%)	Differences
No.1	1.7212	2.1368	24.146%
No.2	2.7093	2.2486	-17.004%
No.3	0.8337	0.9358	12.247%
No.4	0.2919	0.3396	16.341%
No.5	0.3654	1.2283	236.152%
No.6	1.2179	0.6014	-102.511%

D.2 Damage IV

Table D.2.1 Vertical Frequency Changes before and after all Damages Occurred

Mode No.	Frequency at intact condition	Frequency for all damages	Differences
No.1	33.805 Hz	31.696 Hz	-6.238%
No.2	52.664 Hz	50.052 Hz	-4.960%
No.3	93.250 Hz	98.132 Hz	5.235%
No.4	115.474 Hz	111.465 Hz	-3.472%
No.5	140.516 Hz	149.099 Hz	6.108%
No.6	169.174 Hz	164.987 Hz	-2.475%
No.7	185.429 Hz	176.355 Hz	-4.894%

Table D.2.2 Transverse Frequency Changes before and after all Damages

Mode No.	Frequency at intact condition	Frequency for all damages	Differences
No.1	28.966 Hz	28.063 Hz	-3.117%
No.2	51.016 Hz	49.170 Hz	-3.620%
No.3	115.657 Hz	109.568 Hz	-5.265%
No.4	143.798 Hz	140.036 Hz	-2.616%
No.5	169.301 Hz	166.101 Hz	-1.890%
No.6	196.259 Hz	188.180 Hz	-4.117%

Table D.2.3 Damping Ratio Changes (Vertical Mode Shape) before and after Girder 1, Girder 3, and Bearing Damages Occurred

Mode No.	Damping Ratio at intact condition (%)	Damping Ratio for girder 1, girder 3, and bearing damages (%)	Differences
No.1	1.0454	1.2647	20.978%
No.2	1.2836	1.1989	-6.599%
No.3	1.7555	0.3327	-81.048%
No.4	0.8967	0.7560	-15.691%
No.5	3.0321	1.2236	-59.645%
No.6	0.7698	0.9697	25.968%
No.7	1.7754	1.6436	-7.423%

Table D.2.4 Damping Ratio Changes (Transverse Mode Shape) before and after Girder 1, Girder 3, and Bearing Damages Occurred

Mode No.	Damping Ratio at intact condition (%)	Damping Ratio for girder 1, girder 3, and bearing damages (%)	Differences
No.1	1.7212	1.6202	-5.868%
No.2	2.7093	2.8199	4.082%
No.3	0.8337	0.6921	-16.985%
No.4	0.2919	0.2772	-0.504%
No.5	0.3654	0.7242	98.194%
No.6	1.2179	2.9684	143.731%

References

A

Abdo, M. A.-B. and Hori, M. (2002), "A numerical study of structural damage detection using changes in the rotation of mode shapes", Journal of Sound and Vibration, Vol. 251, No. 2, March, 2002, pp. 227-239.

Abe, M., Fujino,Y., et al. (1999), "Monitoring of long span suspension bridge by ambient vibration measurement," Proceedings of the 2nd international Workshop on Structural Health Monitoring, Stanford University, Stanford, CA, Sept., 1999**,** pp. 400-407.

Adams,R.D., Cawley, P., Pye, C.J., and Stone, B.J. (1978), " A vibration technique for nondestructively assessing the integrity of structures.", Journal of Mechanical Engineering Science, Vol. 20, 1978, pp. 93-100.

Alampalli, S., Fu, G., and Aziz, I.A. (1992), " Modal analysis as a bridge inspection tool", Proceedings of the 10th Int'l Modal Analysis Conference (IMAC), pp. 1359-1366, San Diego, CA, 1992.

Alampalli,S. and Fu, G. (1994), "Remote bridge monitoring systems for bridge condition.", Client Rep. 70, Engrg. Res. and Devel. Bureau, New York State Dept. of Transp., Albany, N.Y., 1994.

Alampalli, S. (2000), " Effects of testing, analysis, damage, and environment on modal parameters", Mechanical System. and Signal Processing, 14 (1), pp. 63-74.

Allemang, R.L., and Brown, D.L. (1995), "Experimental modal analysis", ***Shock and Vibration Handbook***, 4th edition, Chapter 18, Harris, C.M. eds., McGraw Hill, N.Y.

Alvin, K.F., Peterson, L.D., and park, K.C. (1995), "Method for determining minimum-order mass and stiffness matrices from modal test data," AIAA Journal, Vol. 33, No. 1, January 1995, pp. 128-135.

Alvin, K.F., and park, K.C. (1999), " Extraction of substructural flexibility from global frequencies and mode shapes", AIAA Journal, Vol. 37, No. 11, Nov., 1999, pp. 1444-1451.

Aktan, A.E., Farhey, D.N., Helmicki, D.J. et al. (1997), "Structural identification for condition assessment: experimental arts", Journal of Struct. Engrg., ASCE, Vol. 123, No. 12, pp. 1674-1684 .

Aktan, A.E., Catbas, F.N., Turer A. and Zhang, Z.F. (1998), "Structural identification, Analytical aspect ", Journal of Struct. Engrg., ASCE , 124(7), pp. 817-829 .

Aktan, A.E., Tsikos, C.J., et al. (1999), "Challenge and opportunities in bridge health monitoring", Proceedings of the 2nd international Workshop on Structural Health Monitoring, Stanford University, Stanford, CA, Sept. 1999**,** pp461-473.

Aktan, A.E., et al. (2000), "Integrated field, theoretical and laboratory research for large systems identification problems," Proceedings of the International Conference on Advances in Structural Dynamics, edited by J.M. Ko and Y.L. Xu, The Hongkong Polytechnic University, Hong Kong, Dec., 2000**,** pp. 1-18.

Ansari, F., eds. (2000), "Condition monitoring of materials and structures", ASCE, 1801 Alexander Bell Drive.

Atalla, M.J., and Inman, D.J. (1998), "On model updating using neural networks", Mech.Sys. and Signal Processing, 12 (1 or 2), pp. 135-161.

B

Bakht, B. and Jaeger, L.G. (1990), " Bridge testing - a surprise every time," Journal of Struc. Engrg., ASCE, Vol. 116, No. 5, May, 1990, pp. 605-611.

Banan, M.R. and Hjelmstad, K.D. (1994a, 1994b), " Parameter estimation of structure from static response. I: Computational Aspect; II: Numerical simulation studies", Journal of Struct. Engrg., ASCE, 120(11), pp. 3243-3283 .

Beck, J.L. and Katafygiotis, L.S. (1992), "Probabilistic system identification and health monitoring of structures", Proc., 10th World Conf. on Earthquake Engrg.

Beck, J.L. and Katafygiotis, L.S. (1997), "Updating structural dynamic models and their uncertainties: statistical system identification", Journal of Engrg. Mech, ASCE, 1997.

Bellizzi, S, Guillemain, P, and Kronland-Martinet, R. (2001), "Identification of coupled non-linear modes from free vibration using time-frequency representations", Journal of Sound and Vibration, Vol. 243, No. 2, pp. 191-203.

Bernal, D. (2002), "Load vectors for damage localization", Journal of Engrg. Mech., ASCE, 128(1), pp. 7-14.

Biswas,M., Pandey, A.K., and Samman, M.M. (1990), "Diagnostic experimental spectral/modal analysis of a highway bridge", The Int'l Journal of Analytical and Experimental Modal analysis.

Vol. 5, No. 1, 1990, pp. 33-42.

Blinchikoff, H.J. and Iverev, A.I. (1976), “Filtering in the time and frequency domains”, Hohn-Wiley & Son, Inc., New York, 1976. (Tk7872 F5 B86).

Borse, G.J. (1997), “Numerical methods with MATLAB——a Resource for scientists and engineers”, PWS Publishing Company, Boston.

Brighan, E.O., “The Fast Fourier Transform and its Applications”, Prentice-Hall, Inc. Upper Saddle River, NJ, 1988.

Brown, D.L., Allemang, R.L., Zimmerman, R., and Mergery, M. (1979), “Parameter estimation techniques for modal analysis”, SAE Technical Paper, No.790221, SAE Transactions.

Burkhardt, J. (2001), “Structural damage characterization using free decays”, Journal of Sound and Vibration, 2001, Vol. 246, No. 3, pp. 683-490.

C

Caicedo,J., Dyke, S.J., and Johnson, E.A. (2000), “Health monitoring beased on component transfer functions”, Proceedings of the International Conference on Advances in Structural Dynamics, edited by J.M. Ko and Y.L. Xu, The Hongkong Polytechnic University, Hong Kong, Dec., 2000**,** pp. 997-1004.

Capecchi, D. and Vestroni, F. (1999), “Monitoring of structural systems by using frequency dada”, Earthquake Engrg. and Struct. Dynamics, Vol. 28, pp. 447-461.

Cappellini,V., Consttantinides, A.G., and Emiliani, P. (1978), “Digital filters and their applications”, Academic Press, Inc., 1978. (TK7872 F5 C37), (program attached).

Caravani,P., Waston, M.L., and Thomson, W.T. (1977), “Recursive least-square time domain identification of structural parameters.”, Journal of Applied Mechanics, Vol. 44, pp. 135-140.

Carmichael, D.G. (1979), “ The state estimate problem in experimental structural mechanics”, Proc., 3rd Conf. On Application of Statistics and Probability in Soil and Structural Engrg., Syney, Australia, pp. 802-815.

Casas, J.R. (1995), “Full-scale dynamic testing of the Alamillo Cable-Stayed Bridge in Sevilla”, Earthquake Engineering and Structural Dynamics, Vol. 24, 1995, pp. 35-51.

Casas, J.R. and Aparicio, C.A. (1995), “Structural damage identification from dynamic-test data”, Journal of Struc. Engrg., ASCE, Vol. 120, No. 8., 1995, pp. 2437-2450.

Catbas, F.N., Grimmelsman, K.A., et al. (1999), " Structural Identification and health monitoring of a long-span bridge", Proceedings of the 2nd international Workshop on Structural Health Monitoring, Standford University, Standford, CA, Sep., 1999**,** pp. 417-429.

Cawley, P. and Adams, R.D. (1979), "The location of defects in structures from measurement natural frequencies", Journal of Strain Analysis, Vol. 14, No. 2, 1979, pp. 49-57.

Cha, P.D., and Pillis, L.G. de. (2001), "Model updating by adding known mass", International Journal for Numerical Methods in Engineering, Vol. 50, pp. 2547-2571.

Chang, T.C.P., Chang, C.C., and Xu, Y.G. (1999), "Updating structural parameters: an adaptive neural network approach", Proceedings of the 2nd international Workshop on Structural Health Monitoring, Standford University, Standford, CA, Sep., 1999, pp. 379-389.

Chase, S.B. and Washer, G. (1996-1997), "Nondestructive Evaluation for Bridge Management in the Next Century", Technique Report.

Chase, S.B. and Laman, J.A. (1999), "Dynamic and field testing of bridge in the new millennium: A look forward", A white paper prepared for Transformation Research Board Committee A2C05 Dynamic and Field Testing of Bridges.

Chaudhary, M.T.A., Abe, M., Fujino, Y., and Yoshida, J. (2000), "System identification of two bas-isolated bridges using seismic records", Journal of Structural Engineering, ASCE, Vol. 126, No. 10, Oct., 2000, pp. 1187-1195.

Chen, G.D, Yang, X.B, Alkhrdaji, T., et al. (1999), "Condition assessment of concrete structures by dynamic signature tests", Proc. 13th Engineering Mechanics Specially Conference, ASCE, Baltimore, MD, N. Jones and R. Ghanem, Editors, June 13-16, 1999.

Chiang Dar-Yun and Huang Si-Tsong (1997), "Model parameter identification using simulated evolution," AIAA Journal, Vol. 35, No. 7, July, 1997, pp. 1204-1208. also AIAA Journal, Vol. 37, No. 10, Oct., 1999, pp. 1331-1333..

Chiang Dar-Yun, and Cheng Ming-Si (1999), "Modal parameter identification from ambient response", AIAA Journal, Vol. 37, No. 4, April, 1999, pp. 513-515.

Chiang,W., Liu, K.F.R., and Lee, J. (2000), "Bridge damage assessment through Fuzzy Petri Net based expert system", Journal of Computing in Civil Engineering, ASCE, Vol. 14, No. 2, April, 2000, pp. 141-149.

Chong, Y.H. and Imregun, M. (2000), “Variable modal parameter identification for non-linear MDOF system, Part I: formulation and numerical validation; Part II: Experimental validation and advanced case study”, Shock and vibration, Vol. 7, 2000, pp. 217-240.

Cobb, R.G. and Liebst, B.S. (1997), “Sensor location prioritization and structural damage localization using minimal sensor information,” AIAA, Journal, Vol. 35, No. 2, Feb., 1997, pp. 369-374.

Cobb,R.G. and Liebst, B.S. (1997), “Structural damage identification using assigned partial eigenstructure.”, AIAA, Journal, Vol. 35, No. 1, 1997, pp. 152-158.

Cohen,L. (1995), “Time-frequency analysis”, Prentice Hall, Inc, N.Y, 1995.

Cooley, J.W. and Tukey, J.W. (1965), “An algorithm for the machine calculation of complex Fourier Series”, Mathematics of Computation, Vol. 19, April, 1965. pp. 297-301.

Cui, F. (2000), “Parameter identification and load-carrying capacity evaluation for bridge”, Ph.D. Dissertation, Dept. of Bridge Engineering, Tongji Univ., China, Jan., 2000.

D

Deblauwe, F. and Allemang, R.J., “The Polyreference time-domain technique”, Proceedings of the 10th International Seminar on Modl Analysis, Part IV, Katholike Universiteit Leuven, Nelgium, 1985.

Denoyer, K.K. and Peterson, L.D. (1997), “Method for structural modal update using dynamically measured static flexibility matrices”, AIAA Journal, Vol. 35, No. 2, Feb, 1997, pp. 362-368.

Desroches, R. and Fenves, G.L. (1997). “Evaluation of recorded earthquake response of a curved highway bridge”, Earthquake Spectra，13(3)，pp. 363-386.

DeWolf, J.T. and Zhao, J. (1998), “Dynamic vibration techniques in highway bridge monitoring”, Report to Dept. of Transportation of Connecticut State. Report No. CEE-98-01, University of Connecticut, Storrs, Conn.

Doebling, S.W., Hemez, F.M., Peterson, L.D., and Farhat, C. (1997), “Improved damage location accuracy using strain energy-based on mode selection criteria”, AIAA Journal, 35(4), pp. 693-699.

Doebling, S.W., Farrar, C.R., Prime, M.B., and Shevtiz, D.W. (1998), “A review of damage identification methods that examine changes in dynamic properties”, Shock and vibration Dig.,

30(2), pp.91—105.

Doebling, S.W., Farrar, C.R., et al. (2000), " The State-of-the-art in structural identification of constructed facilities," ASCE Rep. by Comm. on Struc. Identification of Constr. Fac., Uner review. （in press）

Duron, Z.H., Ozisik, H., and Rubin, S. (1995), "Modal test of one span of Benicia –Martinez Bridge", The Aerospace Corporation, EL Segundo, Calif., 1995.

E

Elkordy, M.F., Chang, K.C, and Lee, G.C. (1993), "Neural networks trained by analytically simulated damage states", Journal of Comp. in Civ. Engrg., ASCE, Vol. 7, No. 2, 1993, pp. 130-145.

Ewins, D.J. (1995), "Modal testing: Theory and Practice" (2nd Edition), Research Studies Press Ltd, England, 1995.

F

Farhat, C. and Heemez, F.M. (1993), "Updating finite element dynamic models using an element-by-element sensitivity methodology," AIAA Journal, Vol. 31, No. 9, Sep., 1993, pp. 1702-1711.

Farrar, C.R. and Jaurehui, D. (1996), "Damage detection algorithms applied to experimental and numerical modal data from the I-40 bridge," Los Alamos National Laboratory, Report #LA –13074 –MS, Los Alamos, New Mexico, January.

Farrar, C.R., et al. (1996), "Finite-element analysis of the I-40 bridge over the Rio Grande," Tech. Rept. #LA-12979-MS, Los Alamos National Laboratory Los Alamos, New Mexico.

Foote, P.D. (1999), "Structural health Monitoring - Tales from Europe", Proceedings of the 2nd international Workshop on Structural Health Monitoring, Standford University, Standford, CA, Sep., 1999**,** pp. 24-35.

Frangopol, D.M., Ghosn, M., et al. (1998), "Structural Reliability in the bridge engineering", Journal of Bridge Engineering, ASCE, Vol. 3, No. 4, Nov., 1998, pp. 151-154

Friswell, M.I. and Mottershead, J.E. (1995), "Finite element model updating in structural dynamics", Kluwer Academic Publishers, The Netherlands, 1995.

Friwell, M.I., Penny, J.E.T., and Wilsonm, D.A.L. (1994), "Using vibration data and statistical measures to locate damage in structures", Int. J. Anal. and Experimental Modal Analysis, Vol. 9,

No. 4, 1994, pp. 239-254.

Fridaus, E. Udwadia (1994), “Methodology for optimum sensor locations for parameter identification in dynamic systems”, Journal of Engrg. Mech., ASCE, 120(2).

Fu, G.K. and Moosa, A.G. (2000), “Health monitoring of structures using optical instrumentation and probabilistic diagnosis”, from “Condition Monitoring of Materials and Structures” (Ansari, F. eds), pp. 190-201.

G

Gahboussi, J., Garrett, J.H., And Wu, X. (1991), “Knowledge-based modeling of material behavior with neural networkd”, Journal of Engrg. Mech., ASCE, Vol. 117, No. 1, 1991, pp. 132-153.

Ghanem, R. and Shinozuka,M. (1995), “Structural system identification: I-theory; II-Experimental verification”, J. Engrg. Mech., ASCE, 121(2), pp. 255-273.

Giordano, A.A. (1985), “Least Square Estimation with Application to digital signal processing”, John Wiley & Sons, New York, 1985.

Gola, M.M., Soma, A., and Botto, D. (2001), “On theoretical limits of dynamic model updating using a sensitivity-based approach”, Journal of Sound and Vibration, Vol. 244, No. 4, pp. 583-595.

Golub, G.H. and Van Loan, C.F. (1983), “Matrix computations”, the Johns Hopkins University Press, Baltimore, Maryland.

Graupe, D. (1989), “Time series analysis, Identification and adaptive filtering.”(2nd Edition), Roberte. Krieger Publishing Company, Malabar, Florida, 1989. (QA280 G74). (program attached)

Green, M.F. and Cebon, D. (1994), “ Dynamic response of highway bridges to heavy vehicle loads: theory and experimental validation”, Journal of Sound and Vibration, Vol. 170, No. 1, 1994, pp. 51-78

Gupta, V.K., Nielsen, S.R.K., and Kirkegaard, P.H. (2001), “A preliminary prediction of seismic damage-based degradation in RC structures”, Earthquake Engng. Struct Dyn., Vol. 30, 2001, pp. 981-993.

H

Hajela, P. and Soerio, F.J. (1990), “Structural damage detection based on Static and model

analysis", AIAA Journal, 28(9), pp. 1110-1115.

Halling, M.W., Muhammad,I., and Womack, K.C. (2001), "Dynamic filed testing for condition assessment of bridge bents", Journal of Struc. Engrg., ASCE, Vol. 127, No. 2., Feb., 2001, pp. 161-167.

Hao, H. and Xia, Y. (2002), "Vibration-based damage detection of structures by genetic algorithm", Journal of Computing in Civil Engineering, ASCE, Vol. 16, No. 3, 2002, pp. 222-229.

Haritos, N. (2000), "Dynamic testing techniques for structural identification of bridge superstructures", Proceedings of the International Conference on Advances in Structural Dynamics, edited by J.M. Ko and Y.L. Xu, The Hongkong Polytechnic University, Hong Kong, Dec., 2000**,** pp. 1013-1020.

Harris, C.M. and Crede, C.E. (1996), "Shock and vibration handbook" (4th Edition), McGraw-Hill, 1996.

Hearn, G. and Testa, R.B. (1991), "Modal analysis for damage detection in structures", Journal of Struc. Engrg., ASCE, Vol. 117, No. 10, pp. 3042-3063.

Heemez, F.M. and Farhat ,C. (1995), "Bypassing numerical difficulties associated with updating simultaneously mass and stiffness matrices," AIAA Journal, Vol. 33, No. 3, March, 1995, pp. 539-546.

Helmicki, A., Hunt, V., et al. (1999), "Multidimensional performance monitoring of a recently constructed steel-stringer bridge", Proceedings of the 2nd international Workshop on Structural Health Monitoring, Standford University, Standford, CA, Sep., 1999**,** pp. 408-416.

Hemez, F.M., (1993), "Theoretical and experimental correlation between Finite Element Models and modal tests in the context of large flexible space structure", Ph.D. Dissertation, Dept. of Aerospace Engineering Sciences, Univ. of Colorado, Rept. CU-CAS-93-18, Builder, CO, Aug., 1993.

Hemez, F.M. and Farhat, C. (1994), "An energy based optimum sensor placement criteria and its application to structural damage detection", Proc., 12th Int. Modal Anal. Conf., Society of Experimental Mechanics, Honolulu, 1994, pp. 1568-1575.

Herrmann, T. and Pralwarter,H.J. (1998), "Two-step identification approach for damped finite element models", J. of Engrg. Mech., ASCE, 124(6), pp. 639-647.

Heredia-Zavoni, E. and Esteva, L. (1998), “Optimal instrumentation of uncertain structural systems subject to earthquake motions”, Earthquake Engineering and Structural Dynamics, Vol. 27, pp. 343-362.

Herman Van der Auweraer and Luc Hermans (1999), “Structural model identification from real operating conditions”, Sound and Vibration. Jan., 1999. pp. 34-41.

Hjelmstad, K.D. (1996), “On the uniqueness of modal parameter estimation”, Journal of Sound and Vibration. 192(2), pp. 581-598

Hjelmstad, K.D. and Shin S. (1997), “Damage detection and assessment of structures from static response”, Journal of Engrg. Mech., ASCE , 123(6), pp. 568-576 .

Hoon Sohn, J.A., Czarnecki, and Farrar, C.R. (2000), “Structural health monitoring using statistical process control”, Journal of Structural Engineering, ASCE, Vol. 126, No. 11, Nov., 2000, pp. 1356-1363.

Hoshiya, M. and Statio, E. (1984), “Structural identification by Extended Kalman Filter”, Journal of Engrg. Mech., ASCE, Vol. 110, No. 12, pp. 1757-1770.

Hoshiya, M. and Maruyama, O. (1987), “Structural Identification by extended Kalman Filter”, Journal of Engineering Mechanics, ASCE, Vol. 110, 1987, pp. 1757-1770.

Houge,T.D., Aktan, A.E., and Hoyos, A. (1991), “Localized identification of constructed facilities.”, Journal of Structural Engineering, ASCE, Vol. 117, No. 1, Jan., 1991, pp. 128-148.

Housner,G.W., Bergman,L.A., et al. (1997). “Structural control: Past, present, and future”, Journal of Engineering mechanics, ASCE, Vol. 123, No. 9, Sep., 1997, pp. 897-971.

Huang, C.H. (2001), “An inverse non-linar force vibration problem of estimating the external forces in a damped system with time-dependent system parameters”, Journal of Sound and Vibration, Vol. 242, No. 5, pp. 749-765.

Huang, C.S., Yang,Y.B., Lu, L.Y., and Chen. C.H. (1999), “Dynamic testing and system identification of a multi-span highway bridge”, Earthquake Engineering and Structural Dynamics, Vol. 28, pp. 857-878.

Huang, C.S. (2001), “Structural identification form ambient vibration measurement using the multivariate AR model”, Journal of Sound and Vibration, Vol. 241, No. 3, pp. 337-359.

Huang, C.S. and Liu, H.L. (2001), “Modal identification of structures from ambient vibration,

free vibration, and seismic response data via a subspace approach", Earthquake Engrg. Struct. Dyn., Vol. 30, 2001, pp. 1857-1878.

Huang, T.J. (1997) "Damage probes in structural and mechanisms Utilizing energy-based modal parameter identification", Ph.D. dissertation, State university of New York at Buffalo, New York, Nov., 1997.

Humar, J.L. and Kashif, A.H. (1993), "Dynamic response of bridge under traveling loads", Canadian Journal Of Civil Engineering, Vol. 20, pp. 280-298.

Humar, J.L. and Kashif, A.H. (1995), "Dynamic response analysis of slab-type bridges", Journal Of Structural Engineering, ASCE, Vol. 121, No. 1, 1995, pp. 48-62.

Hwang, H, Jernigan, J.B., and Lin, Y.W. (2000), "Evaluation of seismic dynamic to Memphis bridges and highway systems", Journal of Bridge Engineering, ASCE, Vol. 5, No. 4, Nov., 2000, pp. 322-330.

I

Ibrahim, S.R. (1973), "A time domain vibration testing technique", Ph.D. Dissertation, Dept. of Mechanical Engrg., University of Calgary, Alberta, Canada.

Ibrahim, S.R. and Mikulcik, E.C. (1976), "The experimental determination of vibration parameters from time responses", the Shock and Vibration Bulletin, Vol. 46, No. 5, 1976, pp. 187-196.

Ibrahim, S.R. and Mikulcik, E.C. (1977), "A method for the direct identification of vibration parameters from the free responses", the Shock and Vibration Bulletin, Vol. 47, No. 4, 1977, pp. 117-122.

Ivanovic, S.S, Trifunac, M.D., and Todorovska, M.I. (1999), "On identification of damage in structures via wave travel times", Proc. Nato advanced research workshop on Strong-motion Instrumentation for civil engineering structures. June 2-5, 1999, Istanbul, Turkey, Kluwer Publ.

J

Jang, J.H., Yeo, I., Shin, S., and Chang, S.P. (2002), "Experimental investigation of system-identification-based damage assessment on structures", Journal of Struct. Engrg., ASCE , 128(5), pp. 673-682.

Jensen, H.A. and Sepulveda, A.E. (1998), "Design sensitivity metric for structural dynamic response," AIAA Journal, Vol. 36, No. 9, Sep., 1998, pp. 1686-1693.

Jiang, H.B. (2000), “Damage identification and reliability updating of simple supported beam and continuous beam”, Post-doctor Report in the Department of Civil Engineering, Hunan University, Changsha, China, 2000.

Juang, J.N. and Pappa, R. (1985), “An eigensystem realization algorithm for modal parameter identification and model reduction”, AIAA Journal of Guidance, Control and Dynamics, Vol. 8, No. 5, Sep.-Oct., 1985, pp. 620-627.

Juang, J.N. (1987), “Mathematical Correlation of Modal-Parameter-Identification methods Via system realization theory”, International Journal of Analytical and Experimental Modal Analysis, Vol. 2, No. 1 Jan., 1987.

Juang, J.N. (1994), “Applied system identification”, Prentice-Hall, Inc., Englewood Cliffs, N.J.

K

Kammer, D.C. (1991), “Sensor placement for on orbit modal identification and correlation of large space structures”, AIAA Journal, Vol. 26, No. 1, pp. 104-112.

Kaouk, M. and Zimmerman, D.C., (1994), “structural damage assessment using a generalized minimum rank perturbation theory”, AIAA Journal, 32(4), pp. 836-842.

Katafygiotis, L.S., Yuen, K.V., and Chen, J.C. (2001), “Bayesian modal updating by using of ambient data”, AIAA Journal, Vol. 39, No. 2, pp. 271-278.

Kennedy, J.B. and Grace, N.F. (1990), “Prestressed continuous composite bridges under dynamic load”, Journal of Structural Engineering, ASCE, Vol. 116, No. 6, June, 1990, pp. 1660-1678.

Kerschen, G. and Golinval, J.-C. (2001), “Theoretical and experimental identification of a non-linear beam”, Journal of Sound and Vibration, Vol. 244, No. 4, pp. 597-613.

Khiem, N.T. and Lien, T.V. (2001), “A simplified method for natural frequency analysis of a multiple cracked beam”, Journal of Sound and Vibration, Vol. 245, No. 4, pp. 737-751.

Kim, H.M. and Bartkowicz, T.J. (1997), “A two-step structural damage detection approach with limited instrumentation”, Journal of Vibration Acoust., 119(2), pp. 258-264.

Kim, H.M. and Bartkowics, T.J. (2001), “An experimental study for damage detection using a hexagonal truss”, Computer and Structures, Vol. 79, pp. 173-182.

Kim, D.O. and Lee, I.W. (2000), “Mode localization in structures consisting of the substructures and couplers”, Engineering Structures, Vol. 22, No. 1, pp. 39-48.

Koh, C.G., See, L.M. and Balendra, T. (1991), “Estimation of structural parameters in time domain: a substructure approach”, Earthquake Engrg. and Struct. Dynamics, Vol. 20, pp. 787-801.

Koh, C.G., See, L.M., and Balendra, T. (1995a), “Determination of story stiffness of three-dimensional frame buildings”. Engrg. Struct., Vol. 17, No. 3, pp. 179-186.

Koh, C.G., See, L.M., and Balendra, T. (1995b), “Damage detection of buildings:numerical and experimental studies”, Journal of Struc. Engrg., ASCE, Vol. 121, No. 8, 1995, pp. 1155-1160.

Koh, C.G. Hoon, B., and Liaw, C.Y. (2000), “Parameter identification of large structural systems in time domain”, Journal of Structural Engineering, ASCE, Vol. 126, NO. 8, Aug., 2000, pp. 957-963.

Kong, F., “The application of energy transfer ratio in the bridge condition assessment,” Ph.D. dissertation, State University of New York at Buffalo, 1996.

Kosmatka, J.B. and Ricles, J.M. (1999), “Damage detection in structures by modal vibration characterization”, Journal of Struct. Engrg., ASCE , 125(12), pp. 1384-1392.

Kraus, A.D. (1987), “Matrices for Engineers”, Hemisphere Publishing Corporation.

L

Lardies, J., and Larbi, N. (2001), “A new method for model order selection and modal parameter estimation in time domain”, Journal of Sound and Vibration, Vol. 245, No. 2, pp. 187-203.

Lauzon, R.G. (1997), “Vibration monitoring of a full-scale highway bridge undergoing a destructive test”, Ph.D. Dissertation, University of Connecticut, Storrs, Conn., CT.

Law, S.S., Shi, Z.Y., and Zhang, L.M. (1998), “Structural damage detection from incomplete and noisy modal test data”, Journal of Engrg. Mech., ASCE, 124(11), pp. 1280-1288.

Law, S.S., Chan, T.H.T., and Wu, D. (2001), “Efficient numerical model for the damage detection of large scale structure”, Engineering Structures, Vol. 23, No. 5, 2001, pp. 436-451.

Law, S.S., et al. (2000), “Modal strain energy changes in neural network damage assessment”, Proceedings of the International Conference on Advances in Structural Dynamics, edited by J.M. Ko and Y.L. Xu, The Hongkong Polytechnic University, Hong Kong, Dec., 2000**,** pp. 1037-1044.

Lee, H.S., Kim, Y.H., Park, C.J., and Park, H.W. (1999), “ A new spatial regularization scheme

for the identification of geometric shapes of inclusions in finite bodies", Inter. J. Numer. Methods in Engrg., 46, pp. 973-992.

Lee, C.H., Lin, C.Y., and Huang, C.C. (2000), "Time domain identification of frames under earthquake loadings", Journal of Engineering Mechanics, Vol. 126, No. 7, July, 2000, pp. 693-703.

Levine-west, M., Milman, M., and Kissi, A. (1996), "Mode shape expansion techniques for prediction: Experimental evaluation", AIAA Journal, Vol. 34, No. 4, April, 1996, pp. 821-829.

Levin, R.I. and Lieven, N.A.J. (1998), "Dynamic finite element model updating using neural network', Journal of Sound and Vibration, Vol. 210, No. 5, 1998, pp. 593-607.

Lee, Jiann-shiun (1995), "Using transfer function parameter changes for damage detection of structures", AIAA, Journal, Vol. 33, No. 11, Nov., 1995, pp. 2189-2193.

Lee, G.C. and Liang, Z. (1999), "Development of a Bridge Monitoring System", Proceedings of the 2nd international Workshop on Structural Health Monitoring, Standford University, Standford, CA, Sep., 1999**,** pp. 349-358.

Liang, Z. (1987), "On modal testing in the time domain", Ph.D. Dissertation, Department of Mechanical and Aerospace Engineering, State University of New York at Buffalo, N.Y., 1987.

Liang, Z. and Lee, G.C. (1991), "Damping of structures", National Center for Earthquake Engineering Research, NCEER 91-0004, State University of New York at Buffalo, Buffalo, NY, 1991.

Liang, Z., Tong, M., and Lee, G.C. (1995), "Modal energy measurement of a long steel bridge", 13th IMAC, Orlando, FL.

Lim, T.W. (1991), "Structural damage detection from modal test data", AIAA Journal, 29(12), pp. 2271-2274.

Lim, T.W. and Kashangaki, T.A.L. (1994), "Structural damage detection of space truss structures using best achievable eigenvector," AIAA Journal, 32(5), pp. 1049-1057.

Lin, J.W., Betti, R., Smyth, A.W., And Longman, R.W. (2001), "On-line identification of non-linear hysteretic structural system using a variable trace approach", Earthquake Engng. Struc. Dyn., Vol. 30, 2001, pp. 1279-1303.

Loukas, Papadopoulos and Ephrahim, Garcia (1998), "Structural damage identification: a

probabilistic approach," AIAA Journal, Vol. 36, No. 11, Nov., 1998, pp. 2137-2145.

M

Ma, J. and Pines, D.J. (2001), "Dereverberation and its application to damage detection in one-dimensional structures", AIAA Journal, Vol. 39, No. 5, pp. 902-918.

Maia, N.M.M. and Silva, J.M.M., eds. (1997), "Theoretical and experimental modal analysis", Research Studies Press Ltd., Taunton, U.K.

Mak, P.S and Law, S.S. (2000), "Structural damage assessment by elemental modal strain energy changes", Proceedings of the International Conference on Advances in Structural Dynamics, edited by J.M. Ko and Y.L. Xu, The Hongkong Polytechnic University, Hong Kong, Dec., 2000.

Magid, A.R. (1985), "Applied matrix models - a Second course in linear Algebra with computer applications", John Wiley & Sons.

Marwala, T. and Hunt, H.E.M. (1999), "Fault identification using finite element models and neural networks", Mech. Sys. and Signal Processing, 13(3), pp. 475-490.

Marwala, T. (2000), "Damage identification using committee of neural networks", Journal of Engineering Mechanics, ASCE, Vol. 126, No. 1, 2000, pp. 43-50.

Masri, S.F., Chassiakos, A.G., and Caughey, T.K. (1993), "Identification of nonlinear dynamic systems using neural networks", Journal of Applied Mechanics, Transactions, ASME, Vol. 60, pp. 123-133.

Masri, S.F., Nakamura, M., et al. (1996), "A neural network approach to the detection of changes in structural parameters", Journal of Engrg. Mech., ASCE, Vol. 122, No. 5.

Masri, S.F., Smyth, A.W., Chassiakos, A.G., et al. (2000), "Application of neural network for detection of changes in nonlinear systems", Journal of Engineering Mechanics, ASCE, Vol. 126, No.7, 2000, pp. 666-676.

Mazurek, D.F. and DeWolf, J.T. (1990), "Experimental study of bridge health monitoring technique", Journal of Structural Engineering, ASCE, Vol. 116, No. 9., Sep., 1990, pp. 2532-2549.

Mazurek, D.F. and DeWolf, J.T. (1990), "Experimental study of bridge monitoring techniques", Journal of Struc. Engrg., ASCE, Vol. 116, No. 9, 1990, pp. 2532-2549.

McConnel, K.G. (1995), "Vibration Testing---Theory and Practice", JohnWilly & Sons, Inc.

NewYork, NY, 1995.

Melchers, R.E. (1998), “Structural reliability analysis and prediction”(2nd edition), John Wiley & Sons Ltd.

Messina, A., Willams, E.J., and Contursi, T. (1998), “Structural damage detection by a sensitivity and statistical-based method”, Journal of Sound and Vibration Vol. 216, No. 5, 1998, pp. 791-808.

Mirmiran,A. and Wei, Y.M. (2001), “Damage Assessment of FRP-encased concrete using Ultrasonic Pulse Velocity”, J. of Engrg. Mech., ASCE, Vol. 127, No. 2, Feb., 2001, pp. 126-135.

Morassi, A. and Rovere,N. (1997), “localizing a notch in a steel frame from frequency measurements”, J. of Engrg. Mech., ASCE, Vol. 123, No. 5, May, 1997, pp. 422-432.

Muria-Vala, D., Gomez, R., and king, C. (1991), “Dynamic structural properties of cable-stayed Tampico Bridge,” Journal of Structural Engineering, ASCE, Vol. 117, No. 11, Nov., 1991, pp. 3396-3416.

N

Narayana, K.L. and Jebaraj, C. (1999), “ Sensitivity analysis of local/global modal parameters for identification of a crack in a beam”, Journal of Sound and Vibration Vol. 228, No. 5, 1999, pp. 977-994.

Nashif, A.D., Jones, D.I.G., and Henderdon, J.P. (1985), “Vibration Damping,” John Willy & Sons, Inc. 1985.

Ni, Y.Q. et al. (2000), “Vibration-based damage localization in Ting Kau Bridge using probabilistic neural network”, Proceedings of the International Conference on Advances in Structural Dynamics, edited by J.M. Ko and Y.L. Xu, The Hongkong Polytechnic University, Hong Kong, Dec., 2000.

Nichols, J.M., Virgin, L.N., and Gavin, H.P. (2001), “Damping estimation form experimental non-linear time-series”, Journal of Sound & Vibration. Vol. 246, No. 5, 2001, pp. 815-827.

Nuno, M., Mendes, M., and Silva, J.M.M. (1997), “Theoretical and experimental modal analysis,” Research Studies Press Ltd, England, 1997.

O

Oh, B.H. and Jung, B.S. (1998), “structural damage assessment with combined data of static and modal tests,” Journal of Struct. Engrg., ASCE, 124(8), pp. 956-965 .

Oreta, A.W.C. and Tanabe, T.A. (1994), “Element identification of member properties of framed structures”, Journal of Struc. Engrg., ASCE, Vol. 120, No. 7, 1994, pp. 1961-1967.

Overman, T.R., Shiu,K.N., Weinmann,T.L., Morgan, B.J., and Schultz, D.M. (1987), “Evaluation and surveillance of concrete bridge structures.”, Bridge and Transmission line Structures, L. Tall, ed., ASCE, New York, N.Y., 1987, pp. 224-236.

P

Pai, P.F. and Jin, S. (2000), “Locating structural damage by detecting boundary effects”, Journal of Sound and Vibration Vol. 231, No. 4, 2000, pp. 1079-1110.

Pandey,A.K., Biswas, M., and Samman, M.M., (1991), “Damage detection from changes in curvature mode shapes”, Journal of Sound Vibration. 145(2), pp. 321-332.

Pandey, A.K. and Biswas, M. (1994), “Damage detection in structures using changes in flexibility”, Journal of Sound Vibration. 169(1), pp. 3-17.

Park, K.C. and reich, G.W. (1999), “Model-based health monitoring of structural systems: Progress, Potential, and Challenges”, Proceedings of the 2nd international Workshop on Structural Health Monitoring, Standford University, Standford, CA, Sep., 1999**,** pp. 82-95.

Paultre, P., Proulx, J., and Begin, T. (2000), “Short communication dynamic investigation of a hybrid suspension and cable –stayed bridge”, Earthquake Engineering and Structural Dynamics, Vol. 29, 2000, pp. 731-739.

Peeters, B. and Roeck, G.D. (1999), “Reference-based stochastic subspace identification for output-only modal analysis”, Mechanical System. and Signal Processing, 13(6), pp. 855-878.

Peeters, B. and Roeck, G.D. (2001), “One-year monitoring of the Z24-bridge: environmental effects versus damage events”, Earthquake Engng. Struct. Dyn., Vol. 30, 20001, pp. 149-171.

Penny, J.E.T., Friswell, M.J., and Garvey, S.D. (1994), “Automatic choice of measurement locations for dynamic testing”, AIAA Journal, Vol. 32, No. 2, Feb., 1994, pp. 407-414.

Philip, D., Cha, and Tuck-Lee, J.P. (2000), “Updating structural system parameters using frequency response data”, **J**ournal of Engineering Mechanics, ASCE, Vol. 126, No. 12, Dec., 2000, pp. 1240-1246.

Piombo, B.A.D., Fasana, A., Marchesiello, S. and Ruzzene, M. (2000), “Modeling and identification of the dynamic response of a supported bridge”, Mechanical System and Signal

Processing, Vol. 14, No. 1, 2000, pp. 75-89.

Pollock, D.S.G. (1999), “A Handbook of time-series analysis, signal processing and dynamics”, Academic Press, U.K, 1999.

Prato, C.A. et al. (2000), “Dynamic tests for structural evaluation and repair of cabled-stayed bridges”, Proceedings of the International Conference on Advances in Structural Dynamics, edited by J.M. Ko and Y.L. Xu, The Hongkong Polytechnic University, Hong Kong, Dec., 2000**,** pp. 1079-1084.

Puotolo,R. and Surace, C. (1999), “Using SVD to detect damage in structures with different operational conditions”, Journal of Sound and Vibration Vol. 226, No. 3, 1999, pp. 425-439.

Q

Quek, S.T., Wang, W.P., and Koh, C.G. (1999), “System identification on linear MDOF structures under ambient excitation”, Earthquake Engrg. and Struc. Dynamics, Vol. 28, pp. 61-77.

Qin, Q., Liang, H.B., and Qian, L.Z. (2001), “Modal identification of Tsing Ma bridge by using improved eigensystem realization algorithm”, Journal of Sound and Vibration Vol. 247, No. 2, 2001, pp. 325-341.

R

Raghavendrachar, M., and Aktan, A.E. (1992), “Flexibilty of multireference impact testing for bridge diagnostics”, Journal of Struc. Engrg., ASCE, Vol. 118, No. 8, pp. 2186-2203.

Ren, W.X. and Roeck, G.D. (2002), “Structural damage identification using modal data: I: Simulation verification; II: Test verification”, Journal of Struc. Engrg., ASCE, Vol. 128, No. 1, pp. 87-104.

Reynier, M. and Hisham, A.K. (1999), “Sensors location for updating problems.”, Mechanical System and Signal Processing, Vol. 13, No. 2, 1999, pp. 297-314.

Ricles, J.M. and Kosmatka , J.B. (1992), “Damage detection in elastic structures using vibratory residual forces and weighted sensitivity”, AIAA J., Vol. 30, No. 9, !992, pp. 2310-2316.

S

Salawu, O.S. and William, C. (1995), “Bridge assessment using forced-vibration testing”, Journal of Structural Engineering, ASCE, Vol. 121, No. 2, Feb., 1995, pp. 161-172.

Salawu, O.S. (1997), “Detection of structural damage through changes in frequency: a review”,

Engineering Structures, Vol. 19, No. 9, pp. 718-723.

Sanayei, M. and Scampoli, S.F. (1990), “Structural element stiffness identification from static test data”, Journal of Engrg. Mech., ASCE, 117(5), pp. 1021-1036

Sanayei, M. and Onipede, O. (1991), “Damage assessment of structure using static test data”, AIAA Journal, 29(7), pp. 1174-1179.

Sanayei, M., Onipede, O., and Babu, S.R. (1992), “Selection of noisy measurement location for error reduction in static parameter identification,” AIAA Journal, 30(9), pp. 2299-2309.

Sanayei, M. and Saletnik, M.J. (1996a,b), “Parameter estimation of structures from static strain measurements. I: Formulation ; II: error sensitivity analysis”, Journal of Struc.Engrg., ASCE, Vol. 122, No. 5, 1996, pp. 555-572.

Sanayei, M., Imbaro, G.R., McClaim, J.A.S., and Brown, L.C. (1997), “Structural model updating using experimental static measurements”, Journal of Struct. Engrg., ASCE, 123(6), pp. 792-798 .

Sanayei,M. and Saletnik, M.J. (1997), “Parameter estimation of structures from static strain measurements. I: Formulation; II: Error sensitivity analysis”, Journal of Struct. Engrg., ASCE, 123(5), pp. 555-572 .

Sato,T. and Qi, K. (1998), “Adaptive H-infinity filter: its application to structural identification.”, Journal of Engrg. Mech., ASCE, Vol. 124, No. 11, 1998, pp. 1233-1240.

Sayyer，J.P. and Rao, S.S. (2000), “Structural damage detection and identification using Fuzzy logic.”, AIAA J., Vol. 38, No. 12, 2000, pp. 2328-2335

Sennah, K. and Kennedy, J.B. (1997), “Dynamic characteristics of simply supported curved composite multi-cell bridges”, Canadian Journal of Civil Engineering, Vol. 24, No. 4, 1997, pp. 621-636.

Sennah,K. and Kennedy, J.B.(1998), “Vibration of horizontally curved continuous composite celluar bridges”, Canadian Journal of Civil Engineering, Vol. 25, No. 1, 1998, pp. 139-150.

Shi ,Tinghui, Jones N.P., and Ellis, J.H. (2000), “Simultaneous estimation of system and input parameters from output measurements”, Journal of Engineering Mechanics, ASCE, Vol. 126, No. 7, July, 2000, pp. 746-753.

Shi, Z.Y., Law, S.S., and Zhang, L.M., (2000), “Damage localization by directly using

incomplete mode shapes", Journal of Engrg. Mech., ASCE, 126(6), pp. 656-660 .

Shi, Z.Y., Law, S.S., and Zhang, L.M., (2000), "Structural damage detection from modal strain energy change", Journal of Engrg. Mech., ASCE, 126(12), pp. 1216-1223 .

Shi, Z.Y., Law, S.S., and Zhang, L.M., (2000), "Optimizing sensor placement for structural damage detection", Journal of Engrg. Mech., ASCE, 126(11), pp. 1173-1179 .

Shi, Z.Y., Law, S.S., and Zhang, L.M., (1998), "structural damage localization from model strain energy change", Journal of Sound Vibration. 218(5), pp. 825-844

Shi, Z.Y., Law,S.S., and Zhang, L.M.(2002), "Improved damage quantification from elemental modal strain energy change", Journal of Engrg. Mech., ASCE, 128(5), pp. 521-529 .

Sohn, H. and Law, H.W. (1997), "Bayesian probabilistic approach for structural damage detection", Earthquake Engrg. and Struc. Dynamics, Vol. 26, pp. 1259-1281.

Sohn, H., and Law, H.W. (2000), "Bayesian probabilistic damage detection of a reinforced-concrete bridge column", Earthquake Engrg. and Struc. Dynamics, Vol. 29, 2000, pp. 1131-1152.

Steinberg, D.I. (1974), "Computational matrix algebra", McGraw-Hill Book Company, 1974.

Stubbs, N., Kim, J.T., and Farrar, C.R. (1995), "Field verification of a nondestructive damage localization and severity estimation algorithm", Proceedings of the 13th Int'l Modal Analysis Conference (IMAC), pp. 210-218, Nashville, TN, 1995.

Stubbs, N. and Kim, J.T. (1996), "Damage localization in structures without baseline model parameters," AIAA J., 34(8), pp. 1644-1649.

Szewezyk, P. and Hajela, P. (1994), "Damage detection in structures based on feature-sensitive neural networks," Journal of Comp. In Civ. Engrg., ASCE, Vol. 8, No. 2, 1994, pp. 163- 178.

U

Udwadia, F.E. and Garba, J.A. (1985), "Optimal sensor locations for structural identification", Proc., JPL workshop on Identification and Control of Flexible Space Struc., 1985, pp. 247-261.

V

Vanik, M.W., Beck, J.L., and Au, S.K. (2000), "Bayesian Probabilitic approach to structural health monitoring," Journal of Engineering Mechanics, ASCE, Vol. 126, No. 7, 2000, pp. 738-745.

Vestroni, F. and Capecchi, D. (2000), " Damage detection in beam structures based on frequency measurements", Journal of Engineering Mechanics, ASCE, Vol. 126, No. 7, July, 2000, pp. 761-768.

Vold, H. and Rocklin, G.T. (1982), "The numerical implementation of a Multi-input modal estimation method for mini-computer", Proceedings of the 1st International Modal Analysis Conference (IMAC I), Orlando, Florida, 1982, pp. 542-548.

W

Wahab, M.M.A., Roceck, G.D., and Peeters, B. (1999), "Parameterization of damage in reinforced concrete structures using modal updating", Journal of Sound and Vibration, Vol. 228, No. 4, 1999, pp. 717-730.

Wahab, M.M.A. and Roceck, G.D. (1999), "Damage detection in bridges using modal curvatures: Application to a real damage scenario", Journal of Sound and Vibration, Vol. 226, No. 2, 1999, pp. 217-235.

Wang, D. and Haldar, A. (1994), "Element-level system identification with unknown input", Journal of Engrg. Mech., ASCE, Vol. 120, No. 1, pp. 159-176.

Wang, B.S., et al. (2000), "Comparative study of damage indices in application to a long-span suspension bridge", Proceedings of the International Conference on Advances in Structural Dynamics, edited by J.M. Ko and Y.L. Xu, the Hongkong Polytechnic University, Hong Kong, Dec., 2000**,** pp. 1085-1092.

Wang, X., Hu, N., Fukunaga, H., and Yao, Z.H. (2001), "Structural damage identification using test data and changes in frequencies", Engineering Structures, Vol. 23, No. 6, 2001, pp. 610-621.

Weaver, W., Jr. and Johnston, P.R. (1987), "Structural Dynamics by Finite Elements", Prentice-Hall, Inc., 1987. (TA654W42)

Westermo, B.D. and Thompson, L.D. (1995), "Design and evaluation of passive and active structural health monitoring systems for bridges and buildings", Proc., UCII'95.

Wong Lai-Ah, and Chen Jay-Chung (2000), "Damage Identification of Nonlinear structural systems," AIAA J., Vol. 38, No. 8, 2000, pp. 1444-1452.

Wilson,J.C. (1986). "Analysis of the observed seismic response of a highway bridge", Earthquake Engrg. And Struc. Dyn., Vol. 15, pp. 249-274.

Wu, X., Gahboussi, J., and Garrett, J.H. (1992), "Use of neural networks in detection of

structural damage", Computer and Structures, Vol. 42, No. 4, 1992, pp. 649-659.

X

Xia, Y. and Hao, H. (2000), "Measurement selection for vibration-based structural damage identification", Journal of Sound and Vibration Vol. 236, No. 1, 2000, pp. 89-104.

Xia,Y., Hao,H., Brownjohn, M.W., and Xia, P.Q. (2002), "Damage identification of structures with uncertain frequency and mode shape data", Earthquake Engineering and Structural Dynamics, Vol. 31, No. 5, 2002, pp. 1053-1066.

Y

Yao. J.T.P. and Natke, H.G. (1994). "Damage Detection and Reliability Evaluation of Existing Structures". Structural Safety. Vol. 15, pp. 3-16.

Yang,X.F, Swamidas, A.S.J., and Seshardri, R. (2001), "Crack identification in vibrating beams using the energy method", Journal of Sound and Vibration, Vol. 244, No. 2, pp. 339-357.

Yeo I., Shin, S., Lee, H.S., and Chang, S.P. (2000), " Statistical damage assessment of framed structures from static responses", Journal of Engrg. Mech., ASCE, 126(4), pp. 414-421.

Yun, C.B. and Shinozuka, M. (1980), "Identification of nonlinear structural dynamic system", Journal Struc. Mech., Vol. 8, No. 2, pp. 187-203.

Yun, C.B., Kim,W.J., and Ang, A.H.S. (1988), "Damage assessment of bridge structures by system identification", Proc.Korea-Japan Joint Seminar on Engrg. Technol. In Struc. Engrg. and Mech., pp. 182-193.

Yun, C.B. and Lee, H.J. (1997), "Substructural identification for damage estimation of structures", Struct. Safety, Amsterdam, 19(1), pp. 121-140.

Z

Zang, C., and Imregun, M. (2001), "Structural damage detection using artificial neural networks and measured FRF data reduced via principal component projection", Journal of Sound and Vibration, Vol. 242, No. 5, pp. 813-827.

Zhang, H.C., Foliente, G.C., Yang, Y.M., and Ma, F. (2002), "Parameter identification of inelastic structures under dynamic loads", Earthquake Engineering and Structural Dynamics, Vol. 31, pp. 1113-1130.

Zhang, H., Schulz, M.J., and Ferguson, F. (1999), "structural health monitoring using transmittance functions", Mechanical System and Signal Processing, 13(5), pp. 765-787.

Zhang, Q.W. (1999), “Modal updating and damage detection for bridge structures.”, Ph.D. Dissertation, Dept. of Bridge Engineering, Tongji Univ., China, Feb., 1999.

Zhao, Q., Sawada,T., Hirao, K., and Nariyuki, Y. (1995), “Localized identification of MDOF structures in the frequency domain.”, Earthquake Engrg. and Struct. Dynamics, Vol. 24, pp. 325-338..

Zhao, J. and DeWolf, J.T. (1999), “sensitivity study for vibration parameters used in damage detection”, Journal of Struct. Engrg., ASCE, 125(4), pp. 410-416 .

Zheng, G.T., Buckley, M.A., Kister, G., and Fernando, G.F. (2001), “Blind deconvolution of acoustic emission signals for damage identification in composites”, AIAA Journal, Vol. 39, No. 6, pp. 1198-1205.

Zhu,H.P. and He, B. (2000), “Finite element model updating with modal test results”, Proceedings of the International Conference on Advances in Structural Dynamics, edited by J.M. Ko and Y.L. Xu, The Hongkong Polytechnic University, Hong Kong, Dec., 2000**,** pp. 1117-1124.

Zhuo, W.D. (2000), “Study on ductile seismic design for highway bridges,” Ph.D. Dissertation, Dept. of Bridge Engineering, Tongji Univ., China, June, 2000.

Zimmerman, D.C., Smith, S.W., Kim, H.M., et al. (1996), “An experimental study of structural damage detection using incomplete measurements”, Journal of Vibration Acoust., 118(4), pp. 543-550.

Zou, Y., Tong, L., and Steven, G.P. (2000), “Vibration-based model-dependent damage (delamination) identification and health monitoring for composite structures - a review”, Journal of Sound and Vibration, Vol. 230, No. 2, 2000, pp. 357-378.